

KATHOLIEKE UNIVERSITEIT LEUVEN
FACULTEIT TOEGEPASTE WETENSCHAPPEN
DEPARTEMENT ELECTROTECHNIEK
AFDELING ESAT
Kardinaal Mercierlaan 94 — 3001 Leuven (Heverlee)

ALGORITHMS FOR ANALYSIS AND DESIGN OF ROBUST CONTROLLERS

Jury :
Prof. W. Dutré, vice-dekaan, voorzitter
Prof. J. Vandewalle, promotor
Prof. B. De Moor, promotor
Prof. O. Bosgra (TUD, Delft)
Prof. A. Bultheel
Prof. J. De Schutter
Prof. L. El Ghaoui (ENSTA, Paris)

Proefschrift voorgedragen tot
het behalen van het doctoraat
in de toegepaste wetenschappen

door

Johan DAVID

Voorwoord

Bij het einde van het doctoraat wil ik graag enkele mensen bedanken, zonder wie dit niet mogelijk zou geweest zijn. Eerst en vooral wil ik professor J. Vandewalle bedanken voor de kans die hij mij gegeven heeft om te doctoreren. Het is een boeiende ervaring geweest om in zijn groep te kunnen werken.

Ook wil ik zeker professor B. De Moor bedanken. Zijn creatieve ideeën zijn altijd stimulerend geweest voor mijn onderzoek. Hij heeft me geleerd om grondig fundamenteel onderzoek te doen, en dit zo goed mogelijk te presenteren.

I also thank the members of the reading comitee, prof. Vandewalle, prof. De Moor, prof. El Ghaoui and prof. Bultheel, for carefully rereading the thesis and for their remarks and suggestions for improvement. Verder bedank ik ook de andere leden van de jury, prof. Dutré, prof. Bosgra en prof. De Schutter, voor hun bereidwillige medewerking.

De groep SISTA is de laatste jaren enorm uitgebreid. Dit maakt het niet mogelijk om iedereen op te sommen. Toch wil ik allen in de groep bedanken voor de aangename sfeer op het werk en erbuiten. Ik denk nog met genoegen terug aan de vele discussies over onze regeltechnische en andere problemen. Speciaal wil ik toch Jeroen, Marc, Bart, Paul en Lieven, bedanken voor het herlezen van een deel van de eerste versie van dit doctoraat.

I also wish to thank prof. Boyd of Stanford University for giving me the opportunity to spend a couple of weeks at his lab. During my stay and due to the many discussions with the members of his research group, a large part of the material in chapter 5 has been developed. Further I also thank Laurent El Ghaoui, Lieven Vandenberghe and Jeroen Dehaene for their suggestions and the many discussions on this problem.

Verder wil ik ook het personeel van het departement bedanken, de secretaresses en de computermanagers, voor de hulp die ik van hen kreeg tijdens mijn doctoraatswerk.

Mijn ouders en schoonouders wil ik ook niet vergeten, die mij altijd gesteund hebben om dit doctoraat te realiseren.

Niet in het minst, wil ik Goele, mijn vrouw, bedanken voor de steun die ze me gegeven heeft tijdens de moeilijke momenten, voor het geduld waarmee ze me rustig heeft laten werken, en voor het draaiende houden van ons gezinnetje tijdens de vele uren dat ik op het bureau was en niet thuis.

Ik dank ook het Nationaal Fonds voor Wetenschappelijk Onderzoek voor de financiële steun.

Johan David
maart 1994

Abstract

In this thesis some aspects of analysis and design of robust controllers are studied. The main contributions are:

1. It is shown how directional aspects of two transfer matrices relative to one another, can be studied. The quotient singular value decomposition has to be used. Norms are defined to quantify the relative properties. It is explained how the norms can be computed.

2. It is explained how an algorithm to solve structured total least squares problems can be used to compute real parameter margins when there are more than two parameters.

3. It is shown how a general mixed H_2/H_∞ controller can be designed, by considering the H_2 and the H_∞ constraints separately.

4. Two algorithms are developed to solve minimum rank problems involving linear matrix inequalities. These algorithms can be used to design reduced order robust controllers.

Contents

Nederlandse Samenvatting ix

List of Symbols xxvii

1 Introduction and Outline of the Thesis 1
- 1.1 Analysis and Design of Robust Controllers . . . 2
- 1.2 What is Robustness? . . . 3
  - 1.2.1 Descriptions of the Perturbation . . . 4
  - 1.2.2 Robustness Analysis . . . 6
  - 1.2.3 Robust Synthesis . . . 13
- 1.3 Chapter by Chapter Overview . . . 22
- 1.4 The Ventilator Setup . . . 24
  - 1.4.1 Steady State and Dynamic Model . . . 26
  - 1.4.2 Disturbance model . . . 27
  - 1.4.3 Measurements . . . 28
  - 1.4.4 Controller Design . . . 29

2 Directional Aspects of Two Transfer Matrices 33
- 2.1 Introduction . . . 33
- 2.2 The QSVD . . . 34
- 2.3 Directional Aspects of Matrices . . . 37
  - 2.3.1 The Indicator Ellipsoid . . . 37
  - 2.3.2 Oriented Energy . . . 40
  - 2.3.3 Signal-to-Signal Ratio of Two Matrices . . . 41
- 2.4 Directional Aspects of Transfer Matrices . . . 43
  - 2.4.1 Oriented Energy of Transfer Matrices . . . 43
  - 2.4.2 Signal-to-signal ratio of transfer matrices . . . 45
- 2.5 Norms for Directional Aspects . . . 52

2.5.1 The QH_2 norm 52
2.5.2 The QL_∞ norm and QH_∞ norm 60
2.6 Examples 70
2.6.1 Analysis of Signal to Noise Ratio of Identified Models 70
2.6.2 Application to the Ventilator Setup 73
2.7 Conclusions and Remarks 74
Appendix 1: The State Space Model of the Glass Furnace 77

3 Real Parameter Margins **79**
3.1 Introduction 79
3.2 Preliminaries 80
3.2.1 Definitions 80
3.2.2 Reformulation as a Determinant Problem 81
3.3 The Computation of the 2-Parameter Margin 88
3.4 The Computation of the ∞-Parameter Margin 91
3.5 Examples 91
3.5.1 An Example from [46] 91
3.5.2 The Ventilator Setup 94
3.6 Conclusions and Remarks 96

4 Mixed H_2/H_∞ Controller Design **97**
4.1 Introduction 97
4.2 The Mixed H_2/H_∞ Problem 100
4.2.1 Problem Statement 100
4.2.2 Proposed Solution 101
4.3 The H_∞ Control Part 106
4.4 The Optimal H_2 Controller 107
4.4.1 Parameterization of H_∞ Norm Bounded Transfer Functions 108
4.4.2 H_2 Optimization with an H_∞ Bounded Controller - Necessary Conditions 108
4.4.3 Numerical Computation of Q 112
4.5 Existence of Solutions 112
4.6 Examples 113
4.6.1 A Simple Example 113
4.6.2 The Ventilator Setup 117
4.7 Conclusions and Remarks 121

5 Reduced Order Controller Design by Rank Minimization under LMI Constraints **123**
5.1 Introduction 123
5.2 Minimum Rank Problems in Robust Control 125
5.2.1 Low Order H_∞ Controller Design 125
5.2.2 L_2 Gain Control of a NLDI 127
5.3 Computational Complexity 133
5.4 Convex Optimization 135
5.4.1 Linear Matrix Inequalities 135
5.4.2 Barrier Functions 136
5.4.3 Analytic center 137
5.4.4 Nesterov and Nemirovsky's Newton Algorithm 138
5.5 Inversion of the Analytic Centering 141
5.5.1 Without Constraints $C(x) \geq 0$ 141
5.5.2 All the Constraints are Taken Into Account 143
5.5.3 The Constraints Are Taken Into Account if Needed . . 144
5.5.4 Reduction of the Influence of the Constraints 145
5.6 The Potential Reduction Method 146
5.6.1 Description of the Algorithm 146
5.6.2 Implementation 148
5.6.3 Some Properties 153
5.7 A Comparison of the Two Methods 156
5.8 Convergence properties 158
5.8.1 Optimization paths 158
5.8.2 The Influence of r 166
5.8.3 The Influence of q 168
5.9 Other Minimum Rank Problems 169
5.9.1 Reduced Order Output Feedback Design 169
5.9.2 Reduced Order H_2 Control 172
5.9.3 The Frisch Scheme 176
5.10 Numerical Results 178
5.10.1 Reduced Order H_∞ Design 178
5.10.2 The Design of a Controller for a NLDI 180
5.10.3 Reduced Order H_2 Design 186
5.10.4 The Frisch Scheme 187
5.10.5 The Ventilator Setup 193
5.11 Conclusions and Remarks 195
Appendix 1: An Example of the Least Squares Solution near the Boundary 197

6 Conclusions 199

Bibliography 203

Nederlandse Samenvatting

1. Inleiding

Moderne regelaars zijn meestal modelgebaseerd. Dit betekent dat een mathematisch model van het te controlleren systeem nodig is om een regelaar te ontwerpen. Hoe men een geschikt model opstelt, wordt al lang onderzocht.

Maar een mathematisch model is nooit een exacte beschrijving van het echte systeem. De meeste modellen zijn lineair en tijdsinvariant, terwijl de meeste echte systemen niet-lineair en tijdsvariant zijn. De regelaars worden echter ontworpen op basis van de modellen en niet op basis van de echte systemen. De ontworpen regelaar kan het gesloten lus systeem met het model stabilizeren, maar daarom wordt het echte systeem nog niet gestabilizeerd. Het is dus nodig dat de ontworpen regelaar niet enkel het model stabilizeert, maar alle systemen in een gegeven verzameling rond het model. Zo een regelaar noemt men dan robust.
Robuustheid kunnen we formeel als volgt omschrijven:

> Gegeven een verzameling $\mathcal{S}$ van systemen rond een nominaal systeem P_0, en een eigenschap $\mathcal{P}$. Een regelaar wordt robuust genoemd met betrekking tot een eigenschap $\mathcal{P}$ en een gegeven set $\mathcal{S}$ als niet enkel de lus met het nominaal systeem P_0 de eigenschap $\mathcal{P}$ heeft, maar ook alle gesloten lussen waarin P_0 vervangen is door een systeem uit de verzameling $\mathcal{S}$.

Gewoonlijk worden twee soorten robuustheid onderscheiden:

Stabiliteitsrobuustheid garandeert de stabiliteit niet enkel van de gesloten lus met het nominale systeem P_0, maar van alle gesloten lussen met de systemen in de verzameling $\mathcal{S}$ rond P_0. De eigenschap $\mathcal{P}$ is hier stabiliteit.

Performantierobuustheid garandeert een zekere performantie voor alle systemen in de verzameling $\mathcal{S}$. Bijvoorbeeld de H_2 norm van het gesloten lus systeem moet lager zijn dan een bepaalde waarde.

In deze thesis worden enkele algorithmen beschreven voor het analyseren en het ontwerpen van robuuste regelaars. Analyse en ontwerp kunnen we als volgt omschrijven:

ANALYSE: Ga na of een gesloten lus systeem met een gegeven regelaar voldoet aan de specificaties.

SYNTHESE: Ontwerp een regelaar zodat het gesloten lus systeem voldoet aan de gegeven specificaties.

De belangrijkste bijdragen van de thesis voor het analyseren van systemen zijn:

1. Er wordt aangetoond hoe directionele aspecten van twee transfertmatrices relatief ten opzichte van elkaar, bestudeerd kunnen worden. De quotiënt singuliere waarden ontbinding wordt hiervoor gebruikt. We hebben normen gedefinieerd om de relatieve eigenschappen te quantificeren. Er werd ook aangetoond hoe de normen berekend kunnen worden.

2. Er is aangetoond hoe reële parametermarges berekend kunnen worden met een algorithme voor het oplossen van gestructureerde totale kleinste kwadraten problemen. Dit laat toe om deze reële parametermarges te berekenen als er meer dan twee parameters zijn. Bij een kwadratisch convergerend algorithme in de literatuur, is het aantal parameters beperkt tot twee.

De belangrijkste bijdragen van de thesis voor de synthese van robuuste regelaars zijn:

1. Voor het ontwerp van gemengde H_2/H_∞ regelaars, werd aangetoond dat de H_2 en de H_∞ regelaars apart beschouwd kunnen worden. De H_∞ beperking kan eerst apart genomen worden voor het zoeken van de H_∞ regelaar generator. Daarna kan de regelaar berekend worden die de H_2 norm minimizeert.

2. Twee algorithmes voor het oplossen van minimum rang problemen met affiene matrix ongelijkheden werden ontwikkeld. Deze algorithmen kunnen gebruikt worden bij het ontwerp van lage orde regelaars.

In hoofdstuk 1 wordt verder een beknopt overzicht gegeven van de huidige literatuur in verband met robuuste controle. Ook wordt een reële opstelling beschreven waarop de theoretische resultaten van de thesis geïllustreerd worden. Het is een axiale vertilator met debietmeting. Het doel is een regelaar te ontwerpen om het debiet constant te houden ondanks drukverstoringen. Een beschrijving van de opstelling en het ontwerp van de regelaars vindt men in [33].

2. Directionele aspecten van twee transfertmatrices

Het is bekend dat systemen met meerdere ingangen en meerdere uitgangen, eigenschappen hebben die niet enkel afhangen van de frequentie van de ingangen, maar ook van hun 'richting'. Deze aspecten kunnen bestudeerd worden met de singuliere waardenontbinding. In hoofdstuk 2 wordt aangetoond hoe dit uitgebreid kan worden tot directionele aspecten van twee transfertmatrices, relatief ten opzichte van elkaar. Dit kan bijvoorbeeld gebruikt worden voor het bestuderen van signaal-ruis verhoudingen.

De quotiënt singuliere waardenontbinding is een veralgemening van de singuliere waardenontbinding naar een ontbinding van twee matrices. Twee complexe matrices $A \in \mathbb{C}^{l\times m}$ en $B \in \mathbb{C}^{p\times m}$ met eenzelfde aantal kolommen, kunnen gezamelijk gefactoriseerd worden als

$$\begin{aligned} A &= U_a S_a X^{-1}, \\ B &= U_b S_b X^{-1}, \end{aligned}$$

waarbij $U_a \in \mathbb{C}^{l\times l}$ en $U_b \in \mathbb{C}^{p\times p}$ unitaire matrices zijn, $X \in \mathbb{C}^{m\times m}$ een niet-singuliere matrix en $S_a \in \mathbb{R}^{l\times m}$ en $S_b \in \mathbb{R}^{p\times m}$ zijn matrices met de volgende structuur:

$$S_a = \begin{array}{c} \\ r_{a|b}-r_b \\ r_a+r_b-r_{a|b} \\ l-r_a \end{array} \begin{array}{c} \begin{array}{cccc} r_{a|b}-r_b & r_a+r_b-r_{a|b} & r_{a|b}-r_a & m-r_{a|b} \end{array} \\ \begin{pmatrix} I & 0 & 0 & 0 \\ 0 & D_a & 0 & 0 \\ 0 & 0 & 0 & 0 \end{pmatrix} \end{array},$$

$$S_b = \begin{array}{c} \\ p-r_b \\ r_a+r_b-r_{a|b} \\ r_{a|b}-r_a \end{array} \begin{array}{c} \begin{array}{cccc} r_{a|b}-r_b & r_a+r_b-r_{a|b} & r_{a|b}-r_a & m-r_{a|b} \end{array} \\ \begin{pmatrix} 0 & 0 & 0 & 0 \\ 0 & D_b & 0 & 0 \\ 0 & 0 & I & 0 \end{pmatrix} \end{array},$$

waarbij

$$r_a = \text{rang}(A),\ r_b = \text{rang}(B) \text{ en } r_{a|b} = \text{rang}\begin{pmatrix} A \\ B \end{pmatrix}.$$

Eerst wordt aangetoond hoe directionele aspecten grafisch voorgesteld kunnen worden. Voor één transfertmatrix, kunnen deze voorgesteld worden in de ruimte van de uitgangen door de indicator ellipsoides. In de ingangsruimte komt dit overeen met georiënteerde energie.

In het geval van twee transfertmatrices bekijken we signaal-signaal verhoudingen. De signaal-signaal verhouding in de richting x, voor twee matrices wordt gedefinieerd als:

$$R_x[A,B] = \frac{\|Ax\|}{\|Bx\|}.$$

De extreme richtingen en de overkomstige signaal-signaal verhoudingen kunnen berekend worden met behulp van de quotiënt singuliere waardenontbinding.

Hierbij onderscheiden we twee gevallen:

1. Ofwel hebben de systemen dezelfde ingang en verschillende uitgangen:

$$y_1 = G_1 u, \qquad y_2 = G_2 u.$$

2. Ofwel hebben ze verschillende ingangen maar worden de uitgangen opgeteld:

$$y = G_1 u_1 + G_2 u_2.$$

Dit wordt schematisch voorgesteld in figuur 0.1.

Beschouw eerst het geval waarbij de twee transfertmatrices dezelfde ingang u maar verschillende uitgangen hebben. Veronderstel verder dat G_2 een 'goede' transfertmatrix is, terwijl G_1 een verstorende is. Het is duidelijk dat we de relatieve invloed van u op y_1 klein willen houden, ten opzichte van de invloed van u op y_2. Er kan gemakkelijk aangetoond worden dat dit zo is als de quotiënt singuliere waarden over alle frequenties klein zijn.

Voor de tweede situatie waarbij er twee ingangen zijn en de uitgangen worden opgeteld is de interpretatie als volgt: als de signaal-signaal verhouding in een bepaalde uitgangsrichting y groter is dan één, dan betekent dit dat de invloed van u_1 op deze uitgangsrichting groter is dan de invloed van u_2 op deze uitgangsrichting. Dus als u_2 de ingang is van het echte signaal

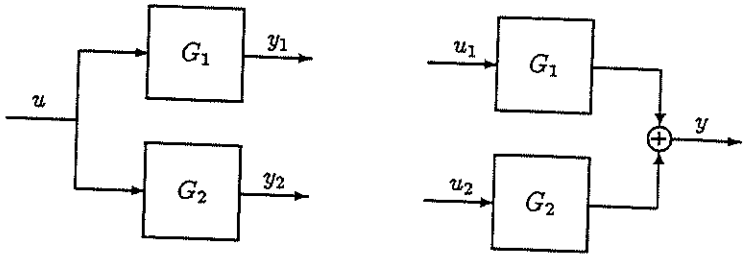

Figure 0.1: Twee configuraties voor de signaal-signaal verhouding van twee transfermatrices.

en u_1 de ruisingang, dan moeten de quotiënt singuliere waarden over alle frequenties zo laag mogelijk zijn.

Voor een grafische voorstelling kan de signaal-signaal verhouding getekend worden voor elke frequentie. Een voorbeeld wordt getoond in figuur 0.2. Op de figuur is duidelijk te zien hoe de signaal-signaal verhouding verandert als functie van de frequentie. De richting en de grootte van de grootste verhouding veranderen voortdurend.

Om de directionele aspecten van twee transfertmatrices te kunnen kwantificeren werden twee nieuwe normen gedefinieerd: de QH_2 en de QH_∞ norm. De QH_2 norm wordt als volgt gedefinieerd:

Definition 1 *De QH_2 norm van een stabiel transfertmatrix paar $(G_1(s), G_2(s))$, met een gelijk aantal ingangen en $G_2(j\omega)$ van volle rang $\forall\omega \in \mathbb{R}$, is*

$$\left\|\frac{G_1}{G_2}\right\|_{Q-2}^2 = \frac{1}{2\pi}\int_{-\infty}^{+\infty} \textit{spoor}\left\{(G_2^*(j\omega)G_2(j\omega))^{-1}(G_1^*(j\omega)G_1(j\omega))\right\}\, d\omega.$$

Het is gemakkelijk aan te tonen dat de QH_2 norm uitgedrukt kan worden in functie van de Q-singuliere waarden:

$$\left\|\frac{G_1}{G_2}\right\|_{Q-2}^2 = \frac{1}{2\pi}\int_{-\infty}^{+\infty} \sum_{i=1}^{r_a}\left(\frac{\alpha_i(j\omega)}{\beta(j\omega)}\right)^2 d\omega,$$

waarbij r_a de generische rang is van $G_1(j\omega)$. Tenslotte wordt er ook nog aangetoond hoe de QH_2 norm berekend kan worden uitgaande van toe-

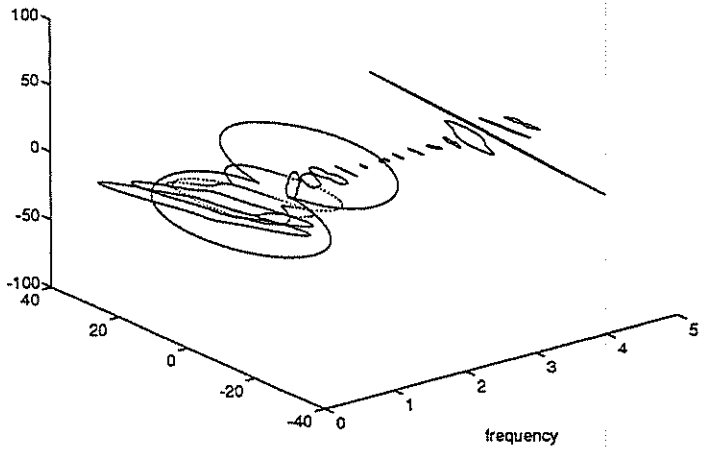

Figure 0.2: Een 3D voorstelling van de signaal-signaal verhouding van twee transfertmatrices.

standsruimtevoorstelling van $G_1(s)$ en $G_2(s)$. Als

$$\begin{pmatrix} G_1 \\ G_2 \end{pmatrix} = \begin{pmatrix} A & B \\ C_1 & 0 \\ C_2 & D_2 \end{pmatrix}$$

de toestandsruimtevoorstelling is van $G_1(s)$ en $G_2(s)$, dan is

$$\left\| \frac{G_1}{G_2} \right\|_{Q-2}^2 = \text{trace}\left\{ C_1 Q C_1^t \right\},$$

waarbij Q de oplossing is van

$$A_x Q + Q A_x^t + B(D_2^t D_2)^{-1} B^t = 0.$$

A_x wordt gedefinieerd als

$$A_x = A - B(D_2^t D_2)^{-1}(D_2^t C_2 + B^t X),$$

met X de oplossing van

$$X\underline{A} + \underline{A}^t X - X\underline{R}X + \underline{Q} = 0,$$

met

$$\begin{aligned} \underline{A} &= A - B(D_2^t D_2)^{-1} D_2^t C_2, \\ \underline{R} &= B(D_2^t D_2)^{-1} B^t, \\ \underline{Q} &= C_2^t C_2 - C_2^t D_2 (D_2^t D_2)^{-1} D_2^t C_2. \end{aligned}$$

De QL_∞ norm wordt gedefinieerd als

Definition 2 *Gegeven twee transfertmatrices $G_1(s)$ en $G_2(s)$ met eenzelfde aantal ingangen. $G_1(s)$ is stabiel en $G_2(s)$ is stabiel en van volle kolomrang over de $j\omega$-as, dan is de QL_∞ norm van de twee transfertmatrices gedefinieerd als*

$$\left\| \frac{G_1}{G_2} \right\|_{Q-\infty} = \sup_{\omega \in \mathbb{R}} \sigma_{q1}(G_1(j\omega), G_2(j\omega)).$$

Hierin stelt σ_{q1} de grootste quotient singuliere waarde van het matrixpaar voor. Voor het berekenen van de QL_∞ norm werd een 'level set' algorithme ontwikkeld. Dit is gebaseerd op het volgende theorema:

Theorem 1 *Beschouw het matrixpaar $G_1(j\omega)$ en $G_2(j\omega)$:*

$$\begin{pmatrix} G_1(j\omega) \\ G_2(j\omega) \end{pmatrix} = \begin{pmatrix} D_1 \\ D_2 \end{pmatrix} + \begin{pmatrix} C_1 \\ C_2 \end{pmatrix} (j\omega I_n - A)^{-1} B.$$

Het paar (α, β) met $\alpha^2 + \beta^2 = 1$ is een quotiënt singuliere waardenpaar van de transfermatrices $G_1(j\omega)$ en $G_2(j\omega)$ op de frequentie ω als $j\omega$ een eigenwaarde is van de matrix M_γ, waarbij

$$\begin{aligned} M_\gamma &= \begin{pmatrix} A^t & 0 & 0 \\ 0 & A^t & 0 \\ 0 & 0 & -A \end{pmatrix} \\ &+ \begin{pmatrix} C_1^t & 0 & 0 \\ 0 & C_2^t & 0 \\ 0 & 0 & -B \end{pmatrix} \begin{pmatrix} -\alpha I & 0 & D_1 \\ 0 & -\beta I & D_2 \\ D_1^t\beta & -D_2^t\alpha & 0 \end{pmatrix}^{-1} \begin{pmatrix} 0 & 0 & -C_1 \\ 0 & 0 & -C_2 \\ -B^t\beta & B^t\alpha & 0 \end{pmatrix}. \end{aligned}$$

De definities zijn gegeven voor twee transfertmatrices die dezelfde ingang hebben. Als de twee transfertmatrices verschillende ingangen hebben en hun uitgangen worden opgeteld, dan zijn de definities gelijkaardig. Het is ook mogelijk om equivalente definities te geven in het discrete tijd domein.

De directionele aspecten van twee transfertmatrices kunnen gebruikt worden om signaal-ruis-verhoudingen te bestuderen. Dit wordt geïllustreerd aan de hand van een stochastisch/deterministisch model van een glasoven. De frequenties en de richtingen van de ingangen waarbij de invloed van de ruis groter is dan die van de controle signalen, kunnen gemakkelijk berekend worden. Eenzelfde analyse werd ook uitgevoerd voor de opstelling met de ventilator.

3. Reële parametermarges

In hoofdstuk 3 beschouwen we systemen met reële parameters. We veronderstellen dat de elementen van de toestandsruimtematrices polynomiaal of rationaal afhankelijk zijn van de parameters a_i:

$$\begin{cases} \dot{x} &= A(a)x + B(a)u \\ y &= C(a)x. \end{cases}$$

De parameters worden samengenomen in een vector a. Voor deze systemen definieerde El Ghaoui twee soorten normen ([44],[45]). Het zijn de maximale normen van de parametervector a die stabiliteit garanderen of die een zekere H_2 performantie garanderen: de q-parameter stabiliteitsmarge en de q-parameter performantiemarge.

De q-parameter stabiliteitsmarge wordt gedefinieerd als

$$q\text{PSM}(A(a)) \triangleq \min_{a\in\mathbb{R}^n} \{\|a\|_q \mid A(a) \text{ is onstabiel}\}.$$

Stel $G(s,a) = C(a)(sI - A(a))^{-1}B(a)$, dan wordt de q-parameter performantiemarge gedefinieerd als

$$q\text{PPM}(G(s,a), J_{ref}) \triangleq \min_{a\in\mathbb{R}^n} \{\|a\|_q \mid \|G(s,a)\|_2 \geq J_{ref}\}.$$

In [44] en [45], werd er aangetoond dat beide uitdrukkingen herschreven kunnen worden als uitdrukkingen in functie van een determinant:

$$\min_{a\in\mathbb{R}^n} \{\|a\|_q \mid det(I + M\Delta) = 0\},$$

waarbij $I + M\Delta = I + a_1M_1 + \ldots + a_nM_n$. In [46] werd er ook een kwadratisch convergerend algorithme voorgesteld om de parametermarges te berekenen als $q = 2$. Dit algorithme kan echter alleen gebruikt worden als er maar twee parameters zijn.

In hoofdstuk 3 stellen we daarom een ander algorithme voor. Het berekenen van de 2-parametermarges kan op dezelfde wijze geformuleerd worden als het oplossen van gestructureerde singuliere waarden problemen ([35]). Het berekenen van de 2-parametermarges kan geformuleerd worden als

$$\min \|a\|_2^2 \quad \text{met beperkingen} \quad \begin{aligned} &M(a)y = 0, \\ &y^ty = 1. \end{aligned}$$

met $M(a) = I + a_1M_1 + \ldots + a_nM_n$. Dit kan opgelost worden met Lagrange vermenigvuldigers. Na enkele substituties en terugsubstituties, bekomen we het volgende niet-lineair-veralgemeend singuliere waarden probleem:

$$\begin{aligned} y &= D_yx\sigma, \\ x &= D_xy\sigma, \end{aligned}$$

met

$$D_x = \sum_{k=1}^{n} (M_k^t x)(M_k^t x)^t,$$
$$D_y = \sum_{k=1}^{n} (M_k y)(M_k y)^t,$$

en $y^t y = 1$, $x^t x = 1$ en $l = x\sigma$. Dit kan opgelost worden met een variant van de 'power'-methode.

Bij deze methode is het aantal parameters niet beperkt. De oplossing wordt recursief berekend. Het is echter niet mogelijk om te garanderen dat het globale minimum altijd bereikt wordt. Het algorithme kan terecht komen in een lokaal minimum. Daarom moet het algorithme een paar keer uitgevoerd worden met verschillende initiële startwaarden.

Het model van de ventilator bevat ook drie parameters. Het beschreven algorithme werd hierop toegepast. De maximale variatie van de parameter vector, die stabiliteit garandeert, is 0.4559. De variatie wordt voornamelijk beperkt door één parameter. Verdere studie toont dat de twee andere parameters veel meer kunnen variëren dan de berekende grenzen.

4. Ontwerp van gemengde H_2/H_∞ regelaars

Hoofdstuk 4 is het eerste hoofdstuk over het ontwerp van regelaars. Bij het ontwerp van H_2/H_∞ regelaars, beschouwen we systemen met drie ingangen en drie uitgangen, zoals voorgesteld in figuur 0.3. Er zijn twee stooringangen w_1 en w_2 en een regelingang u. Er zijn ook twee te regelen uitgangen z_1 en z_2 en een uitgang met metingen voor de regelaar. Het doel is een regelaar te ontwerpen zodat het systeem gestabilizeerd wordt en

$$\min_C \|T_{z_1 w_1}\|_2,$$

$$\text{met beperking} \quad \|T_{z_2 w_2}\|_\infty < \gamma.$$

Om zo een regelaar te ontwerpen stellen we voor om de H_∞ voorwaarde en de H_2 optimizatie te scheiden.

In een eerste stap bekijken we enkel de H_∞ beperking. De ingang w_1 en de uitgang z_1 bekijken we niet. Het is bekend dat, als er een regelaar bestaat die aan de H_∞ voorwaarde voldoet, er niet één maar een verzameling regelaars zijn die er aan voldoen. Die verzameling kan geparametrizeerd

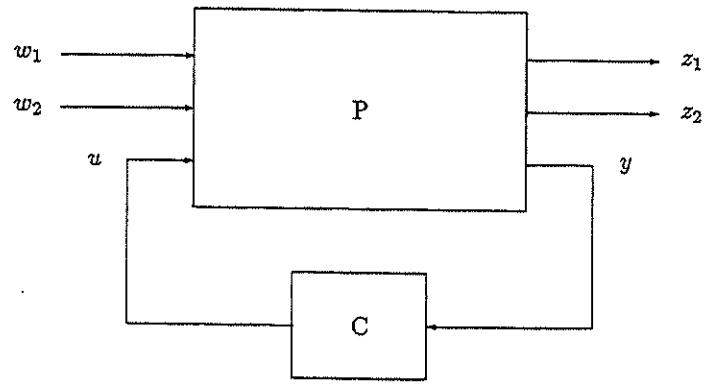

Figure 0.3: De algemene schematische voorstelling voor een gemengd H_2/H_∞ probleem.

worden met een regelaar-generator en een stabiele, H_∞ begrensde transfertfunctie. De H_∞ regelaar-generator K is opnieuw een veralgemeend systeem. De parameter noemen we Q.

In een tweede stap zoeken we in de verzameling van H_∞ regelaars, de regelaar die de H_2 norm minimizeert. Hierbij beschouwen we enkel de ingang w_1 en de uitgang z_1 en bekijken we de ingang w_2 en de uitgang z_2 niet. Om rekening te houden met de H_∞ voorwaarde, hangen we de H_∞ regelaar-generator aan het oorspronkelijke systeem. Het doel is nu om de Q te bepalen zodat de H_2 norm geminimizeerd wordt. Maar Q moet stabiel zijn en begrensd door een H_∞ norm. In de meeste gevallen kan er geen analytische uitdrukking gevonden worden voor de optimale Q, Q_{opt}. Numerieke methoden moeten gebruikt worden.

De resulterende configuratie wordt getoond in figuur 0.4. Als de optimale Q_{opt} gevonden is, dan kan de optimale regelaar berekend worden: $C_{opt} = \mathcal{F}_l(K, Q_{opt})$.

Het zoeken van de optimale Q, komt overeen met H_2 optimizatie met een H_∞ begrensde regelaar. Dit probleem moet meestal numeriek opgelost worden. Hiervoor werden nodige voorwaarden afgeleid.

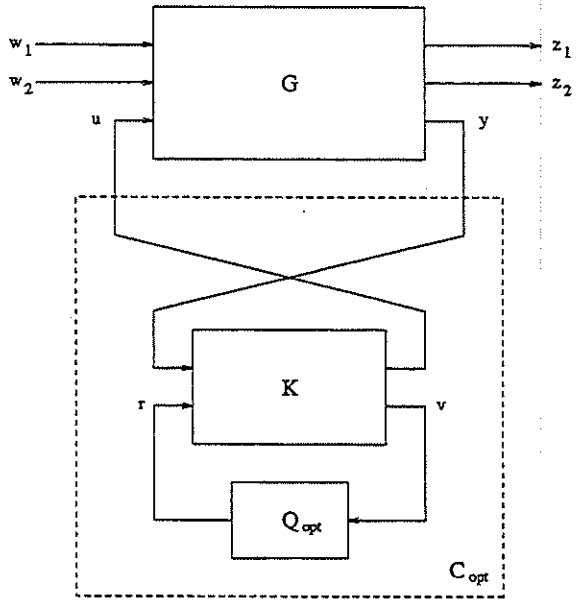

Figure 0.4: De uiteindelijke configuratie voor het gemengde H_2/H_∞ probleem.

Voor de opstelling met de ventilator werden ook een aantal H_2/H_∞ regelaars ontwikkeld. Daarbij werd een additieve onzekerheid verondersteld over het model van de ventilator en de debietmeting. Hierbij blijkt duidelijk dat de H_2 en de H_∞ norm, twee tegenstrijdige beperkingen zijn. Hoe lager de H_∞ norm moet zijn, hoe hoger de laagst mogelijke H_2 norm is. Verder wordt ook getoond dat de minimale H_2 norm lager wordt als de orde van de regelaar verhoogt.

5. Het ontwerp van lage orde regelaars door rang minimizatie met lineaire matrixongelijkheden

Recent werd aangetoond hoe het ontwerp van bepaalde lage orde regelaars met uitgangsterugkoppeling, geformuleerd kan worden als een rang minimizatie van een affiene matrixfunctie met lineaire matrixongelijkheden als beperkingen ([47]). Algemeen kan het probleem als volgt geformuleerd worden:

$$\min_{x\in\mathbb{R}^m} \text{Rang } F(x)$$

$$\text{met beperkingen } \begin{cases} F(x) \geq 0 \\ C(x) \geq 0, \end{cases}$$

waarbij $F(x)$ en $C(x)$ lineaire symmetrische matrixfuncties zijn:

$$F(x) = F_0 + x_1F_1 + x_2F_2 + \ldots + x_mF_m,$$

$$C(x) = C_0 + x_1C_1 + x_2C_2 + \ldots + x_mC_m,$$

met $F_i = F_i^t \in \mathbb{R}^{n_f \times n_f}$ en $C_i = C_i^t \in \mathbb{R}^{n_c \times n_c}$, $i = 0 \ldots m$. Deze problemen komen niet enkel voor bij het ontwerp van lage orde regelaars, maar ook bijvoorbeeld in identificatie. Het Frisch schema is hier een goed voorbeeld van.

In dit hoofdstuk stellen we twee algorithmen voor om deze problemen op te lossen. Beide algorithmen zijn gebaseerd op concepten uit de convexe optimizatie met lineaire matrixongelijkheden. Het probleem met de rang minimizatie is echter niet convex. In dit hoofdstuk wordt ook aangetoond dat het probleem 'NP-hard' is. Daarom zoeken we niet naar een algorithme dat altijd een optimum garandeert. In de praktijk geven de algorithmen meestal een lage orde oplossing binnen een redelijke termijn.

De algorithmen zijn op het volgende gebaseerd. De vectoren x waarvoor $F(x) \geq 0$ vormen een convexe verzameling. De rand van de verzameling

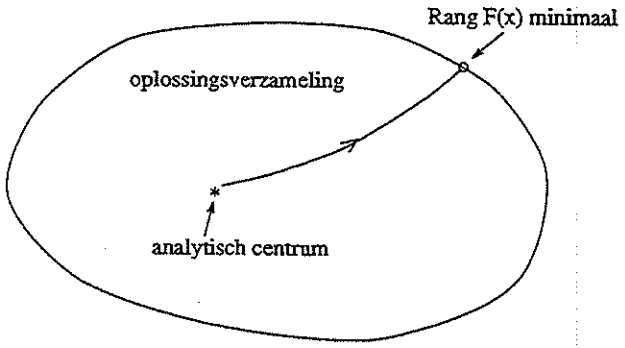

Figure 0.5: Om de minimum rang oplossingen te vinden gaan we van in de convexe verzameling naar de rand die gevormd wordt uit de punten x waarvoor $F(x) \succeq 0$.

wordt gevormd door de vectoren x waarvoor $F(x) \succeq 0$ en singulier is. De algorithmen volgen een pad dat start in de verzameling en naar de rand loopt. Bij voorkeur eindigt het pad in een punt op de rand waar de rang minimaal is. Dit wordt voorgesteld in figuur 0.5.

Het eerste algorithme is gebaseerd op een inversie van de analytisch centrum methode voor convexe optimizatie. De zoekrichting v wordt berekend uit het volgende kleinste kwadratenstelsel:

$$\underset{v}{\text{argmin}} \left\| \begin{pmatrix} I_f & 0 \\ 0 & I_c \end{pmatrix} - \sum_i v_i \begin{pmatrix} Z_F & 0 \\ 0 & Z_C \end{pmatrix} \begin{pmatrix} F_i & 0 \\ 0 & -C_i \end{pmatrix} \begin{pmatrix} Z_F & 0 \\ 0 & Z_C \end{pmatrix} \right\|_F^2.$$

waarbij $Z_F = F(x)^{-1/2}$ en $Z_C = C(x)^{-1/2}$. We nemen echter niet deze stap maar de tegengestelde om een nieuw punt x te vinden. Opdat het volgend punt x ook tot de verzameling zou behoren, wordt de stap geschaald met een factor $\frac{1}{1+\delta(x)}$. $\delta(x)$ wordt berekend als

$$\delta(x)^2 = \left\| \sum_i v_i \begin{pmatrix} Z_F & 0 \\ 0 & Z_C \end{pmatrix} \begin{pmatrix} F_i & 0 \\ 0 & -C_i \end{pmatrix} \begin{pmatrix} Z_F & 0 \\ 0 & Z_C \end{pmatrix} \right\|_F^2,$$

waarbij v de optimale oplossing is uit het kleinste kwadratenstelsel. Bij de rand wordt het aantal eigenwaarden dat naar nul convergeert aangegeven

door

$$\delta_f(x)^2 = \left\| \sum_i v_i Z_F F_i Z_F \right\|_F^2.$$

Om de invloed van de beperkingen $C(x) \succeq 0$ te verminderen worden ze slechts toegevoegd als ze niet meer voldaan zijn. Verder wordt er nog een factor r ingevoerd om hun invloed nog verder te beperken.

Een tweede algorithme is een uitbreiding van de potentiaal reductie methode voor convexe optimizatie naar de minimum rang problemen. Hierbij moet de volgende objectfunctie geminimizeerd worden:

$$\varphi(x) = q \log\det F(x) - \log\det \begin{pmatrix} C(x) & 0 \\ 0 & F(x) \end{pmatrix}.$$

De parameter q weegt de rang minimizatie ten opzichte van de beperkingen $C(x) \succeq 0$ en $F(x) \succeq 0$. Door de eerste term te linearizeren kan de theorie van Nesterov en Nemirovsky opnieuw toegepast worden ([80]). De gelinearizeerde functie in x_k is:

$$\psi(x) = q g_F^t(x_k) x - \log\det \begin{pmatrix} C(x) & 0 \\ 0 & F(x) \end{pmatrix} + c.$$

met

$$g_F^t = \begin{pmatrix} g_1 & g_2 & \cdots & g_m \end{pmatrix} \quad \text{en} \quad g_i = \text{spoor } F(x_k)^{-1} F_i.$$

Omdat de eerste term van $\varphi(x)$ concaaf is, weten we dat $\varphi(x) \leq \psi(x)$. Dus als de gelinearizeerde functie geminimizeerd wordt, dan is de overeenkomstige waarde van echte objectfunctie lager. Als zoekrichting wordt de Newton richting van $\psi(x)$ berekend:

$$-H^{-1}g = \underset{v \in \mathbb{R}^m}{\text{argmin}} \left\| I_c - \sum_{i=1}^m v_i Z_c^{-1} C_i Z_c^{-t} \right\|_F^2 + \left\| I_f (1-q) - \sum_{i=1}^m v_i Z_f^{-1} F_i Z_f^{-t} \right\|_F^2.$$

Opdat de nieuwe x zou voldoen aan de voorwaarden wordt de Newton stap geschaald met de demping factor $\frac{1}{1+\delta(x)}$, met

$$\delta(x) = \left(\left\| \sum_{i=1}^m v_i Z_c^{-1} C_i Z_c^{-t} \right\|_F^2 + \left\| \sum_{i=1}^m v_i Z_f^{-1} F_i Z_f^{-t} \right\|_F^2 \right)^{\frac{1}{2}}.$$

Het aantal naar nul convergerende eigenwaarden kan opnieuw geschat worden. Het wordt aangegeven door

$$\delta_F(x_k)^2 = \left(\frac{\| \sum_{i=1}^{m} Z_F^{-1} F_i Z_F^{-t} \|_F}{q-1} \right)^2 .$$

Dit laat toe om een stopcriterium te definiëren. We beschouwen een eigenwaarde nul als ze kleiner is dan een bepaalde waarde. Het algorithme stopt als het aantal eigenwaarden dat kleiner is dan de drempel gelijk is aan $\delta_F(x_k)^2$.

Voor de potentiaal reductiemethode werd ook een ondergrens voor de parameter q afgeleid. Er werd ook aangetoond dat de eigenwaarden lineair convergeren dicht bij de rand.

Experimenten tonen aan dat de potentiaalreductiemethode veel vlugger werkt dan de methode gebaseerd op de inversie van de analytisch centrum methode.

Een voorbeeld wordt getoond in figuur 0.6. De paden gevolgd door het potentiaal reductie algorithme zijn getekend, vertrekkend van 40 punten rond het analytisch centrum. De randen van het domein waarvoor $F(x) \geq 0$ zijn aangegeven door volle lijnen. Alle paden lopen naar de hoekpunten waar de rang van $F(x)$ minimaal met twee zakt (Op de randen zakt de rang van $F(x)$ maar met één.) Jammer genoeg lopen niet alle paden naar het hoekpunt linksonder waar de rang van $F(x)$ met vijf zakt.

In de thesis worden verschillende regelaars ontworpen met deze methode. Voor de opstelling met de ventilator werd een lage order H_2 en een lage order H_∞ regelaar berekend. Beide regelaars waren echter slechts één order lager dan de orde van het oorspronkelijke model.

6. Besluit

De voornaamste resultaten van de thesis kunnen we als volgt samenvatten. Er is aangetoond hoe directionele aspecten van twee transfermatrices relatief ten opzichte van elkaar bestudeerd kunnen worden. Hiervoor werden ook nieuwe normen gedefinieerd. Voor systemen met reële parameters werd aangetoond hoe de 2-parameter marges berekend kunnen worden met een algorithme gelijkaardig aan dat voor het oplossen van gestructureerde totale kleinste kwadraten problemen. Gemengde H_2/H_∞ regelaars kunnen ontworpen worden door het H_2 en de H_∞ probleem te scheiden. Ten slotte werden

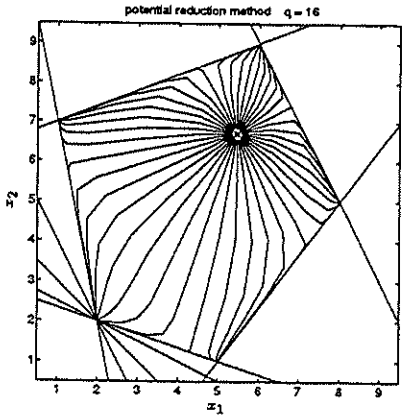

Figure 0.6: Een voorbeeld van de optimizatiepaden gevolgd door de potentiaal reductie methode.

twee algorithmen voorgesteld voor het oplossen van minimum rang problemen met lineaire matrix ongelijkheden. Deze algorithmen kunnen gebruikt worden bij het ontwerp van lage orde regelaars.

List of Symbols

$\mathbb{R}$	The field of real number.
$\mathbb{R}^{p\times q}$	The field of real matrices with p rows and q columns.
$\mathbb{C}$	The field of complex number.
$\mathbb{C}^{p\times q}$	The field of complex matrices with p rows and q columns.
$\mathbb{N}$	The set of integers.
j	The imaginary unit is denoted by $j = \sqrt{-1}$.
A^t	The transpose of the matrix A.
A^*	The complex conjugate transpose of the matrix A.
$A > 0$	A is a positive definite matrix.
$A \geq 0$	A is a positive semi-definite matrix.
$A > B$	$A - B$ is a positive definite matrix.
$A \geq B$	$A - B$ is a positive semi-definite matrix.
$p > q$	$p, q \in \mathbb{R}^n$, then $p_i > q_i$, $i = 1 \ldots n$
$\mathrm{diag}(a, b, \ldots, z)$	$\begin{pmatrix} a & & 0 \\ & b & \\ & & \ddots \\ 0 & & z \end{pmatrix}$, a diagonal matrix.
$\lambda_i(A)$	The ith eigenvalue of the square matrix A.
$\sigma_i(A)$	The ith singular value of the matrix A: $\sigma_i(A) = \lambda_i(A^tA)^{1/2}$.

$\lambda_{\max}(A)$	The largest eigenvalue of the matrix A.
$\overline{\sigma}(A)$	The largest singular value of the matrix A.
$\mu_{\Delta}(A)$	The structured singular value μ, defined on page 10.
$\sigma_{qi}(A,B)$	The ith quotient singular value of the matrix pair (A,B).
$\|A\|$	The induced 2-norm of the matrix A.
$\left(\begin{array}{c\|c} A & B \\ \hline C & D \end{array}\right)$	$= D + C(sI - A)^{-1}B$. A transfer function in terms of state-space data.
$\left(\begin{array}{c\|cc} A & B_1 & B_2 \\ \hline C_1 & D_{11} & D_{12} \\ C_2 & D_{21} & D_{22} \end{array}\right)$	$= \begin{pmatrix} P_{11}(s) & P_{12}(s) \\ P_{21}(s) & P_{22}(s) \end{pmatrix}$ A state-space realization of a generalized plant: $P_{ij}(s) = D_{ij} + C_i(sI - A)^{-1}B_j$.
$\mathcal{F}(P(s),C(s))$	Lower fractional transformation: Given $P(s) = \begin{pmatrix} P_{11}(s) & P_{12}(s) \\ P_{21}(s) & P_{22}(s) \end{pmatrix}$ and $C(s)$ $\mathcal{F}(P(s),C(s)) = P_{11}(s) + P_{12}(s)C(s)\left(I - P_{22}(s)C(s)\right)^{-1}P_{21}(s)$.
$\|G(s)\|_2$	The H_2 norm of a stable transfer function $G(s)$.
$\|G(s)\|_{\infty}$	The H_{∞} norm of a stable transfer function $G(s)$.
$\|G(s)\|_{\Delta}$	The structured singular value norm of a transfer function $G(s)$ with respect to the structured perturbation Δ.

Acronyms

SISO	single-input single-output.
MIMO	multi-input multi-output.
LQG	linear quadratic gaussian.
LTR	loop transfer recovery.
SVD	singular value decomposition.
QSVD	quotient singular value decomposition.
SSR	signal-to-signal ratio.
PSM	parameter stability margin.
PPM	parameter performance margin.
STLS	structured total least squares.
LMI	linear matrix inequality.
NLDI	norm-bound linear differential inclusion.

Chapter 1

Introduction and Outline of the Thesis

Modern control is model based. A mathematical model of the system to be controlled is needed, to design a controller. How to obtain suitable mathematical models has been studied a long time already. We refer to e.g. [73] and [89] for further references.

However, mathematical models are never an exact description of the real system. Most models are linear and time invariant, while real systems are usually non-linear and time-varying. Time variations are due to e.g. aging of the components or because of linearization of non-linear systems. This can change the dynamics of the system. Even if an exact model is known, it is often too complicated. The design of a controller is then often based on a simpler approximate model.

The design of controllers is based on the model and not on the real system. However, if a controller is designed that stabilizes the model, this does not imply that the controller will stabilize the real system. The closed loop of the real plant with the controller can become unstable due to the unmodelled dynamics. Or due to the non-linear or time-varying characteristics, the dynamics of the plant can vary so much that the closed loop also becomes unstable. It is thus necessary to design a controller that not only stabilizes the model, but all the plants in a given set around the model. Such a controller is called robust.

Sometimes a controller has to be designed, that not only guarantees stability of the closed loop but also a certain performance, e.g. the H_2 norm of the closed loop has to be smaller than a given value α. Not only the H_2

norm of the closed loop with the model has to be smaller than α but also the H_2 norm of the loops with a plant close to the model. This is called robust performance.

1.1 Analysis and Design of Robust Controllers

Two main problems can be distinguished:

ANALYSIS: Verify if the closed loop system with a given controller, satisfies the robustness specifications.

SYNTHESIS: The direct design of a controller such that the closed loop satisfies the given robustness specifications.

To analyze control systems the main contributions of the thesis are:

1. It is shown how the directional aspects of transfer matrices can be extended to study the directional aspects of two transfer matrices relative to one another. The quotient singular value decomposition has to be used. Norms are defined to quantify the relative properties. It is explained how the norms can be computed.

2. It is shown how an algorithm to solve structured total least squares problems can be used to compute real parameter margins when there are more than two parameters.

The main contributions for the synthesis of a controller are:

1. It is shown how a general mixed H_2/H_∞ controller can be designed, by considering the H_2 and the H_∞ constraints separately.

2. Two algorithms are developed to solve minimum rank problems involving linear matrix inequalities. These algorithms can be used to design reduced order robust controllers.

In the next section a brief overview is given of some topics that have appeared in the literature on robustness of linear systems. Due to the large number of researchers and the huge amount of articles and books that have been published in this field recently, this overview is not intended to be complete. However, we hope the reader will be able to situate better the contributions of this thesis. After the short survey, a chapter by chapter

overview of the thesis is given. The contributions of the thesis will be illustrated on a practical example that returns in each chapter: The control of the air flow rate through an axial fan. As this example will be used in each of the chapters, the setup is described in the last section of this chapter.

1.2 What is Robustness?

Robustness of control systems has always been a major concern for control engineers. A mathematical model is never a perfect description of the real system. Furthermore, most systems are more or less time varying. It is thus important to design a controller not only for the nominal plant model but for a whole class of models around it. In this section we try to give a short overview of the area of robust control. As this is a very large domain of research, we do not claim to be complete.
Robustness can be defined as follows:

> Given a set $\mathcal{S}$ around a nominal plant P_0 and a property $\mathcal{P}$. A control system is called robust with respect to a property $\mathcal{P}$ and to a given set $\mathcal{S}$ if not only the loop with the nominal plant P_0 possesses this property $\mathcal{P}$, but also the loops with the nominal plant replaced by one of a given set $\mathcal{S}$, possess the property $\mathcal{P}$.

Usually two kinds of robustness are distinguished: *robust stability* and *robust performance*:

Robust stability guarantees stability not only of the closed loop with the nominal plant P_0 but for the closed loop with all the plants in a set $\mathcal{S}$ around the nominal plant. Usually robust stability is the most important property of the closed loop system. Obviously, a closed loop control system that is not stable is useless. However, not only the closed loop with the nominal plant and the designed controller has to be stable, but also the closed loop with the plants in $\mathcal{S}$.

Robust performance guarantees a certain performance for all the plants in a given set $\mathcal{S}$, e.g. the H_2 norm of the closed loop has to be smaller than a given value for all the plants of the given set. Robust performance is opposed to nominal performance where only the performance of the controller with respect to the nominal model P_0 is important.

In the remaining part of this section a short overview of robust control is given. First we show how the uncertainty can be modeled. Then some

robustness measures are introduced to analyze the robustness of the systems. Finally some robust design methodologies are described briefly.

1.2.1 Descriptions of the Perturbation

In this section the main disturbance descriptions are mentioned. The model of the plant obtained from identification is called the *nominal model* P_0. The real plant is denoted by P. The difference Δ between the nominal plant P_0 and the real plant P can be described as e.g.

1. an additive perturbation.
2. a multiplicative perturbation.
3. an upper or lower fractional transformation.
4. perturbations on the coprime factors.

- **Additive perturbations.** A perturbation Δ_a is an additive perturbation if $P = P_0 + \Delta_a$.

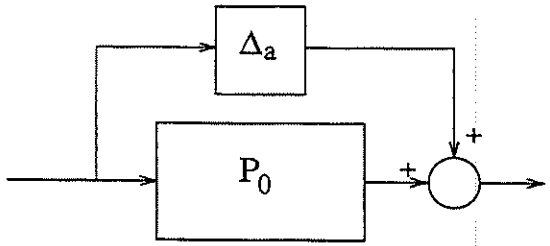

- **Multiplicative perturbations.** A perturbation Δ_m is a multiplicative perturbation if $P = P_0(I + \Delta_m)$.

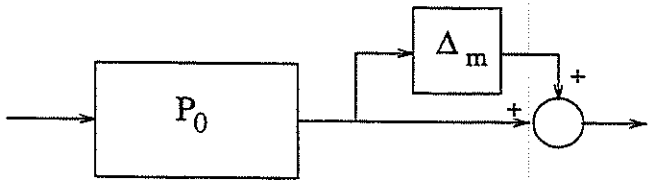

- **Upper or lower fractional transformation.** We illustrate the description as an upper fractional transformation. The nominal model P_0 is divided into four blocks:

$$\begin{pmatrix} d \\ y \end{pmatrix} = P_0 \begin{pmatrix} e \\ u \end{pmatrix} = \begin{pmatrix} P_{11} & P_{12} \\ P_{21} & P_{22} \end{pmatrix} \begin{pmatrix} e \\ u \end{pmatrix}$$

and the perturbation Δ operates between the outputs d and the inputs e: $e = \Delta d$. The actual plant P is then described by: $P = \mathcal{F}_u(P_0, \Delta) = P_{21}\Delta(I - P_{11}\Delta)^{-1}P_{12} + P_{22}$.

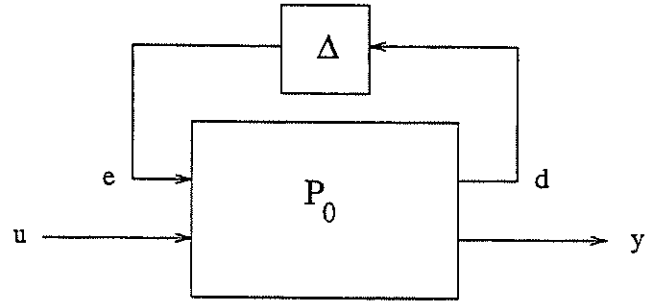

This is the most general form to describe perturbations.

- **Perturbations on the coprime factors.** ([77]) The nominal plant P_0 can be factorized in coprime factors: $P_0 = M^{-1}N$. The perturbations can be described as additive perturbation on the coprime factors: $P = (M + \Delta_m)^{-1}(N + \Delta_n)$.

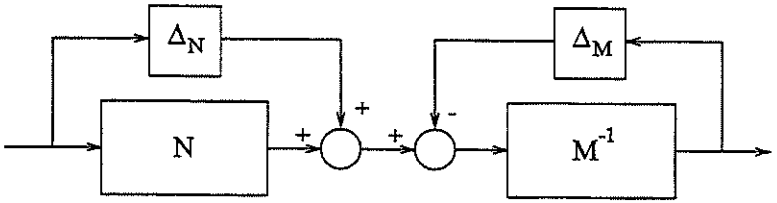

Other descriptions of the perturbations also exist. However the above descriptions are used most.

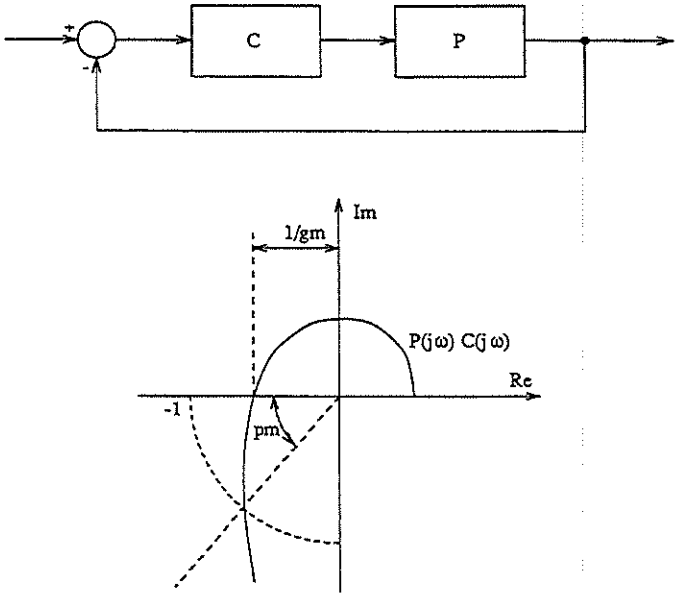

Figure 1.1: The upper figure is a classical one degree-of-freedom feedback system with a plant P and a controller C. The gain and phase margin can easily be read from the Nyquist plot of a SISO system, shown in the lower plot.

1.2.2 Robustness Analysis

Robust stability has always been a major concern in the design of controllers. The gain and phase margins in classical control are nice illustrations ([81]). These measures give the maximal gain variations and the maximal phase shift that can be allowed in the open loop gain PC without destabilizing the closed loop, where P is the transfer function of the controlled plant and C of the controller (see figure 1.1). They can easily be visualized on e.g. a Nyquist plot as shown in figure 1.1. The gain and phase margin are defined for single-input single-output (SISO) systems. There are extensions to multi-input multi-output (MIMO) systems. However, they are not easy to compute and not so often used ([4]).

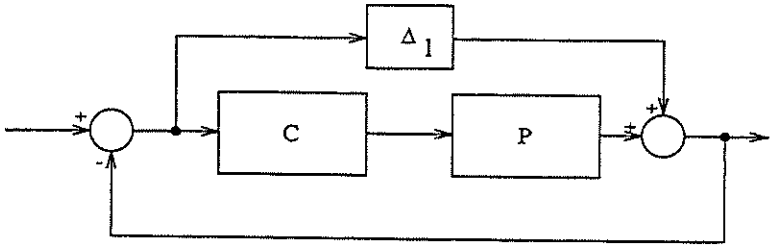

Figure 1.2: The M-circle is the largest H_∞ norm of an additive perturbation of the open loop that ensures stability of the closed loop.

The gain and phase margins are difficult to extend to MIMO systems. Therefore a new measure has been introduced that combines more or less the gain and phase margin and that can also be used for MIMO systems. This new measure is called the M-circle ([5]). Its definition is based on the H_∞ norm. The H_∞ norm of a stable linear time invariant transfer function $F(s)$ is defined as:

$$\|F(s)\|_\infty \triangleq \sup\{\overline{\sigma}(F(s)) : \text{Re } s > 0\},$$

where $\overline{\sigma}(.)$ denotes the largest singular value of the matrix. By the maximum modulus theorem, the open right half plane can be replaced by the imaginary axis:

$$\|F(s)\|_\infty = \sup\{\overline{\sigma}(F(j\omega)) : \omega \in \mathbb{R}\}.$$

Consider now the closed loop shown in figure 1.2, with plant P and controller C. The M-circle is defined as

$$M = \frac{1}{\|(I+PC)^{-1}\|_\infty}.$$

For SISO systems, the M-circle has an interpretation in the Nyquist plane. It is the inverse of the radius of the largest circle around $(-1, 0)$ that does not cross the loop gain PC. This is shown in figure 1.3. It is clear that the M-circle combines in a certain sense the gain and phase margin.

The M-circle is the largest possible H_∞ norm of an additive uncertainty, Δ_l, allowed on the loop gain PC, such that the closed loop is guaranteed

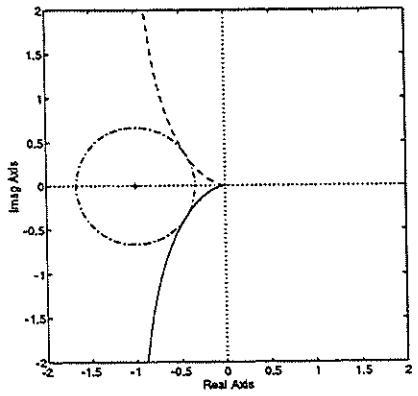

Figure 1.3: For SISO systems the M-radius can easily be plotted on the Nyquist plot. The M-radius is the radius of the largest circle around $(-1, 0)$ that does not cross the Nyquist plot.

to be stable. Another measure of robustness is the D-circle. Consider the configuration shown in figure 1.4. The D-circle is defined as ([5])

$$D = \frac{1}{\|C(I+PC)^{-1}\|_\infty}.$$

The D-circle is the largest additive uncertainty Δ_a, of the plant P, that can be allowed without destabilizing the closed loop. These two measures are conservative. When the H_∞ norm of the uncertainty is larger than the M or D-circle, this does not imply that the closed loop will be unstable. On the other hand there exist disturbances, with H_∞ norm equal to the M or D-circle that destabilize the closed loop. However, it is not sure that these disturbances will or can occur in practice. From their definitions it is clear that the use of the M and the D-circle is not restricted to SISO plants. They can also be used in the case of MIMO plants.

The previous measures are called unstructured. All the uncertainties are localized in one large block. It is assumed that all the uncertainties influence each other. Even if a specific structure of the disturbance is known, it is not taken into account. Uncertainties that cannot occur in reality are also considered. Therefore these unstructured measures are often conservative.

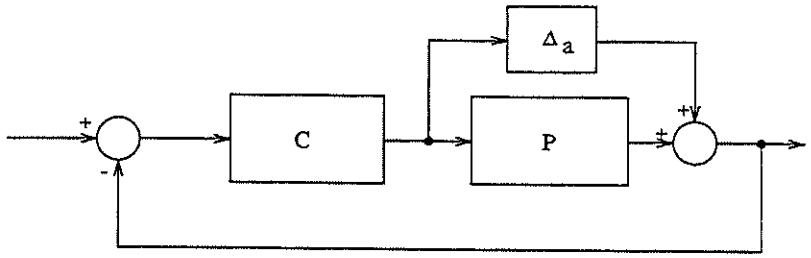

Figure 1.4: The D-circle is the largest H_∞ norm of an additive perturbation of the plant, that ensures stability of the closed loop.

To analyze structured disturbances, the μ theory is developed.

In the μ theory the disturbances are described in one block diagonal matrix. The specific form of this disturbance matrix is taken into account to compute the robustness. Consider matrices $M \in \mathbb{C}^{n\times n}$ and an underlying block structure Δ. Δ belongs to the following set:

$$\begin{aligned}\Delta \;=\; \{\Delta = \mathrm{diag}(\delta_1 I_{r_1}, \ldots, \delta_S I_{r_S}, \Delta_1, \ldots, \Delta_F) | \delta_i \in \mathbb{C}, \Delta_j \in \mathbb{C}^{m_j \times m_j},\\ \sum_{i=1}^{S} r_i + \sum_{j=1}^{F} m_j = n\}.\end{aligned}$$

There are two types of blocks: Repeated scalar blocks S and full blocks F. The sizes of the different blocks are given by r_i for the repeated blocks and by m_j for the full blocks.

The structured singular value μ of M with respect to the block structure of Δ is defined as ([38],[42]):

$$\mu_\Delta(M) \triangleq \frac{1}{\min\{\overline{\sigma}(\Delta) : \Delta \in \mathbf{\Delta}, \det(I - M\Delta) = 0\}}$$

unless no $\Delta \in \mathbf{\Delta}$ makes $(I - M\Delta)$ singular, in which case $\mu_\Delta(M) = 0$. The following theorem shows how the structured singular value can be used for robust stability. Consider a stable linear time invariant transfer matrix $G(s)$ and a structured uncertainty $\Delta(s)$. Let $\mathcal{M}_S$ denote the set of real-rational, proper, stable, transfer matrices. Associated with any block structure Δ, let

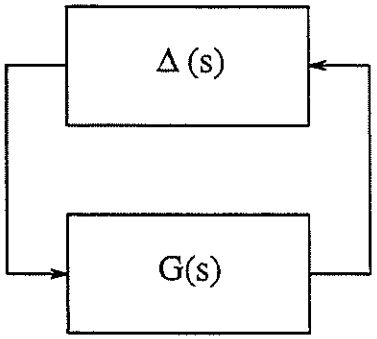

Figure 1.5: This loop is stable if and only if $\|G\|_\Delta = \sup_{\omega\in\mathbb{R}} \mu_\Delta(G(j\omega)) \leq \beta$.

$\mathcal{M}(\Delta)$ denote the set of all block diagonal, stable rational transfer functions, with a block structure like Δ:

$$\mathcal{M}(\Delta) = \{\Delta(.) \in \mathcal{M}_S : \Delta(s_0) \in \Delta \text{ for all } s_0 \in \overline{\mathbb{C}}_+\}.$$

The following theorem can be proved ([2]):

Theorem 2 *Let $\beta > 0$. The loop shown in figure 1.5 is well-posed and internally stable for all $\Delta(.) \in \mathcal{M}(\Delta)$ with $\|\Delta\| < \frac{1}{\beta}$ if and only if*

$$\|G\|_\Delta \triangleq \sup_{\omega\in\mathbb{R}} \mu_\Delta(G(j\omega)) \leq \beta.$$

The μ singular value has to be computed at each frequency. In practice it is computed at some discrete frequencies ω only. This is called a frequency sweep.

As an example consider the configuration in figure 1.6. There is a plant P with an additive uncertainty Δ_P and a sensor S with a multiplicative uncertainty Δ_S. The H_∞ norms of Δ_P and Δ_S are known. By introducing appropriate weighting functions W_P and W_S, the H_∞ norms of Δ_P and Δ_S can always be scaled to 1. The configuration can be redrawn in the form of figure 1.5 by extracting the two uncertainty blocks, as shown in figure 1.7 (C is fixed for analysis). It is now obvious to identify $G(s)$ as the transfer function from d to e and the uncertainty $\Delta(s)$ as

$$\Delta(s) = \begin{pmatrix} \Delta_P(s) & 0 \\ 0 & \Delta_S(s) \end{pmatrix}.$$

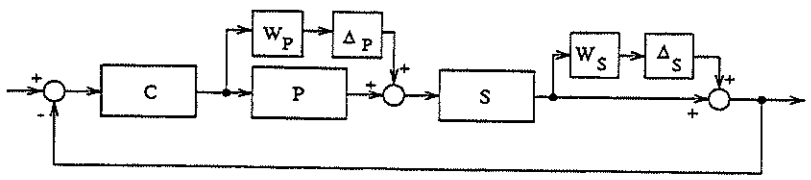

Figure 1.6: A configuration with two uncertainty blocks.

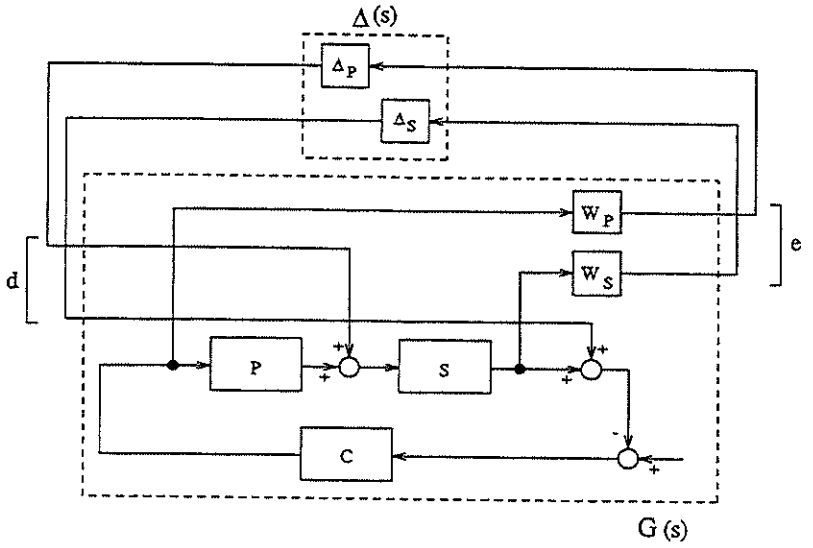

Figure 1.7: The redrawn configuration with two uncertainties.

This closed loop system will be stable with respect to Δ_P and Δ_S if

$$\mu_{\Delta}(G(s)) < 1.$$

However, the computation of the μ singular value is hard. In the general case only upper and lower bounds are computed.

The definition of the structured singular value μ, still assumes that all the disturbances are complex. The problem becomes even harder if some disturbances are real parametric. This is the case when a model is known but real parameters can vary. These problems can be solved in the framework of the real μ theory ([88]). The real structured singular value is however not a continuous function of frequency, even for linear time invariant systems ([3],[70]). There is a real risk that discontinuities are missed in a frequency sweep. This can result in erroneous bounds because not all the frequencies can be tested. Still this problem is studied because it is less conservative than the complex μ problem for systems with real parameter uncertainties.

Another approach can be found in [44] and [96]. In these papers it is proposed to check the maximal real parameter variations without performing a frequency sweep. All the real parameters are put into one vector. The maximal norm of the vector is computed that ensures stability or a certain H_2 performance. When the l_2 norm is used for the parameter vector, these norms are called the l_2 parameter stability margin and the l_2 parameter performance margin, respectively. When the l_∞ norm is used for the parameter vector, these norms are called l_∞ parameter margins. A more complete description is given in Chapter 3. In that chapter, an algorithm is presented to compute the l_2 parameter margins when there are more than two parameters.

Other researchers have been working on the stability of systems when the coefficients of the denominator polynomial of the transfer function, can vary between certain bounds. These are the Kharitonov and related theories ([61],[69]). The design of robust controllers in this way is often very conservative. An example is shown in [62].

Finally we also want to discuss another aspect of MIMO systems that is not directly related to robustness. It is well known that the output of a MIMO system is not only dependent on the frequency but also on the direction of the input. These properties are called directional aspects. In this thesis we show how this can be extended to study the directional aspects of two transfer matrices relative to one another. Therefore a generalization of the singular value decomposition, the quotient singular value decomposition is used. This is shown in Chapter 2.

1.2.3 Robust Synthesis

H_∞ Control

A major area in robust control design is H_∞ control. The goal in H_∞ control design is to minimize the H_∞ norm of a transfer function. The robustness of the H_∞ control is based on the small gain theorem ([43]). Consider the configuration shown in figure 1.8. The closed loop will be stable if

$$\overline{\sigma}(G(j\omega)\Delta(j\omega)) < 1 \qquad \forall \omega \in \mathbb{R}.$$

It is easily derived that

$$\begin{aligned} \overline{\sigma}(G(j\omega)\Delta(j\omega)) &\leq \|G(s)\Delta(s)\|_\infty \\ &\leq \|G(s)\|_\infty \|\Delta(s)\|_\infty. \end{aligned}$$

The last step is called the submultiplicative property of the ∞ norm. Suppose an upper bound on the H_∞ norm of $\Delta(s)$ is known:

$$\|\Delta(s)\|_\infty < \gamma.$$

Then it follows immediately, that stability of the closed loop is guaranteed if

$$\|G(s)\|_\infty < \frac{1}{\gamma}.$$

This formulation is, however, conservative. If

$$\|\Delta(s)\|_\infty > \frac{1}{\|G(s)\|_\infty}$$

this does not imply that the closed loop system will be unstable. However, there exists at least one Δ, with $\|\Delta\|_\infty = \gamma$ that will make the closed loop unstable.

In figure 1.9 the general setup for solving the H_∞ control problem is shown. The problem is first transformed into a so-called standard plant configuration. The standard plant setup has two sets of inputs and two sets of outputs:

- The *actuator signal vector*, denoted by u, consists of the inputs to the model that can be *manipulated* by the controller.
- The *exogenous input vector*, denoted by w, consists of all other input signals to the model.

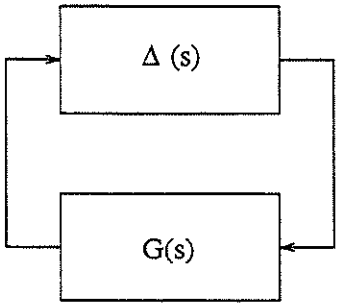

Figure 1.8: The setup for the small gain theorem.

Similarly, the output of the model consists of two vector signals:

- The *sensor signal vector*, denoted by y, consists of output signals that are accessible to the controller.
- The *regulated outputs signal vector*, denoted by z, consists of every signal from the model, which is of interest to the designer.

The dynamic behaviour of the plant is described by the following transfer matrix:

$$\begin{pmatrix} z \\ y \end{pmatrix} = P(s) \begin{pmatrix} w \\ u \end{pmatrix} = \begin{pmatrix} P_{11}(s) & P_{12}(s) \\ P_{21}(s) & P_{22}(s) \end{pmatrix} \begin{pmatrix} w \\ u \end{pmatrix}.$$

The goal in H_∞ controller design is to find a stabilizing controller $C(s)$, $u = C(s)y$, such that the H_∞ norm of the transfer function from w to z T_{zw}, is minimized:

$$\min_{C \text{ stabilizing controller}} \|T_{zw}\|_\infty$$

or

$$\min_{C \text{ stabilizing controller}} \|P_{11} + P_{12}C(I - P_{22}C)^{-1}P_{21}\|_\infty.$$

This is called the *standard problem* in H_∞ ([49]).
To illustrate how a problem can be converted into the standard form, consider the setup shown in figure 1.10. In figure 1.11 the setup is redrawn in the standard plant configuration. The goal is to minimize the sensitivity

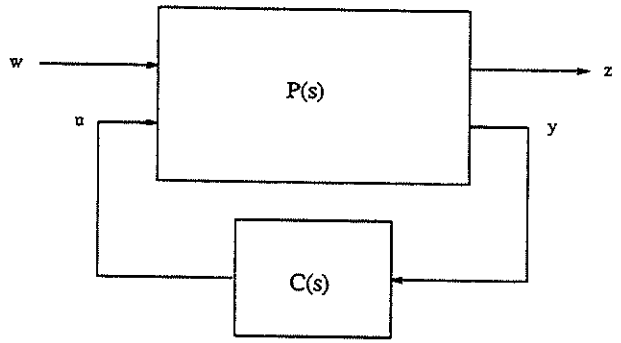

Figure 1.9: The standard plant configuration.

of the closed loop, while at the same time a certain robustness has to be guaranteed with respect to a multiplicative perturbation Δ. To minimize the sensitivity, the norm of the transfer function from r to e_1 has to be minimized. To guarantee robustness the largest singular value of the transfer function from d_2 to e_2 has to be smaller than the largest singular value of the disturbance at each frequency. The transfer function from d_2 to e_2 is equivalent to the transfer function from r to e_2. Thus the robustness specification can be expressed as:

$$\overline{\sigma}(T_{e_2r}(j\omega)) < \overline{\sigma}(\Delta(j\omega)), \qquad \forall\omega \in \mathbb{R}.$$

If for the disturbance we have

$$\overline{\sigma}(\Delta(j\omega)) < |W_3(j\omega)^{-1}|, \qquad \forall\omega \in \mathbb{R},$$

we can write

$$\|W_3T_{e_2r}\|_\infty < 1.$$

Similarly, if the sensitivity should be lower than a given function W_1, we require

$$\|W_1T_{e_1r}\|_\infty < 1.$$

Usually these last two conditions are combined:

$$\left\| \begin{matrix} W_1S \\ W_3T \end{matrix} \right\|_\infty < 1,$$

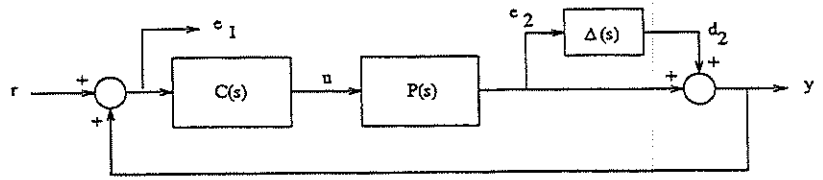

Figure 1.10: The mixed sensitivity setup.

where $S = (I + PC)^{-1}$ is the sensitivity function and $T = PC(I + PC)^{-1}$ is the complementary sensitivity function. If the last inequality is satisfied, the former two are satisfied within a factor $\sqrt{2}$. This problem is usually called the mixed sensitivity problem. If there exists a controller such that the H_∞ norm is lower than one, there is a solution to the problem. In other cases, the constraints on the sensitivity function have to be weakened.

The start of the research in this domain is mainly credited to Zames ([103]). However, the first analytic solutions to this problem come from Doyle ([39]), as e.g. described in the book of Francis ([49]). They optimize the H_∞ norm of a transfer function from the input to the output of a standardized plant. An optimal controller was found using factorizations and a Nehari approximation. The designed controllers, however, are of large order. A few years later articles appeared in which the design of an H_∞ controller was reduced to the solution of two algebraic Riccati equations, as in the case of H_2 optimal controllers ([40],[56],[57]). The order of the resulting controllers is equal or less than the order of the plant. It was also shown how different problems could be reformulated as a problem in the form of a standard plant.

The design of a good H_∞ controller is not so easy. Suitable weighting functions have to be determined. This is usually a hard problem. Furthermore, there are a lot of mathematical and numerical problems involved. Due to mathematical reasons, zeros are not allowed on certain transfer functions. Although it is already shown how most of these problems can be circumvented ([60],[94]), still computing the solution of the algebraic Riccati equations and the consecutive computation of the optimal controller is a hard numerical problem. Recently some articles appeared that tackle this problem solving the H_∞ problem using the bounded real lemma ([51],[52]). Extensions of the existing H_∞ theories to time varying systems also exist ([71],[95]).

The main disadvantage of the H_∞ theory is that the nominal and the

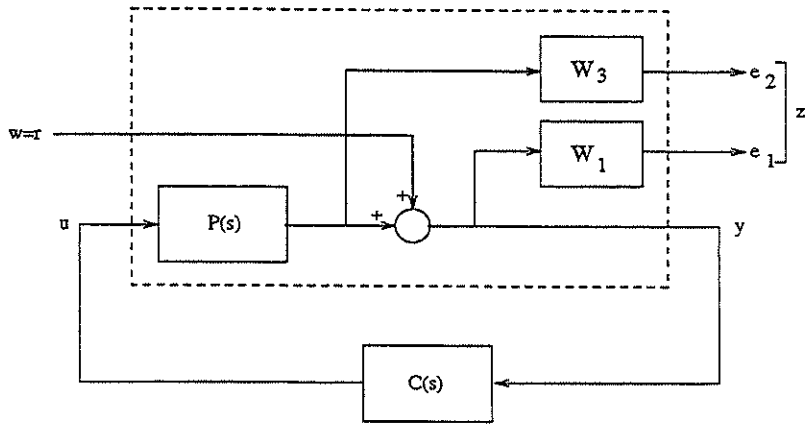

Figure 1.11: The mixed sensitivity setup redrawn in the standard plant configuration. Weighting functions W_1 and W_3 are introduced to 'shape' the sensitivity function S and the complementary sensitivity function T.

perturbed plant need to have the same number of unstable poles. This is a disadvantage when additive or multiplicative disturbance descriptions are used. It makes it sometimes not very useful for systems with poles near the imaginary axis or the unit circle. Therefore the design of H_∞ controllers for perturbations on coprime factors is developed ([77]). Other metrics also have been designed, e.g. the graph metric ([100]) and the gap metric ([54]). However, up to now, these are mainly used for theoretical purpose.

μ Synthesis

As already mentioned the H_∞ controller design can be rather conservative. To make use of the specific structure of the uncertainty, the μ theory is used. Consider the configuration as in figure 1.7. The two uncertainties are combined into one large block Δ:

$$\Delta = \begin{pmatrix} \Delta_P & 0 \\ 0 & \Delta_S \end{pmatrix}.$$

The weighting functions W_P and W_S are determined such that $\|\Delta_P\|_\infty < 1$ and $\|\Delta_S\|_\infty < 1$. In the H_∞ control a controller C is designed, but it is assumed that Δ is a full matrix. This introduces conservatism as the design

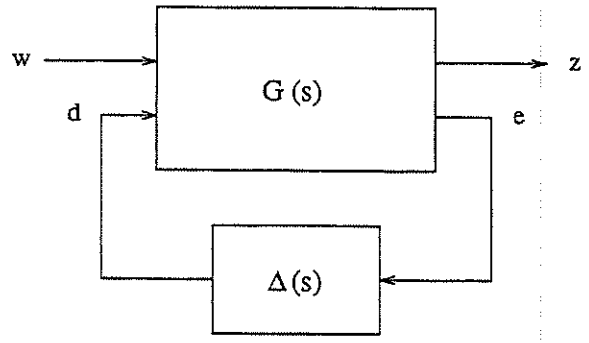

Figure 1.12: The setup for a robust performance design via μ synthesis.

can take destabilizing Δs into account that cannot occur, e.g. a destabilizing block with a non-zero upper right or lower left block. μ control will take into account the specific structure of the disturbance. The goal is to design a controller such that

$$\|G(C)\|_{\mu_\Delta} < 1.$$

Where $G(C)$ is the transfer function from the input d to the output e as a function of the controller C.

μ synthesis can also be used for robust performance. The effect of perturbations Δ can increase drastically when disturbances are present. Hence the need for a robust performance test. Such a test will indicate the worst-case level of performance degradation associated with a given level of perturbations. Consider the setup as shown in figure 1.12. $G(s)$ is a stable, proper transfer function with $n_w + n_d$ inputs and $n_z + n_e$ outputs. Let $\Delta \subset \mathbb{C}^{n_d \times n_e}$ be the set of disturbances Δ, with a specified block structure and $\|\Delta\|_\infty < 1$. Define an augmented block structure

$$\Delta_P = \left\{ \begin{pmatrix} \Delta_F & 0 \\ 0 & \Delta \end{pmatrix} : \Delta \in \Delta, \Delta_F \in \mathbb{C}^{n_w \times n_z} \right\}.$$

The following theorem is proved ([42]):

Theorem 3 *The following conditions are equivalent*

$$\mu_{\Delta_P}(G) < 1 \equiv \begin{cases} \mu_\Delta(G_{22}) < 1 \\ \max_{\Delta \in \Delta} \mu_{\Delta_F}(F_l(G, \Delta)) < 1. \end{cases}$$

The lower fractional transformation $F_l(G, \Delta)$ is well posed and the performance specification $\mu_{\Delta_P}(F_l(G, \Delta)) < 1$ for all uncertainties $\Delta \in \Delta$ if and only if $\mu_{\Delta_P}(G) < 1$.

As already mentioned, computing μ is a very hard problem. Only, upper and lower bounds are rather easy to compute. The μ controller design problem has not been solved yet. Iterative methods based on H_∞ controller design exist, like the $D - K$ ([2]) and $\mu - K$ iteration ([72]). However, the resulting controllers are of very high order. Still, a lot of research is going on in this field.

Robust LQG

It is well known that the gain and phase margins of the LQ control (state feedback) are very good. However, these robustness properties can completely disappear when an observer is used to estimate the states ([36]). The LQG/LTR design methodology is developed to recover the robustness properties of the original LQ design as much as possible. So, the robustness of the LQG design is improved ([37],[74]).

Also a lot of research has been done on the stabilizability of uncertain linear systems. Especially if the systems are *quadratically* stabilizable. A system is quadratically stable if there exists a quadratic Lyapunov equation to prove stability. The considered systems are linear containing unknown-but-bounded uncertain parameters. We refer to the following papers e.g. [7], [8], [63], [85]. Most of these papers also deal with LQ-control. An upper bound, usually called *guaranteed cost*, is minimized.

Mixed H_2/H_∞

As mentioned above, the dynamic LQG output feedback controller has no guaranteed robustness margins. Stability with respect to uncertainties has to be included in another way. On the other hand it has been shown in [40] that H_2 and H_∞ controllers can be computed in a similar way. The controllers are both based on the solutions of two algebraic Riccati equations. Therefore people have been trying to design controllers when the two constraints are present.

Consider a setup as shown in figure 1.13. Two sets of disturbance inputs are considered now: w_1 and w_2. Similarly two sets of controlled outputs are assumed: z_1 and z_2. The mixed H_2/H_∞ problem is formulated as:

$$\min_{C \text{ stabilizing controller}} \|T_{z_1 w_1}\|_2$$

$$\text{subject to } \|T_{z_2 w_2}\|_\infty < \gamma.$$

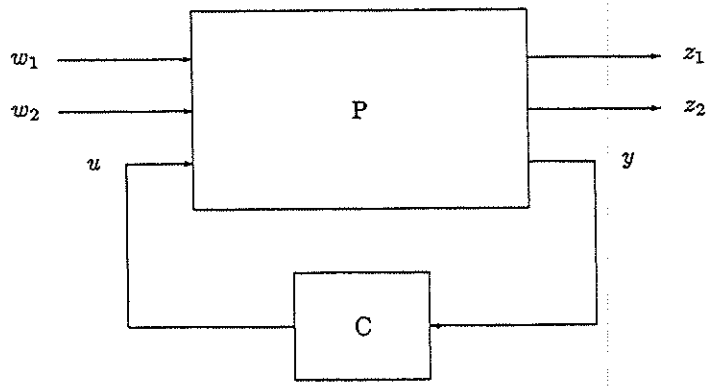

Figure 1.13: The general setup for the mixed H_2/H_∞ problem.

Where $T_{z_1 w_1}$ is the closed loop transfer function from w_1 to z_1 and $T_{z_2 w_2}$ is the closed loop transfer function from w_2 to z_2. However, usually an upper bound is optimized instead of the real H_2 norm. The mixed H_2/H_∞ problem will be discussed in Chapter 4.

Controller Design via Convex Optimization

As already mentioned, there exist analytic solutions to some control problems like the H_2 and H_∞ control design problems. However, for most design problems no analytic solutions exist, e.g. when two or more constraints have to be satisfied simultaneously. In those cases the controller has to be designed using numerical optimization. Numerical optimization, however, has a lot of disadvantages. Good methods to find the global minimum do not exist. Often the minimization gets stuck in local minima. Sometimes no analytic formula exists for the gradients, which then have to be computed numerically. A special class of optimization problems are the convex optimization problems. This is a class of problems that has only one minimum, the global one. Fast and reliable algorithms exist to solve these problems ([12],[13],[80],[97]). Therefore a lot of researchers have tried to (re)formulate control problems as convex optimization problems.

In [12] Boyd and Barratt show that quite some specifications in control are convex. It is also shown how a controller can be computed via the Youla parametrization of all stabilizing controllers. However, there is a disadvantage. To obtain a convex problem the parameter in the Youla

parametrization, that has to be a stable function, is approximated by a sum of functions with a fixed denominator. This often results in controllers of very high order before a reasonable performance is obtained. The advantage of the method is that multiple constraints can be specified, as long as they are convex.

More recently it has been shown how some analysis and design problems can be rewritten as convex problems involving linear matrix inequalities:

$$F(x) > 0,$$

where $F(x) \in \mathbb{R}^{n \times n}$ is an affine function of the parameters x. The entries of $F(x)$ are linearly dependent on the parameters x:

$$F(x) = F_0 + x_1 F_1 + \ldots + x_m F_m,$$

where $F_i = F_i^t \in \mathbb{R}^{n \times n}$, $i = 0 \ldots m$, are constant matrices and $x_i \in \mathbb{R}$, $i = 0 \ldots m$, are the real unknown parameters. The set of positive definite matrices is a convex set.

To solve these positive definite problems, very efficient interior point methods exist ([13],[80],[97]). Some problems that can be solved this way are given in [14] and [82]. These formulations are usually not restricted to linear time invariant systems. Uncertain systems that can be described as polytopic linear differential inclusions or norm bound linear differential inclusions can also be treated in this framework ([14]). Usually it is not possible to compute norms or to design controllers for these systems, analytically. Due to the formulation as a convex problem, these problems can be solved easily. Unfortunately, only state feedback problems and some output feedback control problems can be solved via convex optimization. The design of an H_∞ controller for a linear time invariant system is one of the problems ([51],[52]). Most dynamic output feedback problems have to be solved in another way.

Reduced Order Controller Design

Most modern controller design techniques, like H_2 and H_∞ designs, result in controllers of high order. This makes the implementation harder. If necessary, model reduction can be applied to reduce the order. Different strategies can be used. The order of the original model can be reduced first, and a controller is then designed based on the reduced model. On the other hand a controller can be designed on the full order model and the order of the controller can be reduced afterwards. Several techniques for model reduction

exist ([55],[78]). The open loop model reduction can sometimes be dangerous as some dynamics in the plant can be neglected that are important in the closed loop. Therefore closed loop model reduction has been studied too. Closed loop model reduction reduces the order of the controller, taking into account the dynamics of the controller *and* the plant ([65]).

Due to the model reduction the optimality of the design is lost. Therefore it is better to design a low order controller directly. The structure of the controller is specified in advance and the parameters are designed to optimize the design criteria. Numerical optimization techniques have to be used. These problems are however usually very hard to solve. An example is the controller design in Chapter 4.

More recently another framework for controller design has been proposed. In [47] it is shown how many important reduced order output feedback problems can be reduced to the following generic (non-convex) optimization problem:

$$\min_{x \in \mathbb{R}^m} \text{Rank } F(x) \qquad \text{subject to} \begin{cases} F(x) \geq 0 \\ C(x) \geq 0, \end{cases}$$

where $F(x)$ and $C(x)$ are symmetric matrix functions which are affine in the decision vector $x \in \mathbb{R}^m$. The lower the rank of $F(x)$ the lower the rank of the resulting controller. This problem is not convex. In Chapter 5 two algorithms are described to solve these minimum rank problems involving linear matrix inequalities.

Other reduced rank formulations can be found in [6] and [14]. An advantage of this framework is that the order of the controller is not specified in advance. The lowest possible order of the controller that satisfies the specifications, is looked for.

The minimum rank problems also appear in the output feedback control design for norm bound linear differential inclusions. More details can be found in Chapter 5.

1.3 Chapter by Chapter Overview

The thesis consists of two main parts. The two chapters of the first part study measures to analyze systems. The second part has two chapters that deal with controller design.

ANALYSIS

In **Chapter 2** it is described how the quotient singular value decomposition can be used to study directional aspects of two transfer matrices. It is well known that multiple input multiple output transfer matrices have properties that vary not only with frequency but also with the 'direction' of the input. It is also known how to study these aspects for one transfer matrix in the output space. In this chapter it is shown how these directional aspects of one transfer matrix can be represented graphically in the input space. These results are extended to the properties of two transfer matrices relative to one another. It is also shown how the definitions of the H_2 and H_∞ norms for one transfer matrix can be extended to the case of two transfer matrices.

In **Chapter 3** systems with real parameters are studied. The aim is to compute the largest change in the parameters, that ensures stability or a certain performance (the H_2 performance). Therefore all the parameters are put together in a vector. The goal is to find the largest norm of the vector that ensures the desired performance. Especially the 2 norm of the parameter vector is looked at. This 2 parameter norm is hard to compute. An algorithm has already been proposed when there are only two parameters. This algorithm converged quadratically. In this chapter we present a new algorithm to compute the 2 parameter norm without restrictions on the number of parameters. It is based on a similar algorithm to compute structured total least square problems. Unfortunately, convergence is not guaranteed in this case. However, experiments show that when the algorithm is executed with different initial points the global optimum is usually found.

SYNTHESIS

Chapter 4 is the first chapter that deals with robust controller design. The mixed H_2/H_∞ control design problem is studied. The last few years a lot of researchers have studied these controllers that optimize a H_2 norm and at the same time satisfy a H_∞ constraint. In most cases not the real H_2 norm but an upper bound is minimized. In this chapter we want to design a controller that minimizes the real H_2 norm. It is also shown how the design of the controller can be done for the two objectives separately.

First the H_∞ constraint is looked at. There is a set of controllers that satisfies this constraint. In a second step the controller that minimizes the H_2 performance is determined. Therefore, a H_2 controller design problem with an H_∞ bounded controller has to be solved. However, only necessary conditions for the solution are obtained.

A lot of research has been done on controller design using convex optimization and linear matrix inequalities. As these problems are convex, fast algorithms exist to solve them, e.g. the method of centers. It is, however, impossible to rewrite most output feedback problems in such a form, e.g. reduced order controller designs. Some of these problems can be rewritten as minimum rank problems subject to linear matrix inequalities. However, these problems are not convex. In **Chapter 5** two heuristic algorithms are presented to solve these reduced rank problems. The first one is based on the inversion of the analytic centering method. The second is an extension of a potential reduction method for optimizing a linear objective over a convex set. Not only problems in robust control but a lot of other problems can be rewritten in this form. Of course other output feedback problems fit into this framework, but also identification problems like the Frisch scheme.

In **Chapter 6** the conclusions are summarized and suggestions for further research are given.

1.4 The Ventilator Setup

In this section a practical control problem is described that is used as an example to illustrate the theoretical contributions of the coming chapters. The goal is to control the air flow rate through an axial fan. The control of the air flow rate is important to control the microclimate in confined spaces.

The air flow rate $f(t)$ through the ventilator is not only dependent on the voltage $v(t)$, but also on the pressure difference over the ventilator. The ventilator can thus be modeled as a system with two inputs and one output. The output is the air flow rate. The inputs are the voltage over the ventilator $v(t)$, as the controlled input, and the pressure over the ventilator $p(t)$ as a disturbance input. The pressure over the ventilator is disturbed by e.g. the wind.

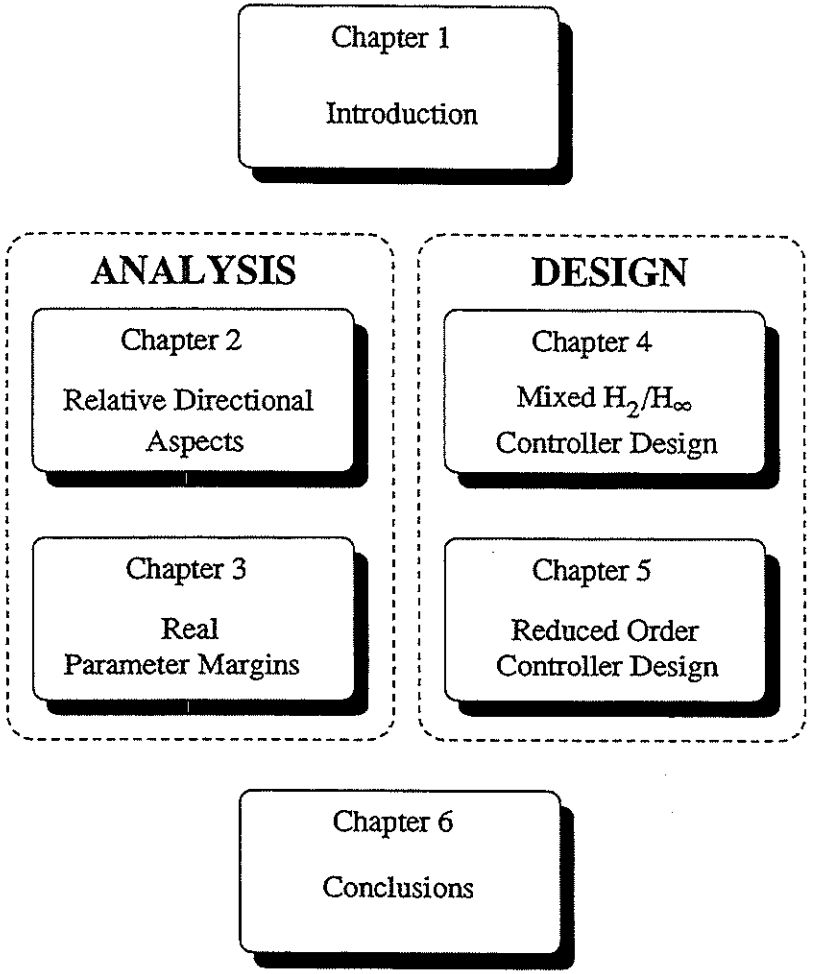

Figure 1.14: A schematic overview of the contents of the thesis.

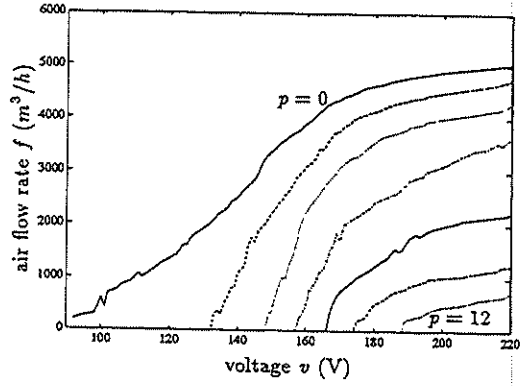

Figure 1.15: Equilibrium curves of the ventilator for different values of the pressure difference over the ventilator. The air flow rate f is given in m^3/h, the voltage in V and the pressure difference in mm water globe. ($p = 0, 2, 4, 6, 8, 10, 12$)

In this section we briefly describe how a simple model of the ventilator can be obtained and how controllers are designed. More details can be found in [33]. A first order model is derived from static measurements as no dynamic measurements were available. The used ventilator is a Siemens 450.

1.4.1 Steady State and Dynamic Model

Curves of equilibrium triplets (v_{eq}, f_{eq}, p_{eq}), shown in figure 1.15, were obtained from static experiments. In a first step of the modeling process, the equilibrium curves were fitted using a non-linear least squares approach. The proposed equilibrium model is:

$$f_{eq}(v_{eq}, p_{eq}) = f_\infty(1 - (\frac{v_0}{v_{eq}})^{\frac{1}{\eta}}), \tag{1.1}$$

where the dead zone v_0, the exponent η and the asymptotic value f_∞ are functions of the pressure p_{eq}.

Our next task is to obtain a dynamic model, the steady state of which coincides with the measured steady state curves. Assume that the ventilator

is operating in the neighborhood of an equilibrium point $(p_{lin}, v_{lin}, f_{lin})$. We *postulate* that the dynamic behavior of the system in this neighborhood can be approximated as:

$$\dot{f} = \alpha(f - f_{lin}) + \beta(v - v_{lin}) + \gamma(p - p_{lin}). \tag{1.2}$$

The value of α is determined from experiments. Once α is known, β and γ are obtained from differentiations of the equilibrium model around the operating point.

Equation (1.2) can be transformed in a state space model:

$$\begin{cases} \dot{x}_p &= \alpha x_p + \beta v_1 + \gamma p_1 \\ f &= x_p + f_{lin}, \end{cases}$$

where $v_1 = v - v_{lin}$, $p_1 = p - p_{lin}$. The signal p_1, which represents variations in pressure due to wind, will be further modeled. Define also $f_1 = f - f_{lin}$: The variations of the air flow rate around the equilibrium. We shall analyze several controllers for the linear model around the equilibrium point

$$(\ v_{lin}\ ,\ f_{lin}\ ,\ p_{lin}\ ) = (\ 170,\ 3509\ ,\ 2\ ). \tag{1.3}$$

The time constant of the ventilator gives us $\alpha = -\frac{1}{1.987} = 0.503$. The other coefficients are $\beta = 21.999$ and $\gamma = -248.249$. Actually, the value of β that will be used is 13 times higher, a factor which comes from a simplified model of a DC/AC conversion.

1.4.2 Disturbance model

A typical disturbance for a ventilator is the wind. The wind is modeled based on power spectrum data. A good model for the wind disturbances is obtained with a third order system driven by white noise. The result of the fit is shown in figure 1.16. The obtained model is scaled to make its H_2 norm equal to one. The resulting model is

$$\begin{cases} \dot{x}_d &= A_d x_d + B_d w_d \\ p_1 &= C_d x_d + D_d w_d, \end{cases}$$

with

$$A_d = \begin{pmatrix} -3.64e-01 & -2.61e-02 & -1.41e-03 \\ 1.00e+00 & 0.0 & 0.0 \\ 0.0 & 1.00e+00 & 0.0 \end{pmatrix}, \quad B_d = \begin{pmatrix} 4.37e-01 \\ 0.0 \\ 0.0 \end{pmatrix},$$

$$C_d = (\ 1.58e+00 \quad 1.51e-01 \quad 1.30e-03\ ), \qquad D_d = 0.$$

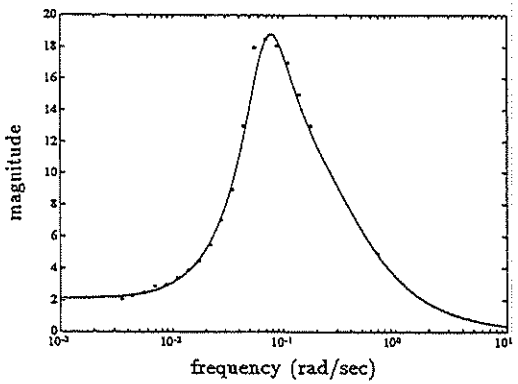

Figure 1.16: The fit of the wind spectrum. (Dots: measured data, full line: model.)

The signal w_d is assumed to be white noise, zero mean, Gaussian with variance $\sigma^2_{w_d} = 1$.

1.4.3 Measurements

The measurement of the flow rate f is modeled as a first order linear dynamical system with additive measurement noise:

$$\begin{cases} \dot{x}_m &= \alpha_m x_m + \beta_m f \\ v_m &= \gamma_m x_m + \delta_m w_m. \end{cases} \tag{1.4}$$

Since measuring a flow rate is quite difficult, we model the inaccuracy of the measurements by additive zero mean Gaussian white noise with variance $\sigma^2_{w_m} = 100$. The variance is derived from the known accuracy of the sensor around the equilibrium point (1.3).

The output v_m is a voltage which will be fed back to the input via a controller. From experiments on the measurement equipment, the following values were obtained:

$$\alpha_m = -\tfrac{1}{5.582}, \qquad \beta_m = 0.0627,$$
$$\gamma_m = 1/140, \qquad \delta_m = 1/140.$$

1.4.4 Controller Design

The controller has to keep the air flow rate through the ventilator, f_{lin}, constant. This will be called the set point. Using equations (1.4) the desired air flow rate is converted into an *equivalent* voltage v_{ref}. In the noiseless case, $w_m = 0$, we would like that in equilibrium the set point $v_{ref} = v_m$. Hence $v_{ref} = -\frac{\gamma_m \beta_m}{\alpha_m} f_{lin}$. The error signal $e(t)$ is obtained as $e = v_{ref} - v_m$. In general the controller will be represented by the state space model:

$$\begin{cases} \dot{x}_c &= A_c x_c + B_c e \\ v_1 &= C_c x_c + D_c e. \end{cases}$$

The models of the ventilator, the wind and the sensor can now be combined into one generalized plant. The block diagram of the generalized plant is shown in figure 1.17. The dashed box is the generalized plant. The inputs and outputs can be defined as:

- external inputs: $w = \begin{pmatrix} w_d & w_m \end{pmatrix}^t$.
- controller input: $u = v_1$.
- output to be minimized: $z = \begin{pmatrix} f_1 & \sqrt{\rho} v_1 \end{pmatrix}^t$.
- measurement output to the controller: $y = v_m$.

The output vector z contains all the signals to be controlled. Therefore, the controlled output z does not only contain the air flow rate variations f_1, but also the actuator output v_1. The controller energy should not be to excessive. The controller output was also scaled with a parameter $\sqrt{\rho}$ to influence the allowed control energy. In this text ρ is taken to be 1.

The resulting generalized model for this example is therefore given by:

$$\begin{pmatrix} P_{11} & P_{12} \\ P_{21} & P_{22} \end{pmatrix} = \left(\begin{array}{c|cc} A & B_1 & B_2 \\ \hline C_1 & D_{11} & D_{12} \\ C_2 & D_{12} & D_{22} \end{array}\right)$$

$$= \left(\begin{array}{ccccc|cc|c} -0.5033 & -392.8866 & -37.5781 & -0.3238 & 0 & 0 & 0 & 286.0103 \\ 0 & -0.3643 & -0.0261 & -0.0014 & 0 & 0.4375 & 0 & 0 \\ 0 & 1.0000 & 0 & 0 & 0 & 0 & 0 & 0 \\ 0 & 0 & 1.0000 & 0 & 0 & 0 & 0 & 0 \\ 0.0627 & 0 & 0 & 0 & -0.1791 & 0 & 0 & 0 \\ \hline 1.0000 & 0 & 0 & 0 & 0 & 0 & 0 & 0 \\ 0 & 0 & 0 & 0 & 0 & 0 & 0 & 1 \\ \hline 0 & 0 & 0 & 0 & -0.0071 & 0 & -0.0071 & 0 \end{array}\right). \tag{1.5}$$

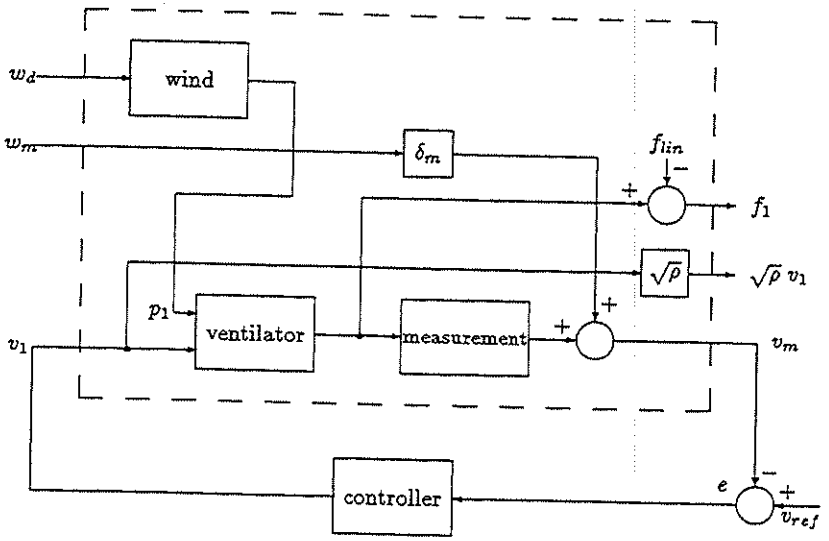

Figure 1.17: The generalized plant block diagram of the ventilator configuration

where the five states are due to one plant state, three states of the wind model and one state of the measurement.

Three different types of controllers were designed: a PI-controller, an H_2 controller and an H_∞ controller. The state space realizations of the controllers are shown below:

- The state space realization of the PI controller:

$$\left(\begin{array}{c|c} A_c & B_c \\ \hline C_c & D_c \end{array}\right) = \left(\begin{array}{c|c} 0 & 3.04 \\ \hline 1 & 7.82 \end{array}\right).$$

- The H_2 controller is the controller that minimizes $\|T_{zw}\|_2$, where T_{zw} is the closed loop transfer function from the disturbance input w to the controlled output z. Its state space realization is:

$$\left(\begin{array}{c|c} A_c & B_c \\ \hline C_c & D_c \end{array}\right)$$

$$= \left(\begin{array}{rrrrr|r} -286 & -1.059 & -0.1007 & -0.002498 & -15.25 & -2136 \\ 0 & -0.3643 & -0.02607 & -0.001408 & 0.01984 & 2.778 \\ 0 & 1 & 0 & 0 & 0.06023 & 8.432 \\ 0 & 0 & 1 & 0 & 0.07063 & 9.888 \\ 0.0627 & 0 & 0 & 0 & -1.395 & -170.2 \\ \hline -0.9982 & 1.37 & 0.131 & 0.001124 & 0 & 0 \end{array}\right).$$

- The H_∞ controller is the controller that minimizes $\|T_{zw}\|_\infty$. Its state space realization is:

$$\left(\begin{array}{c|c} A_c & B_c \\ \hline C_c & D_c \end{array}\right)$$

$$= \left(\begin{array}{rrrr|r} -0.1811 & -3.11 & -0.7282 & -0.7139 & 457.3 \\ 4.421 & -254.7 & -59.92 & -58.65 & 3.745e+04 \\ 1.684 & -61.3 & -15 & -14.79 & 9053 \\ 2.273 & -77.82 & -17.94 & -17.49 & 1.142e+04 \\ \hline 1.662 & -15.16 & -3.595 & -3.525 & 2235 \end{array}\right).$$

These controllers are used in the next chapters.

Chapter 2

Directional Aspects of Two Transfer Matrices

2.1 Introduction

It is well-known that the "size" of the output of a multiple input-multiple output (MIMO) system is not only dependent on the frequency of the input, but also on its 'direction'. These are called *directional aspects* of transfer matrices. It is known in the control community that directional aspects of transfer matrices can be studied using the singular value decomposition (SVD) ([17]).

As an example consider a stable, linear, time invariant 2×2 MIMO system. To find the sinusoidal input signal that is amplified most, a SVD is needed. The frequency of the sinusoidal input will be any frequency ω_0 where the H_∞ norm of the transfer matrix is attained. The H_∞ norm is defined as

$$\|G\|_\infty = \sup_{\omega \in \mathbb{R}} \sigma_{\max}(G(j\omega)),$$

where $\sigma_{\max}(.)$ denotes the largest singular value of the matrix between brackets. Let the SVD of $G(j\omega_0)$ be given by

$$G(j\omega_0) = \begin{pmatrix} u_1 & u_2 \end{pmatrix} \begin{pmatrix} \sigma_1 & 0 \\ 0 & \sigma_2 \end{pmatrix} \begin{pmatrix} v_1^* \\ v_2^* \end{pmatrix},$$

where $v_1 = \begin{pmatrix} \alpha + j\beta \\ \gamma + j\delta \end{pmatrix}$ with $v_1^* v_1 = 1$ or $\alpha^2 + \beta^2 + \gamma^2 + \delta^2 = 1$.

The input signal that will be amplified most is then given by:

$$u(t) = \begin{pmatrix} \sqrt{\alpha^2+\beta^2}\sin(\omega_0 t + \arctan\frac{\beta}{\alpha}) \\ \sqrt{\gamma^2+\delta^2}\sin(\omega_0 t + \arctan\frac{\delta}{\gamma}) \end{pmatrix}.$$

With $u_1 = \begin{pmatrix} \epsilon + j\phi \\ \kappa + j\lambda \end{pmatrix}$ and $u_1^* u_1 = 1$, the corresponding output vector will be given by

$$y(t) = \sigma_1 \begin{pmatrix} \sqrt{\epsilon^2+\phi^2}\sin(\omega_0 t + \arctan\frac{\phi}{\epsilon}) \\ \sqrt{\kappa^2+\lambda^2}\sin(\omega_0 t + \arctan\frac{\lambda}{\kappa}) \end{pmatrix}.$$

In this chapter it will be shown how this can be extended to study directional aspects of two transfer matrices relative to one another. We will show how this can be used to study signal-to-noise ratios. Therefore the quotient singular value decomposition (QSVD), a generalization of the singular value decomposition, is used. Using the QSVD it is possible to compute the ratios and the extremal directions.
In section 2.2 the main results of the QSVD are summarized. In a second section we briefly recapitulate how directional aspects of matrices can be studied. In a next section it is shown how this can be used to study the directional aspects of transfer matrices. It is also possible to define norms for these directional aspects. The definitions are given in section 2.4, where it is also explained how these norms can be computed. Finally, everything will be illustrated with an example.

2.2 The QSVD

In this section the main results on the QSVD are summarized. While the SVD was already discovered more than 100 years ago (see [32] for a collection of historical references), the QSVD is much more recent and is only one member of an infinite set of generalizations of the SVD for any number of matrices ([32]). A standardized nomenclature for these generalizations was proposed in [30].

Theorem 4 *Any pair of complex matrices, $A \in \mathbb{C}^{l\times m}$ and $B \in \mathbb{C}^{p\times m}$ with the same number of columns, can be jointly factorized as*

$$A = U_a S_a X^{-1}, \quad B = U_b S_b X^{-1},$$

where $U_a \in \mathbb{C}^{l\times l}$ and $U_b \in \mathbb{C}^{p\times p}$ are unitary, $X \in \mathbb{C}^{m\times m}$ is a nonsingular square matrix and $S_a \in \mathbb{R}^{l\times m}$ and $S_b \in \mathbb{R}^{p\times m}$ are matrices with the following structure:

$$S_a = \begin{array}{c} \\ r_{a|b}-r_b \\ r_a+r_b-r_{a|b} \\ l-r_a \end{array} \begin{array}{c} \begin{array}{cccc} r_{a|b}-r_b & r_a+r_b-r_{a|b} & r_{a|b}-r_a & m-r_{a|b} \end{array} \\ \begin{pmatrix} I & 0 & 0 & 0 \\ 0 & D_a & 0 & 0 \\ 0 & 0 & 0 & 0 \end{pmatrix} \end{array},$$

$$S_b = \begin{array}{c} \\ p-r_b \\ r_a+r_b-r_{a|b} \\ r_{a|b}-r_a \end{array} \begin{array}{c} \begin{array}{cccc} r_{a|b}-r_b & r_a+r_b-r_{a|b} & r_{a|b}-r_a & m-r_{a|b} \end{array} \\ \begin{pmatrix} 0 & 0 & 0 & 0 \\ 0 & D_b & 0 & 0 \\ 0 & 0 & I & 0 \end{pmatrix} \end{array},$$

where

$$r_a = rank(A),\ r_b = rank(B)\ and\ r_{a|b} = rank\begin{pmatrix} A \\ B \end{pmatrix}.$$

This decomposition is called the quotient singular value decomposition.

Proof:
Our proof of the QSVD is constructive and uses three SVDs: First consider the SVD of the concatenation of the matrices A and B:

$$\begin{pmatrix} A \\ B \end{pmatrix} = U \begin{array}{c} \begin{array}{cc} r_{a|b} & m-r_{a|b} \end{array} \\ \begin{pmatrix} S & 0 \\ 0 & 0 \end{pmatrix} \end{array} V^* = \begin{array}{c} \\ l \\ p \end{array} \begin{array}{c} \begin{array}{cc} r_{a|b} & m-r_{a|b} \end{array} \\ \begin{pmatrix} U_1 & 0 \\ U_2 & 0 \end{pmatrix} \end{array} \begin{array}{c} \begin{array}{cc} r_{a|b} & m-r_{a|b} \end{array} \\ \begin{pmatrix} S & 0 \\ 0 & I \end{pmatrix} \end{array} V^*.$$

Next consider the SVDs of the matrices U_1 and U_2:

$$U_1 = U_{u_1} S_{u_1} V_{u_1}^*, \qquad U_2 = U_{u_2} S_{u_2} V_{u_2}^*.$$

From the orthonormality of U follows that

$$U_1^* U_1 + U_2^* U_2 = I_{r_{a|b}}$$

$$V_{u_1} S_{u_1}^t S_{u_1} V_{u_1}^* + V_{u_2} S_{u_2}^t S_{u_2} V_{u_2}^* = I_{r_{a|b}}$$

$$V_{u_1} S_{u_1}^t S_{u_1} V_{u_1}^* = V_{u_2} \left(I_{r_{a|b}} - S_{u_2}^t S_{u_2}\right) V_{u_2}^*$$

$$S_{u_1}^t S_{u_1} = V_{u_1}^* V_{u_2} \left(I_{r_{a|b}} - S_{u_2}^t S_{u_2}\right) V_{u_2}^* V_{u_1}.$$

The latter equation represents a similarity transformation. As $S_{u_1}^t S_{u_1}$ and $\left(I_{r_{a|b}} - S_{u_2}^t S_{u_2}\right)$ are diagonal matrices, the values of S_{u_2} can always be re-ordered such that

$$S_{u_1}^t S_{u_1} = \left(I_{r_{a|b}} - S_{u_2}^t S_{u_2}\right).$$

This implies that $S_{u_1}^t S_{u_1} + S_{u_2}^t S_{u_2} = I_{r_{a|b}}$ and $V_{u_1} = V_{u_2}$ so that

$$A = U_a(\; S_1 \;\; 0 \;)X^{-1}, \qquad B = U_b(\; S_2 \;\; 0 \;)X^{-1},$$

where

$$U_a = U_{u_1}, \;\; U_b = U_{u_2}, \;\; S_1 = S_{u_1}, \;\; S_2 = S_{u_2},$$

$$X^{-1} = \begin{pmatrix} V_1^* & 0 \\ 0 & I \end{pmatrix} \begin{pmatrix} S & 0 \\ 0 & I \end{pmatrix} V^*.$$

This basically proves the theorem. The structure of S_a and S_b follows from the ranks of A, B and $\begin{pmatrix} A \\ B \end{pmatrix}$. □

If A and B are real matrices, all the SVDs in the constructive proof are real and this automatically results in a real version of the QSVD.

The original formulation of the QSVD (which used to be called *the generalized SVD*, but see also [29]) is due to Paige and Saunders ([83]) and Van Loan ([98]).
D_a and D_b are diagonal matrices with size $r_q = r_a + r_b - r_{a|b}$. The diagonal elements are strictly positive and smaller than 1. Let $\alpha_1, \ldots, \alpha_{r_q}$ be the diagonal elements of D_a, and $\beta_1, \ldots, \beta_{r_q}$ those of D_b. The pairs of real numbers (α_i, β_i), $i = 1, \ldots, r_q$ are called the quotient singular value pairs and by convention, we put $\alpha_i^2 + \beta_i^2 = 1$ and order the pairs so that

$$\frac{\alpha_1}{\beta_1} \geq \frac{\alpha_2}{\beta_2} \geq \cdots$$

The convention $\alpha_i^2 + \beta_i^2 = 1$ follows from the construction in the proof and makes this matrix decomposition unique. The ratios will be called the *quotient singular values* (QSV). We will use an extended definition of the QSV: Take as α_i the diagonal elements of S_a. Let β_i be the elements on the diagonal of S_b that contains the diagonal elements of D_b, where i is now an index ranging from $1, ..., r_{a|b}$. With this definition, the QSVs may be 0, when A is singular, and they may be infinite, when B is singular. The QSVs will be denoted as σ_{qi}, where σ_{qi} is the ith QSV.

Note that the block dimension $r_a + r_b - r_{a|b}$ gives the dimension of the intersection of the row spaces of A and B.
We will also need the following lemma:

Lemma 1 *Let u, v and x be three vectors satisfying*

$$Ax = u\alpha, \quad Bx = v\beta, \quad A^*u\beta = B^*v\alpha,$$

where α and β are two real numbers satisfying $\alpha^2 + \beta^2 = 1$. Then, u, v and x are corresponding column vectors of matrices U_a, U_b and X that form the QSVD of (A, B) as described in Theorem 1.

The proof is straightforward.

2.3 Directional Aspects of Matrices

In this section, directional aspects of matrices are studied. It will be shown how they can be represented graphically. First, we will show how directional aspects of one matrix can be represented. Then the case of two matrices will be considered.

2.3.1 The Indicator Ellipsoid

A complete picture of the action of a matrix $A \in \mathbb{C}^{l \times m}$ is provided by the image under A of the unit sphere of $\mathbb{C}^m$:

Theorem 5 Indicator ellipsoid of a matrix $A \in \mathbb{C}^{l \times m}$ *([17])*

Let $A \in \mathbb{C}^{l \times m}$ be of rank r and consider the linear transformations $y = Ax$. The domain and codomain transformations induced by its SVD $A = U\Sigma V^*$, where $\Sigma = diag(\sigma_i)$ contains the singular values σ_i, are $x = V\xi$ and $y = U\eta$. Let $S_m = \{ \; x \in \mathbb{C}^m \mid \|x\| = 1 \; \}$ denote the unit sphere of $\mathbb{C}^m$. Let $A[S_m]$ denote the image under A of S_m. Then the following properties hold:

If $r = l = m$: $A[S_m] = \{ \; y \in \mathbb{C}^l \mid y = U\eta \; , \; \sum_{i=1}^r (\eta_i/\sigma_i)^2 = 1 \; \}$.

If $r = l < m$: $A[S_m] = \{ \; y \in \mathbb{C}^l \mid y = U\eta \; , \; \sum_{i=1}^r (\eta_i/\sigma_i)^2 \leq 1 \; \}$.

If $r = m < l$: $A[S_m] = \{ \; y \in \mathbb{C}^l \mid y = U\eta \; , \; \sum_{i=1}^r (\eta_i/\sigma_i)^2 = 1, \eta_{r+1} = \ldots = \eta_l = 0 \}$.

If $r < min(l,m)$: $A[S_m] = \{\ y \in \mathbb{C}^l | y = U\eta, \sum_{i=1}^{r}(\eta_i/\sigma_i)^2 \leq 1, \eta_{r+1} = \ldots = \eta_l = 0\ \}$.

The matrix A maps the unit sphere S_m of $\mathbb{C}^m$ onto an r-dimensional ellipsoid in $\mathbf{R}(A)$ with as principal axes the left singular vectors u_i of U that correspond to nonzero singular values $\sigma_i > 0$. If A is not of full column rank, the points in $\mathbf{R}(A)$ interior to the ellipsoid have to be included. If A has full row rank, the ellipsoid has l principal axes with positive length. Note that the four cases of the theorem are mutually exclusive.
Let $A \in \mathbb{C}^{l \times m}$, $x \in \mathbb{C}^m$ and $y = Ax$. Then

$$\max_{\|x\|=1} \|y\| = \sigma_1 \quad \text{and} \quad \min_{\|x\|=1} \|y\| = \begin{cases} \sigma_m & \text{if } l \geq m \\ 0 & \text{if } l < m. \end{cases}$$

For the case $l \geq m$, the following minimax properties hold:

$$\begin{aligned} \max_{Q^r \subset \mathbb{C}^m} \{ \min_{x \in Q^r, \|x\|=1} \|y\| \} &= \sigma_r, \\ \min_{Q^r \subset \mathbb{C}^m} \{ \max_{x \in Q^r, \|x\|=1} \|y\| \} &= \sigma_{m-r+1}, \end{aligned}$$

where 'max' and 'min' denote operators, maximizing or minimizing over all r-dimensional subspaces Q^r of the ambient range space $\mathbb{C}$. These are the classical (Courant-Fisher) minimax characterizations of the singular values (see e.g. [58]).

The Frobenius norm of A is defined as $\|A\|_F^2 = \sum_{i=1}^{l}\sum_{j=1}^{m} |a_{ij}|^2$. It is easy to show that $\|A\|_F^2 = \text{trace}(A^*A) = \text{trace}(AA^*)$. Using the fact that $\|UA\|_F = \|AV\|_F = \|A\|_F$ for arbitrary unitary matrices U and V (i.e. the Frobenius norm is *unitarily invariant*), we find from the SVD of A that

$$\|A\|_F^2 = \|U\Sigma V^*\|_F^2 = \|U^*U\Sigma V^*V\|_F^2 = \|\Sigma\|_F^2 = \sigma_1^2 + \sigma_2^2 + \ldots + \sigma_r^2.$$

Summarizing, we have $\|A\|_F^2 = \sum_{i=1}^{r} \sigma_i^2 = \text{trace}(A^*A) = \text{trace}(AA^*)$.
There is also a result which puts the indicator ellipsoid in a statistical framework. For the time being, we will restrict ourselves to the real case.
Let $x \in \mathbb{R}^m$ be a random vector, normally distributed with zero mean and covariance I_m. This implies that the directional distribution of x, which is the distribution of the projections of x onto the unit sphere in $\mathbb{R}^m$, is uniform: All directions in $\mathbb{R}^m$ are equally probable. We find for the average length of x:

$$\mathrm{E}\|x\|^2 = m.$$

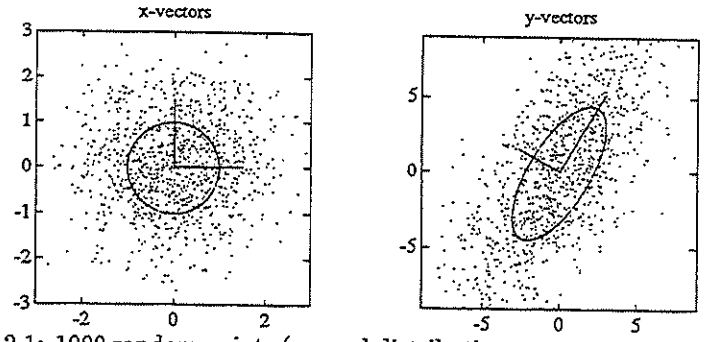

Figure 2.1: 1000 random points (normal distribution, zero mean, covariance I_2) are shown in the left plot. The unit circle is generated by normalizing these random points to have norm one. For each random point x, we compute $y = Ax$ and show the obtained points y in the right plot. The ellipsoid is obtained by plotting the image under A of the points on the unit circle. Observe that its principal axes lie in the direction of the left singular vectors, with half lengths equal to the singular values.

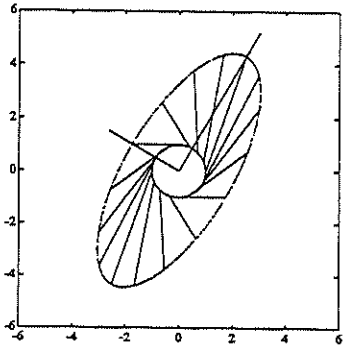

Figure 2.2: The small circle is generated by 1000 random points on the unit circle, representing input vectors. Also shown are the 1000 corresponding points on the indicator ellipsoid, some of which are connected by a line with their corresponding point on the unit circle. The right singular vectors are in the directions $(1,0)$ for $\sigma_1 = 5$ and $(0,1)$ for $\sigma_2 = 2$. The directions of the left singular vectors are given by the long lines. It can be observed that on the average points are relatively more 'attracted' to the left singular vector corresponding to the largest singular value, especially in the neighborhood of the right singular vector corresponding to the smallest singular value.

Next let $y = Ax$ with $A = U\Sigma V^t$ the singular value decomposition of A. Then $y \in \mathbb{R}^l$ will be normally distributed too by linearity and

$$\mathbf{E}\|y\|^2 = \mathbf{E}(x^t A^t A x) = \mathbf{E}(z^t \Sigma^t \Sigma z) = \sigma_1^2 \zeta_1^2 + \ldots + \sigma_r^2 \zeta_r^2,$$

where $z = V^t x = (\ \zeta_1\ ,\ \ldots\ ,\ \zeta_m\ )$ and $r = \text{rank}(A)$. As the 2 norm is unitarily invariant, we find that

$$\mathbf{E}\|y\|^2 = \sigma_1^2 + \ldots + \sigma_r^2.$$

Hence, we have proved:

Theorem 6 *Let $x \in \mathbb{R}^m$ be a random vector, which is independently and identically normally distributed with mean zero and covariance matrix I_m. Then $y = Ax$ is normally distributed with mean zero and covariance matrix AA^t and $\mathbf{E}\|y\|^2 = \sigma_1^2 + \ldots + \sigma_r^2 = \|A\|_F^2$.*

Example:
The statistical interpretation of the SVD is illustrated in figures 2.1 and 2.2 for the matrix:

$$A = \begin{pmatrix} 2.5 & -1.7321 \\ 4.3301 & 1 \end{pmatrix} = \begin{pmatrix} 0.5 & -0.866 \\ 0.866 & 0.5 \end{pmatrix} \begin{pmatrix} 5 & 0 \\ 0 & 2 \end{pmatrix} \begin{pmatrix} 1 & 0 \\ 0 & 1 \end{pmatrix}.$$

2.3.2 Oriented Energy

The geometrical interpretation of the static transfer performed by a matrix A can also be shown in another way. Let x be a unit vector in $\mathbb{R}^m$ and $y = Ax \in \mathbb{R}^l$. An *oriented energy plot* can be obtained by plotting the vector

$$x\sqrt{x^t A^t A x}$$

for each unit vector x. Such a plot tells us how much a vector x will get amplified when the matrix A is applied to it. The quantity $\|Ax\|$ will be called the oriented energy of the matrix A in the direction of the vector x. In general, there is one maximum (in the direction of the first right singular vector) and one minimum (in the direction of the m-th right singular vector). The other extrema, which are saddle points, occur at the remaining right singular vectors. An illustration can be found in figure 2.3. There is an important difference between the *indicator ellipsoid* and an *oriented energy plot*: The indicator ellipsoid is a 'picture' in the output space $\mathbb{R}^l$ of the

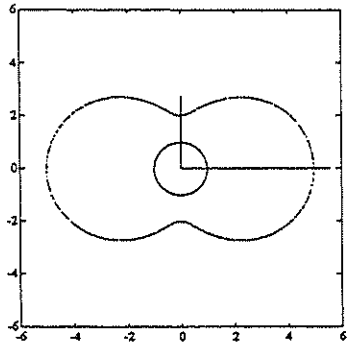

Figure 2.3: Shown is the unit circle obtained by normalizing 1000 random points (normal distribution, zero mean, covariance I_2) to have norm 1. For each normalized point x, the corresponding point $x\|Ax\|$ is also plotted, generating the oriented energy plot. The minimum and maximum occur at the directions of the *right* singular vectors, which are indicated by the lines.

vectors y while the oriented energy plot is a 'picture' in the domain $\mathbb{R}^m$ of the input space.

The indicator ellipsoid and the oriented energy plot give complementary information about the action of a linear transformation, represented by a matrix A, on an input vector x resulting in an output vector y. The indicator ellipsoid shows the geometric extent of the set of vectors y that can be reached by applying a unit input vector x. If however we pick one point on the indicator ellipsoid, it does not tell us in which direction the corresponding input vector x could be situated. This is revealed by an oriented energy plot, which shows, in the input space, the effect of a certain input direction, on the energy of the output. Clearly, such information has its value in the sense that the input causally affects the output. If certain effects are to be avoided, for instance by designing an appropriate controller, one should operate in the input space. Hence the importance of an oriented energy plot.

2.3.3 Signal-to-Signal Ratio of Two Matrices

Until now we have been looking at the properties of only one matrix. In this section, we look at the properties of one matrix *relative* to another one. Hereto, we introduce:

Definition 3 *The signal-to-signal ratio SSR of two real matrices A and B in the direction x is the ratio of the oriented energies of the matrices A and B in the direction x:*

$$R_x[A,B] = \frac{\|Ax\|}{\|Bx\|}.$$

Consider two matrices A and B with an equal number of columns and let their QSVD be:

$$\begin{cases} A = U_a S_a X^{-1}, \\ B = U_b S_b X^{-1}. \end{cases}$$

Let us now demonstrate how the QSVD provides a canonical decomposition for the signal-to-signal ratios just as the SVD does for the oriented energy. Hereto, consider the QSVD of $[A,B]$, then,

$$R_x^2[A,B] = \frac{x^t A^t A x}{x^t B^t B x} = \frac{(x^t X^{-t}) S_a^t S_a (X^{-1}x)}{(x^t X^{-t}) S_b^t S_b (X^{-1}x)}.$$

Obviously, when $x = x_i$, the ith column of X, then

$$R_{x_i}[A,B] = \frac{\alpha_i}{\beta_i}.$$

Let $A \in \mathbb{C}^{l\times m}$ and $B \in \mathbb{C}^{p\times m}$, with $l \geq m$ and $p \geq m$, then

$$\begin{aligned} \max_{x,\|x\|=1} R_x[A,B] &= \frac{\alpha_1}{\beta_1}, \\ \min_{x,\|x\|=1} R_x[A,B] &= \frac{\alpha_m}{\beta_m}. \end{aligned}$$

The directions of maximal and minimal SSR are given by column x_1 and x_m of X. These extremal directions are, in general, *not* orthogonal to one another, because X is not an orthogonal matrix. Other relative minimax properties are:

$$\begin{aligned} \mathrm{MmR}[A,B,r] \equiv \max_{Q^r \subset \mathbb{C}^m} \{\min_{x\in Q^r} R_x[A,B]\} &= \frac{\alpha_r}{\beta_r} \\ \mathrm{mMR}[A,B,r] \equiv \min_{Q^r \subset \mathbb{C}^m} \{\max_{x\in Q^r} R_x[A,B]\} &= \frac{\alpha_{m-r+1}}{\beta_{m-r+1}}. \end{aligned}$$

In words: Consider two matrices A and B and a certain r-dimensional subspace Q^r. Then there is a direction $x \in Q^r$ for which the signal-to-signal ratio is minimal. If we now manipulate also Q^r, we can find the maximum of

all these minima, which is exactly $\frac{\alpha_r}{\beta_r}$. This ratio will be called the maximal minimal signal-to-signal ratio over r-dimensional subspaces: $\mathrm{MmR}[A,B,r]$. The corresponding subspace is the range of the matrix $[x_1,\ldots,x_r]$ where x_i, $i = 1,\ldots,r$, are the first r vectors of X. A dual argument applies for the minimal maximal signal-to-signal ratio $\mathrm{mMR}[A,B,r]$.

A signal-to-signal ratio plot is obtained by plotting the vector $x\frac{\|Ax\|}{\|Bx\|}$ for each unit direction x. Again, a SSR-plot is a picture in the input space. The extremal directions, which are given by the column vectors of X, are not orthogonal.

Example:
The signal-to-signal ratio is plotted for two pairs of matrices: $[A,B_1]$ and $[A,B_2]$

$$A = \begin{pmatrix} .25 & 0 \\ 0 & 2 \end{pmatrix}, \quad B_1 = \begin{pmatrix} 1 & -1.5 \\ 0 & 1.5 \end{pmatrix}, \quad B_2 = \begin{pmatrix} 1 & 2 \\ 3 & 2 \end{pmatrix}.$$

The directions of maximal and minimal SSR are shown and also the circle with radius $\frac{\alpha_1}{\beta_1}$ and $\frac{\alpha_2}{\beta_2}$. The maximal SSR is given by $\frac{\alpha_1}{\beta_1}$ and the minimal by $\frac{\alpha_2}{\beta_2}$. The directions of maximal and minimal SSR are given by the column vectors of the matrix X in the QSVD. These directions are *not* orthogonal as in the case of the oriented energy. The direction and size of the maximal SSR is dependent on the two matrices, as can be seen in the figure.

2.4 Directional Aspects of Transfer Matrices

The directional aspects of matrices can easily be extended to transfer matrices. In this section we present how this can be done.

2.4.1 Oriented Energy of Transfer Matrices

Let us consider complex transfer matrices, that are a function of frequency. The SVD of a transfer matrix is defined as

$$y(s) = G(s)u(s) = U(s)S(s)V(s)^* u(s),$$

where $U(s), S(s)$ and $V(s)$ are such that at each s, $U(s)S(s)V(s)^*$ is the SVD of $G(s)$. The entries of $U(s)$ and $V(s)$ are in general not rational, even if $G(s)$ contains only rational entries.

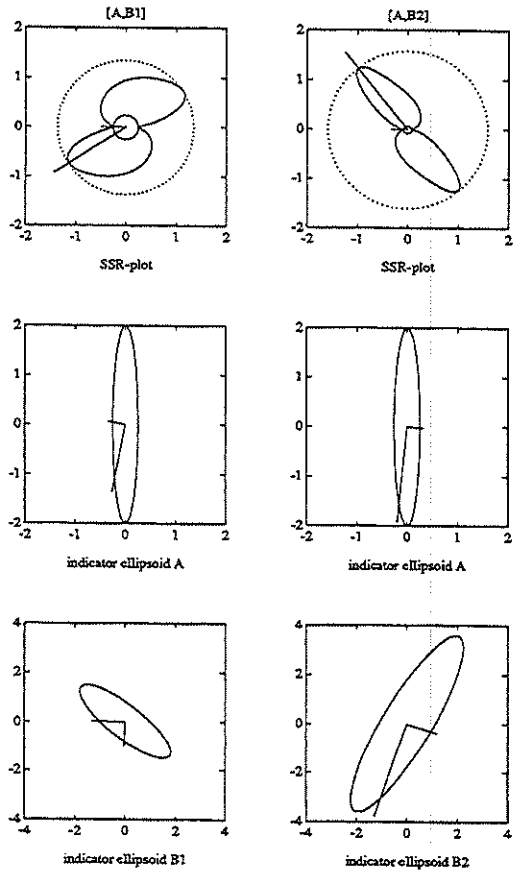

Figure 2.4: Left, the SSR and indicator ellipsoids of the matrix pair $[A, B_1]$ and right those of $[A, B_2]$. The circles have a radius corresponding to $\frac{\alpha_1}{\beta_1}$ and $\frac{\alpha_2}{\beta_2}$. Also shown are the column vectors x_1 and x_2 of X, which are the directions of maximal and minimal SSR. They are not orthogonal. Observe how the plot for the pair $[A, B_1]$ differs considerably from that of $[A, B_2]$. The lines on the plots of the indicator ellipsoids, are the directions of maximal and minimal SSR in the output space. In the output space these directions are orthogonal! However, they do not coincide with semi-axes of the indicator ellipsoids of each matrix separately.

Here we are only interested in the frequencies at the imaginary axis $s = j\omega$. If $G(s)$ has no poles on the imaginary axis, the singular values $\sigma_i(j\omega)$ are continuous, but in general non-differentiable functions of ω. However, the next theorem relates the singular values on the imaginary axis with real analytic functions:

Theorem 7 *There are real analytic functions $f_i : \mathbb{R} \to \mathbb{R}$, $i = 1, \ldots, m$, such that for all $\omega \in \mathbb{R}$,*

$$\{\sigma_1(G(j\omega)), \ldots, \sigma_m(G(j\omega))\} = \{|f_1(\omega)|, \ldots, |f_m(\omega)|\}.$$

The functions $f(.)$ form an *unsigned singular value decomposition* (USVD) of the transfer matrix $G(s)$. Further details can be found in [11] and [31].

It is also possible to show the oriented energy as a function of frequency. This is illustrated with an example.

Example:
Consider a 2×2 transfer matrix, which is for convenience, real on the imaginary axis:

$$G(j\omega) = \begin{pmatrix} 5 & \frac{8-\omega^2}{16.5-\omega^2} \\ \frac{19-\omega^2}{16.5-\omega^2} & \frac{8-\omega^2}{1.4-\omega^2} \end{pmatrix}.$$

The oriented energy plot $u\|G(j\omega)u\|$ is shown in figure 2.5. u varies over all unit norm input vectors. In this case the vector represents the amplitudes and phases of sine waves with frequency ω at the inputs. Putting all these plots one behind the other we obtain the 3-dimensional plot shown in figure 2.6.
At $\omega = \sqrt{8} = 2.828$, $G(j\omega)$: $G(s)$ drops rank. As can be seen on the corresponding plot, this does not imply that the output is zero. The output is zero only when the correct input direction is applied. In all other cases there is still an output signal. This directional aspect does not occur with SISO transfer functions which themselves become zero at a system zero.

2.4.2 Signal-to-signal ratio of transfer matrices

Let us now look at the signal-to-signal ratio of two transfer matrices as a function of frequency. Two different situations can be considered (see figure 2.7), either two systems with the same input and two outputs:

$$y_1 = G_1 u, \qquad y_2 = G_2 u,$$

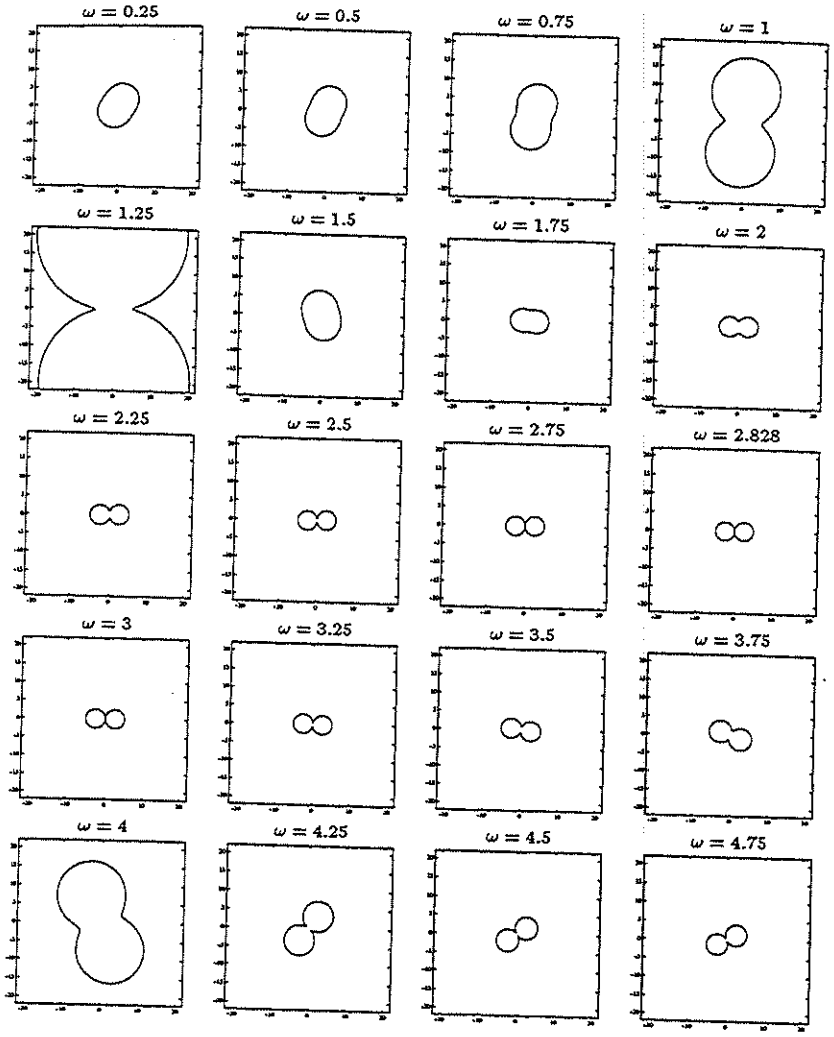

Figure 2.5: The oriented energy plots of $G(j\omega)$ for different values of ω. The direction and size of the largest amplification change drastically. The largest changes occur at the poles: $\omega = \sqrt{1.4}$ and $\omega = \sqrt{16.5}$. Observe also that even at a zero of the transfer matrix ($\omega = 2.828$) on the imaginary axis the output is non-zero unless the input has the correct orientation.

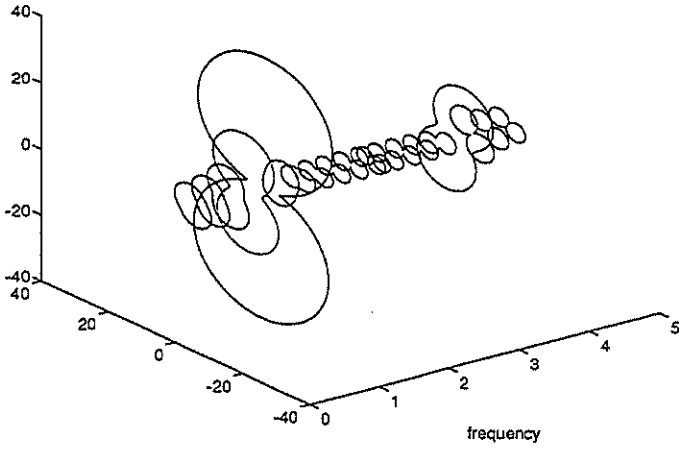

Figure 2.6: A 3D-plot of the oriented energy of a 2×2 transfer matrix.

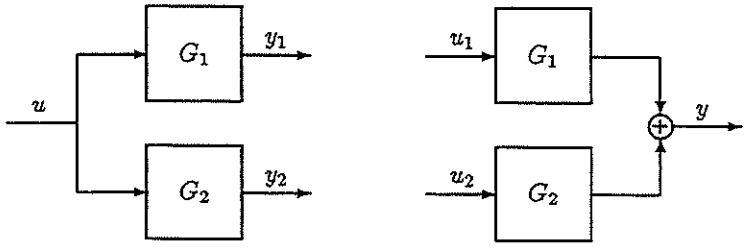

Figure 2.7: Two configurations for the oriented signal-to-signal ratio of two transfer matrices.

or two systems with different inputs, but with a summation of the outputs:

$$y = G_1 u_1 + G_2 u_2.$$

Consider first the case where the two transfer functions have the same input u but different outputs y_1 and y_2. For an interpretation assume that G_2 is a 'good' transfer matrix while G_1 is a disturbing one. Obviously, we would like the relative influence of u on y_1 to be small compared to its influence on y_2. In other words: At each frequency ω, we want the SSR $R_u[G_1(j\omega), G_2(j\omega)]$ as small as possible. Calculate the QSVD at each frequency:

$$y(s) = \begin{pmatrix} y_1(s) \\ y_2(s) \end{pmatrix} = \begin{pmatrix} G_1(s) \\ G_2(s) \end{pmatrix} u(s) = \begin{pmatrix} U_1(s)S_1(s)X^{-1}(s) \\ U_2(s)S_2(s)X^{-1}(s) \end{pmatrix} u(s).$$

The signal-to-signal ratio will be small if the Q-singular values are small for all frequencies. The QSVD reveals the size and the direction of the largest signal-to-signal ratio at each frequency. In control applications the output of the 'disturbing' transfer function G_1 has to be minimized relatively to the output of the 'good' transfer function G_2. The control engineer has to design a controller that minimizes the Q-singular values over all frequencies.

In the second situation there are different inputs u_1 and u_2 and one output y. In matrix notation this becomes:

$$y = \begin{pmatrix} G_1 & G_2 \end{pmatrix} \begin{pmatrix} u_1 \\ u_2 \end{pmatrix}.$$

For each frequency, define the QSVD of G_1 and G_2 as

$$G_1 = YS_1U^* = Y \begin{pmatrix} I & 0 & 0 \\ 0 & D_1 & 0 \\ 0 & 0 & 0 \\ 0 & 0 & 0 \end{pmatrix} U^*,$$

$$G_2 = YS_2V^* = Y \begin{pmatrix} 0 & 0 & 0 \\ 0 & D_2 & 0 \\ 0 & 0 & I \\ 0 & 0 & 0 \end{pmatrix} V^*,$$

with an appropriate partitioning for all matrices. G_1 and G_2 have an equal number of rows. Their common factor is thus the left factor in the product. The right factors U and V are now orthogonal. Then we can write:

$$y = y_1 + y_2 = G_1 u_1 + G_2 u_2 = YS_1U^*u_1 + YS_2V^*u_2.$$

Partition Y, U and V:

$$Y = \begin{pmatrix} Y_1 & Y_2 & Y_3 & Y_4 \end{pmatrix}, \; U = \begin{pmatrix} U_1 & U_2 & U_3 \end{pmatrix}, \; V = \begin{pmatrix} V_1 & V_2 & V_3 \end{pmatrix}.$$

Now decompose the inputs u_1 and u_2 as

$$u_1 = U_1p_1 + U_2p_2 + U_3p_3, \;\; u_2 = V_1q_1 + V_2q_2 + V_3q_3$$

for some vectors p_1, p_2, p_3, q_1, q_2 and q_3. Then

$$\begin{aligned} y &= \begin{pmatrix} Y_1 & Y_2D_1 & 0 \end{pmatrix} \begin{pmatrix} p_1 \\ p_2 \\ p_3 \end{pmatrix} + \begin{pmatrix} 0 & Y_2D_2 & Y_3 \end{pmatrix} \begin{pmatrix} q_1 \\ q_2 \\ q_3 \end{pmatrix} \\ &= Y_1p_1 + Y_2(D_1p_2 + D_2q_2) + Y_3q_3 \\ &= \begin{pmatrix} Y_1 & Y_2 & Y_3 \end{pmatrix} \begin{pmatrix} p_1 \\ D_1p_2 + D_2q_2 \\ q_3 \end{pmatrix}. \end{aligned}$$

From this we can conclude that there is a directional decoupling. Some directions in the output space can only be influenced by the first input. In these directions the Q-singular values $\frac{\alpha_i}{\beta_i}$ are infinite. Other directions can only be controlled by the second input. In these directions the Q-singular values $\frac{\alpha_i}{\beta_i}$ are 0. Finally, there are directions that are controlled by both inputs.

The SSR is, in this case, a ratio of input signals. Suppose u_1 and u_2 are vectors of sinusoidal signals with the same frequency ω. Call u_{1y} the input signal that produces an output signal in the direction y, when no input u_2 is present. Define u_{2y} as the input signal u_2 that produces the same output y, when $u_1 = 0$. Then the SSR in the output direction y, is the ratio of the norms of the input signals u_{2y} and u_{1y}. A SSR value larger than one shows that the corresponding direction y is controlled relatively more by u_1 than by u_2. Or the same output signal y can be generated by a smaller signal u_1 than u_2.

For a control interpretation, suppose that u_2 is the 'good' input while u_1 is the disturbing one. Thus y has to be controlled mainly by u_2. A controller has to be designed that minimizes the Q-singular values of the pair $(G_1(j\omega), G_2(j\omega))$ at all frequencies.

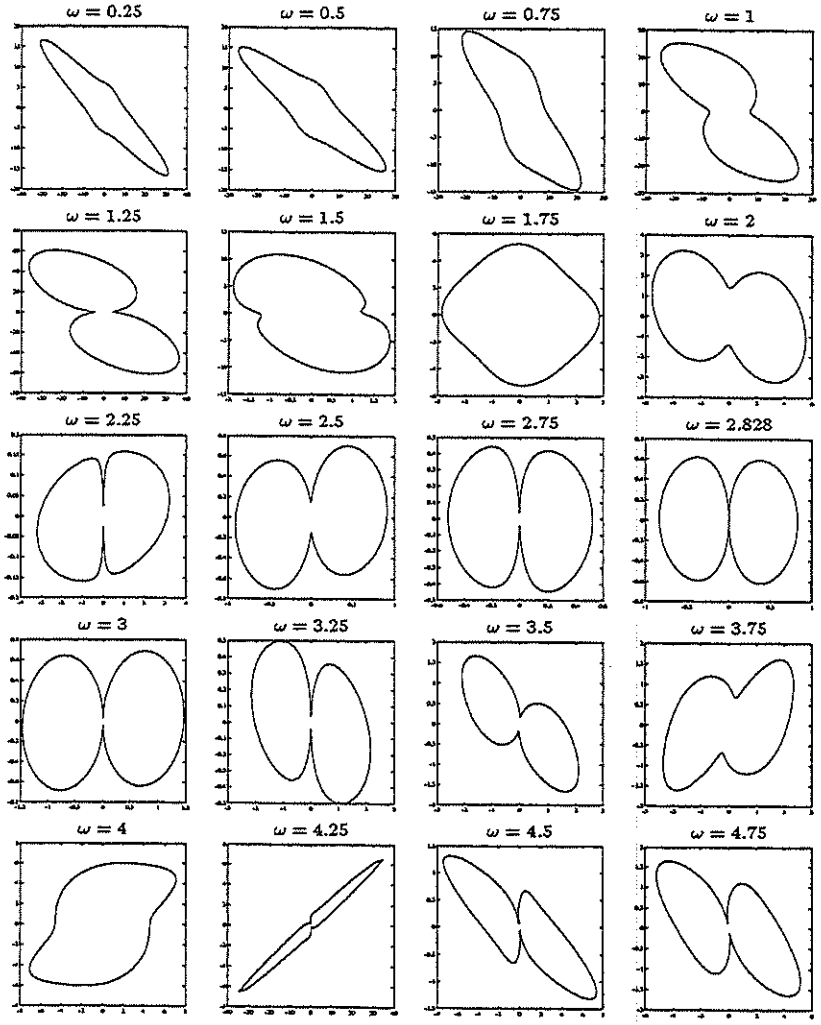

Figure 2.8: The SSR-plot at different frequencies ω, of two transfer matrices with two inputs for all unit norm input vectors. The direction and size of the SSR-plot can change drastically with the frequency. Note that the plots have different scales! Notice that the directions of maximal and minimal SSR are, in general, not orthogonal.

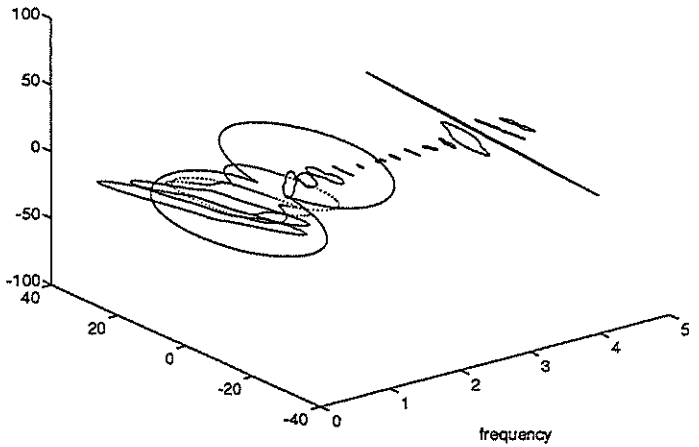

Figure 2.9: A 3D view of the signal-to-signal ratio of two transfer matrices.

Example:

As an example, take two transfer matrices in the first configuration (with the same input u):

$$G_1(s) = \begin{pmatrix} 5 & \frac{s^2+8}{s^2+16.5} \\ \frac{s^2+19}{s^2+16.5} & \frac{s^2+8}{s^2+1.4} \end{pmatrix}, \qquad G_2(s) = \begin{pmatrix} \frac{1}{s^2+2.5} & \frac{s^2+3}{s^2+5} \\ \frac{2}{s^2+13} & \frac{s^2+5}{s^2+10} \\ \frac{s^2+2}{s^2+7} & \frac{s^2+11}{s^2+19} \end{pmatrix}.$$

The signal-to-signal ratio is plotted for different values of ω in figure 2.8. The maximal and minimal signal-to-signal ratio and direction vary quite drastically with changing ω. Notice that when G_2 becomes small, the signal-to-signal ratio becomes large (around $\omega = 1.25$). If G_1 has a zero on the imaginary axis, the SSR becomes zero in one direction.

The directions and sizes of the maximum and minimum SSR can be obtained using the QSVD. Recall once more that these directions are in general *not* orthogonal in the input space.

2.5 Norms for Directional Aspects of Two Transfer Matrices

In this section some new norms are defined that characterize directional aspects of two transfer matrices relative to one another. They are extensions of the classical H_2 and H_∞ norms for one transfer matrix to the case of two matrices.

2.5.1 The QH_2 norm

In this section we introduce the QH_2 norm for two transfer matrices as a generalization of the classical H_2 norm. We show its connection with the H_2 norm and derive its calculation from the state space models of the transfer matrices.

Definition

The H_2 norm of a stable $l \times m$ transfer matrix $G(s) = C(sI - A)^{-1}B$ is defined as

$$\|G\|_2^2 = \frac{1}{2\pi}\int_{-\infty}^{+\infty} \text{trace}\{G(j\omega)^* G(j\omega)\} d\omega.$$

This can also be expressed in terms of its singular values:

$$\|G\|_2^2 = \frac{1}{2\pi}\int_{-\infty}^{+\infty} \sum_{i=1}^{\min(l,m)} \sigma_i^2(G(j\omega))\, d\omega.$$

The H_2 norm of a transfer matrix G can easily be calculated from its state space representation. If L_c denotes the controllability Gramian of G and L_o denotes its observability Gramian, satisfying the following Lyapunov equations

$$AL_c + L_cA^t + BB^t = 0, \qquad A^tL_o + L_oA + C^tC = 0,$$

then

$$\|G\|_2^2 = \text{trace}(CL_cC^t) = \text{trace}(B^tL_oB).$$

Similarly, we will define the QH_2 norm for a pair of matrices and give its calculation from a state space realization.

Consider the setup with one set of inputs and two sets of outputs (situation 1) with state space model:

$$G(s) = \begin{pmatrix} G_1(s) \\ G_2(s) \end{pmatrix} = \left(\begin{array}{c|c} A & B \\ \hline C_1 & D_1 \\ C_2 & D_2 \end{array}\right),$$

where $G_1(s) = D_1 + C_1(sI - A)^{-1}B$ and $G_2(s) = D_2 + C_2(sI - A)^{-1}B$. If A is stable, we call the transfer matrix pair $(G_1(s), G_2(s))$ stable.

Definition 4 *The QH_2 norm of a stable transfer matrix pair $(G_1(s), G_2(s))$, with an equal number of inputs and $G_2(j\omega)$ of full column rank $\forall\omega \in \mathbb{R}$, is*

$$\left\|\frac{G_1}{G_2}\right\|_{Q-2}^2 = \frac{1}{2\pi}\int_{-\infty}^{+\infty} \text{trace}\Big\{(G_2^*(j\omega)G_2(j\omega))^{-1}(G_1^*(j\omega)G_1(j\omega))\Big\}\, d\omega.$$

It is obvious that the QH_2 norm is only finite if

$$(G_2^*(\infty)G_2(\infty))^{-1}(G_1^*(\infty)G_1(\infty)) = 0.$$

As $G_2^*(\infty)G_2(\infty)$ has to be invertible, this implies that $G_2(\infty)$ is of full column rank and $G_1(\infty) = 0$.
The QH_2 norm can also be expressed in terms of the Q-singular values:

Lemma 2 *Suppose G_1 and G_2 are two transfer functions with m inputs, and $G_2(j\omega)$ is of full column rank $\forall\omega \in \mathbb{R}$, then*

$$\left\|\frac{G_1}{G_2}\right\|_{Q-2}^2 = \frac{1}{2\pi}\int_{-\infty}^{+\infty} \sum_{i=1}^{r_a} \left(\frac{\alpha_i(j\omega)}{\beta_i(j\omega)}\right)^2 d\omega,$$

where r_a is the generic rank of $G_1(j\omega)$.

Proof:
$G_1(s)$ $(l \times m)$ and $G_2(s)$ $(p \times m)$ can always be factored such that

$$G_1(s) = U_1(s)S_1(s)X^{-1}(s), \quad G_2(s) = U_2(s)S_2(s)X^{-1}(s),$$

where $U_1(s)$ and $U_2(s)$ are unitary, and $X(s)$ is a nonsingular square matrix. Because G_2 is of full column rank on the imaginary axis, the following statements hold on the $j\omega$-axis: rank $G_2 = m$ and rank $\begin{pmatrix} G_1 \\ G_2 \end{pmatrix} = m$.

The matrices S_1 and S_2 have the following structure:

$$S_1 = \begin{array}{c} \\ r_a \\ l-r_a \end{array} \begin{array}{c} \begin{array}{cc} r_a & m-r_a \end{array} \\ \begin{pmatrix} D_a & 0 \\ 0 & 0 \end{pmatrix} \end{array}, \quad S_2 = \begin{array}{c} \\ p-m \\ r_a \\ m-r_a \end{array} \begin{array}{c} \begin{array}{cc} r_a & m-r_a \end{array} \\ \begin{pmatrix} 0 & 0 \\ D_b & 0 \\ 0 & I \end{pmatrix} \end{array},$$

where

$$D_a = \begin{pmatrix} \alpha_1 & 0 & & 0 \\ 0 & \alpha_2 & & 0 \\ & & \ddots & 0 \\ 0 & 0 & & \alpha_{r_a} \end{pmatrix}, \quad D_b = \begin{pmatrix} \beta_1 & 0 & & 0 \\ 0 & \beta_2 & & 0 \\ & & \ddots & 0 \\ 0 & 0 & & \beta_{r_a} \end{pmatrix},$$

such that $\alpha_i^2 + \beta_i^2 = 1$.

This yields

$$\begin{aligned} \left\| \frac{G_1}{G_2} \right\|_{Q-2}^2 &= \frac{1}{2\pi} \int_{-\infty}^{+\infty} \text{trace} \left\{ (G_2^* G_2)^{-1} (G_1^* G_1) \right\} d\omega \\ &= \frac{1}{2\pi} \int_{-\infty}^{+\infty} \text{trace} \left\{ (X^{-*} S_2^t S_2 X^{-1})^{-1} (X^{-*} S_1^* S_1 X^{-1}) \right\} d\omega \\ &= \frac{1}{2\pi} \int_{-\infty}^{+\infty} \text{trace} \left\{ X (S_2^t S_2)^{-1} X^* X^{-*} (S_1^t S_1) X^{-1} \right\} d\omega \\ &= \frac{1}{2\pi} \int_{-\infty}^{+\infty} \text{trace} \left\{ (S_2^t S_2)^{-1} (S_1^t S_1) \right\} d\omega \\ &= \frac{1}{2\pi} \int_{-\infty}^{+\infty} \text{trace} \left\{ \begin{pmatrix} D_b^2 & 0 \\ 0 & I \end{pmatrix}^{-1} \begin{pmatrix} D_a^2 & 0 \\ 0 & 0 \end{pmatrix} \right\} d\omega \\ &= \frac{1}{2\pi} \int_{-\infty}^{+\infty} \sum_{i=1}^{r_a} \left(\frac{\alpha_i}{\beta_i} \right)^2 d\omega. \end{aligned}$$

□

Observe that the full column rank assumption for G_2 implies that G_2 has no finite pure imaginary transmission zeros.

Similarly for the case of two inputs and a summation of the outputs, the following state space model is considered:

$$G(s) = \begin{pmatrix} G_1(s) & G_2(s) \end{pmatrix} = \left(\begin{array}{c|cc} A & B_1 & B_2 \\ \hline C & D_1 & D_2 \end{array} \right),$$

where $G_1(s) = D_1 + C(sI - A)^{-1}B_1$ and $G_2(s) = D_2 + C(sI - A)^{-1}B_2$. If A is stable, the transfer matrix pair $\begin{pmatrix} G_1(s) & G_2(s) \end{pmatrix}$ is called stable.

Definition 5 *The QH_2 norm of a stable transfer matrix pair $(G_1(s), G_2(s))$, with an equal number of outputs and $G_2(j\omega)$ of full row rank $\forall \omega \in \mathbb{R}$, is*

$$\left\| \; G_1 \mid G_2 \; \right\|_{Q-2}^2 = \frac{1}{2\pi} \int_{-\infty}^{+\infty} \text{trace} \left\{ (G_2(j\omega) G_2^*(j\omega))^{-1} (G_1(j\omega) G_1^*(j\omega)) \right\} d\omega.$$

Again $G_2(\infty)$ has to be full row rank and $G_1(\infty) = 0$. The norm can also be expressed in terms of the Q-singular values:

$$\begin{aligned} \left\| \; G_1 \mid G_2 \; \right\|_{Q-2}^2 &= \frac{1}{2\pi} \int_{-\infty}^{+\infty} \sum_{i=1}^{r_a} \sigma_{qi}(G_1(j\omega, G_2(j\omega))^2 \, d\omega \\ &= \frac{1}{2\pi} \int_{-\infty}^{+\infty} \sum_{i=1}^{r_a} \left(\frac{\alpha_i(j\omega)}{\beta_i(j\omega)} \right)^2 d\omega. \end{aligned}$$

Observe also that the full row rank assumption for G_2 implies that G_2 has no finite pure imaginary transmissions zeros and no zeros at ∞.

Both definitions are equivalent. It is easily observed that

$$\| \; G_1 \mid G_2 \; \|_{Q-2} = \left\| \frac{G_1^*}{G_2^*} \right\|_{Q-2}.$$

The norm of the system with two inputs and one output can thus be computed as the norm of the system with one output and two inputs, replacing $G_1(s)$ and $G_2(s)$ by $G_1(s)^*$ and $G_2(s)^*$. Therefore, we will only look at the setup with one input and two outputs in the next chapters. However, everything can be generalized to the other case.

Relation with the H_2 norm.

Let us now investigate the relation between the H_2 norm and the QH_2 norm. Recall that the QSVD of a matrix pair (A, B) is related to the SVD of AB^{-1} if B is invertible:

$$AB^{-1} = U S_a X^{-1} X S_b^{-1} V^* = U (S_a S_b^{-1}) V^*.$$

The same observation applies for transfer matrices with however one complication if G_2 is non-minimum phase. First, consider the special case where G_2 is stably invertible. $D_1 = 0$ to ensure a finite QH_2 norm.

$$\left\{ \begin{array}{rcl} \dot{x} & = & Ax + Bu \\ y_1 & = & C_1 x \\ y_2 & = & C_2 x + D_2 u, \end{array} \right.$$

so that

$$u = D_2^\dagger y_2 - D_2^\dagger C_2 x,$$

where $D_2^\dagger$ denotes the pseudo inverse of D_2. Substitution in the state space realization of G_1 yields (with $D_1 = 0$):

$$\left\{ \begin{array}{rcl} \dot{x} & = & (A - BD_2^\dagger C_2)x + BD_2^\dagger y_2 \\ y_1 & = & C_1 x. \end{array} \right.$$

This is exactly the state space realization of $G_1 G_2^\dagger$. Thus the QH_2 norm of $\begin{pmatrix} G_1 \\ G_2 \end{pmatrix}$ can be computed from

$$\|G_1 G_2^\dagger\|_2.$$

More general, if G_2 contains zeros in the right half plane (non-minimum-phase zeros), it has no stable inverse. However, one can then compute a unique minimum phase spectral factor G_3 of $G_2^* G_2$, which has a stable inverse.

Lemma 3 *If $G_1(s)$ and $G_2(s)$ are stable, have an equal number of inputs and $G_2(s)$ is of full column rank on the $j\omega$-axis, then*

$$\left\| \frac{G_1}{G_2} \right\|_{Q-2}^2 = \|G_1 G_3^{-1}\|_2^2,$$

where G_3 is the spectral factor of $G_2^* G_2$:

$$G_2^* G_2 = G_3^* G_3,$$

with G_3 as well as G_3^{-1} stable.

Proof:
Because G_2 is full column rank on the $j\omega$-axis, a spectral factor G_3 exists such that $G_2^* G_2 = G_3^* G_3$ ([49]). The spectral factor is square.

$$\begin{aligned} \left\| \frac{G_1}{G_2} \right\|_{Q-2} &= \frac{1}{2\pi} \int_{-\infty}^{+\infty} \text{trace} \left\{ (G_2^* G_2)^{-1} (G_1^* G_1) \right\} d\omega \\ &= \frac{1}{2\pi} \int_{-\infty}^{+\infty} \text{trace} \left\{ (G_3^* G_3)^{-1} (G_1^* G_1) \right\} d\omega \\ &= \frac{1}{2\pi} \int_{-\infty}^{+\infty} \text{trace} \left\{ G_3^{-1} G_3^{-*} G_1^* G_1 \right\} d\omega \\ &= \frac{1}{2\pi} \int_{-\infty}^{+\infty} \text{trace} \left\{ (G_1 G_3^{-1})^* (G_1 G_3^{-1}) \right\} d\omega \\ &= \|G_1 G_3^{-1}\|_2. \end{aligned}$$

□

Computing the QH_2 norm

Suppose a stable state space realization of $G_1(s)$ and $G_2(s)$ is known:

$$\begin{pmatrix} G_1 \\ G_2 \end{pmatrix} = \left(\begin{array}{c|c} A & B \\ \hline C_1 & 0 \\ C_2 & D_2 \end{array} \right).$$

If $G_2(s)$ is of full column rank on the $j\omega$-axis and its state space realization $D_2 + C_2(sI - A)^{-1}B$ is minimal, then the QH_2 norm can easily be computed from the state space realization. This is shown in the following lemma:

Lemma 4 *If $G_1(s)$ and $G_2(s)$ have an equal number of inputs, G_1 is strictly proper and $G_2(s)$ is stable and of full column rank on the $j\omega$-axis and (A, B, C_2, D_2) a minimal realization of G_2, then*

$$\left\| \frac{G_1}{G_2} \right\|_{Q-2}^2 = \textit{trace} \left\{ C_1 Q C_1^t \right\}$$

where Q is the solution of

$$A_x Q + Q A_x^t + B(D_2^t D_2)^{-1} B^t = 0. \tag{2.1}$$

A_x is defined as

$$A_x = A - B(D_2^t D_2)^{-1}(D_2^t C_2 + B^t X),$$

and X is the solution of

$$X\underline{A} + \underline{A}^t X - X\underline{R}X + \underline{Q} = 0, \tag{2.2}$$

where

$$\begin{aligned} \underline{A} &= A - B(D_2^t D_2)^{-1} D_2^t C_2, \\ \underline{R} &= B(D_2^t D_2)^{-1} B^t, \\ \underline{Q} &= C_2^t C_2 - C_2^t D_2 (D_2^t D_2)^{-1} D_2^t C_2. \end{aligned}$$

Proof:
From the previous lemma we know that we first have to find a spectral factor G_3 of $G_2^* G_2$. A state space realization of G_3 is ([49]):

$$G_3 = \left(\begin{array}{c|c} A & B \\ \hline \underline{D}^{-\frac{1}{2}}(D_2^t C_2 + B^t X) & \underline{D}^{-\frac{1}{2}} \end{array} \right), \tag{2.3}$$

where $\underline{D} = D_2^t D_2$ and X is the solution of (2.2).
The state space realization of G_3^{-1} is

$$H_3^{-1} = \left(\begin{array}{c|c} A_{3i} & B_{3i} \\ \hline C_{3i} & D_{3i} \end{array} \right),$$

where

$$\begin{aligned} A_{3i} &= A - B\underline{D}^{-1}(D_2^t C_2 + B^t X), & B_{3i} &= B\underline{D}^{-\frac{1}{2}} \\ C_{3i} &= -\underline{D}^{-1}(D_2^t C_2 + B^t X), & D_{3i} &= \underline{D}^{-\frac{1}{2}}. \end{aligned}$$

Multiplying G_1 and G_3^{-1} yields

$$G_1 G_3^{-1} = \left(\begin{array}{cc|c} A & -B\underline{D}^{-1}(D_2^t C_2 + B^t X) & B\underline{D}^{-\frac{1}{2}} \\ 0 & A - B\underline{D}^{-1}(D_2^t C_2 + B^t X) & B\underline{D}^{-\frac{1}{2}} \\ \hline C_1 & 0 & 0 \end{array} \right).$$

Apply a similarity transformation with $T = \begin{pmatrix} I & I \\ 0 & I \end{pmatrix}$. The matrices of $G_1 G_3^{-1}$ are transformed in

$$T^{-1} \begin{pmatrix} A & -B\underline{D}^{-1}(D_2^t C_2 + B^t X) \\ 0 & A - B\underline{D}^{-1}(D_2^t C_2 + B^t X) \end{pmatrix} T = \begin{pmatrix} A & 0 \\ 0 & A - B\underline{D}^{-1}(D_2^t C_2 + B^t X) \end{pmatrix},$$

$$T^{-1} \begin{pmatrix} B\underline{D}^{-\frac{1}{2}} \\ B\underline{D}^{-\frac{1}{2}} \end{pmatrix} = \begin{pmatrix} 0 \\ B\underline{D}^{-\frac{1}{2}} \end{pmatrix}, \quad \begin{pmatrix} C_1 & 0 \end{pmatrix} T = \begin{pmatrix} C_1 & C_1 \end{pmatrix}.$$

Hence,

$$G_1 G_3^{-1} = \left(\begin{array}{cc|c} A & 0 & 0 \\ 0 & A - B\underline{D}^{-1}(D_2^t C_2 + B^t X) & B\underline{D}^{-\frac{1}{2}} \\ \hline C_1 & C_1 & 0 \end{array} \right).$$

Deleting the uncontrollable part yields

$$G_1 G_3^{-1} = \left(\begin{array}{c|c} A - B\underline{D}^{-1}(D_2^t C_2 + B^t X) & B\underline{D}^{-\frac{1}{2}} \\ \hline C_1 & 0 \end{array} \right). \tag{2.4}$$

$\|G_1 G_3^{-1}\|_2$ can now be calculated as trace$\{C_1 Q C_1^t\}$ where Q is the solution of (2.1). □

If $D_2 + C_2(sI - A)^{-1}B$ is not a minimal state space realization of G_2, then first a minimal realization has to be obtained. (2.2) is still valid using for A, B, C_2 and D_2 a minimal realization of G_2. However, (2.4) and (2.1) cannot be used any more. For a state space realization of the spectral factor G_3, see e.g. [49].

Example:
Let G_1 and G_2 be 2×2 transfer matrices with the following state space realization:

$$\begin{pmatrix} G_1 \\ G_2 \end{pmatrix} = \left(\begin{array}{c|c} A & B \\ \hline C_1 & D_1 \\ C_2 & D_2 \end{array} \right)$$

$$= \left(\begin{array}{cccc|cc} -1.7248 & -0.5282 & 0.4624 & 1.4348 & -1.2735 & 175.6686 \\ 1.5608 & -3.0347 & 1.6567 & 0.1683 & -231.5284 & 122.1187 \\ 0.6891 & -0.6996 & -2.4053 & 0.6253 & -154.1046 & -31.8661 \\ -1.1154 & 0.5728 & 0.5063 & -0.1347 & -37.6361 & -29.0237 \\ \hline -166.7150 & 149.5111 & -76.6974 & 102.4094 & 0 & 0 \\ 161.0284 & 54.7933 & -84.4153 & -13.9756 & 0 & 0 \\ \hline -1.2019 & -1.1340 & 0.1163 & -0.5071 & 0.4003 & 1.4079 \\ -0.2919 & -0.0209 & -0.6422 & -0.6246 & -0.6395 & 0.6615 \end{array} \right).$$

Applying the procedure described above, the QH_2 norm is 4.5521e+03.

Similar formulas to compute the QH_2 norm can be derived in the discrete time case.

2.5.2 The QL_∞ norm and QH_∞ norm

The L_∞ norm and H_∞ norm can also be generalized for the ratio of the outputs of two transfer functions. A level set algorithm to calculate the norm is also described.

Definitions

Definition 6 *If $G_1(s)$ and $G_2(s)$ are two transfer matrices with the same number of inputs, $G_1(s)$ has no imaginary poles and $G_2(s)$ is of full column rank on the $j\omega$-axis, then the QL_∞ norm of the two transfer matrices is defined as*

$$\left\| \frac{G_1}{G_2} \right\|_{Q-\infty} = \sup_{\omega \in \mathbb{R}} \sigma_{q1} \left(G_1(j\omega), G_2(j\omega) \right).$$

Definition 7 *If $G_1(s)$ and $G_2(s)$ are two transfer matrices with the same number of inputs, $G_1(s)$ is stable and $G_2(s)$ is stable and of full column rank on the right half plane, then the QH_∞ norm of the transfer matrices is defined as*

$$\left\| \frac{G_1}{G_2} \right\|_{Q-\infty} = \sup_{Re(s) \geq 0} \sigma_{q1} \left(G_1(s), G_2(s) \right).$$

When G_1 is stable and all the zeros of G_2 are in the open left half plane, then the QL_∞ and QH_∞ norm coincide. We use the same notation for the QL_∞ and the QH_∞ norm. What norm is used is clear in the context.
The definition of the norms are given for the case with one common inputvector and two outputvectors. However, it is clear that a similar definition can be given for the case with two inputs and one output.
The QH_∞ norm is the largest ratio of the energies of the output signals, over all frequencies.
Again G_2 is assumed to be of full rank on the $j\omega$-axis. Otherwise one of the Q-singular values would become $\frac{1}{0}$ or $\frac{0}{0}$. This would make the QH_∞ norm ∞ or undefined. This property also corresponds to the condition that G_2 has to be analytic in the right half plane.

Because G_2 is of full column rank, the Q-singular values will be equal to the singular values of $(G_1^* G_1 (G_2^* G_2)^{-1})^{\frac{1}{2}}$. Thus, all the properties on the singular values of a transfer matrix of [11] are also valid for the Q-singular values, under the usual conditions. Some of these properties are ([11], [31]):

1. If $\sigma_{qi}(G_1(j\omega_0), G_2(j\omega_0)) > 0$ and has multiplicity one, then $\sigma_{qi}(G_1(j\omega), G_2(j\omega)) > 0$ is *real analytic* near ω_0.
2. There are real analytic functions f_i: $\mathbb{R} \to \mathbb{R}, i = 1, \ldots, m$, such that for all $\omega \in \mathbb{R}$,

   $$\{\sigma_{q1}(G_1(j\omega), G_2(j\omega)), \ldots, \sigma_{qm}(G_1(j\omega), G_2(j\omega))\} = \{|f_1(\omega)|, \ldots, |f_m(\omega)|\}.$$

   These functions f_i can be considered as *unordered, unsigned* 'Q-singular values'. We will illustrate this with an example.

   Example:

   The first plot in figure 2.10 shows the Q-singular values of a pair of transfer matrices. The functions $\sigma_{qi}(j\omega)$ are continuous but non-differentiable functions. The second plot shows continuous differentiable functions that can be interpreted as unordered, unsigned Q-singular values.
3. If $\sigma_{q1}(G_1(j\omega), G_2(j\omega))$ has a local maximum at ω_M, then near ω_M, it has a continuous second derivative.

It is well-known that the H_∞ norm of a transfer function is smaller than γ, if there exists a positive definite solution to a certain Riccati equation ([101]). This is extended to the QH_∞ norm.

Lemma 5 *Consider*

$$\begin{pmatrix} G_1 \\ G_2 \end{pmatrix} = \left(\begin{array}{c|c} A & B \\ \hline C_1 & 0 \\ C_2 & D_2 \end{array} \right).$$

If $G_2(s)$ is of full column rank and (A, C) is observable and (A, B) is controllable, where

$$C = \begin{pmatrix} C_1 \\ C_2 \end{pmatrix},$$

then the following statements are equivalent:

(i)

$$\left\| \frac{G_1(s)}{G_2(s)} \right\|_{Q-\infty} < \gamma. \tag{2.5}$$

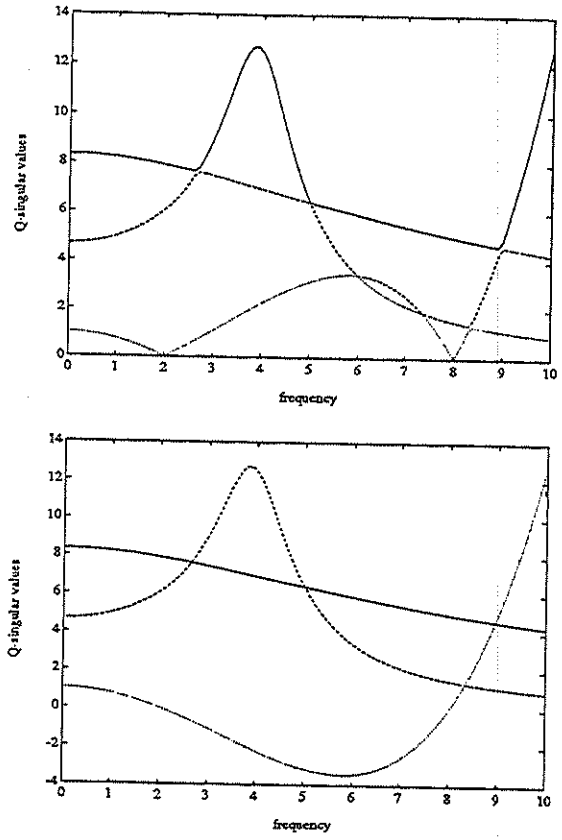

Figure 2.10: In the first plot the Q-singular values of a transfer matrix pair are plotted. The second plot are real analytic functions f_i, such that the set of absolute values at each frequency is equal to the set of Q-singular values. Observe that the functions f_i are allowed to become negative.

(ii) $\exists X = X^t > 0$ *and* $\exists P = P^t > 0$ *satisfying the Riccati equations*

$$X\underline{A} + \underline{A}^t X - X\underline{R}X + \underline{Q} = 0, \tag{2.6}$$

$$PA_t + A_t^t P + \gamma^{-2} PB\underline{D}^{-1}B^t P + C_1^t C_1 = 0, \tag{2.7}$$

where

$$\begin{aligned} \underline{A} &= A - B\underline{D}^{-1}D_2^t C_2, \\ \underline{R} &= B\underline{D}^{-1}B^t, \\ \underline{Q} &= C_2^t(I - D_2\underline{D}^{-1}D_2^t)C_2, \\ \underline{D} &= D_2^t D_2, \\ A_t &= A - B\underline{D}^{-1}(D_2^t C_2 + B^t X), \end{aligned}$$

such that $A_t + \gamma^{-2}B\underline{D}^{-1}B^t P$ *is stable.*

(iii) $\exists X = X^t > 0$ *and* $\exists S = S^t > 0$ *satisfying the Riccati equations*

$$X\underline{A} + \underline{A}^t X - X\underline{R}X + \underline{Q} = 0, \tag{2.8}$$

$$A_t S + SA_t^t + \gamma^{-2} SC_1^t C_1 S + B\underline{D}^{-1}B^t = 0, \tag{2.9}$$

such that $A_t + \gamma^{-2}SC_1^t C_1$ *is stable.*

Proof: This is a direct extension of the H_∞-case because we can find an invertible spectral factor G_3 of $G_2^* G_2$. □

In discrete time similar definitions can be given. The $j\omega$-axis is replaced by the unit circle and the right half plane by the region outside the unit disk.

A Level Set Algorithm for QL_∞ norm

In [11] a quadratically convergent algorithm for computing the L_∞ norm is described. This algorithm can be generalized to compute the QL_∞ norm. The main idea exploited in [11] is the following:
Let σ be a singular value of the transfer matrix $G(j\omega)$ at a certain frequency ω, then

$$\begin{aligned} (D + C(j\omega I_n - A)^{-1}B)v &= u\sigma, \\ (D^t + B^t(-j\omega I_n - A^t)^{-1}C^t)u &= v\sigma, \end{aligned}$$

for two vectors u and v. The idea is now to determine the *level set* of σ, i.e. the set of values ω for which σ is a singular value. Further it is shown

that the level set follows from the pure imaginary eigenvalues of a certain Hamiltonian matrix. Here, a similar approach will be followed to prove the next theorem:

Theorem 8 *Consider the transfer matrix pair $G_1(j\omega)$ and $G_2(j\omega)$:*

$$\begin{pmatrix} G_1(j\omega) \\ G_2(j\omega) \end{pmatrix} = \begin{pmatrix} D_1 \\ D_2 \end{pmatrix} + \begin{pmatrix} C_1 \\ C_2 \end{pmatrix} (j\omega I_n - A)^{-1} B.$$

The pair (α, β) with $\alpha^2 + \beta^2 = 1$ is a quotient singular value pair of the pair of transfer matrices $G_1(j\omega)$ and $G_2(j\omega)$ at the frequency ω if $j\omega$ is an eigenvalue of the matrix M_γ, where

$$\begin{aligned} M_\gamma &= \begin{pmatrix} A^t & 0 & 0 \\ 0 & A^t & 0 \\ 0 & 0 & -A \end{pmatrix} \\ &+ \begin{pmatrix} C_1^t & 0 & 0 \\ 0 & C_2^t & 0 \\ 0 & 0 & -B \end{pmatrix} \begin{pmatrix} -\alpha I & 0 & D_1 \\ 0 & -\beta I & D_2 \\ D_1^t\beta & -D_2^t\alpha & 0 \end{pmatrix}^{-1} \begin{pmatrix} 0 & 0 & -C_1 \\ 0 & 0 & -C_2 \\ -B^t\beta & B^t\alpha & 0 \end{pmatrix}. \end{aligned}$$

Proof:
Let (α, β) with $\alpha^2 + \beta^2 = 1$ be a quotient singular value pair of the pair of transfer matrices $G_1(j\omega)$ and $G_2(j\omega)$ at a certain frequency ω where

$$G(j\omega) = \begin{pmatrix} G_1(j\omega) \\ G_2(j\omega) \end{pmatrix} = \begin{pmatrix} D_1 \\ D_2 \end{pmatrix} + \begin{pmatrix} C_1 \\ C_2 \end{pmatrix} (j\omega I_n - A)^{-1} B.$$

From Lemma 1 we find that there must exist three vectors u, v and x such that

$$\begin{aligned} (D_1 + C_1(j\omega I_n - A)^{-1}B)x &= u\alpha, \\ (D_2 + C_2(j\omega I_n - A)^{-1}B)x &= v\beta, \\ (D_1^t + B^t(-j\omega I_n - A^t)^{-1}C_1^t)u\beta &= (D_2^t + B^t(-j\omega I_n - A^t)^{-1}C_2^t)v\alpha, \end{aligned}$$

with $\alpha^2 + \beta^2 = 1$. Now call

$$\begin{aligned} y &= (j\omega I_n - A)^{-1}Bx, \\ p &= (-j\omega I_n - A^t)^{-1}C_1^t u, \\ q &= (-j\omega I_n - A^t)^{-1}C_2^t v, \end{aligned}$$

then

$$\begin{pmatrix} -\alpha I & 0 & D_1 \\ 0 & -\beta I & D_2 \\ D_1^t\beta & -D_2^t\alpha & 0 \end{pmatrix} \begin{pmatrix} u \\ v \\ x \end{pmatrix} = \begin{pmatrix} 0 & 0 & -C_1 \\ 0 & 0 & -C_2 \\ -B^t\beta & B^t\alpha & 0 \end{pmatrix} \begin{pmatrix} p \\ q \\ y \end{pmatrix},$$

$$\begin{pmatrix} -j\omega I_n - A^t & 0 & 0 \\ 0 & -j\omega I_n - A^t & 0 \\ 0 & 0 & -j\omega I_n + A \end{pmatrix} \begin{pmatrix} p \\ q \\ y \end{pmatrix} = \begin{pmatrix} C_1^t & 0 & 0 \\ 0 & C_2^t & 0 \\ 0 & 0 & -B \end{pmatrix} \begin{pmatrix} u \\ v \\ x \end{pmatrix}.$$

We would now like to eliminate the vector $(u^t\ v^t\ x)^t$ which obviously requires the non-singularity of the matrix

$$\begin{pmatrix} -\alpha I & 0 & D_1 \\ 0 & -\beta I & D_2 \\ D_1^t\beta & -D_2^t\alpha & 0 \end{pmatrix}.$$

It is straightforward to show that this matrix is nonsingular if (α, β) is not a quotient singular value pair of (D_1, D_2). This can be seen as follows. Let the QSVD of D_1, D_2 be given as

$$D_1 = U_1 S_1 X^{-1}, \quad D_2 = U_2 S_2 X^{-1},$$

where (α_i, β_i) are the quotient singular value pairs, then

$$\begin{aligned} &\begin{pmatrix} -\alpha I & 0 & D_1 \\ 0 & -\beta I & D_2 \\ D_1^t\beta & -D_2^t\alpha & 0 \end{pmatrix} \\ &= \begin{pmatrix} U_1 & 0 & 0 \\ 0 & U_2 & 0 \\ 0 & 0 & X^{-t} \end{pmatrix} \begin{pmatrix} -\alpha I & 0 & S_1 \\ 0 & -\beta I & S_2 \\ S_1^t\beta & -S_2^t\alpha & 0 \end{pmatrix} \begin{pmatrix} U_1^t & 0 & 0 \\ 0 & U_2^t & 0 \\ 0 & 0 & X^{-1} \end{pmatrix}. \end{aligned}$$

While the left and right factors are clearly non-singular, the determinant of the middle factor will be a product of determinants of the form

$$\det \begin{pmatrix} -\alpha & 0 & \alpha_i \\ 0 & -\beta & \beta_i \\ \alpha_i\beta & -\beta_i\alpha & 0 \end{pmatrix} = \alpha_i^2\beta^2 - \alpha^2\beta_i^2.$$

Hence, the determinant is only zero when (α, β) coincides with a quotient singular value pair of D_1, D_2.
Elimination of the vector $(\ u^t\ v^t\ x^t\ )^t$ now results in the eigenvalue problem

$$\left[\begin{pmatrix} A^t & 0 & 0 \\ 0 & A^t & 0 \\ 0 & 0 & -A \end{pmatrix} + \begin{pmatrix} C_1^t & 0 & 0 \\ 0 & C_2^t & 0 \\ 0 & 0 & -B \end{pmatrix} \begin{pmatrix} -\alpha I & 0 & D_1 \\ 0 & -\beta I & D_2 \\ D_1^t\beta & -D_2^t\alpha & 0 \end{pmatrix}^{-1} \cdot \begin{pmatrix} 0 & 0 & -C_1 \\ 0 & 0 & -C_2 \\ -B^t\beta & B^t\alpha & 0 \end{pmatrix}\right] \begin{pmatrix} p \\ q \\ y \end{pmatrix} = \begin{pmatrix} p \\ q \\ y \end{pmatrix} (-j\omega).$$

Define M_γ as

$$M_\gamma = \begin{pmatrix} A^t & 0 & 0 \\ 0 & A^t & 0 \\ 0 & 0 & -A \end{pmatrix} + \begin{pmatrix} C_1^t & 0 & 0 \\ 0 & C_2^t & 0 \\ 0 & 0 & -B \end{pmatrix} \begin{pmatrix} -\alpha I & 0 & D_1 \\ 0 & -\beta I & D_2 \\ D_1^t\beta & -D_2^t\alpha & 0 \end{pmatrix}^{-1} \begin{pmatrix} 0 & 0 & -C_1 \\ 0 & 0 & -C_2 \\ -B^t\beta & B^t\alpha & 0 \end{pmatrix}.$$

The pure imaginary eigenvalues of M_γ are the frequencies at which there is a Q-singular value $\gamma = \frac{\alpha}{\beta}$. In other words: $-j\omega$ is an eigenvalue of

$$M_\gamma x = -j\omega x,$$

if and only if for some i, $\sigma_{qi}(G_1(j\omega), G_2(j\omega)) = \gamma$. □

A similar theorem exists in the case of discrete transfer matrices. Then a generalized eigenvalue problem has to be solved:

Theorem 9 *Consider the discrete transfer matrix pair with sampling frequency T, $G_1(e^{j\omega T})$ and $G_2(e^{j\omega T})$:*

$$\begin{pmatrix} G_1(e^{j\omega T}) \\ G_2(e^{j\omega T}) \end{pmatrix} = \begin{pmatrix} D_1 \\ D_2 \end{pmatrix} + \begin{pmatrix} C_1 \\ C_2 \end{pmatrix} (e^{j\omega T} I_n - A)^{-1} B.$$

The pair (α, β) with $\alpha^2 + \beta^2 = 1$ is a quotient singular value pair of the pair of transfer matrices $G_1(e^{j\omega T})$ and $G_2(e^{j\omega T})$ at the frequency ω if $e^{j\omega T}$ is a generalized eigenvalue of the matrix pair (V_γ, W_γ), where

$$V_\gamma = \begin{pmatrix} I & 0 & 0 \\ 0 & A^t & 0 \\ 0 & 0 & A^t \end{pmatrix} + \begin{pmatrix} 0 & 0 & 0 \\ C_1^t & 0 & 0 \\ 0 & C_2^t & 0 \end{pmatrix} \begin{pmatrix} \alpha I & 0 & -D_1 \\ 0 & \beta I & -D_2 \\ D_1^t\beta & -D_2^t\alpha & 0 \end{pmatrix}^{-1} \begin{pmatrix} C_1 & 0 & 0 \\ C_2 & 0 & 0 \\ 0 & -B^t\beta & B^t\alpha \end{pmatrix},$$

$$W_\gamma = \begin{pmatrix} A & 0 & 0 \\ 0 & I & 0 \\ 0 & 0 & I \end{pmatrix} + \begin{pmatrix} 0 & 0 & B \\ 0 & 0 & 0 \\ 0 & 0 & 0 \end{pmatrix} \begin{pmatrix} \alpha I & 0 & -D_1 \\ 0 & \beta I & -D_2 \\ D_1^t\beta & -D_2^t\alpha & 0 \end{pmatrix}^{-1} \begin{pmatrix} C_1 & 0 & 0 \\ C_2 & 0 & 0 \\ 0 & -B^t\beta & B^t\alpha \end{pmatrix}.$$

Proof:
Let (α, β) with $\alpha^2 + \beta^2 = 1$ be a quotient singular value pair of the pair of discrete transfer matrices $G_1(e^{j\omega T})$ and $G_2(e^{j\omega T})$ at a certain frequency ω where

$$\begin{pmatrix} G_1(e^{j\omega T}) \\ G_2(e^{j\omega T}) \end{pmatrix} = \begin{pmatrix} D_1 \\ D_2 \end{pmatrix} + \begin{pmatrix} C_1 \\ C_2 \end{pmatrix} (e^{j\omega T} I_n - A)^{-1} B.$$

Then, from Lemma 1 we find that there must exists three vectors u, v and x such that

$$\begin{aligned} (D_1 + C_1(e^{j\omega T} I_n - A)^{-1} B)x &= u\alpha, \\ (D_2 + C_2(e^{j\omega T} I_n - A)^{-1} B)x &= v\beta, \\ (D_1^t + B^t(e^{-j\omega T} I_n - A^t)^{-1} C_1^t)u\beta &= (D_2^t + B^t(e^{-j\omega T} I_n - A^t)^{-1} C_2^t)v\alpha, \end{aligned}$$

with $\alpha^2 + \beta^2 = 1$. Now call

$$\begin{aligned} y &= (e^{j\omega T} I_n - A)^{-1} Bx, \\ p &= (e^{-j\omega T} I_n - A^t)^{-1} C_1^t u, \\ q &= (e^{-j\omega T} I_n - A^t)^{-1} C_2^t v, \end{aligned}$$

then

$$\begin{pmatrix} -\alpha I & 0 & D_1 \\ 0 & -\beta I & D_2 \\ D_1^t\beta & -D_2^t\alpha & 0 \end{pmatrix} \begin{pmatrix} u \\ v \\ x \end{pmatrix} = \begin{pmatrix} 0 & 0 & -C_1 \\ 0 & 0 & -C_2 \\ -B^t\beta & B^t\alpha & 0 \end{pmatrix} \begin{pmatrix} p \\ q \\ y \end{pmatrix},$$

$$e^{j\omega T}\begin{pmatrix} I & 0 & 0 \\ 0 & A^t & 0 \\ 0 & 0 & A^t \end{pmatrix}\begin{pmatrix} y \\ p \\ q \end{pmatrix} + e^{j\omega T}\begin{pmatrix} 0 & 0 & 0 \\ C_1^t & 0 & 0 \\ 0 & C_2^t & 0 \end{pmatrix}\begin{pmatrix} u \\ v \\ x \end{pmatrix}$$
$$= \begin{pmatrix} A & 0 & 0 \\ 0 & I & 0 \\ 0 & 0 & I \end{pmatrix}\begin{pmatrix} y \\ p \\ q \end{pmatrix} + \begin{pmatrix} 0 & 0 & B \\ 0 & 0 & 0 \\ 0 & 0 & 0 \end{pmatrix}\begin{pmatrix} u \\ v \\ x \end{pmatrix}. \quad (2.10)$$

We would now like to eliminate the vector $(u^t\ v^t\ x)^t$ which obviously requires the non-singularity of the matrix

$$\begin{pmatrix} -\alpha I & 0 & D_1 \\ 0 & -\beta I & D_2 \\ D_1^t\beta & -D_2^t\alpha & 0 \end{pmatrix}.$$

The proof is similar as in the previous theorem.
Elimination of the vector $\begin{pmatrix} u^t & v^t & x^t \end{pmatrix}^t$ results in the generalized eigenvalue problem:

$$V_\gamma \begin{pmatrix} p \\ q \\ y \end{pmatrix} = e^{-j\omega T} W_\gamma \begin{pmatrix} p \\ q \\ y \end{pmatrix}.$$

The generalized eigenvalues with modulus 1 of the pair (V_γ, W_γ) are the frequencies where a Q-singular value is equal to $\gamma = \frac{\alpha}{\beta}$. In other words, $e^{-j\omega T}$ is a generalized eigenvalue of

$$V_\gamma x = e^{j\omega T} W_\gamma x,$$

if and only if for some i, $\sigma_{qi}(G_1(e^{j\omega T}), G_2(e^{j\omega T})) = \gamma$. □

The QH_∞ norm for discrete systems can of course also be computed via a bilinear transformation to the continuous time domain.

A quadratic convergent algorithm for computing the QL_∞ norm

As in [11] the level set described in the previous section, can be used in a quadratically convergent algorithm for computing the QL_∞ norm.

The frequencies ω_i with a Q-singular value equal to γ can be obtained by taking:

$$\alpha = \frac{\gamma}{\sqrt{\gamma^2+1}}, \quad \beta = \frac{1}{\sqrt{\gamma^2+1}},$$

and find the eigenvalues of M_γ. The imaginary eigenvalues of M_γ are the requested frequencies.

Also the slope of the Q-singular values at ω can be computed. Suppose that $\sigma_{qi}(j\omega_k) = \gamma$, $M_\gamma p = -j\omega_k p$ and $q^* M_\gamma = -j\omega_k q^*$. Here p and q are the right and left eigenvectors corresponding to $-j\omega$. The slope is then:

$$\left.\frac{\partial \sigma_{qi}(G(j\omega))}{\partial \omega}\right|_{\omega=\omega_k} = \left(q^* \frac{\partial M_\gamma}{\partial \gamma} p\right)^{-1} (jq^*p).$$

Suppose we order the ω's in ascending order and $\gamma > \max\{\sigma_{q1}(0), \sigma_{q1}(\infty)\}$. The sign of the slope of the singular value at ω_1 is positive. Then we go through the list to find the corresponding frequency. That is the frequency ω_k for which the sum of the signs up to that frequency is zero. We know that $\sigma_{q1}(j\omega) > \gamma$ for all ω's in the interval $[\omega_1, \omega_k]$. The next ω, ω_{k+1} will also correspond to a largest singular value and we can repeat the procedure to find the next interval where $\sigma_{q1}(j\omega) > \gamma$.
To find the maximal singular value, apply the following algorithm:

set $\gamma = \max(\sigma_{q1}(0), \sigma_{q1}(\infty))$
while (imaginary eigenvalues of $M_{\gamma(1+\epsilon)}$)
  find the intervals where $\sigma_{q1}(j\omega) > \gamma(1+\epsilon)$
  for each interval set ω_k = midpoint of the interval
  $\gamma = \max_k \sigma_{q1}(j\omega_k)$
end

ϵ is the tolerance on γ.
This algorithm will converge quadratically. The proof is similar to the one given in [11]. This algorithm converges much faster than a bisection algorithm based on the same level set procedure.

Example:
Take the same transfer matrices as in the example of section 2.4.2. We want to find the QH_∞ norm with the quadratically convergent algorithm. The algorithm looks for the frequency intervals where the largest quotient value is larger than the level γ. At the midpoints of these intervals, the largest QSV is calculated. The maximum QSV at all the midpoints is taken as the new level γ for a new iteration. The solution was found in 3 iterations within a relative accuracy of $\epsilon = 1e-4$. These are shown in figure 2.11. The first plot just shows the quotient singular values as function of the frequency. The next plots show the different iterations. The dotted line is the level γ.

The first level is at the $\sigma_{q1}(0)$. The plus-signs indicate the calculated largest QSV at the midpoint of an interval. The plus-sign of the maximum QSVs at all the midpoints is replaced by a star. The resulting QL_∞ norm is 508.9. This occurs at $\omega = \omega_m = 136.9$ rad/sec. Using the QSVD the direction of the worst case input signal can be found:

$$x_1 = \begin{pmatrix} 0.0026 - 0.0015i \\ 0.0023 + 0.0005i \end{pmatrix}.$$

From ω_m and x_1 we find that the worst case input signal is:

$$u(t) = \begin{pmatrix} 0.0030 \sin(136.9t - 0.5143) \\ 0.0024 \sin(136.9t + 0.2069) \end{pmatrix}.$$

2.6 Examples

In this section, the theory is illustrated with two examples. The signal to noise ratio is checked of a glass furnace model and of the axial fan set-up.

2.6.1 Analysis of Signal to Noise Ratio of Identified Models

Some identification models generate a model from the measured inputs to the measured outputs, together with a stochastic model from white noise inputs to the outputs. These include well-known models such as the ARMAX models ([73]):

$$y(k) = \frac{B(z)}{A(z)}u(k) + \frac{C(z)}{A(z)}e(k)$$

and the stochastic/deterministic subspace models in forward innovation form ([99]):

$$\begin{cases} x(k+1) &= Ax(k) &+B_1u(k) &+B_2e(k) \\ y(k) &= Cx(k) &+D_1u(k) &+D_2e(k). \end{cases}$$

These models have two sets of inputs and one set of outputs. The output can be interpreted as a summation of the outputs of two separate models. The relative influence of the real inputs and the disturbance inputs on the output can easily be studied using the methods described in this chapter.

The state space model of the glass furnace is shown in appendix 1 of this chapter. It is a discrete time $10th$ order model with two outputs, two control inputs and two disturbance inputs. The model is scaled and the sampling

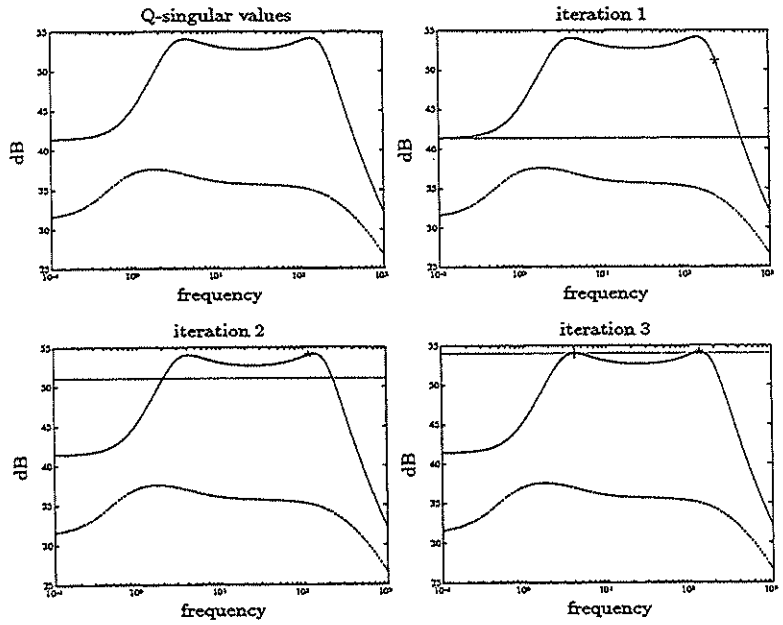

Figure 2.11: An illustration of the quadratically convergent algorithm for calculating the QH_∞ norm. The first plot shows the Q-singular values. The next plots show the algorithm at work. The dotted line is the level γ. The plus-signs indicate the maximum quotient singular values at the midpoints of the intervals. The plus-sign that indicates the largest quotient singular value, is replaced by a star. Only at the third iteration, there are two intervals.

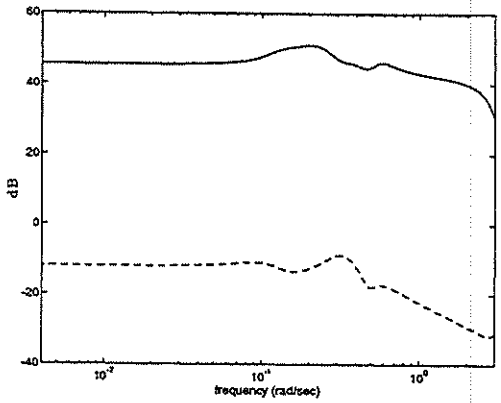

Figure 2.12: The Q-singular values of the scaled glass furnace model. One Q-singular value is much larger than 1 (=0dB) and one is smaller than 1. This implies that there are output directions where the influence of the control is much lower than the influence of the noise, and there are output directions where the noise has more influence than the control input.

time is assumed to be 1. The Q-singular value plot is shown in figure 2.12. The ratio of the control inputs over the disturbance inputs is plotted. The magnitude is expresses in dB. This is $20\log_{10}(\sigma_{qi})$. One Q-singular value is about 50dB. This implies that in a certain output direction the disturbance input signal has to be 50dB larger than the control input signal to have an equal influence on the output signal in that direction. For those output directions there is a good signal to noise ratio if the inputs have about the same magnitudes. However, in another output direction the Q-singular value is smaller than 1. This means that the signal-to-noise ratio is bad in that direction. The influence of the noise inputs is larger than those of the control inputs in that output direction. To improve the signal to noise ratio in the latter direction, the smallest Q-singular value should be increased.

Using the QH_∞ routine it is possible to find the largest signal-to-noise ratio, the output direction in which it occurs and the corresponding input directions:

$$\left\| \left(\begin{array}{c|cc} A & B_1 & B_2 \\ \hline C & D_1 & D_2 \end{array} \right) \right\|_{Q-\infty} = 355.39 = 51.01\text{dB}.$$

This is reached at 0.2053 rad/sec. The corresponding output direction is

$$y = \begin{pmatrix} 0.7579 & -0.1970i \\ 50.8274 & -31.3575i \end{pmatrix} \rightarrow y(t) = \begin{pmatrix} 0.7831\sin(0.2053t - 0.2543) \\ 59.722\sin(0.2053t - 0.5528) \end{pmatrix}.$$

The controlled input direction that generates this output direction is

$$u = \begin{pmatrix} -0.8038 & -0.5948i \\ 0.0009 & +0.0025i \end{pmatrix} \rightarrow u(t) = \begin{pmatrix} 1.0000\sin(0.2053t - 2.5045) \\ 0.0026\sin(0.2053t + 0.5268) \end{pmatrix},$$

and the disturbance input is

$$e = \begin{pmatrix} 0.8273 & +0.2934i \\ 0.4531 & +0.1556i \end{pmatrix} \rightarrow e(t) = \begin{pmatrix} 0.8778\sin(0.2053t + 0.3408) \\ 0.4791\sin(0.2053t + 1.0109) \end{pmatrix}.$$

As it is possible to compute the signal-to-noise ratios in different directions, a controller could be designed that optimizes them. E.g. in this case there are output directions where the noise has more influence than the input. A controller should be designed that makes the smallest Q-singular values as large as possible for all the frequencies that we are interested in.

2.6.2 Application to the Ventilator Setup

This analysis can also be applied to the axial fan setup. There is one control input: the voltage of the fan or the desired input air flow rate if a controller is present. There is one disturbance signal: the wind signal. The wind model will be added to the model of the fan. The noise input is then a fictitious white noise that drives the wind model. It is now possible to study the relative influence of the inputs on the outputs for the different frequencies. Applying the Q-singular value decomposition is a bit trivial in this case as there is only one output signal, one controller input signal and one disturbance input.

The plots with the influence of the reference signal, v_{ref}, with respect to the disturbance signal is given in figure 2.13. Three Q-singular values plots are shown:

1. of the open loop (no controller, v_1 is the reference signal).
2. of the closed loop with a H_2 controller.
3. of the closed loop with a H_∞ controller.

The controllers are designed with another model for the wind. The used model is of first order that overbounds the wind model, but remains high at low frequencies. The performances of this controller at low frequencies is better. In the Q-singular value plot of the open loop, we see that the Q-singular value is larger than 1 for most frequencies. For these frequencies the control input has more influence on the output than the disturbance signal. However, there is a frequency range where the disturbance signal has relatively more influence than the control signal.

With the the controllers the Q-singular values increase. This implies that the influence of the wind is reduced considerably. Still the Q-singular values decrease in the frequency range where the wind spectrum is high.

2.7 Conclusions and Remarks

In this chapter it has been shown how the QSVD can be used to study properties of transfer matrices relative to one another. It is also shown how directional aspects of transfer matrices can be represented graphically. The extremal directions of the properties of two transfer matrices relative to one another, can be computed from the QSVD.

Norms are defined to quantify the relative aspects. The H_2 norm was extended to the QH_2 norm, and the H_∞ norm to the QH_∞ norm. Two different situations are possible:

1. The two systems have the same input but different outputs.
2. The two systems have different inputs and the global output is the sum of the two individual outputs.

The QH_2 norm is a measure for the energy in the first output signal relative to the energy in the second signal, when white noise is present at the input (situation 1). In that case the QH_∞ norm is the worst case energy amplification relative to energy amplification of the second system.

For the second situation, the norms give the relative influence of the first input on the output compared to the influence of the second input.

It is also shown how the norms can be computed. Formulas are derived for the QH_2 norm. A level set algorithm is developed for the QH_∞ norm.

The QSVD is only one member of a whole set of decompositions of two and more matrices ([30]). So, one might also define other norms for more than two transfer matrices. However, in that case the interpretation of the result gets complicated.

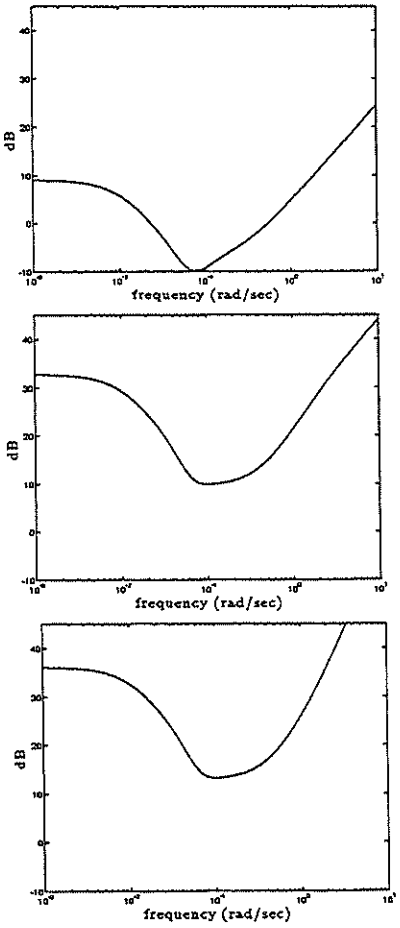

Figure 2.13: The Q-singular values of the ventilator model. The first plot shows the Q-singular values of model without controller. The second and third plot show the Q-singular values of the closed loop with H_2 controller and H_∞ controller.

In this chapter we have shown how to analyze directional aspects. Based on the norms defined in this chapter, one could also design controllers. E.g. minimize the QH_∞ norm to reduce the relative influence of the noise in all input directions over all frequencies. However, the design of controllers based on these norms has not been studied yet.

Appendix 1: The State Space Model of the Glass Furnace

The glass furnace is modeled with two inputs and two outputs. The model of a glass furnace below is obtained with a subspace algorithm for combined deterministic stochastic identification. It is a $10th$ order model with two inputs w_1, two outputs z and two disturbance inputs w_2. The model is scaled in all directions

$$\begin{cases} x(k+1) &= Ax(k) + B_1 w_1(k) + B_2 w_2(k) \\ z(k) &= Cx(k) + D_1 w_1(k) + D_2 w_2(k), \end{cases}$$

where

$$A = \begin{pmatrix} 0.8329 & 0.0851 & 0.0183 & 0.2603 & -0.0209 \\ 0.0405 & 0.8852 & 0.0812 & -0.2377 & 0.0183 \\ -0.1904 & -0.1100 & 0.8674 & 0.1093 & -0.1969 \\ -0.3772 & 0.1130 & -0.1340 & -0.0930 & 0.3072 \\ 0.0831 & -0.0135 & 0.2750 & 0.0843 & 0.9069 \\ 0.0194 & 0.1091 & 0.1766 & -0.2859 & -0.2005 \\ 0.1132 & -0.1468 & 0.0713 & -0.1213 & 0.0150 \\ 0.1762 & -0.0976 & 0.0872 & -0.3029 & 0.0817 \\ 0.1162 & -0.0750 & 0.1105 & -0.0267 & -0.0292 \\ -0.0286 & -0.0160 & -0.0519 & 0.1221 & -0.0462 \end{pmatrix}$$

$$\begin{pmatrix} 0.0310 & -0.0022 & 0.0112 & -0.0141 & -0.0063 \\ -0.0625 & 0.0049 & -0.0258 & 0.0293 & 0.0143 \\ -0.0517 & -0.0491 & 0.0493 & -0.0549 & -0.0210 \\ -0.1405 & 0.1919 & 0.1931 & 0.1176 & -0.0473 \\ 0.2179 & -0.0673 & -0.0844 & 0.0068 & 0.0192 \\ 0.8195 & 0.0629 & 0.1421 & 0.1383 & -0.0163 \\ 0.0127 & 0.9328 & -0.1628 & 0.0365 & 0.0696 \\ -0.1718 & 0.0390 & 0.7687 & -0.3696 & 0.2094 \\ -0.2324 & -0.1082 & 0.1894 & 0.8520 & 0.1760 \\ 0.0983 & -0.0839 & -0.1250 & 0.0368 & 0.8856 \end{pmatrix},$$

$$\left(B_1 \,\middle|\, B_2 \right) = \left(\begin{array}{cc|cc} -14.9432 & 0.0102 & 0.0461 & 0.1082 \\ 6.0855 & 0.0286 & -0.0108 & -0.1456 \\ -5.0042 & 0.0333 & 0.0295 & 0.1149 \\ -38.4368 & 0.0021 & -0.1544 & 0.0330 \\ 8.6269 & -0.0055 & 0.0343 & 0.0432 \\ -4.0363 & -0.0392 & -0.1497 & -0.0344 \\ 6.1004 & 0.0187 & -0.1064 & -0.0799 \\ 4.8929 & -0.0056 & -0.1585 & -0.0705 \\ 2.1959 & -0.0155 & 0.0925 & -0.2822 \\ 0.9502 & 0.0205 & -0.2621 & 0.0338 \end{array}\right),$$

$$C = \begin{pmatrix} 0.0273 & -0.0020 & 0.0001 & -0.0012 & -0.0006 \\ 0.0048 & -0.0059 & 0.0013 & 0.0038 & 0.0001 \\ -0.0003 & -0.0008 & -0.0005 & -0.0002 & -0.0002 \\ 0.0002 & 0.0001 & 0.0002 & -0.0001 & -0.0001 \end{pmatrix},$$

$$\left(D_1 \vdots D_2 \right) = \left(\begin{array}{cc:cc} -0.0045 & 0.0002 & 0.0026 & -0.0001 \\ -0.1384 & -0.0001 & -0.0001 & 0.0021 \end{array} \right).$$

Chapter 3

Real Parameter Margins

3.1 Introduction

Classical norms for robustness are the well-known gain and phase margins, which are mainly intended for SISO systems. To quantify the robustness of MIMO systems the M and D-circle were defined. However, these measures are unstructured. To deal with structured uncertainties the structured singular value μ has been developed. The structured singular value, however, assumes that all the disturbances are complex. This can still be conservative if the disturbances are known to be real.

In this chapter two measures are described that deal with robustness against real structured disturbances. The first measure gives the largest possible deviation that ensures stability of the system. The second ensures a certain H_2 norm of the system. The latter is a robust performance measure. It gives the largest allowable deviation of the parameters without violating a given bound for the H_2 norm. The only restriction is that the entries of the state space matrices of the system have to be polynomially or rationally dependent on the parameters.

In [44], El Ghaoui defined the l_2 and l_∞ parameter margins. It is the largest 2 or ∞ norm of the parameter vector that ensures stability or H_2 performance. In [46] a quadratically convergent algorithm was presented to compute the l_2 norm when there are only two uncertain parameters. However, the algorithm does not converge globally. The computation of the l_2 parameter margin can also be formulated in the framework of structured total least squares (STLS) ([35]). Using this algorithm there are no restrictions on the number of parameters. Unfortunately, global convergence is not

ensured either.

In section 3.2 some definitions will be recapitulated. It is also shown how the l_2 parameter margin can reformulated as a determinant problem. In section 3.3 it is shown how the l_2 parameter problem can be solved using the STLS algorithm. In section 3.4 the l_∞ parameter margin is discussed briefly. An example is given in section 3.5. The conclusions are summarized in section 3.6.

3.2 Preliminaries

In this section, the basic definitions are recapitulated for the q-parameter stability margin (qPSM) and the q-parameter performance margin (qPPM). It is also shown how they can be reformulated as determinant problems. This section is based on [44], [45] and [46].

3.2.1 Definitions

The q-Parameter Stability Margin

Consider a linear, time-invariant closed-loop system of order p

$$\dot{x} = A(a)x,$$

where x is the state and $A(a)$ is the $p \times p$ dynamic matrix of the plant. The entries of $A(a)$ are polynomially dependent on the parameter vector a with length n. The nominal value of a is assumed to be 0. This is not a restriction.
The qPSM of $A(a)$ is defined as

$$q\text{PSM}(A(a)) \triangleq \min_{a \in \mathbb{R}^n} \{\|a\|_q \mid A(a) \text{ is unstable}\}. \tag{3.1}$$

Only the 2 norm and the ∞ norm will be considered ($q = 2, \infty$).

The q-Parameter Performance Margin

Consider a stable plant $G(s,a) = C(a)\left(sI - A(a)\right)^{-1} B(a)$. The matrices $A(a)$, $B(a)$ and $C(a)$ are all dependent on the real parameter vector a. For a stable plant the H_2 norm is defined as

$$\|G(s)\|_2 = \left(\frac{1}{2\pi}\int_{-\infty}^{+\infty} \text{trace}\ \left(G(j\omega)^* G(j\omega)\right)\, d\omega\right)^{\frac{1}{2}}.$$

As $G(s,a)$ is dependent on the real parameter vector a, the qPPM is defined as:

$$q\text{PPM}(G(s,a), J_{\text{ref}}) \triangleq \min_{a \in \mathbb{R}^n} \{\|a\|_q \mid \|G(s,a)\|_2 \geq J_{\text{ref}}\}.$$

It is the maximal variation of the parameters that ensures that the H_2 norm of the transfer function does not exceed a given value J_{ref}. In other words, it guarantees a certain H_2 performance.

3.2.2 Reformulation as a Determinant Problem

The q-Parameter Stability Margin

In (3.1) $A(a)$ becomes unstable if $A(a)$ has eigenvalues on the imaginary axis. Thus (3.1) can be reformulated as

$$q\text{PSM}(A(a)) = \min_{a \in \mathbb{R}^n} \{\|a\|_q \mid \det(A(a) - j\omega I) = 0 \text{ for some } \omega \in \mathbb{R}\}.$$

To compute the qPSM a frequency sweep should be performed. This also occurs in e.g. μ analysis to find the global minimum over all frequencies. In this case, however, it is possible to avoid this frequency sweep. The method proposed in [46] is to express the critical constraint, that $A(a)$ has an eigenvalue on the $j\omega$-axis, as a determinant expression:

$$q\text{PSM}(A(a)) = \min_{a \in \mathbb{R}^n} \{\|a\|_q \mid \det\left(\mathbf{B}(a)\right) = 0\}. \tag{3.2}$$

$\mathbf{B}(a)$ is real, polynomial matrix of order $\frac{p(p+1)}{2}$, called a Lyapunov matrix. The eigenvalues of the Lyapunov matrix are the sums of the eigenvalues of $A(a)$. Thus if $A(a)$ is real and has eigenvalues on the imaginary axis, then $\mathbf{B}(a)$ is singular and $\det\left(\mathbf{B}(a)\right) = 0$. How the Lyapunov matrix is constructed, is explained in the next paragraph.

The Construction of the Lyapunov Matrix The construction of the Lyapunov matrix is described in [66]. It is based on the following observation. The Lyapunov equation

$$AL + LA^t + BB^t = 0, \tag{3.3}$$

is linear in the entries of L. Before continuing a new operator is defined. Given a symmetric $n \times n$ matrix Q, let $\text{vec}(Q)$ denote a vector of length

$n(n+1)/2$ consisting of the elements of Q on and above the diagonal. The elements of the upper triangle of Q are stored column by column:

$$\mathrm{vec}(Q) = \begin{pmatrix} q_{11} \\ q_{12} \\ q_{22} \\ q_{13} \\ q_{23} \\ \vdots \\ q_{nn} \end{pmatrix}.$$

The solution of the Lyapunov equation can then be rewritten as

$$\mathrm{vec}(L) = \mathrm{A}^{-1}\mathrm{vec}(-BB^t).$$

Here A is a matrix of order $n(n+1)/2$, called the Lyapunov matrix. Multiplying out (3.3) and collecting the terms, we find

$$\mathrm{A} = \begin{pmatrix} 2a_{11} & 2a_{12} & 0 & 2a_{13} & 0 & 0 & \cdots \\ a_{21} & a_{22}+a_{11} & a_{12} & a_{23} & a_{13} & 0 & \cdots \\ 0 & 2a_{21} & 2a_{22} & 0 & 2a_{23} & 0 & \cdots \\ a_{31} & a_{32} & 0 & a_{33}+a_{11} & a_{12} & a_{13} & \cdots \\ 0 & a_{31} & a_{32} & a_{21} & a_{33}+a_{11} & a_{23} & \cdots \\ 0 & 0 & 0 & 2a_{31} & 2a_{32} & 2a_{33} & \cdots \\ \vdots & \vdots & \vdots & \vdots & \vdots & \vdots & \ddots \end{pmatrix}.$$

In [66] is described how to construct A when A is given. A can be written as the sum of n square matrices of order $\frac{n(n+1)}{2}$, constructed according a rule based on a triangular array of integers.
Construct first a triangle of all integers from 1 to $\frac{n(n+1)}{2}$:

$$\begin{array}{cccccc} 1 & & & & & \\ 2 & 3 & & & & \\ 4 & 5 & 6 & & & \\ 7 & 8 & 9 & 10 & & \\ \vdots & \vdots & \vdots & \vdots & \ddots & \\ . & . & . & . & \cdots & \frac{1}{2}n(n+1). \end{array}$$

Complete this to the symmetrical square array:

$$\begin{array}{ccccccc} 1 & 2 & 4 & 7 & \cdots & . \\ 2 & 3 & 5 & 8 & \cdots & . \\ 4 & 5 & 6 & 9 & \cdots & . \\ 7 & 8 & 9 & 10 & \cdots & . \\ \vdots & \vdots & \vdots & \vdots & \ddots & \vdots \\ . & . & . & . & \cdots & \frac{1}{2}n(n+1). \end{array} \tag{3.4}$$

The n matrices that are summed to form A are obtained as follows. Each of the rows of (3.4) represents one of the n matrices. In each of the rows of (3.4) some integers are missing. The missing integers in the first row represent the rows and columns of the first matrix of order $\frac{n(n+1)}{2}$, that consist wholly of zeros. Similarly, for the second row and column, the missing integers represent the rows and columns of the second matrix that consist wholly of zeros. In the remaining positions the elements of A are filled in. Finally the rows in the n matrices corresponding to the integers that lie on the main diagonal of (3.4) are to be multiplied by 2.

A 'Linearization' of the Determinant Constraint Suppose we have a determinant constraint:

$$\det(\mathrm{B}(a)) = 0,$$

where $a = (a_1\ a_2\ \ldots\ a_n)$ is the parameter vector. If all the entries of $A(a)$ are linear dependent on the parameters a, then the entries of $\mathrm{B}(a)$ will be linear dependent on the parameters a too. However, if the entries of $A(a)$ are polynomially or rational dependent on the parameters, the entries of $B(a)$ will be so too. It is, however, possible to 'linearize' the determinant constraint:

$$\det(\mathrm{B}(a)) = \det(B_0 + \sum_{i=1}^{n} a_i B_i),$$

where B_i $(i = 0 \ldots n)$ are constant matrices.
Consider the case where the entries of B are polynomially dependent on only one parameter a. The general case can be linearized by applying the procedure for one parameter repeatedly. Extensions to matrices that are rationally dependent on the parameters are also possible. See e.g. [19].
Consider the following problem:

$$\det(B_0 + \sum_{i=1}^{n} a^i B_i) = 0,$$

where B_i $(i = 0 \ldots n)$ are real, square, constant matrices and a is a real, scalar parameter. The determinant expression is then equivalent to

$$\det \begin{pmatrix} B_0 + aB_1 & aB_2 & aB_3 & \cdots & aB_{n-2} & aB_{n-1} & aB_n \\ -aI & I & 0 & \cdots & 0 & 0 & 0 \\ 0 & -aI & I & \ddots & 0 & 0 & 0 \\ \vdots & \vdots & \ddots & \ddots & \ddots & \vdots & \vdots \\ 0 & 0 & 0 & \ddots & I & 0 & 0 \\ 0 & 0 & 0 & \ddots & -aI & I & 0 \\ 0 & 0 & 0 & \cdots & 0 & -aI & I \end{pmatrix}.$$

I is the unit matrix of the same dimensions as B_i. This is easily proved using the properties of determinants: Add the last block column multiplied by a to the one but last. Then add the one but last block column, multiplied by a, to the second last one. Continue this until the second block column is added to the first one. This does not change the determinant, by the first property. The result is:

$$\det \begin{pmatrix} B_0 + \sum_{i=1}^{n} a^i B_i & * \\ 0 & I \end{pmatrix} = \det(B_0 + \sum_{i=1}^{n} a^i B_i),$$

where '*' denotes an irrelevant block. This proves the equivalence. The resulting structure is clearly in the form:

$$\det(C_0 + aC_1),$$

where C_0 and C_1 are constant matrices. See also [96], where a similar way of 'linearizing' the determinant expression is described.

Reducing the Size of the Linearized Problem First it is shown how to convert

$$\det(B_0 + \sum_{i=1}^{n} a_i B_i) = 0 \tag{3.5}$$

into

$$\det(I + M\Delta(a)) = 0$$

with

$$\Delta(a) = \text{block diag} \begin{pmatrix} a_1 I_{r_1} & a_2 I_{r_2} & \cdots & a_n I_{r_n} \end{pmatrix}.$$

The condition (3.5) implies

$$\exists x \neq 0 \; : \; (B_0 + \sum_{i=1}^{n} a_i B_i)x = 0. \tag{3.6}$$

Using the singular value decomposition $B_i = U_i \Sigma_i V_i^t$ with $\Sigma_i \in \mathbb{R}^{r_i \times r_i}$, where r_i is the rank of B_i, (3.6) can be rewritten as

$$\exists x \neq 0 \; : \; (B_0 + \sum_{i=1}^{n} U_i \Sigma_i a_i I_{r_i} V_i^t)x = 0, \tag{3.7}$$

or

$$\exists x \neq 0 \; : \; B_0 x + \underline{U}\Delta(a)\underline{V}x = 0, \tag{3.8}$$

where

$$\begin{aligned} \Delta &= \begin{pmatrix} a_1 I_{r_1} & & & \\ & a_2 I_{r_2} & & \\ & & \ddots & \\ & & & a_n I_{r_n} \end{pmatrix}, \\ \underline{U} &= \begin{pmatrix} U_1\Sigma_1 & U_2\Sigma_2 & \cdots & U_n\Sigma_n \end{pmatrix}, \\ \underline{V} &= \begin{pmatrix} V_1^t \\ V_2^t \\ \vdots \\ V_n^t \end{pmatrix}. \end{aligned}$$

This is equivalent to

$$\begin{cases} \exists x, y, z \neq 0 \; : & B_0 x + \underline{U} y = 0 \\ & z = \underline{V} x \\ & y = \Delta z \end{cases}$$

$$\Leftrightarrow \begin{cases} \exists y, z \neq 0 \; : & z = -\underline{V} B_0^{-1} \underline{U} y \\ & y = \Delta z. \end{cases}$$

This describes an inner loop (see e.g. [2]):

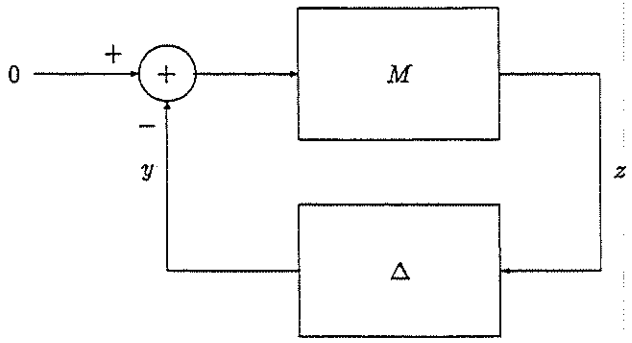

There are solutions $y, z \neq 0$ if and only if $I + M\Delta$ is singular or $\det(I + M\Delta) = 0$, where $M = \underline{V} B_0^{-1} \underline{U}$.
The matrix M can be reduced even further, such that all the block rows and columns have full rank. This is explained in [46].
How these (hard) problems can be solved, is explained in sections 3.3 and 3.4, for the cases $q = 2, \infty$.

The q-Parameter Performance Margin

With the qPPM we want to ensure a certain H_2 performance. For a stable transfer function $G(s)$ the H_2 norm of the transfer function is:

$$\|G\|_2 = \left(\frac{1}{2\pi} \int_{-\infty}^{+\infty} \text{trace}\left(G(j\omega)^* G(j\omega)\right)\, d\omega \right)^{\frac{1}{2}}.$$

For a given state space realization of $G(s) = C(sI - A)^{-1}B$, the H_2 norm of the transfer function can be computed as

$$\|G\|_2^2 = \text{trace}(LC^tC),$$

where L is the controllability gramian of (A, B). L is the solution of a Lyapunov equation:

$$AL + LA^t + BB^t = 0.$$

As already shown, this equation can be rewritten as

$$\mathrm{A}l = b,$$

where $l := vec(L)$, $b = vec(-BB^t)$ and A is the Lyapunov matrix, a real matrix of order $n(n+1)/2$, whose elements are linear combinations of the entries of A.
The H_2 norm of a transfer function can thus be written as:

$$\|G\|_2^2 = c\mathrm{A}^{-1}b,$$

where $c^t = vec(C^tC. * H)$. '.*' denotes the elementwise product of two matrices. H is defined as

$$H = \begin{pmatrix} 1 & 2 & 2 & 2 & \cdots \\ 2 & 1 & 2 & 2 & \cdots \\ 2 & 2 & 1 & 2 & \cdots \\ 2 & 2 & 2 & 1 & \cdots \\ \vdots & \vdots & \vdots & \vdots & \ddots \end{pmatrix}.$$

If G is perturbed by n real parameters, our performance index becomes

$$J(a) = \|G\|_2^2 = c(a)\mathrm{A}(a)^{-1}b(a).$$

The entries of A, B and C have to be polynomial or rational in the parameters a_i. Given a given scalar J_{ref}, a measure of the robustness in H_2 performance is defined as:

$$q\text{PPM}(J_{\text{ref}}) = \min_{a \in \mathbb{R}^n} \{ \|a\|_q \mid J(a) \geq J_{\text{ref}} \}.$$

We look for the minimum norm ($q = 2$ or ∞) of the parameter vector which increases the performance index $J(a)$ up to a certain level above the reference value J_{ref}.
Using the identity

$$\det(I + uv^t) = 1 + v^t u,$$

we obtain

$$J(a) = J_{\text{ref}} \Leftrightarrow \det(\mathrm{A} - \frac{1}{J_{\text{ref}}} bc) = 0.$$

Therefore, the performance margin can be written as:

$$q\text{PPM} = \min_{a \in \mathbb{R}^n} \left\{ \|a\|_q \,\middle|\, \det(\mathrm{A}(a) - \frac{1}{J_{\text{ref}}} b(a)c(a)) = 0 \right\}.$$

This is exactly the same form as $\det(\mathrm{B}(a)) = 0$. It can be solved similarly: Linearize the constraint and reduce its size. The resulting form is again $\det(I + M\Delta)$.
When $J_{\text{ref}} \to \infty$, the parameter stability margin is obtained.

3.3 The Computation of the 2-Parameter Margin

To solve the 2-parameter margin, a new method, described in [35] is used. In [35] structured total least square problems are studied. The computation of the 2-parameter margin can be formulated as an optimization problem that has the same form as the optimization problems in structured total least squares. An iterative method based on the inverse power method is used to solve the optimization problem. It is not guaranteed to converge to the global optimum. In most cases, however, the method works well and fast. The 2-parameter margin problem

$$\min_{a\in\mathbb{R}^n} \{\|a\|_2 \mid \det(I + M\Delta) = 0\}$$

can be reformulated as

$$\min \|a\|_2^2 \quad \text{subject to} \quad \begin{array}{l} M(a)y = 0 \\ y^t y = 1 \end{array}$$

where $M(a) = I + M\Delta = I + a_1M_1 + a_2M_2 + \ldots + a_nM_n$.
This problem can easily be solved using Lagrange multipliers. The Lagrangian is

$$\mathcal{L} = \|a\|_2^2 + 2l^tM(a)y + \lambda(y^ty - 1),$$

where l is a vector of Lagrange multipliers and λ is a scalar Lagrange multiplier. Differentiation with respect to the different unknowns yields necessary conditions for the solution

$$\frac{\partial\mathcal{L}}{\partial a_k} : a_k + l^tM_ky = 0 \tag{3.9}$$

$$\frac{\partial\mathcal{L}}{\partial y} : M(a)^tl + y\lambda = 0 \tag{3.10}$$

$$\frac{\partial\mathcal{L}}{\partial\lambda} : y^ty = 1 \tag{3.11}$$

$$\frac{\partial\mathcal{L}}{\partial l} : M(a)y = 0. \tag{3.12}$$

Now, we will manipulate these formulas to bring them in a specific form. Premultiplying (3.10) with y^t and using (3.11) and (3.12) yields:

$$y^tM(a)^tl + y^ty\lambda = 0 \quad \Rightarrow \lambda = 0.$$

With $\lambda = 0$, (3.10) becomes

$$M(a)^tl = 0. \tag{3.13}$$

Substituting (3.9) in (3.13) yields

$$\left(I - \sum_{k=1}^{n} M_k^tl^tM_ky\right) l = 0.$$

This can be rewritten as

$$l = \sum_{k=1}^{n} M_k^tl(l^tM_ky) \Leftrightarrow l = \sum_{k=1}^{n}(M_k^tl)(M_k^tl)^ty \Leftrightarrow l = \left[\sum_{k=1}^{n}(M_k^tl)(M_k^tl)^t\right] y. \tag{3.14}$$

Similarly, when (3.9) is substituted in (3.12):

$$M(a)y = 0 \Leftrightarrow \left(I - \sum_{k=1}^{n} M_ky(y^tM_k^tl)\right) y = 0 \Leftrightarrow y = \left[\sum_{k=1}^{n}(M_ky)(M_ky)^t\right] l. \tag{3.15}$$

The length of l is normalized. Call $x = \frac{l}{\|l\|}$ and $\sigma = \|l\|$. Substitution in (3.14) and (3.15) yields

$$x = D_xy\sigma, \qquad y = D_yx\sigma,$$

where

$$D_x = \sum_{k=1}^{n}(M_k^tx)(M_k^tx)^t, \qquad D_y = \sum_{k=1}^{n}(M_ky)(M_ky)^t,$$

and $y^ty = 1$, $x^tx = 1$ and $l = x\sigma$. This looks like a non-linear generalized singular value problem. It is solved using a variant of the power method ([35]). Until now, convergence is not guaranteed. However, in practice, most problems converge fast and accurately. Once x, y and σ are found, the optimal parameters a can easily be computed using (3.9).
The algorithm could look as follows:

1. Start with a random x and y with length 1.
2. Compute a new x: $x_n = D_xy$.
3. Normalize x_n: $x_n \leftarrow \frac{x_n}{\|x_n\|}$.
4. Compute a new y using the new x_n: $y_n = D_yx_n$.

5. Take $\sigma = \frac{1}{\|y_n\|}$.
6. Normalize y_n: $y_n \leftarrow \frac{y_n}{\|y_n\|}$.
7. Substitute $x = x_n$ and $y = y_n$.
8. If convergence stop, else goto step 2.

Other iteration schemes are possible, where a new x or y is computed taking as much as possible old information into account. Here is an example where y is computed using as much information as possible:

1. Start with a random x and y with length 1.
2. Compute a new y: $y_n = D_y D_x y$.
3. Normalize y_n: $y_n \leftarrow \frac{y_n}{\|y_n\|}$
4. If D_{y_n} is invertible
   (a) Compute a new x: $x_n = D_{y_n}^{-1} y_n$
   (b) $\sigma = \|x\|$
   (c) Normalize x_n: $x_n \leftarrow \frac{x_n}{\|x_n\|}$

   else
   (a) Compute a new x: $x_n = D_x y_n$
   (b) $\sigma = 1/\|x\|$
   (c) Normalize x_n: $x_n \leftarrow \frac{x_n}{\|x_n\|}$
5. Substitute $x = x_n$ and $y = y_n$.
6. If convergence stop, else goto step 2.

Convergence can be checked by e.g. computing the singular values of $I + M\Delta$. When they are small enough, stop the iteration.
A disadvantage is that the convergence is only guaranteed locally. If the initial point is close enough to a local minimum it will converge to it. Therefore, the algorithm should be used several times from different starting points. The resulting parameter vector with the lowest norm is taken to be the solution.

3.4 The Computation of the ∞-Parameter Margin

In the examples the 2-parameter margins are compared with the ∞-parameter margins. Therefore we briefly recapitulate their computation. The computation of the ∞-parameter margin is normally a very hard problem. However, as pointed out by El Ghaoui([45]), in most practical cases, the largest box touches the constraints in one of its corners. Our experiments confirmed this. In that case the ∞-parameter margin can easily be found solving 2^{n-1} eigenvalue problems (n is the number of parameters.).

Suppose we want to know in a certain direction in the parameter space, the distance from the origin to the constraint

$$\det(I + M\Delta(a)) = 0.$$

In a certain direction of the parameter space, this can be rewritten as

$$\det(I + \lambda M_a) = 0,$$

where $M_a = M\Delta(a)$ with a fixed. The problem can now be formulated as: Find the λ with the smallest absolute value that satisfies the constraint. First rewrite the problem

$$\det(\frac{1}{\lambda} I + M_a) = 0.$$

The solution is the inverse of the spectral radius of M_a.
To find the largest box, check all the corner directions:

$$\left(a_1, \ a_2, \ \cdots \ a_n \right) = \left(1, \ \pm 1, \ \cdots \ \pm 1 \right).$$

The inverse of the maximum of all the largest eigenvalues is the ∞-parameter margin.

3.5 Examples

3.5.1 An Example from [46]

In this section we will show an example. First an example with two parameters is given for graphical reasons. The example of [45] is used, slightly

modified. Consider the following state feedback problem

$$\begin{aligned}
\dot{x} &= \begin{pmatrix} -1 & 0 \\ 0 & -2 \end{pmatrix} x + \begin{pmatrix} 7+a_1 & -8+a_2 \\ 6 & -7 \end{pmatrix} w + \begin{pmatrix} 7+a_1 & -8+a_2 \\ 6 & -7 \end{pmatrix} u \\
z &= \begin{pmatrix} 1 & 0 \\ 0 & 1 \\ 0 & 0 \\ 0 & 0 \end{pmatrix} x + \begin{pmatrix} 0 & 0 \\ 0 & 0 \\ \sqrt{10} & 0 \\ 0 & \sqrt{10} \end{pmatrix} u \\
y &= \begin{pmatrix} 1 & 0 \\ 0 & 1 \end{pmatrix} x.
\end{aligned}$$

The nominal LQR controller is ($a = 0$):

$$u = -Kx = -\begin{pmatrix} 0.1413 & 0.0736 \\ -0.1604 & -0.0872 \end{pmatrix} x.$$

For this example the l_2 and l_∞ parameter robustness margin were computed and the l_2 and l_∞ parameter performance margin. For the performance margins J_{ref} was chosen to be three times the nominal H_2 performance, $J_{\text{ref}} = 3J(0)$. The computed margins are:

2PSM	17.7664
∞PSM	12.5795
2PPM($\rho = 3$)	14.6019
∞PPM($\rho = 3$)	10.9439

The result is shown in figure 3.1. The largest circle (2-parameter margin) and box (∞-parameter margin) for $J_{\text{ref}} = 3J(0)$ are shown. The lines are lines of equal H_2 norm as a function of a_1 and a_2. The box and the circle touch the curve of H_2 norm equal to $3J(0)$. The 2-parameter performance margin is 14.60. The ∞-parameter performance margin is 10.94. The 2-parameter performance margin touches the boundary at $(a_1, a_2) = (-14.46, -2.05)$. The box touches the boundary at its upper right hand corner.

Remark that the 2-parameter margin (circle) is not necessary more conservative than the ∞-parameter margin (box). This can clearly be observed on the plots. Which region is more conservative only depends on the location of the constraint.

In figure 3.2, ∞PPM and 2PPM are plotted as a function of ρ. ∞PPM and 2PPM increase monotonically with ρ. As $\rho \to \infty$, the performance margins approach the stability margins.

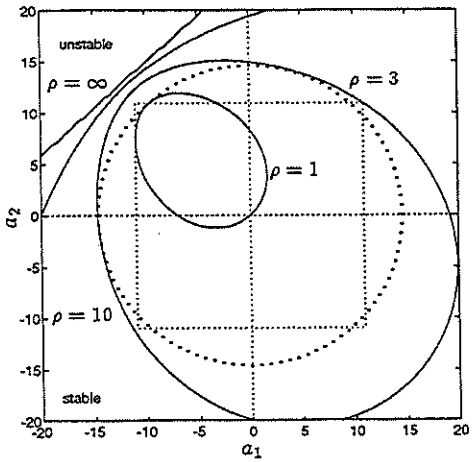

Figure 3.1: An example of the 2 and ∞ parameter margin for a system with two uncertain parameters. The constraint is a H_2 performance loss of 3 times the nominal H_2 performance. The full lines are the lines of equal H_2 norm for $\rho = 1, 3, 10, \infty$.

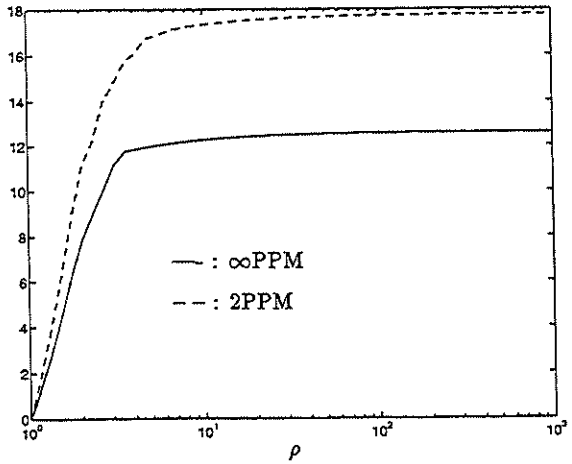

Figure 3.2: 2PPM and ∞PPM as a function of $\rho J(0)$, where $J(.)$ is the H_2 norm. As $\rho \to \infty$, the PPMs converge to the PSMs.

3.5.2 The Ventilator Setup

In the introduction it is shown how a very simple first order model of a ventilator can be obtained around a working point. The model has three parameters α, β and γ. Here we try to compute the parameter margins for these three parameters, when the fan is controlled with the H_2 controller. The nominal values of α, β and γ are given in the introduction: $(\alpha, \beta, \gamma) = (0.503, 285.986, -248.249)$. The resulting closed loop is ($D_c = 0$ for the H_2 controller):

$$\left(\begin{array}{cccc|cc} A_d & 0 & 0 & 0 & B_d & 0 \\ \gamma C_d & \alpha & 0 & \beta C_c & 0 & 0 \\ 0 & \beta_m & \alpha_m & 0 & 0 & 0 \\ 0 & 0 & -B_c\gamma_m & A_c & 0 & -B_c\delta_m \\ \hline 0 & 1 & 0 & 0 & 0 & 0 \\ 0 & 0 & 0 & C_c & 0 & 0 \end{array}\right)$$

How far can the parameters vary while still ensuring stability? What is the maximal variation that ensures an H_2 performance degradation of at most twice the nominal performance? The results are given below:

2PSM	0.4559
∞PSM	0.4558
2PPM($\rho = 2$)	0.4115
∞PPM($\rho = 2$)	0.4106

This implies that each of the parameters α, β and γ can vary with 0.4558 from their nominal value without destabilizing the system. In practice the PSM and PPM are mainly determined by the variations on α. α is the pole of the ventilator. When it is pushed to much towards the imaginary axis, the closed loop becomes unstable. Experiments show that β and γ can vary much more without destabilizing the system. The margins are thus rather conservative for variations on β and γ.

The evolution of the 2PPM and ∞PPM as a function of ρ is shown in figure 3.3. The two margins are almost equal. As $\rho \to \infty$, the performance margins tend to the stability margins.

As an example of the convergence of the algorithm, the computation of the 2PSM of the ventilator is shown. In figure 3.4 the singular values of $M_0 + a_1M_1 + a_2M_2 + a_3M_3$ are shown as a function of the number of iterations. One of the singular values decreases to 0 in 36 iterations. On this logarithmic scale it decreases linearly as a function of the number of iterations.

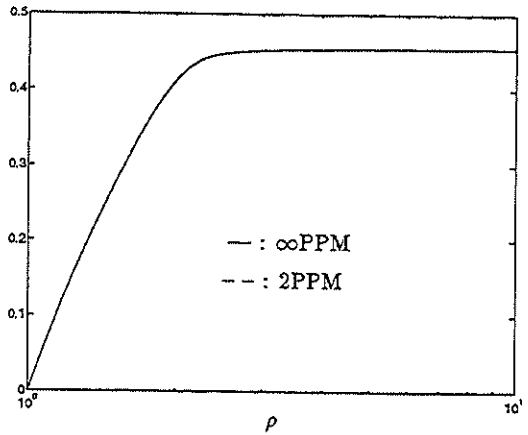

Figure 3.3: The ventilator example: the 2PPM and ∞PPM as a function of $\rho J(0)$, where $J(.)$ is the H_2 norm.

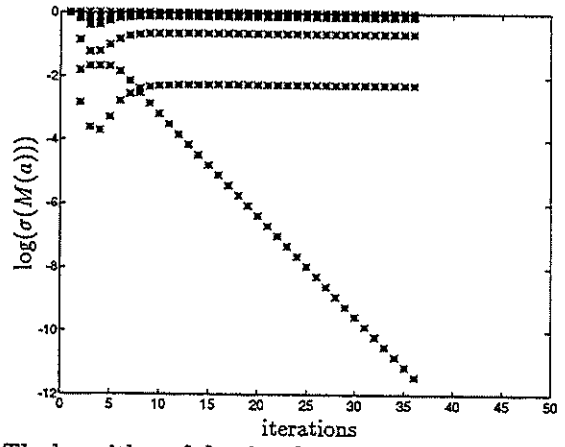

Figure 3.4: The logarithm of the singular values values of $M(a)$ as a function of the number of iterations. The example is the computation of the 2PSM of the ventilator. One eigenvalue converges to 0, which implies that $M(a)$ becomes singular.

3.6 Conclusions and Remarks

In this section robustness margins for systems that depend on real parameters are studied. The entries of the state space matrices of the systems are assumed to depend polynomially or rationally on the parameters. The studied margins are the largest norms of the parameter vector that still ensures stability or a certain H_2 performance.

A new algorithm is presented to compute the 2-parameter stability margin and the 2-parameter performance margin. The number of parameters can be larger than two for this algorithm. This overcomes a problem of a previously proposed algorithm where the number of parameters is restricted to two ([46]). The algorithm is an iterative process to find a singular matrix. It is solved using a variant of the power method. Unfortunately, convergence is not always guaranteed. In practice it converges fast and accurately in most cases. However, global convergence is not ensured.

Chapter 4

Mixed H_2/H_∞ Controller Design

4.1 Introduction

In recent years there has been a lot of interest in controller design that combines the H_2 and H_∞ norms. The general setup for the mixed H_2/H_∞ problem is shown in figure 4.1. It consists of a plant with three sets of inputs and three sets of outputs. There are two sets of disturbance inputs w_1 and w_2, and a set of controller inputs u. Equivalently there are two sets of regulated outputs z_1 and z_2, and a set of measurements y for the controller. The goal is to find a controller C such that the H_2 norm of the transfer function from w_1 to z_1 is minimized, while at the same time the H_∞ norm of the transfer function from w_2 to z_2 has to be smaller than or equal to a predefined value γ (or has to be minimized):

$$\min_C \|T_{z_1 w_1}\|_2 \qquad \text{subject to } \|T_{z_2 w_2}\|_\infty < \gamma,$$

where $T_{z_1 w_1}$ is the closed loop transfer function from w_1 to z_1 and $T_{z_2 w_2}$ the closed loop transfer function from w_2 to z_2. Without loss of generality γ can be taken to be 1. The mixed H_2/H_∞ problem combines performance and robustness aspects. The H_2 norm is usually related with the performance of the closed loop system, while the H_∞ norm ensures robustness against stable norm bounded plant variations.

As far as we know this problem has not been solved yet. However, several related problems have already been solved. Most of them consider an upper bound for the H_2 norm. This upper bound is minimized taking into account

a H_∞ norm constraint. Mustafa and Glover solved the minimum entropy controller problem ([79]). This is a mixed H_2/H_∞ problem where $w_1 = w_2$ and $z_1 = z_2$. The purpose is to find a feedback controller which stabilizes the system subject to an H_∞ norm bound, $\|T_{zw}\|_\infty < \gamma$, while simultaneously minimizing the entropy, defined as ([79]):

$$I(H,\gamma) = -\frac{\gamma^2}{2\pi}\int_{-\infty}^{\infty} \ln|\det(I-\gamma^{-2}H^*(j\omega)H(j\omega))|\,d\omega.$$

The entropy is an upper bound for the H_2 norm. The solution in this case is known. It is the so-called central suboptimal H_∞ controller.
The first paper on the mixed H_2/H_∞ problem is due to Bernstein and Haddad [9]. They consider the case with two different disturbance inputs but with only one output ($z_1 = z_2$). Again, not the real H_2 norm is optimized but an upper bound. The solution is now found by numerical optimization. Doyle, Zhou and Bodenheimer considered the problem with one input and two outputs. In [68], Khargonekar and Rotea show how the mixed H_2/H_∞-problem considered by Bernstein and Haddad can be solved by a convex optimization approach. Stoorvogel describes in [93] a more analytic approach to the problem. In [102], Yeh *et al.* show that the problem of Bernstein and Haddad and the problem of Doyle *et al.* are in fact duals of one another. They also give necessary and sufficient conditions for the problems to have a solution.

More recently, the general mixed H_2/H_∞ problem was studied by Ridgely *et al.* ([86]). They minimize the real H_2 norm of the nominal transfer function from w_1 to z_1. They show how a solution can be computed numerically when the order of the controller is fixed. However, in general, the optimal solution is not known yet. The general problem probably can also be solved using a method proposed by Boyd and Barratt, as described in [10]. However, the software currently available is only for discrete time systems and the L_∞ norm can only be given approximately as a bound for SISO transfer functions.

In [92], Steinbuch and Bosgra consider a related problem: the minimization of the real H_2 norm for a given set of stable, proper, H_∞ norm bounded disturbances between z_2 and w_2. The worst case H_2 norm from w_1 to z_1 is minimized over this set, under the constraint that the closed loop has to remain stable. This is a robust performance problem. Again the solution is not known. It is only possible to derive necessary conditions for a fixed order controller. In [93], Stoorvogel also considers this problem. However, he minimizes upper bounds instead of the real H_2 norm.

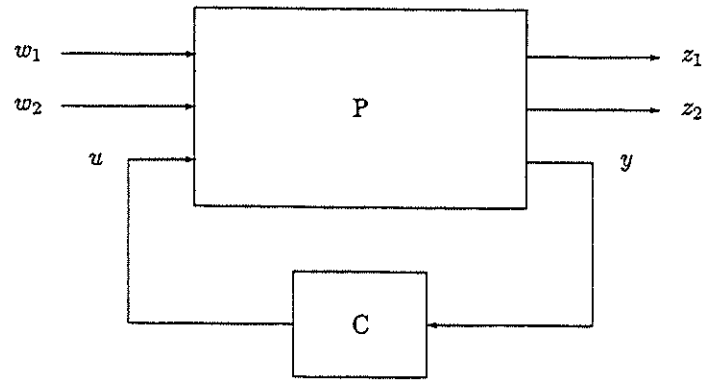

Figure 4.1: The general setup for the mixed H_2/H_∞ problem.

In this chapter, the general mixed H_2/H_∞ problem is studied. We want to minimize the real H_2 norm of the nominal transfer function between w_1 and z_1, not an upper bound. It is shown how a mixed H_2/H_∞ controller can be designed by separating the two objectives. First the H_∞ problem is considered. Afterwards the H_2 norm is minimized while the H_∞ constraint remains satisfied. In section 4.2 we give a formulation of the problem and an outline of how it can be solved. Section 4.3 recapitulates the main facts of H_∞ controller design. In section 4.4 it is explained how the H_2 norm can be minimized, to find the optimal H_2/H_∞ controller. An example is given in section 4.5. In section 4.6, the conclusions are summarized.

4.2 The Mixed H_2/H_∞ Problem

4.2.1 Problem Statement

Consider the configuration in figure 4.1. A state space realization of the plant P is:

$$\left\{\begin{array}{rcl} \dot{x} &=& Ax + B_{w_1}w_1 + B_{w_2}w_2 + B_u u \\ z_1 &=& C_{z_1}x + D_{z_1w_1}w_1 + D_{z_1w_2}w_2 + D_{z_1u}u \\ z_2 &=& C_{z_2}x + D_{z_2w_1}w_1 + D_{z_2w_2}w_2 + D_{z_2u}u \\ y &=& C_y x + D_{yw_1}w_1 + D_{yw_2}w_2 + D_{yu}u \end{array}\right. \tag{4.1}$$

The objective in mixed H_2/H_∞ controller design is to find a stabilizing controller C, $u = Cy$, such that

$$\min_C \|T_{z_1w_1}\|_2 \tag{4.2}$$

$$\|T_{z_2w_2}\|_\infty < \gamma. \tag{4.3}$$

Without loss of generality, we take $\gamma = 1$. This can always be realized with an appropriate scaling of the matrices. If the state space realization of the controller is:

$$\left\{\begin{array}{rcl} \dot{\hat{x}} &=& A_c\hat{x} + B_c y \\ u &=& C_c\hat{x} + D_c y \end{array}\right.$$

then

$$T_{z_1w_1} = \left(\begin{array}{cc|c} A + B_u D_c M^{-1} C_y & B_u \overline{M}^{-1} C_c & B_{w_1} + B_u D_c M^{-1} D_{yw_1} \\ B_c M^{-1} C_y & A_c + B_c M^{-1} D_{yu} C_c & B_c M^{-1} D_{yw_1} \\ \hline C_{z_1} + D_{z_1u} D_c M^{-1} C_y & D_{z_1u}\overline{M}^{-1} C_c & D_{z_1w_1} + D_{z_1u} D_c M^{-1} D_{yw_1} \end{array}\right)$$

$$T_{z_2w_2} = \left(\begin{array}{cc|c} A + B_u D_c M^{-1} C_y & B_u \overline{M}^{-1} C_c & B_{w_2} + B_u D_c M^{-1} D_{yw_2} \\ B_c M^{-1} C_y & A_c + B_c M^{-1} D_{yu} C_c & B_c M^{-1} D_{yw_2} \\ \hline C_{z_2} + D_{z_2u} D_c M^{-1} C_y & D_{z_1u}\overline{M}^{-1} D_{yu})C_c & D_{z_2w_2} + D_{z_2u} D_c M^{-1} D_{yw_2} \end{array}\right)$$

where $M = I - D_{yu}D_c$ and $\overline{M} = I - D_c D_{yu}$. The feedthrough matrix of $T_{z_1w_1}$ has to be zero to obtain a finite H_2 norm. To ensure a finite H_2 norm, the following is assumed:

$$D_{z_1w_1} = 0, \quad D_c = 0.$$

We also assume:

$$D_{yu} = 0.$$

This assumption is only made for the clarity of the formulas. However, it is not a restriction. Afterwards the controller can easily be transformed to

take into account $D_{yu} \neq 0$ ([56]). With these assumptions the equations of $T_{z_1w_1}$ and $T_{z_2w_2}$ simplify to:

$$T_{z_1w_1} = \left(\begin{array}{cc|c} A & B_u C_c & B_{w_1} \\ B_c C_y & A_c & B_c D_{yw_1} \\ \hline C_{z_1} & D_{z_1u} C_c & 0 \end{array}\right),$$

$$T_{z_2w_2} = \left(\begin{array}{cc|c} A & B_u C_c & B_{w_2} \\ B_c C_y & A_c & B_c D_{yw_2} \\ \hline C_{z_2} & D_{z_2u} C_c & D_{z_2w_2} \end{array}\right).$$

4.2.2 Proposed Solution

To solve this problem, we propose to consider the H_∞ constraint and the H_2 objective function separately.

In the first step we only look at the H_∞ constraint as shown in figure 4.2. The input w_1 and the output z_1 are 'removed'. It is well-known that if the H_∞ constraint can be satisfied, there is not a single controller that satisfies this constraint but a whole set of controllers ([40],[57]). This set can be parameterized. A controller generator can be computed and the parameter is a stable, H_∞ norm bounded function. The H_∞ controller generator K is again a generalized plant. The parameter will be called Q. This is shown in figure 4.3.

In a second step, the controller of the set that minimizes the H_2 norm will be computed. We concentrate now on the input w_1 and the output z_1, and 'remove' the input w_2 and the output z_2. To take into account the set of feasible H_∞ controllers, the H_∞ controller generator is attached to the plant. Again, we obtain a generalized plant with inputs w_1 and r and outputs z_1 and v. This is shown in figure 4.4. The goal is now to find the Q, $r = Qv$, that minimizes the H_2 norm. However, Q has to be stable and H_∞ norm bounded. In most cases no analytic solution can be found for Q_{opt}. Numerical methods have to be used.

The resulting configuration is shown in figure 4.5. When the optimal Q_{opt} is found, the optimal controller is $C_{opt} = \mathcal{F}_l(K, Q_{opt})$, where $\mathcal{F}_l(.,.)$ represent the lower fractional transformation.

The following sections explain the two steps in detail.

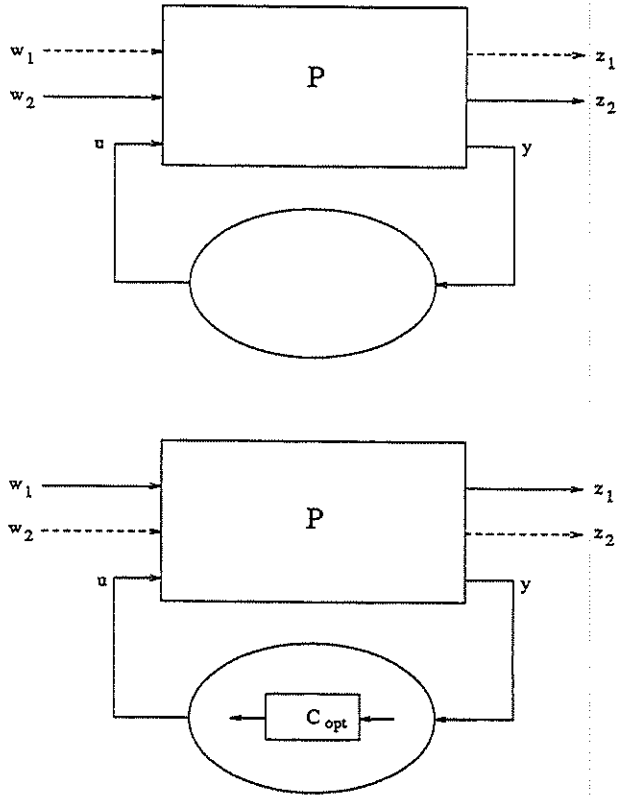

Figure 4.2: A schematic representation of the proposed solution to solve the mixed H_2/H_∞ problem. In the first step, only the H_∞ problem is considered. The controller generator of the set of controllers that satisfy the H_∞ constraint is computed. In the second step, the controller in the set, which minimizes the H_2 norm has to be found.

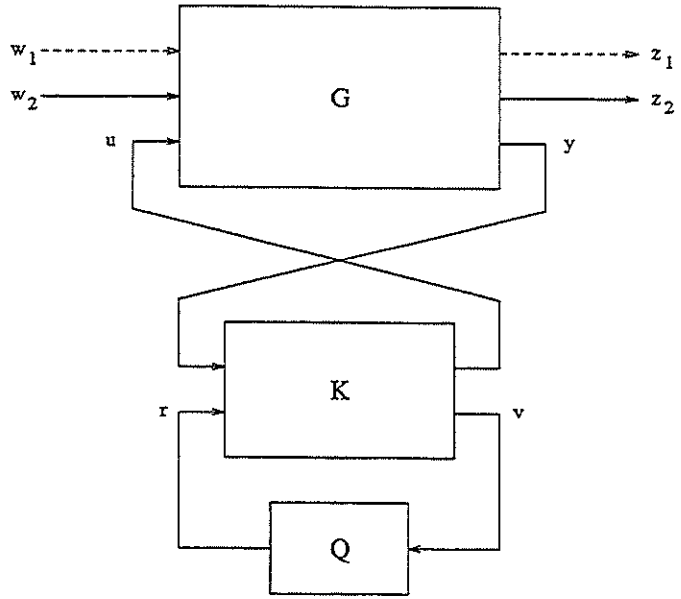

Figure 4.3: The set of controllers that satisfy the H_∞ constraint can be parameterized by a controller generator and a parameter Q. The resulting H_∞ controllers are a lower fractional transformation of the controller generator K and a stable transfer function Q: $C = \mathcal{F}_l(K, Q)$.

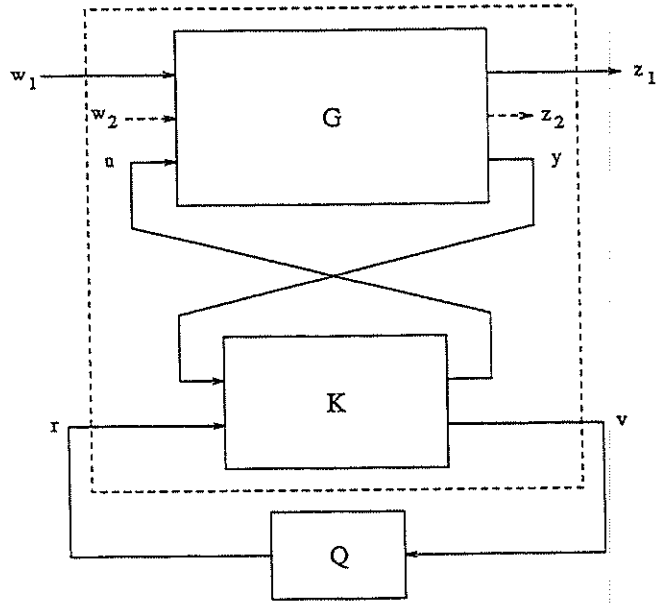

Figure 4.4: The solution of the H_2 control part. The H_∞ controller generator is attached to the plant G. This results in a new generalized plant. The stable and H_∞ norm bound transfer function Q has to be found that minimizes $\|T_{z_1 w_1}\|_2$.

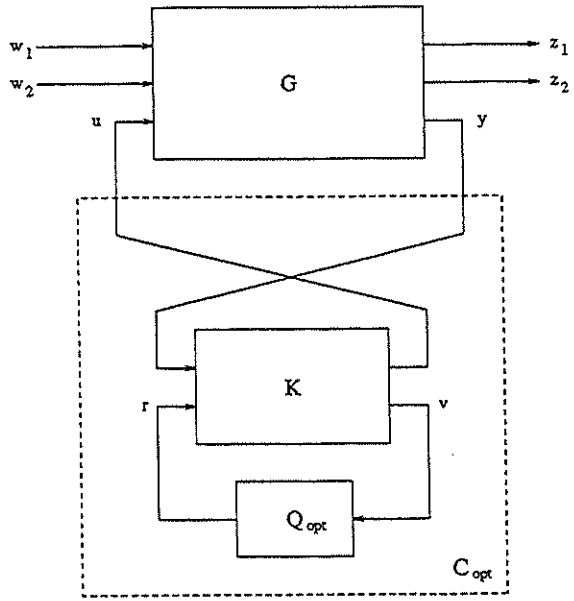

Figure 4.5: The resulting configuration for the mixed H_2/H_∞ controller.

4.3 The H_∞ Control Part

In general, there is a set of solutions to the suboptimal H_∞ control problem, if there exists a solution ([40],[57]). Without loss of generality, the H_∞ control problem can always be solved such that the H_∞ norm of the closed loop is smaller than 1. The set of controllers satisfying this conditions is parameterized by a *controller generator* and a feedback Q, where Q is a stable, H_∞ norm bounded transfer function.

Below we show the realization of the controller generator for $\gamma = 1$, as derived in [57]. It is given in a descriptor form. $D_{11} = 0$ and $D_{22} = 0$ are assumed. See [57] for formulas if $D_{z_2w_2} \neq 0$. $D_{yu} = 0$ for notational reasons. It is also assumed that $D_{z_2u}^t D_{z_2u} = I$ and $D_{yw_2} D_{yw_2}^t = I$. This can always be achieved by an appropriate scaling.
Consider the following two algebraic Riccati equations:

$$\begin{aligned}&(A - B_u D_{z_2u}^t C_{z_2})^t P + P(A - B_u D_{z_2u}^t C_{z_2}) \\ &\quad -P(B_u B_u^t - B_{w_2} B_{w_2}^t)P + C_{z_2}^t D_\perp D_\perp^t C_{z_2} = 0, \qquad (4.4)\\ &(A - B_{w_2} D_{yw_2}^t C_y)S + S(A - B_{w_2} D_{yw_2}^t C_y)^t \\ &\quad -S(C_y^t C_y - C_{z_2}^t C_{z_2})S + B_{w_2} \tilde{D}_\perp^t \tilde{D}_\perp B_{w_2}^t = 0. \qquad (4.5)\end{aligned}$$

$D_\perp$ and $\tilde{D}_\perp$ are orthogonal complements of D_{z_2u} and D_{yw_2} such that $\begin{pmatrix} D_{z_2u} & D_\perp \end{pmatrix}$ and $\begin{pmatrix} D_{yw_2}^t & \tilde{D}_\perp^t \end{pmatrix}$ are square and orthogonal.
There exists a solution to the suboptimal H_∞ problem if the following three conditions hold:

1. $\overline{\sigma}(D_{z_2w_2}) < \gamma$.
2. There exist positive definite solutions P and S of the algebraic Riccati equation (4.4) and (4.5).
3. $\lambda_{\max}(PS) < 1$.

The resulting controller generator K is given by:

$$\left\{\begin{array}{rcl} E_k\dot{x}_k &=& A_k x_k + B_{k1} y + B_{k2} r \\ u &=& C_{k1} x_k + D_{k11} y + D_{k12} r \\ v &=& C_{k2} x_k + D_{k21} y + D_{k22} r, \end{array}\right. \qquad (4.6)$$

where

$$E_k = I - SP,$$

$$\begin{aligned} B_{k1} &= -(B_{w_2} D_{yw_1}^t + \gamma^2 S C_y^t), \\ C_{k1} &= -(D_{z_2u}^t C_{z_2} + \gamma^2 B_u^t P), \\ D_{k11} &= 0, \qquad D_{k12} = -I, \\ D_{k21} &= -I, \qquad D_{k22} = 0, \\ A_k &= E_k\{A + B_u C_{k1}\} + B_{k1} C_y + \{E_k B_1 + B_{k1} D_{21}\} B_1^t P, \\ B_{k2} &= -(B_u + S C_{z_2}^t D_{z_2u}), \\ C_{k2} &= -(C_y + D_{yw_2} B_{w_2}^t P). \end{aligned}$$

All the controllers C, $u = Cy$, that satisfy the H_∞ (sub-)optimal control problem are given by the controller generator (4.6) and a transfer function Q: $C = \mathcal{F}_l(K, Q)$. If $\|Q\|_\infty < 1$, the resulting controller C is stabilizing. This is used to solve the mixed H_2/H_∞ control problem. The general H_2/H_∞ setup is shown in figure 4.3. G is the plant model, K is the H_∞ (sub-) optimal controller generator and Q is the parameter. From this derivation it is clear that the lowest possible γ for the mixed H_2/H_∞ problem, is the lowest possible norm that can be achieved for the H_∞ problem.

4.4 The Optimal H_2 Controller

In the previous section it was shown how the set of controllers that satisfy the H_∞ constraint can be determined. For the H_2 problem only the input w_1 and the output z_1 are considered. Now we still have to find the transfer function Q that minimizes the H_2 norm from w_1 to z_1. If there exists a solution to the H_∞ problem, append the H_∞ controller generator to the plant model. This is a so-called Redheffer star product, often used in μ-synthesis ([2],[42]).

Within the set of controllers that stabilize the closed loop and satisfy the H_∞ condition $\|T_{z_2w_2}\|_\infty < 1$, find the controller that minimizes the H_2 norm of $T_{z_1w_1}$. Therefore, we search for the transfer function Q, $r = Qv$, that minimizes the H_2 norm from z_1 to w_1.

The transfer function Q, however, should be such that it does not destabilize $T_{z_2w_2}$ and keeps the H_∞ norm of $T_{z_2w_2}$ less than or equal to 1. Therefore, we know from the H_∞ control theory, that Q has to be a stable transfer function such that $\|Q\|_\infty < 1$. The problem can now be stated as:

$$\min_Q \|T_{z_1w_1}\|_2 \qquad \text{subject to} \quad \|Q\|_\infty < 1.$$

We call this problem a H_2 control design with an H_∞ bounded controller. To obtain a finite H_2 norm the following conditions must hold:

1. $D_{z_1 w_1} = 0$.

2. Q has to be strictly proper.
   A state space realization of Q is

$$\begin{cases} \dot{x}_q &= A_q x_q &+ B_q v \\ r &= C_q x_q. \end{cases}$$

Thus Q has to be stable, strictly proper and H_∞ norm bounded transfer function: $\|Q\|_\infty < 1$. Unfortunately, no analytic solution has been found yet. We will only show how such a controller can be computed numerically. A parameterization of all strictly, proper, norm bounded H_∞ transfer functions, proposed by Steinbuch and Bosgra ([92]), will be used. Necessary conditions for the solution will be derived.

4.4.1 Parameterization of H_∞ Norm Bounded Transfer Functions

In [92], Steinbuch and Bosgra describe a parameterization for strictly proper, stable, norm-bounded finite-dimensional transfer functions:

Lemma 6 *Let the set Ω_γ^* be defined as*

$$\Omega_\gamma^* = \{F(s) \mid \|F(s)\|_\infty < \gamma, F(s) \text{ stable, real rational,}$$

$$\text{strictly proper and of McMillan degree} \leq n\}$$

and consider the set Ω_γ

$$\Omega_\gamma = \{C(sI - A)^{-1}B | A = A_s + A_k, A_s = -\frac{1}{2}\gamma^{-2}BB^t - \frac{1}{2}C^tC,$$

$$A_k = -A_k^t \in \mathbb{R}^{n\times n}, B \in \mathbb{R}^{n\times n_w}, C \in \mathbb{R}^{n_z \times n}\}$$

then $\Omega_\gamma = \Omega_\gamma^*$.

4.4.2 H_2 Optimization with an H_∞ Bounded Controller - Necessary Conditions

In this section necessary conditions are derived for a H_∞ norm bounded controller that minimizes an H_2 norm. We will call this problem a constrained H_2 problem.

Consider the following linear, time invariant plant:

$$\begin{cases} \dot{x} &= Ax &+ B_1 w &+ B_2 u \\ z &= C_1 x &+ D_{11} w &+ D_{12} u \\ y &= C_2 x &+ D_{21} w &+ D_{22} u. \end{cases} \tag{4.7}$$

Now find a dynamic, stable, strictly proper, H_∞ norm bounded controller K, $u = Ky$, that stabilizes the closed loop and such that the H_2 norm of the closed loop transfer function from w to z is minimized. K has to belong to Ω_γ. Again without loss of generality $\gamma = 1$ is assumed. The state space realization of the controller is then:

$$\begin{cases} \dot{x}_c &= A_c x_c &+ B_c y \\ u &= C_c x_c. \end{cases} \tag{4.8}$$

To make the 2 norm of the closed loop finite, D_{11} has to be 0. For notational reasons, we also assume that $D_{22} = 0$. This is not a limitation, as the controller is strictly proper. This is shown e.g. in the paper of Doyle and Glover [38].
From (4.7) and (4.8) the state space realization of the closed loop can be derived ($D_{11} = 0$ and $D_{22} = 0$):

$$\begin{cases} \begin{pmatrix} \dot{x} \\ \dot{x}_c \end{pmatrix} &= \begin{pmatrix} A & B_2C_c \\ B_cC_2 & A_c \end{pmatrix} \begin{pmatrix} x \\ x_c \end{pmatrix} + \begin{pmatrix} B_1 \\ B_cD_{21} \end{pmatrix} w \\ z &= \begin{pmatrix} C_1 & D_{12}C_c \end{pmatrix} \begin{pmatrix} x \\ x_c \end{pmatrix} \end{cases} \tag{4.9}$$

Define

$$\overline{A} = \begin{pmatrix} A & B_2C_c \\ B_cC_2 & A_c \end{pmatrix}, \quad \overline{B} = \begin{pmatrix} B_1 \\ B_cD_{21} \end{pmatrix}, \quad \overline{C} = \begin{pmatrix} C_1 & D_{12}C_c \end{pmatrix}.$$

The control objective can be expressed as:

$$\min_{K\in\Omega_1} \text{trace}\{\overline{C}^t\overline{C}S\},$$

where S is the solution of

$$\overline{A}S + S\overline{A}^t + \overline{B}\overline{B}^t = 0.$$

Necessary conditions for this problem are given in the following lemma.

Lemma 7 *Necessary conditions for the constrained H_2 problem.*

Given the state space realization of (4.7), a stable, finite dimensional, strictly proper controller K, with H_∞ norm smaller than 1, that stabilizes the closed loop and minimizes the H_2 norm of the closed loop transfer function from w to z satisfies the following equations:

$$\begin{aligned} \overline{A}S + S\overline{A}^t + \overline{B}\overline{B}^t &= 0, \\ P\overline{A} + \overline{A}^t P + \overline{C}^t\overline{C} &= 0, \end{aligned}$$

$$\begin{pmatrix} P_{12}^t & P_{22} \end{pmatrix} \begin{pmatrix} S_{12} \\ S_{22} \end{pmatrix} = \begin{pmatrix} S_{12}^t & S_{22} \end{pmatrix} \begin{pmatrix} P_{12} \\ P_{22} \end{pmatrix},$$

$$A_s + \frac{1}{2}B_cB_c^t + \frac{1}{2}C_c^tC_c = 0,$$

$$B_c = \left[\begin{pmatrix} S_{12}^t & S_{22} \end{pmatrix} \begin{pmatrix} P_{12} \\ P_{22} \end{pmatrix} \right]^{-1} \begin{pmatrix} P_{12}^t & P_{22} \end{pmatrix} \begin{pmatrix} S_{11} \\ S_{12}^t \end{pmatrix} C_2^t,$$

$$C_c \begin{pmatrix} S_{12}^t & S_{22} \end{pmatrix} \begin{pmatrix} P_{12} \\ P_{22} \end{pmatrix} - D_{12}^t D_{12} C_c S_{22} = D_{12}^t C_1 S_{12} + B_2^t \begin{pmatrix} P_{11}^t & P_{12} \end{pmatrix} \begin{pmatrix} S_{12} \\ S_{22} \end{pmatrix},$$

where $A_c = A_s + A_k$ with $A_s = A_s^t$ and $A_k = -A_k^t$. S and P have to be positive definite $S > 0$ and $P > 0$. The inverse

$$\left[\begin{pmatrix} S_{12}^t & S_{22} \end{pmatrix} \begin{pmatrix} P_{12} \\ P_{22} \end{pmatrix} \right]^{-1}$$

has to exist.

Proof:
The necessary conditions can easily be derived using Lagrange multipliers. The Lagrangian we obtain is:

$$\begin{aligned} \mathcal{L} &= \text{trace}\left\{ \begin{pmatrix} C_1^tC_1 & C_1^tD_{12}C_c \\ C_c^tD_{12}^tC_1 & C_c^tD_{12}^tD_{12}C_c \end{pmatrix} \begin{pmatrix} S_{11} & S_{12} \\ S_{12}^t & S_{22} \end{pmatrix} \right\} \\ &+ \text{trace}\left\{ \begin{pmatrix} P_{11} & P_{12} \\ P_{12}^t & P_{22} \end{pmatrix} \left[\begin{pmatrix} A & B_2C_c \\ B_cC_2 & A_c \end{pmatrix} \begin{pmatrix} S_{11} & S_{12} \\ S_{12}^t & S_{22} \end{pmatrix} \right.\right. \\ &\quad \left.\left. + \begin{pmatrix} S_{11} & S_{12} \\ S_{12}^t & S_{22} \end{pmatrix} \begin{pmatrix} A^t & C_2^tB_c^t \\ C_c^tB_2^t & A_c^t \end{pmatrix} + \begin{pmatrix} B_1B_1^t & B_1D_{21}^tB_c^t \\ B_cD_{21}B_1^t & B_cD_{21}D_{21}^tB_c^t \end{pmatrix} \right] \right\} \\ &+ \text{trace}\left\{ Q\left(A_s + \frac{1}{2}B_cB_c^t + \frac{1}{2}C_c^tC_c \right) \right\}, \end{aligned}$$

where $A_c = A_s + A_k$ and $A_s = A_s^t$, $A_k = -A_k^t$. This last constraint is not taken into account explicitly into the Lagrangian but will be used implicitly in the derivation of the necessary conditions.

Taking the derivatives we obtain the following necessary conditions:

$$\frac{\partial \mathcal{L}}{\partial P} : \overline{A}S + S\overline{A}^t + \overline{B}\overline{B}^t = 0, \tag{4.10}$$

$$\frac{\partial \mathcal{L}}{\partial S} : P\overline{A} + \overline{A}^tP + \overline{C}^t\overline{C} = 0, \tag{4.11}$$

$$\frac{\partial \mathcal{L}}{\partial Q} : A_s + \frac{1}{2}B_cB_c^t + \frac{1}{2}C_c^tC_c = 0, \tag{4.12}$$

$$\frac{\partial \mathcal{L}}{\partial A_s} : S_{12}^tP_{12} + P_{12}^tS_{12} + S_{22}P_{22} + P_{22}S_{22} + Q = 0, \tag{4.13}$$

$$\frac{\partial \mathcal{L}}{\partial A_k} : -S_{12}^tP_{12} + P_{12}^tS_{12} - S_{22}P_{22} + P_{22}S_{22} = 0, \tag{4.14}$$

$$\frac{\partial \mathcal{L}}{\partial B_c} : 2P_{12}^tS_{11}C_2^t + 2P_{22}S_{12}^tC_2^t + 2P_{12}^tB_1D_{21}^t + 2P_{22}B_cD_{21}D_{21}^t + QB_c = 0, \tag{4.15}$$

$$\frac{\partial \mathcal{L}}{\partial C_c} : 2D_{12}^tC_1S_{12} + 2D_{12}^tD_{12}C_cS_{22} + 2B_2^tP_{11}S_{12} + 2B_2^tP_{12}S_{22} + C_cQ = 0. \tag{4.16}$$

From (4.14) we find

$$\begin{pmatrix} P_{12}^t & P_{22} \end{pmatrix} \begin{pmatrix} S_{12} \\ S_{22} \end{pmatrix} = \begin{pmatrix} S_{12}^t & S_{22} \end{pmatrix} \begin{pmatrix} P_{12} \\ P_{22} \end{pmatrix}. \tag{4.17}$$

Substitution into (4.13), (4.15) and (4.16) yields:

$$Q = -2\begin{pmatrix} S_{12}^t & S_{22} \end{pmatrix} \begin{pmatrix} P_{12} \\ P_{22} \end{pmatrix}, \tag{4.18}$$

$$B_c = \left[\begin{pmatrix} S_{12}^t & S_{22} \end{pmatrix} \begin{pmatrix} P_{12} \\ P_{22} \end{pmatrix} \right]^{-1} \begin{pmatrix} P_{12}^t & P_{22} \end{pmatrix} \begin{pmatrix} S_{11} \\ S_{12}^t \end{pmatrix} C_2^t, \tag{4.19}$$

$$\begin{aligned} &C_c \begin{pmatrix} S_{12}^t & S_{22} \end{pmatrix} \begin{pmatrix} P_{12} \\ P_{22} \end{pmatrix} - D_{12}^tD_{12}C_cS_{22} \\ &\quad = D_{12}^tC_1S_{12} + B_2^t \begin{pmatrix} P_{11} & P_{12} \end{pmatrix} \begin{pmatrix} S_{12} \\ S_{22} \end{pmatrix}. \end{aligned} \tag{4.20}$$

□

4.4.3 Numerical Computation of Q

$Q(s)$ can be found as the solution of an unconstrained minimization problem. The objective function is

$$\text{trace}\{\overline{C}^t \overline{C} S\}$$

and the unknown parameters are A_k, B_c and C_c. A_s can be obtained from (4.12). When A_s is known, P and S can be computed from (4.10) and (4.11). Q has to satisfy (4.13). The gradients of A_k, B_c and C_c are then given by (4.14), (4.15) and (4.16). Of course these gradients will only be zero in the (local) minimum.

The results of section 4.6 are obtained with the unconstrained optimization function of the optimization toolbox of the software package MATLAB.

4.5 Existence of Solutions

In [86], Ridgely *et al.* prove some facts about the existence of a controller that satisfies the constraints. They can easily be understood from the above theory. We add a new observation concerning Q. The following definitions are needed:

- Call C_2 the H_2 controller that minimizes $\|T_{z_1 w_1}\|_2$ without the H_∞ constraint on $T_{z_2 w_2}$ (or $\gamma = +\infty$).
- Call C_∞ the 'central' H_∞ controller that minimizes $\|T_{z_2 w_2}\|_\infty$ without the H_2 constraint on $T_{z_1 w_1}$.

Based on C_2 and C_∞ the following values are defined:

$\gamma_2 = \|T_{z_2 w_2}\|_\infty$ when $C = C_2$.

$\gamma_0 = \|T_{z_2 w_2}\|_\infty$ when $C = C_\infty$.

$\alpha_0 = \|T_{z_1 w_1}\|_2$ when $C = C_2$.

With these definitions the following observations can easily be checked:

- If $\gamma < \gamma_0$ then no solution to the mixed H_2/H_∞ problem exists, as no controllers exist that satisfy the H_∞ constraint.
- If $\gamma > \gamma_2$ then the optimal controller is C_2, as C_2 is in the set of controllers that satisfy the H_∞ constraint.

- From the definition of α_0, it is clear that $\|T_{z_1 w_1}\|_2 \geq \alpha_0$ if a controller C exists that satisfies the constraints.
- Consider now the generalized plant with the H_∞ controller attached. If $\gamma > \gamma_2$ and Q is computed as the optimal H_2 controller, then $\|Q\|_\infty < 1$. This is easily explained: As C_2 is in the set of admissible controllers, there has to exist a Q, $\|Q\|_\infty < 1$, such that $\mathcal{F}_l(K, Q) = C_2$. An example is shown in the next section.

From these observations it is clear that the controller has to be computed numerically only if $\gamma_0 \leq \gamma < \gamma_2$.

4.6 Examples

4.6.1 A Simple Example

In this section an example is given of the calculation of an optimal mixed H_2/H_∞-controller. Consider the following example:

$$\left(\begin{array}{c|ccc} A & B_{w_1} & B_{w_2} & B_u \\ \hline C_{z_1} & D_{z_1 w_1} & D_{z_1 w_2} & D_{z_1 u} \\ C_{z_2} & D_{z_2 w_1} & D_{z_2 w_2} & D_{z_2 u} \\ C_y & D_{y w_1} & D_{y w_2} & D_{y u} \end{array}\right) = \left(\begin{array}{cc|cc|cc} 0.2 & 0.5 & 3 & 0 & 1 & 1 \\ -1 & -5 & 1 & 1 & 0 & 2 \\ \hline 2 & 4 & 0 & 0 & 0 & 0 \\ 0 & 0 & 0 & 0 & 0 & 1 \\ \hline 1 & 0 & 0 & 0 & 0 & 1 \\ 0 & 1 & 0 & 1 & 10 & 0 \end{array}\right)$$

Suppose now that a controller has to be designed such that

$$\min_C \|T_{z_1 w_1}\|_2$$

$$\text{subject to } \|T_{z_2 w_2}\|_\infty \leq 55.$$

The problem $\|T_{z_2 w_2}\|_\infty \leq 55$ can always be reduced to a problem $\|T_{z_2 w_2}\|_\infty \leq 1$ by an appropriate scaling of the matrices. First the controller generator is calculated for the H_∞ problem from w_1 to z_1. Then the H_2 norm is optimized over the parameter Q. We compute the optimal Q of order $2n = 4$. As an initial guess for $Q(s)$, the optimal H_2 controller is calculated from w_1 to z_1, when the H_∞ controller generator K is attached to the plant. This Q is however unstable. Thus an optimal Q has to be found by optimization. As an initial guess, the computed Q is taken with the unstable poles mirrored in the left half plane. If Q was stable and $\|Q\|_\infty > 1$, the initial guess would be

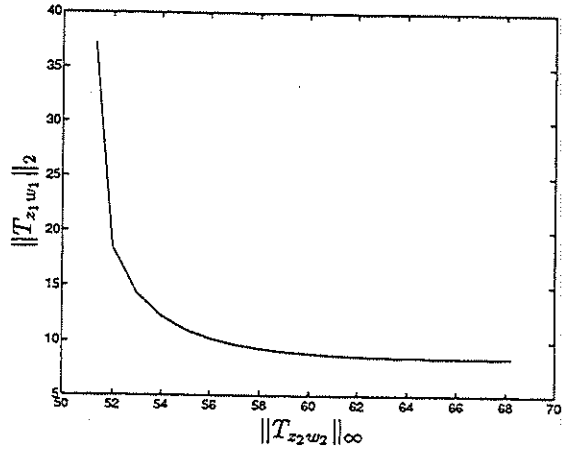

Figure 4.6: $\|T_{z_1w_1}\|_2$ versus $\|T_{z_2w_2}\|_\infty$ for the simple example. $\|T_{z_1w_1}\|_2$ and $\|T_{z_2w_2}\|_\infty$ form a trade-off: $\|T_{z_1w_1}\|_2$ increases for decreasing $\|T_{z_2w_2}\|_\infty$.

the Q scaled such that $\|Q\|_\infty < 1$. After optimization the H_∞ norm of the transfer function Q is equal to 1. The resulting closed loop transfer function is stable and the H_2 and H_∞ norms are:

$$\begin{aligned} \|T_{z_1w_1}\|_2 &= 10.98, \\ \|T_{z_2w_2}\|_\infty &= 55. \end{aligned}$$

The solution as a function of γ can also be studied. The problem solved is

$$\min_C \|T_{z_1w_1}\|_2$$

$$\|T_{z_2w_2}\|_\infty < \gamma.$$

First γ_2, γ_0 and α_0 are computed:

$$\gamma_2 = 68.17, \quad \gamma_0 = 51.23, \quad \alpha_0 = 8.454.$$

In the different plots, γ is varied between 51.3 and 80. In figure 4.6, the resulting optimal $\|T_{z_1w_1}\|_2$ is plotted versus $\|T_{z_2w_2}\|_\infty$. $\|T_{z_2w_2}\|_\infty$ and $\|T_{z_1w_1}\|_2$ form a trade-off: If $\|T_{z_2w_2}\|_\infty$ decreases, $\|T_{z_1w_1}\|_2$ has to increase. It is easily checked that the highest occurring value of $\|T_{z_2w_2}\|_\infty$ is γ_2, although γ ranges until 80. The lowest value of $\|T_{z_1w_1}\|_2$ is α_0.

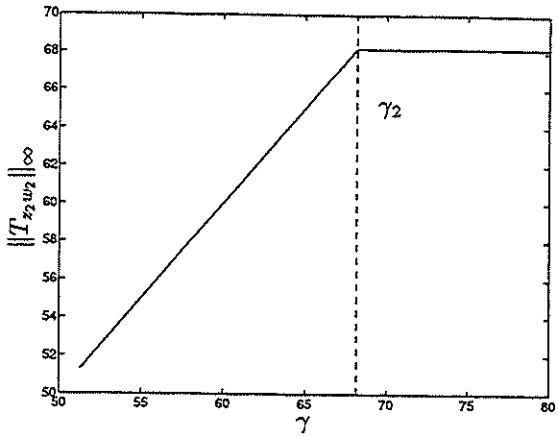

Figure 4.7: $\|T_{z_2w_2}\|_\infty$ versus γ for the simple example. For small γ's, $\|T_{z_2w_2}\|_\infty$ will decrease with decreasing γ. For large γ's, $\|T_{z_2w_2}\|_\infty$ will remain constant independent of the value of γ.

In figure 4.7, the H_∞ norm of $T_{z_2w_2}$ is plotted versus γ. $\|T_{z_2w_2}\|_\infty$ decreases with γ when $\gamma < \gamma_2$. If $\gamma > \gamma_2$, $\|T_{z_2w_2}\|_\infty$ remains constant. This illustrates a statement of section 4.5.

Consider now the computation of Q, the parameter of the set of admissible H_∞ controllers. Suppose Q is computed as the H_2 controller of $T_{z_1w_1}$ when the H_∞ controller generator is attached to the original plant, without checking the constraint $\|Q\|_\infty < 1$. Call this optimal unconstrained H_2 controller Q_2. In figure 4.8, the H_∞ norm of Q_2 is plotted versus γ. It is easily observed that $\|Q_2\|_\infty > 1$ when $\gamma < \gamma_2$. Below a certain γ, Q_2 is even unstable, such that an H_∞ norm does not exist. If $\gamma > \gamma_2$, then $\|Q_2\|_\infty < 1$. This implies that Q_2 belongs to the set of admissible H_∞ controllers. The resulting controller $C = \mathcal{F}_l(K, Q_2)$ is in fact the optimal controller C_2. There are pole-zero cancellations such that $\mathcal{F}_l(K, Q_2) = C_2$.

Until now the studied controllers are of order $3n$, where n is the order of the plant. This is of course a very high order. However, in the optimization routine for the H_∞ bounded H_2 controller any order can be taken. In figure 4.9, $\|T_{z_1w_1}\|_2$ is plotted as a function of the order of Q for $\gamma = 55$. The optimal H_2/H_∞ controller is computed with the order of Q between 0 and 12. Order 0 corresponds to the central H_∞ controller as D_c has to be 0.

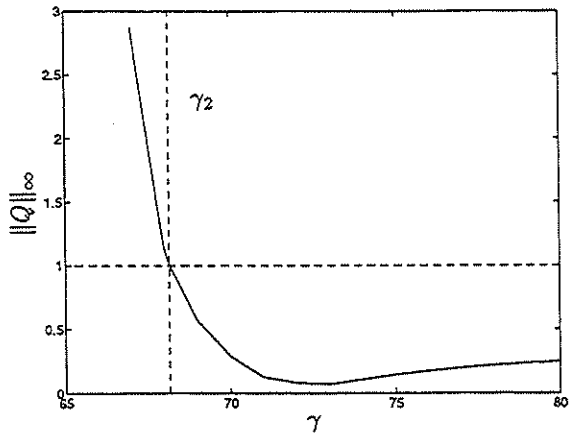

Figure 4.8: $\|Q_2\|_\infty$ versus γ where Q_2 is the optimal unconstrained H_2 controller for $\|T_{z_1w_1}\|$ when the controller generator K is attached to the plant. $\|Q_2\|_\infty > 1$ or Q_2 is unstable when $\gamma < \gamma_2$. $\|Q\|_\infty < 1$ when $\gamma > \gamma_2$. When $\gamma > \gamma_2$, C_2 is in the set of admissible H_∞ controllers. It is thus normal that there exists a Q_2, $\|Q_2\|_\infty < 1$, such that $C_2 = \mathcal{F}_l(K, Q_2)$.

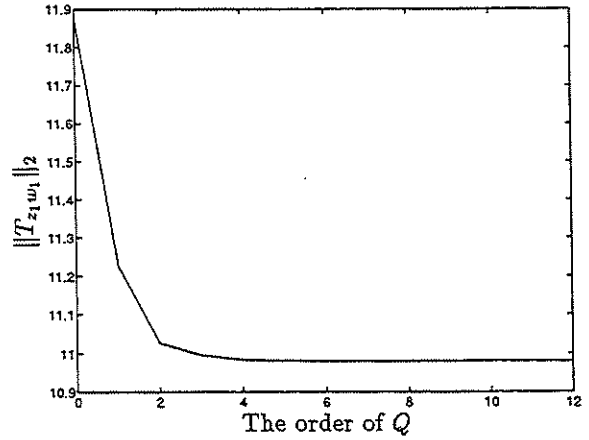

Figure 4.9: $\|T_{z_1w_1}\|_2$ versus the order of Q for $\gamma = 55$. $\|T_{z_1w_1}\|_2$ decreases slowly when the order of Q increases. Order 0 corresponds to the central H_∞ controller C_∞.

$\|T_{z_1w_1}\|_2$ decreases slowly as the order of Q increases. Even if the order is larger than $2n$, $\|T_{z_1w_1}\|_2$ still decreases. For low orders the norm decreases a lot and it seems to converge as the order increases. However, to our knowledge this has not been proved yet. However, it is clear that $\|T_{z_1w_1}\|_2$ can still decrease if the order of Q is larger than $2n$, which is 4 in this case.

4.6.2 The Ventilator Setup

In this section a mixed H_2/H_∞ controller is designed for the ventilator setup. Suppose we want to minimize the H_2 norm from $\begin{pmatrix} w_d & w_m \end{pmatrix}^t$ to $\begin{pmatrix} f_1 & u \end{pmatrix}^t$ and there is an additive perturbation over the ventilator and the flow rate measurement. The corresponding block scheme is shown in figure 4.10. This can be rearranged into the general plant shown in figure 4.11.

The state space model of the resulting generalized plant is:

$$\left(\begin{array}{c|ccc} A & B_{w_1} & B_{w_2} & B_u \\ \hline C_{z_1} & D_{z_1w_1} & D_{z_1w_2} & D_{z_1u} \\ C_{z_2} & D_{z_2w_1} & D_{z_2w_2} & D_{z_2u} \\ C_y & D_{yw_1} & D_{yw_2} & D_{yu} \end{array}\right) = \left(\begin{array}{ccc|ccc|c} \alpha & \gamma C_d & 0 & 0 & 0 & 0 & \beta \\ 0 & A_d & 0 & B_d & 0 & 0 & 0 \\ \beta_m & 0 & \alpha_m & 0 & 0 & 0 & 0 \\ \hline 1 & 0 & 0 & 0 & 0 & 0 & 0 \\ 0 & 0 & 0 & 0 & 0 & 0 & 1 \\ \hline 0 & 0 & 0 & 0 & 0 & 0 & 1 \\ \hline 0 & 0 & \gamma_m & 0 & \delta_m & 1 & 0 \end{array}\right)$$

The model is of order five. First we compute γ_2, γ_0 and α_0:

$$\gamma_2 = 8.3001, \quad \gamma_0 = 7.6294e-06, \quad \alpha_0 = 173.7161.$$

The results are shown in figures 4.12, 4.13 and 4.14. They are similar to the results shown for the artificial example. The H_2 norm and the H_∞ norm form a trade-off. The robustness against uncertainties can be increased at the expense of more H_2 norm. The robustness increases with decreasing H_∞ norm. This is a direct consequence of the small gain theorem. In figure 4.13, remark that $\|T_{z_2w_2}\|_\infty = \gamma_2$ and constant, if $\gamma \geq \gamma_2$. When $\gamma < \gamma_2$, $\|T_{z_2w_2}\|_\infty$ is almost equal to γ. The H_∞ norm is increased as much as allowed by the constraint. In figure 4.14, observe that $\|Q_2\|_\infty > 1$ if $\gamma < \gamma_2$ and $\|Q_2\|_\infty \leq 1$ if $\gamma \geq \gamma_2$, if Q_2 is computed as the optimal H_2 controller of the plant with the controller generator attached. In figure 4.15, $\|T_{z_1w_1}\|_2$ is plotted versus the order of Q, for $\gamma = 4$. The H_2 norm slightly decreases with increasing order of Q.

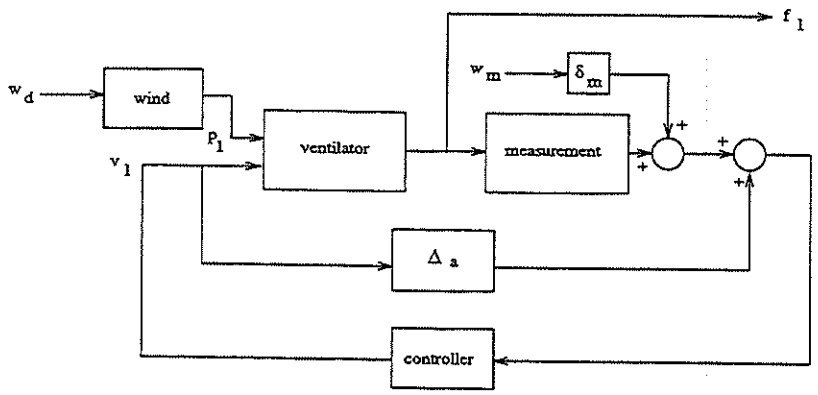

Figure 4.10: The block scheme of the ventilator setup with the additive disturbance.

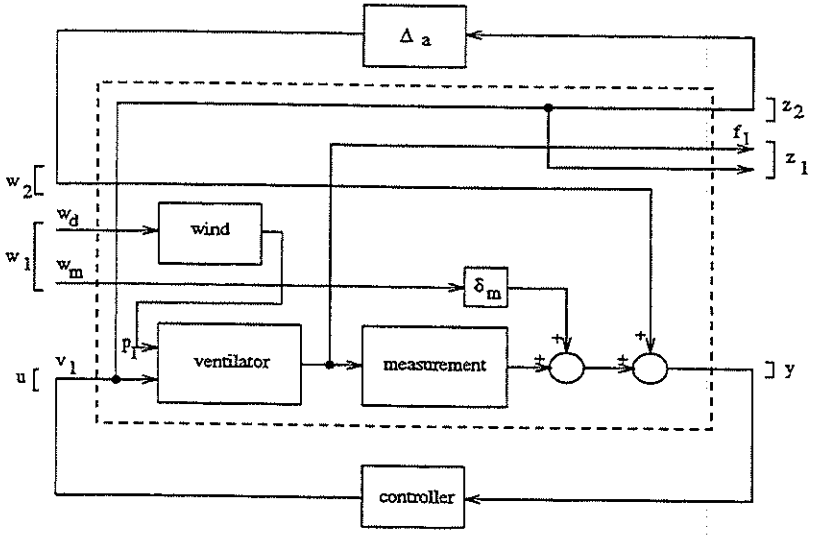

Figure 4.11: The block scheme of the ventilator setup with the additive disturbance, rearranged in a generalized plant form.

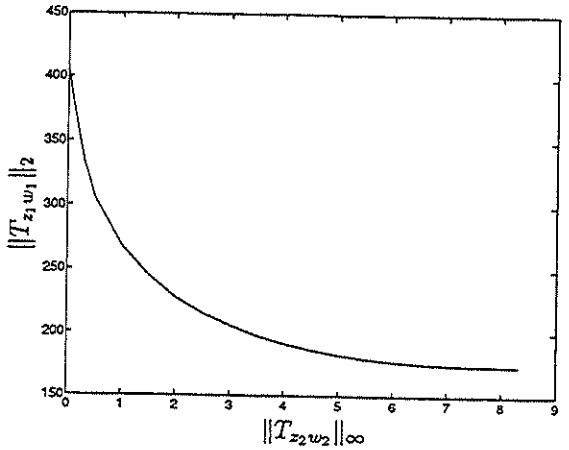

Figure 4.12: $\|T_{z_1 w_1}\|_2$ versus $\|T_{z_2 w_2}\|_\infty$ for the ventilator setup. The order of Q is $2n = 10$. $\|T_{z_1 w_1}\|_2$ and $\|T_{z_2 w_2}\|_\infty$ form a trade-off: $\|T_{z_1 w_1}\|_2$ increases for decreasing $\|T_{z_2 w_2}\|_\infty$. The lowest possible H_2 norm is α_0. The lowest possible H_∞ norm is γ_0. $\|T_{z_2 w_2}\|_\infty$ does not exceed γ_2.

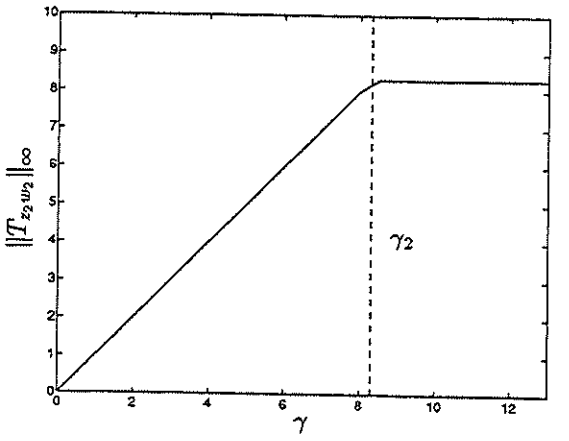

Figure 4.13: $\|T_{z_2 w_2}\|_\infty$ versus γ for the ventilator setup. For small γs, $\|T_{z_2 w_2}\|_\infty$ will decrease with decreasing γ. For large γ's, $\|T_{z_2 w_2}\|_\infty$ will remain constant independent of the value of γ.

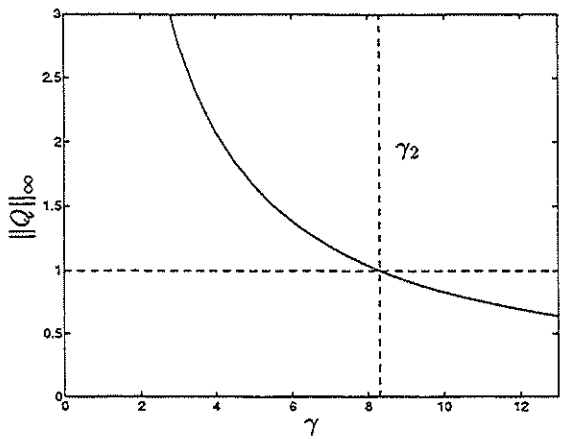

Figure 4.14: $\|Q_2\|_\infty$ versus γ, where Q_2 is the optimal unconstrained H_2 controller for $\|T_{z_1 w_1}\|$ when the controller generator K is attached to the plant. $\|Q_2\|_\infty > 1$ or Q_2 is unstable when $\gamma < \gamma_2$. $\|Q_2\|_\infty < 1$ when $\gamma > \gamma_2$. When $\gamma > \gamma_2$, C_2 is in the set of admissible H_∞ controllers. It is thus normal that there exists a Q_2, $\|Q_2\|_\infty < 1$, such that $C_2 = \mathcal{F}_l(K, Q_2)$.

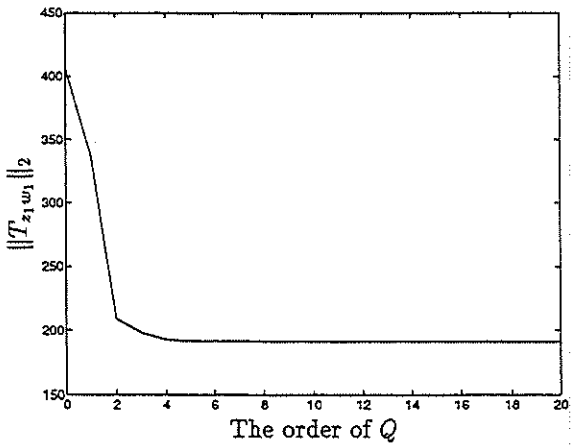

Figure 4.15: $\|T_{z_1 w_1}\|_2$ versus the order of Q for $\gamma = 4$. $\|T_{z_1 w_1}\|_2$ decreases slowly when the order of Q increases. Order 0 corresponds to the central H_∞ controller C_∞.

4.7 Conclusions and Remarks

In this chapter a new approach to the general mixed H_2/H_∞ problem is presented. To solve the problem, the H_∞ and the H_2 problems are separated. In this way, the exact problem can be minimized and not a kind of upper bound.

First, the controller generator for the H_∞ problem is calculated. Using this controller generator, the whole set of controllers satisfying the H_∞ criterion, can be parameterized. In this set of controllers the one that minimizes the H_2 norm of $T_{z_1 w_1}$ has to be found. This can be done using a parameterization of H_∞ norm bounded transfer functions. Therefore, a constrained H_2 problem has to be solved. The controller that minimizes the H_2 norm, and with H_∞ norm lower than 1, has to be found. Necessary conditions for this controller are also derived. It is also shown that the H_2 and the H_∞ norm seem to form a trade off. Also the problem of a fast calculation of the optimal controller is still under investigation.

The full mixed H_2/H_∞ problem is not solved yet. In this chapter we have shown how a controller can be designed that minimizes the H_2 norm given a certain order of the controller. However, it is not known what the order of the optimal controller is, except in special cases, as discussed in e.g. [68] and [87].

A disadvantage of our method is the high order of the resulting controller. However, the complexity of the computations is lower than in the case of a direct design with the two constraints involved simultaneously.

It would have been nice if the full mixed H_2/H_∞ problem could be cast as an LMI problem. Then a fast and reliable algorithm would exist to compute a controller that satisfies the constraints. However, this seems not to be possible.

Chapter 5

Reduced Order Controller Design by Rank Minimization under LMI Constraints

5.1 Introduction

Fast and reliable algorithms exist to solve convex problems ([12],[80],[97]). This has motivated many researchers to formulate or reformulate problems in systems and control theory as convex problems. We refer to [12], [14] and the references therein. For instance, it has been shown how the design of some output feedback controllers can be formulated as a convex problem. In [12], convex design specifications are studied. It is proposed to design output feedback controllers using the Youla parameterization of all stabilizing controllers. To obtain a convex problem the stable parameter of the Youla parameterization is approximated by a series of stable functions. Unfortunately, the resulting controllers are usually of very high order. More recently it has been shown how some output feedback design problems can be formulated as convex problems involving linear matrix inequalities (LMI) ([6], [14], [52]). In this case the order of the controller is usually equal to the order of the plant. However, it is not possible to include many specifications simultaneously.

In [47] a framework for the design of reduced order output feedback controllers has been proposed. It also involves LMIs. However, the problem

is not convex any more: The rank of an affine matrix function has to be minimized subject to LMIs. The general formulation of the problem is:

$$\min_{x\in\mathbb{R}^m} \text{Rank } F(x), \qquad \text{subject to } \begin{cases} F(x) \geq 0 \\ C(x) \geq 0, \end{cases} \tag{5.1}$$

where $F(x)$ and $C(x)$ are symmetric affine matrix functions:

$$F(x) = F_0 + x_1F_1 + x_2F_2 + \ldots + x_mF_m,$$

$$C(x) = C_0 + x_1C_1 + x_2C_2 + \ldots + x_mC_m,$$

with $F_i = F_i^t \in \mathbb{R}^{n_f \times n_f}$ and $C_i = C_i^t \in \mathbb{R}^{n_c \times n_c}$, $i = 0 \ldots m$.

This problem arises not only in control but also in identification. E.g. the Frisch scheme can easily be formulated as a minimum rank problem involving LMIs ([28],[67]).

In this chapter two heuristic algorithms are presented to solve these problems. They are both based on algorithms for convex optimization involving LMIs. The first algorithm is based on an inversion of the analytic centering used in the method of centers. The second algorithm is an extension of a potential reduction method for the optimization of a linear objective over a convex set. Although the minimum rank problems are not convex, these heuristic algorithms still find reduced rank solutions very fast.

It is shown how the search direction can be computed as the solution of a least squares problem ([13]). The feasibility of the step can be ensured using the appropriate damping factor. Finally, easy stopping criteria can be derived.

This chapter is structured as follows. First some examples in robust control where minimum rank problems appear, are presented to motivate the development of an algorithm for solving these problems. In section 5.3 it is shown that the minimum rank problem is NP-hard. In section 5.4 some aspects of interior point methods for positive definite problems are briefly described. Section 5.5 presents the algorithm based on the inversion of analytic centering, to solve the minimum rank problems. The extension of the potential reduction method is described in section 5.6. The two algorithms are compared in section 5.7. Some convergence aspects of the algorithms are discussed in section 5.8. Section 5.9 contains numerical results. In section 5.10 other problems that can be cast as minimum rank problems are presented. The conclusions are summarized in section 5.11.

5.2 Minimum Rank Problems in Robust Control

In this section we give some examples of problems in robust control that can be solved as minimum rank problems. The examples are taken from [14], [47] and [52].

5.2.1 Low Order H_∞ Controller Design

In [47] El Ghaoui and Gahinet propose a framework for low order controller design. It is shown how the design of a reduced order H_∞ controller fits in the framework (5.1). To design a reduced order controller a minimum rank problem has to be solved.
Given the generalized plant $P(s)$:

$$\begin{cases} \dot{x} &= Ax &+B_ww &+B_uu \\ z &= C_zx &+D_{zw}w &+D_{zu}u \\ y &= C_yx &+D_{yw}w &+D_{yu}u, \end{cases} \tag{5.2}$$

where $A \in \mathbb{R}^{n\times n}, B_w \in \mathbb{R}^{n\times n_w}, B_u \in \mathbb{R}^{n\times n_u}, C_z \in \mathbb{R}^{z\times n}, D_{zw} \in \mathbb{R}^{n_z\times n_w}, D_{zu} \in \mathbb{R}^{n_z\times n_u}, C_y \in \mathbb{R}^{n_y\times n}, D_{yw} \in \mathbb{R}^{n_y\times n_w}, D_{yu} \in \mathbb{R}^{n_y\times n_u}$ and given a value γ. The standard H_∞ control problem is to find a dynamic controller $K(s)$:

$$\begin{cases} \dot{x}_c &= A_cx_c &+B_cy \\ u &= C_cx_c &+D_cy, \end{cases}$$

with $A_c \in \mathbb{R}^{n_c\times n_c}, B_c \in \mathbb{R}^{n_c\times n_y}, C_c \in \mathbb{R}^{n_u\times n_c}, D_c \in \mathbb{R}^{n_u\times n_y}$, such that $\|\mathcal{F}_l(P,K)\|_\infty < \gamma$, where $\mathcal{F}_l(.,.)$ represents the lower fractional transformation.
The following assumptions are made:

1. (A, B_u, C_y) is stabilizable and detectable.
2. D_{zu} has full column rank and D_{yw} has full column rank.
3. $D_{zu}^t \begin{pmatrix} D_{zu} & C_z \end{pmatrix} = \begin{pmatrix} I & 0 \end{pmatrix}$.
4. $D_{yw} \begin{pmatrix} D_{yw}^t & B_w^t \end{pmatrix} = \begin{pmatrix} I & 0 \end{pmatrix}$.
5. $D_{zw} = 0$.
6. $D_{yu} = 0$.

Assumption 1 is needed to ensure stabilizability of the closed loop using a dynamic output feedback controller. Assumption 2 can be removed as shown in [94], for instance. Assumptions 3, 4 and 5 are made for the clarity of the presentation. Assumption 6 is not necessary. If $D_{yu} \neq 0$, the controller can be adapted afterwards. Compute first the controller with $D_{yu} = 0$. Suppose that the resulting is $K_0(s)$ with state space realization:

$$K_0(s) = \left(\begin{array}{c|c} A_c & B_c \\ \hline C_c & D_c \end{array}\right).$$

The controller $K(s)$ that generates the same closed loop with $D_{yu} \neq 0$ is:

$$\begin{aligned} K(s) &= K_0(s)\left(I + D_{yu}K_0(s)\right)^{-1} \\ &= \left(\begin{array}{c|c} A_c - B_c(I + D_{yu}D_c)^{-1}D_{yu}D_c & B_c(I + D_{yu}D_c)^{-1} \\ \hline -(I + D_cD_{yu})^{-1}C_c & (I + D_cD_{yu})^{-1}D_c \end{array}\right). \end{aligned}$$

Of course, this is only valid if the inverses exist. When $D_{yu} \neq 0$ there is a possibility of the feedback system becoming ill-posed due to

$$\det(I + D_cD_{yu}) = 0.$$

The following theorem can be found in [47]:

Theorem 10 *Given a proper plant $P(s)$ with a given minimal state space realization (5.2) and satisfying the assumptions 1-6. There exists a dynamic γ-suboptimal controller of order k if and only if there exists a pair of symmetric matrices R and $S \in \mathbb{R}^{n\times n}$ such that*

$$AR + RA^t + RC_z^tC_zR + \gamma^{-2}B_wB_w^t - B_uB_u^t < 0, \tag{5.3}$$

$$A^tS + SA + SB_wB_w^tS + \gamma^{-2}C_z^tC_z - C_y^tC_y < 0, \tag{5.4}$$

$$\begin{pmatrix} R & \gamma^{-1}I \\ \gamma^{-1}I & S \end{pmatrix} \geq 0 \quad \textit{and} \quad \textit{Rank}\begin{pmatrix} R & \gamma^{-1}I \\ \gamma^{-1}I & S \end{pmatrix} \leq n + k.$$

The proof is given in [51] and [52]. □

To find a controller with the lowest order, the rank of the matrix

$$\begin{pmatrix} R & \gamma^{-1}I \\ \gamma^{-1}I & S \end{pmatrix}$$

has to be minimized, subject to the LMIs (5.3) and (5.4). This problem has the form of the general problem (5.1). The algebraic Riccati inequalities can easily be transformed into linear matrix inequalities (see e.g. [13]). In [47] similar formulas are derived for μ-synthesis with constant scalings.

5.2.2 L_2 Gain Control of a NLDI

In this section we derive formulas for designing a linear time invariant controller that guarantees a bound on the L_2 gain of a norm-bound linear differential inclusion (NLDI). A NLDI can be described by the following equations ([14]):

$$\left\{\begin{array}{rcllll} \dot{x} &=& Ax &+B_ww &+B_uu &+B_pp \\ z &=& C_zx &+D_{zw}w &+D_{zu}u &+D_{zp}p \\ y &=& C_yx &+D_{yw}w &+D_{yu}u &+D_{yp}p \\ q &=& C_qx &+D_{qw}w &+D_{qu}u &+D_{qp}p, \end{array}\right. \tag{5.5}$$

$$p = \Delta(t)q, \qquad \|\Delta(t)\| \leq 1,$$

with $A \in \mathbb{R}^{n\times n}$, $B_w \in \mathbb{R}^{n\times n_w}$, $B_u \in \mathbb{R}^{n\times n_u}$, $B_p \in \mathbb{R}^{n\times n_p}$, $C_z \in \mathbb{R}^{n_z\times n}$, $C_y \in \mathbb{R}^{n_y\times n}$, $C_q \in \mathbb{R}^{n_q\times n}$, $D_{zw} \in \mathbb{R}^{n_z\times n_w}$, $D_{zu} \in \mathbb{R}^{n_z\times n_u}$, $D_{zp} \in \mathbb{R}^{n_z\times n_p}$, $D_{yw} \in \mathbb{R}^{n_y\times n_w}$, $D_{yu} \in \mathbb{R}^{n_y\times n_u}$, $D_{yp} \in \mathbb{R}^{n_y\times n_p}$, $D_{qw} \in \mathbb{R}^{n_q\times n_w}$, $D_{qu} \in \mathbb{R}^{n_q\times n_u}$, $D_{qp} \in \mathbb{R}^{n_q\times n_p}$. $\Delta(t) \in \mathbb{R}^{n_p\times n_q}$ is a time varying uncertainty with norm smaller than one. $\|.\|$ denotes the induced 2-norm for matrices.
The goal is to design a linear time invariant controller $K(s)$, $u = K(s)y$, such that the L_2 gain of the closed loop transfer function from w to z is lower than a given value γ. The L_2 gain of the system is defined as:

$$\sup_{\|w\|_2<1} \|z\|_2 = \sup_{\|w\|_2\neq 0} \frac{\|z\|_2}{\|w\|_2},$$

where $\|.\|_2$ is the L_2 norm of the signal:

$$\|w\|_2^2 = \int_0^{+\infty} w(t)^tw(t)\,dt.$$

The state space realization of the controller is assumed to be

$$\left\{\begin{array}{rcl} \dot{\hat{x}} &=& A_c\hat{x} + B_cy \\ u &=& C_c\hat{x} + D_cy, \end{array}\right.$$

with $A_c \in \mathbb{R}^{n_c\times n_c}$, $B_c \in \mathbb{R}^{n_c\times n_y}$, $C_c \in \mathbb{R}^{n_u\times n_y}$ and $D_c \in \mathbb{R}^{n_u\times n_y}$.
Again it is assumed that $D_{yu} = 0$. For notational reasons, D_{zw}, D_{zu}, D_{zp}, D_{yw}, D_{yp} and D_{qp} are also assumed to be zero. However, the formulas can easily be extended to include the non-zero cases. The formulas presented here, will be needed for an example of section 5.9.
The following theorem can be proved from arguments in [14]:

Theorem 11 *A controller of order n_c that guarantees that the L_2 gain of the NLDI (5.5) is lower than γ, exists if matrices $P = P^t > 0$ and $Q = Q^t > 0$, and positive scalars λ, μ and σ can be found such that*

$$\lambda = \mu^{-1}, \tag{5.6}$$

$$\begin{pmatrix} P & I \\ I & Q \end{pmatrix} \geq 0, \tag{5.7}$$

$$\begin{pmatrix} QA^t + AQ + \gamma^{-2}B_w B_w^t + \mu B_p B_p^t & QC_z^t & QC_q^t + \gamma^{-2}B_w D_{qw}^t \\ C_z Q & -I & 0 \\ C_q Q + \gamma^{-2}D_{qw}B_w^t & 0 & -\mu I + \gamma^{-2}D_{qw}D_{qw}^t \end{pmatrix}$$
$$< \sigma \begin{pmatrix} B_u \\ 0 \\ D_{qu} \end{pmatrix} \begin{pmatrix} B_u^t & 0 & D_{qu}^t \end{pmatrix}, \tag{5.8}$$

$$\begin{pmatrix} A^tP + PA + C_z^tC_z + \lambda C_q^tC_q & PB_w + \lambda C_q^tD_{qw} & PB_p \\ B_w^tP + \lambda D_{qw}^tC_q & -\gamma^2 I + \lambda D_{qw}^tD_{qw} & 0 \\ B_p^tP & 0 & -\lambda I \end{pmatrix}$$
$$< \sigma \begin{pmatrix} C_y^t \\ 0 \\ 0 \end{pmatrix} \begin{pmatrix} C_y & 0 & 0 \end{pmatrix}, \tag{5.9}$$

and

$$Rank \begin{pmatrix} P & I \\ I & Q \end{pmatrix} \leq n + n_c.$$

Proof:
The proof is similar to proofs given in [14].
The state space matrices of the controller are combined into one matrix K:

$$K = \begin{pmatrix} A_c & B_c \\ C_c & D_c \end{pmatrix}.$$

The closed loop matrices can be written as:

$$\begin{cases} \dot{\tilde{x}} &= (\tilde{A} + \tilde{B}_u K \tilde{C}_y)\tilde{x} \quad + \tilde{B}_w w \quad + \tilde{B}_p p \\ z &= \tilde{C}_z \tilde{x} \\ q &= (\tilde{C}_q + \tilde{D}_{qu} K \tilde{C}_y)\tilde{x} \quad + \tilde{D}_{qw} w, \end{cases} \tag{5.10}$$

$$p = \Delta(t) q, \qquad \|\Delta(t)\| \leq 1,$$

where

$$\tilde{x} = \begin{pmatrix} x \\ \hat{x} \end{pmatrix}, \quad \tilde{A} = \begin{pmatrix} A & 0 \\ 0 & 0 \end{pmatrix}, \quad \tilde{B}_w = \begin{pmatrix} B_w \\ 0 \end{pmatrix}, \quad \tilde{B}_u = \begin{pmatrix} 0 & B_u \\ I & 0 \end{pmatrix},$$

$$\tilde{C}_z = \begin{pmatrix} C_z & 0 \end{pmatrix}, \quad \tilde{C}_y = \begin{pmatrix} C_y & 0 \\ 0 & I \end{pmatrix}, \quad \tilde{C}_q = \begin{pmatrix} C_q & 0 \end{pmatrix},$$

$$\tilde{D}_{qw} = D_{qw}, \qquad \tilde{D}_{qu} = \begin{pmatrix} D_{qu} & 0 \end{pmatrix}.$$

If there exists a matrix $\tilde{P} = \tilde{P}^t \in \mathbb{R}^{(n+n_c)\times(n+n_c)}$ and $\tilde{P} > 0$, such that for all t

$$\frac{d}{dt}V(\tilde{x}) + z(t)^t z(t) - \gamma^2 w(t)^t w(t) \leq 0 \tag{5.11}$$

whenever

$$p(t)^t p(t) \leq q(t)^t q(t), \tag{5.12}$$

then the L_2 gain of the closed loop is less than γ. We look for a quadratic Lyapunov function $V(\tilde{x}) = \tilde{x}^t \tilde{P} \tilde{x}$, with $\tilde{P}$ a positive definite matrix. Substituting (5.10) in (5.11) and (5.12) yields

$$\left[\tilde{x}^t(\tilde{A} + \tilde{B}_u K \tilde{C}_y)^t + w^t \tilde{B}_w^t + p^t \tilde{B}_p^t\right] \tilde{P}\tilde{x} + \tilde{x}^t \tilde{P} \left[(\tilde{A} + \tilde{B}_u K \tilde{C}_y)\tilde{x} + \tilde{B}_w w + \tilde{B}_p p\right]$$
$$+ \tilde{x}^t \tilde{C}_z^t \tilde{C}_z \tilde{x} - \gamma^2 w^t w < 0, \tag{5.13}$$

$$p^t p - \left[\tilde{x}^t(\tilde{C}_q + \tilde{D}_{qu} K \tilde{C}_y)^t + w^t \tilde{D}_{qw}^t\right] \left[(\tilde{C}_q + \tilde{D}_{qu} K \tilde{C}_y)\tilde{x} + \tilde{D}_{qw} w\right] \leq 0. \tag{5.14}$$

Applying the $\mathcal{S}$-procedure ([14]) to (5.13) and (5.14), implies that a controller exists if there exist a $\tilde{P} > 0$, K and a scalar $\lambda > 0$ such that the following inequality holds for every $\tilde{x}$, w and p:

$$\tilde{x}^t \left[(\tilde{A} + \tilde{B}_u K \tilde{C}_y)^t \tilde{P} + \tilde{P}(\tilde{A} + \tilde{B}_u K \tilde{C}_y) + \tilde{C}_z^t \tilde{C}_z \right.$$
$$\left. + \lambda(\tilde{C}_q + \tilde{D}_{qu} K \tilde{C}_y)^t (\tilde{C}_q + \tilde{D}_{qu} K \tilde{C}_y)\right] \tilde{x}$$
$$+ \quad 2\tilde{x}^t \left[\tilde{P}\tilde{B}_w + \lambda(\tilde{C}_q + \tilde{D}_{qu} K \tilde{C}_y)^t \tilde{D}_{qw}\right] w + 2\tilde{x}^t \tilde{P} \tilde{B}_p p$$
$$+ \quad w^t(-\gamma^2 I + \lambda \tilde{D}_{qw}^t \tilde{D}_{qw})w - \lambda p^t p < 0.$$

This is equivalent with

$$\begin{pmatrix} (\tilde{A}+\tilde{B}_u K\tilde{C}_y)^t\tilde{P}+\tilde{P}(\tilde{A}+\tilde{B}_u K\tilde{C}_y)+\tilde{C}_z^t\tilde{C}_z+\lambda(\tilde{C}_q+\tilde{D}_{qu}K\tilde{C}_y)^t(\tilde{C}_q+\tilde{D}_{qu}K\tilde{C}_y) \\ \tilde{B}_w^t\tilde{P}+\lambda\tilde{D}_{qw}^t(\tilde{C}_q+\tilde{D}_{qu}K\tilde{C}_y) \\ \tilde{B}_p^t\tilde{P} \end{pmatrix}$$

$$\begin{pmatrix} \tilde{P}\tilde{B}_w+\lambda(\tilde{C}_q+\tilde{D}_{qu}K\tilde{C}_y)^t\tilde{D}_{qw} & \tilde{P}\tilde{B}_p \\ -\gamma^2 I+\lambda\tilde{D}_{qw}^t\tilde{D}_{qw} & 0 \\ 0 & -\lambda I \end{pmatrix} < 0$$

or

$$\begin{pmatrix} \tilde{A}^t\tilde{P}+\tilde{P}\tilde{A}+\tilde{C}_z^t\tilde{C}_z & \tilde{P}\tilde{B}_w & \tilde{P}\tilde{B}_p & \tilde{C}_q^t \\ \tilde{B}_w^t\tilde{P} & -\gamma^2 I & 0 & \tilde{D}_{qw}^t \\ \tilde{B}_p^t\tilde{P} & 0 & -\lambda I & 0 \\ \tilde{C}_q & \tilde{D}_{qw} & 0 & -\lambda^{-1}I \end{pmatrix}$$
$$+ \begin{pmatrix} \tilde{P}\tilde{B}_u \\ 0 \\ 0 \\ \tilde{D}_{qw} \end{pmatrix} K \begin{pmatrix} \tilde{C}_y & 0 & 0 & 0 \end{pmatrix} + \begin{pmatrix} \tilde{C}_y^t \\ 0 \\ 0 \\ 0 \end{pmatrix} K^t \begin{pmatrix} \tilde{B}_u^t\tilde{P} & 0 & 0 & \tilde{D}_{qu}^t \end{pmatrix} < 0. \tag{5.15}$$

A solution K exists if a scalar $\tilde{\sigma} > 0$ exists such that the following two constraints are satisfied ([47]):

$$\begin{pmatrix} \tilde{A}^t\tilde{P}+\tilde{P}\tilde{A}+\tilde{C}_z^t\tilde{C}_z & \tilde{P}\tilde{B}_w & \tilde{P}\tilde{B}_p & \tilde{C}_q^t \\ \tilde{B}_w^t\tilde{P} & -\gamma^2 I & 0 & \tilde{D}_{qw}^t \\ \tilde{B}_p^t\tilde{P} & 0 & -\lambda I & 0 \\ \tilde{C}_q & \tilde{D}_{qw} & 0 & -\lambda^{-1}I \end{pmatrix}$$
$$< \tilde{\sigma} \begin{pmatrix} \tilde{P}\tilde{B}_u \\ 0 \\ 0 \\ \tilde{D}_{qw} \end{pmatrix} \begin{pmatrix} \tilde{B}_u^t\tilde{P} & 0 & 0 & \tilde{D}_{qu}^t \end{pmatrix}, \tag{5.16}$$

$$\begin{pmatrix} \tilde{A}^t\tilde{P}+\tilde{P}\tilde{A}+\tilde{C}_z^t\tilde{C}_z & \tilde{P}\tilde{B}_w & \tilde{P}\tilde{B}_p & \tilde{C}_q^t \\ \tilde{B}_w^t\tilde{P} & -\gamma^2 I & 0 & \tilde{D}_{qw}^t \\ \tilde{B}_p^t\tilde{P} & 0 & -\lambda I & 0 \\ \tilde{C}_q & \tilde{D}_{qw} & 0 & -\lambda^{-1}I \end{pmatrix}$$
$$< \tilde{\sigma} \begin{pmatrix} \tilde{C}_y^t \\ 0 \\ 0 \\ 0 \end{pmatrix} \begin{pmatrix} \tilde{C}_y & 0 & 0 & 0 \end{pmatrix}. \tag{5.17}$$

These inequalities are equivalent to

$$\begin{pmatrix} \tilde{Q}\tilde{A}^t+\tilde{A}\tilde{Q}+\gamma^{-2}\tilde{B}_w\tilde{B}_w^t+\mu\tilde{B}_p\tilde{B}_p^t & \tilde{Q}\tilde{C}_q^t+\gamma^{-2}\tilde{B}_w\tilde{D}_{qw}^t & \tilde{Q}\tilde{C}_z \\ \tilde{C}_q\tilde{Q}+\gamma^{-2}\tilde{D}_{qw}\tilde{B}_w^t & -\mu I+\gamma^{-2}\tilde{D}_{qw}\tilde{D}_{qw}^t & 0 \\ \tilde{C}_z\tilde{Q} & 0 & -I \end{pmatrix}$$
$$< \tilde{\sigma} \begin{pmatrix} \tilde{B}_u \\ \tilde{D}_{qw} \\ 0 \end{pmatrix} \begin{pmatrix} \tilde{B}_u^t & \tilde{D}_{qw}^t & 0 \end{pmatrix}, \tag{5.18}$$

$$\begin{pmatrix} \tilde{A}^t\tilde{P}+\tilde{P}\tilde{A}+\tilde{C}_z^t\tilde{C}_z+\lambda\tilde{C}_q^t\tilde{C}_q & \tilde{P}\tilde{B}_w+\lambda\tilde{C}_q^t\tilde{D}_{qw} & \tilde{P}\tilde{B}_p \\ \tilde{B}_w^t\tilde{P}+\lambda\tilde{D}_{qw}^t\tilde{C}_q & -\gamma^2 I+\lambda\tilde{D}_{qw}^t\tilde{D}_{qw} & 0 \\ \tilde{B}_p^t\tilde{P} & 0 & -\lambda I \end{pmatrix}$$
$$< \tilde{\sigma} \begin{pmatrix} \tilde{C}_y^t \\ 0 \\ 0 \end{pmatrix} \begin{pmatrix} \tilde{C}_y & 0 & 0 \end{pmatrix}, \tag{5.19}$$

where $\tilde{Q} = \tilde{P}^{-1}$ and $\mu = \lambda^{-1}$. (5.18) and (5.19) are LMIs in $\tilde{P}$, $\tilde{Q}$, λ and μ. Let P and Q denote the upper $n \times n$ blocks of $\tilde{P}$ and $\tilde{Q}$. It is known from a theorem in [47], that if a $P > 0$ and $Q > 0$ exist such that

$$\begin{pmatrix} P & I \\ I & Q \end{pmatrix} \geq 0 \quad \text{and} \quad \text{Rank} \begin{pmatrix} P & I \\ I & Q \end{pmatrix} \leq n + n_c, \tag{5.20}$$

then there exists a $\tilde{P}$ and $\tilde{Q} \in \mathbb{R}^{(n+n_c)\times(n+n_c)}$ such that $\tilde{P} = \tilde{Q}^{-1}$. Further it is easily shown that if there exist a $P > 0$, $Q > 0$, $\lambda > 0$, $\mu > 0$ and $\sigma > 0$ satisfying (5.20) and

$$\begin{pmatrix} QA^t+AQ+\gamma^{-2}B_wB_w^t+\mu B_pB_p^t & QC_q^t+\gamma^{-2}B_wD_{qw}^t & QC_z \\ C_qQ+\gamma^{-2}D_{qw}B_w^t & -\mu I+\gamma^{-2}D_{qw}D_{qw}^t & 0 \\ C_zQ & 0 & -I \end{pmatrix}$$
$$< \sigma \begin{pmatrix} B_u \\ D_{qw} \\ 0 \end{pmatrix} \begin{pmatrix} B_u^t & D_{qw}^t & 0 \end{pmatrix}, \tag{5.21}$$

$$\begin{pmatrix} A^tP+PA+C_z^tC_z+\lambda C_q^tC_q & PB_w+\lambda C_q^tD_{qw} & PB_p \\ B_w^tP+\lambda D_{qw}^tC_q & -\gamma^2 I+\lambda D_{qw}^tD_{qw} & 0 \\ B_p^tP & 0 & -\lambda I \end{pmatrix}$$

$$< \sigma \begin{pmatrix} C_y^t \\ 0 \\ 0 \end{pmatrix} \begin{pmatrix} C_y & 0 & 0 \end{pmatrix}, \tag{5.22}$$

then there exists a $\tilde{P}$, $\tilde{Q}$ and $\tilde{\sigma} \geq \sigma > 0$ such that (5.18) and (5.19) are satisfied and $\tilde{P} = \tilde{Q}^{-1}$. For a proof we refer to the proof in section 5.9.2, where the same is proved for a simpler LMI.

This completes the proof. □

σ can be removed from (5.8) and (5.9). Call N_B a matrix that spans the null space of $\begin{pmatrix} B_u^t & 0 & D_{qu}^t \end{pmatrix}$ and N_C a matrix that spans the null space of $\begin{pmatrix} C_y & 0 & 0 \end{pmatrix}$:

$$\begin{pmatrix} B_u^t & 0 & D_{qu}^t \end{pmatrix} N_B = 0, \quad \begin{pmatrix} C_y & 0 & 0 \end{pmatrix} N_C = 0,$$

then (5.8) and (5.9) are equivalent to

$$N_B^t \begin{pmatrix} QA^t + AQ + \gamma^{-2} B_w B_w^t + \mu B_p B_p^t & QC_z^t & QC_q^t + \gamma^{-2} B_w D_{qw}^t \\ C_z Q & -I & 0 \\ C_q Q + \gamma^{-2} D_{qw} B_w^t & 0 & -\mu I + \gamma^{-2} D_{qw} D_{qw}^t \end{pmatrix} N_B < 0,$$

$$N_C^t \begin{pmatrix} A^t P + PA + C_z^t C_z + \lambda C_q^t C_q & PB_w + \lambda C_q^t D_{qw} & PB_p \\ B_w^t P + \lambda D_{qw}^t C_q & -\gamma^2 I + \lambda D_{qw}^t D_{qw} & 0 \\ B_p^t P & 0 & -\lambda I \end{pmatrix} N_C < 0.$$

Computing a controller is more involved than finding a reduced order H_∞ controller for linear time invariant systems, as a λ and μ have to be found such that $\lambda = \mu^{-1}$. To find a $\lambda = \mu^{-1}$, El Ghaoui ([48]) proposed to apply the following procedure: First find P, Q, λ and μ that satisfy (5.7), (5.8) and (5.9) and

$$\begin{pmatrix} \lambda & 1 \\ 1 & \mu \end{pmatrix} \geq 0. \tag{5.23}$$

Then apply a rank minimization on (5.23) subject to (5.7), (5.8) and (5.9). When a rank 1 matrix is found, $\lambda = \mu^{-1}$ holds. If a rank 1 solution for (5.23) exists and the other constraints are also satisfied, a full order controller that satisfies the given specifications exists. If no rank 1 solution can be found, it does not imply that there does not exist a controller such that the L_2-gain is smaller than γ. The formulas are *only sufficient* for NLDIs and *not necessary* ([14]).

Once a suitable λ and μ are found a reduced order controller can be designed: Fix λ and μ and reduce the order of the controller by minimizing

the rank of (5.7) subject to (5.8) and (5.9). From the resulting P and Q, $\tilde{P}$ can be constructed. A controller that satisfies the constraints can be computed by substituting $\tilde{P}$ and λ in (5.15) and solving the convex feasibility problem. A solution is guaranteed to exist as a $\tilde{P}$, $\tilde{Q}$ and $\tilde{\sigma}$ exist that satisfy (5.18) and (5.19).

When these formulas are used for a time invariant system, this is a system with $B_p = D_{zp} = D_{yp} = D_{qp} = D_{qw} = C_q = 0$, the H_∞ controller is obtained. The derived formulas are *necessary and sufficient* for time invariant plants.

5.3 Computational Complexity

In this section we determine the computational complexity of the minimum rank problem. To apply computational complexity theory, the minimum rank problem is formulated as a *rank decision problem* (The answer is "yes" or "no".). We show that this decision problem is NP-hard, i.e. at least as hard as the NP-complete problems.

To prove the NP-hardness the following procedure is used. First it is shown that *zero-one integer programming* can be cast as a minimum rank problem. Since zero-one integer programming is NP-complete, the rank decision problem must be NP-hard.

The zero-one integer programming problem can be formulated as:

> Given a matrix $A \in \mathbb{R}^{m \times n}$ and a vector $b \in \mathbb{R}^m$, is there an n-vector x with all entries belonging to $\{0, 1\}$ that satisfies $Ax \leq b$?

This problem can be linked to a decision problem involving the rank of $F(x)$ (In this text it is called the rank decision problem.):

> Given $k \in \mathbb{N}$, and linear matrix inequalities $F(x) \geq 0$ and $C(x) \geq 0$ does there exist an $x \in \mathbb{R}^n$ such that the rank of $F(x) \leq k$, and which satisfies the constraints $F(x) \geq 0$ and $C(x) \geq 0$?

The following theorem shows how the zero-one integer programming problem can be cast as a decision problem on the rank of $F(x)$:

Theorem 12 *Given a matrix $A \in \mathbb{R}^{m \times n}$ and a vector $b \in \mathbb{R}^m$, define*

$$F(x) = \begin{pmatrix} diag(x) & 0 \\ 0 & I_n - diag(x) \end{pmatrix}$$

and

$$C(x) = diag(b) - \sum_{i=1}^{n} diag(A_{.i}x_i),$$

where $A_{.i}$ is the ith column of A.
Then there exists an x such that rank $F(x) \leq n$, $F(x) \geq 0$ and $C(x) \geq 0$ if and only if x is an n-vector x with entries belonging to $\{0,1\}$, satisfying $Ax \leq b$.

Proof:
The rank of $F(x)$ can only drop if the entries of x are either 0 or 1. If all the components of x belong to $\{0,1\}$, then rank $F(x) = n$. This is the lowest attainable rank. However, these vectors do not necessarily satisfy the constraints $C(x) \geq 0$.

It is obvious that the constraint $C(x) \geq 0$ is equivalent with $Ax \leq b$. Thus if there exists a solution x such that the rank $F(x) = n$ (which is equivalent with rank $F(x) \leq n$, in this case) and $C(x) \geq 0$, then x is a vector consisting of all zeros and ones and a solution of the zero-one integer program. If the lowest possible rank of $F(x)$ is larger than n, then there does not exist a x satisfying the zero-one integer program.

The transformation that casts the zero-one integer programming problem as a rank decision problem is a polynomial transformation. When A and b are given and if all the matrices that form the LMIs $F(x)$ and $C(x)$ are constructed, then $4n^2(n+1)+m^2(n+1)$ memory locations are needed. This grows only polynomially with n and m, although it is a very inefficient way of storing the matrices. □

Now it is easy to prove that the rank decision problem is NP-hard.

Theorem 13 *Checking if there exists an x such that rank $F(x) \leq k$, $F(x) \geq 0$ and $C(x) \geq 0$, is NP-hard.*

Proof:
Zero-one integer programming is NP-complete ([53, p. 245]). It polynomially reduces to a rank decision problem by theorem 12. Thus the rank decision problem is at least as difficult as the zero-one integer programming problem. Therefore, we conclude that the rank decision problem is NP-hard. □

The minimum rank problem is at least as difficult to solve as the rank decision problem, since the solution of the rank decision problem immediately follows from the solution of the minimum rank problem.

We also refer to [16], where a similar procedure is used to prove the NP-hardness of the μ calculation.

In fact it can be shown that the rank decision problem is NP-complete. The only thing left to show is that it belongs to the class of NP problems. If an x is given, we can check in polynomial time if the x satisfies the convex constraints $F(x) \geq 0$ and $C(x) \geq 0$. This is a convex feasibility problem that can be solved in polynomial time. Checking if rank $F(x) \leq k$, can also be done in polynomial time.

As the minimum rank problems are NP-hard, we did not look for algorithms that are efficient in all cases. In this chapter two heuristic algorithms are presented. In most practical cases they give a reduced rank solution $F(x)$. However, it is not guaranteed that the minimal rank is reached. Nevertheless, although we have proved that the general minimum rank problem is NP-hard, we have not proved that each of the particular problems we consider, are NP-hard.

5.4 Convex Optimization

Although the minimum rank problems are not convex, the heuristic algorithms are based on methods for convex optimization. Several methods for convex optimization exist: The cutting plane algorithm, ellipsoid algorithms, etc. ([12],[14]). The algorithms for solving the minimum rank problems are based on the concepts of the interior point methods for positive definite problems of Nesterov and Nemirovsky. The most important concepts are explained below based on [13]. In [13] Boyd and El Ghaoui show how generalized eigenvalue problems can be solved using the method of centers based on Nesterov and Nemirovsky's theory.

5.4.1 Linear Matrix Inequalities

An inequality

$$F(x) = F_0 + x_1F_1 + \ldots + x_mF_m > 0$$

with $F_i = F_i^T \in \mathbb{R}^{n\times n}$, $i = 0 \ldots m$, given matrices, and $x_i \in \mathbb{R}$, $i = 1 \ldots m$, the unknown parameters, is called a *linear matrix inequality*. The set of all feasible points x is called $\mathcal{X}$:

$$\mathcal{X} \triangleq \{x \in \mathbb{R}^m | F(x) > 0\}.$$

Two LMIs

$$\begin{cases} F_1(x) > 0 \\ F_2(x) > 0 \end{cases}$$

can always be combined into one block diagonal LMI

$$\begin{pmatrix} F_1(x) & 0 \\ 0 & F_2(x) \end{pmatrix} > 0.$$

Consider the constraints having a "Schur complement form":

$$Q(x) - S(x)R(x)^{-1}S(x)^t > 0, \qquad R(x) > 0,$$

where $Q(x) = Q(x)^t$, $S(x)$ and $R(x) = R(x)^t$ are matrices of appropriate size that depend affinely on the vector x. These constraints can be represented by an LMI:

$$\begin{pmatrix} Q(x) & S(x) \\ S(x)^t & R(x) \end{pmatrix} > 0.$$

An example is the algebraic Riccati inequality:

$$A^tP(x) + P(x)A + P(x)BR^{-1}B^tP(x) + Q < 0,$$

where $P(x) = P(x)^t$ is an affine function of x, and A, B, $Q = Q^t$, $R = R^t > 0$ are matrices of appropriate size. This can be expressed as the LMI

$$\begin{pmatrix} -A^tP(x) - P(x)A - Q & P(x)B \\ B^tP(x) & R \end{pmatrix} > 0.$$

5.4.2 Barrier Functions

Consider a linear matrix inequality

$$F(x) > 0,$$

with $F(x) = F(x)^t \in \mathbb{R}^{n\times n}$. With this inequality a barrier function $\phi(x)$ is associated:

$$\phi(x) \triangleq \begin{cases} \log\det F(x)^{-1} & \text{if } x \in \mathcal{X} \\ \infty & \text{if } x \notin \mathcal{X}. \end{cases}$$

This barrier function is finite if $x \in \mathcal{X}$ and becomes ∞ at the borders. It has some nice properties and it is analytic and convex when $x \in \mathcal{X}$. As the determinant is the product of the eigenvalues of a matrix, $\phi(x)$ can also be expressed as:

$$\phi(x) = -\sum_{i=1}^{n} \log \lambda_i,$$

when $F(x)$ is positive definite. λ_i is the ith eigenvalue of $F(x)$. The barrier function is the sum of the logarithms of the eigenvalues. The lower the eigenvalues become the larger the corresponding value of the barrier function will be. If one or more of the eigenvalues tend to zero, the barrier will tend to ∞. The border of the feasible region consists of all points where $F(x)$ is singular. The barrier function becomes ∞ at these points.

The formulas for the gradient $g(x)$ and the Hessian $H(x)$ of $\phi(x)$ at $x \in \mathcal{X}$ are readily derived ([13]):

$$\begin{aligned} g_i(x) &= -\text{trace } F(x)^{-1}F_i = -\text{trace } F(x)^{-1/2}F_iF(x)^{-1/2} \\ &\qquad\qquad \text{for } i = 1\ldots m \end{aligned}$$

$$\begin{aligned} H_{ij}(x) &= \text{trace } F(x)^{-1}F_iF(x)^{-1}F_j \\ &= \text{trace } (F(x)^{-1/2}F_iF(x)^{-1/2})(F(x)^{-1/2}F_jF(x)^{-1/2}) \\ &\qquad \text{for } i,j = 1\ldots m. \end{aligned}$$

5.4.3 Analytic center

The analytic center x^* of an LMI is defined as the x that minimizes the barrier function:

$$x^* \triangleq \underset{x}{\text{argmin}}\ \phi(x).$$

We illustrate this with a simple one-dimensional example. Suppose we want to find the analytic center of the following two constraints:

$$5 - x > 0, \qquad 1 + x > 0.$$

These two constraints can be combined into one LMI:

$$F(x) = \begin{pmatrix} 5 & 0 \\ 0 & 1 \end{pmatrix} + x\begin{pmatrix} -1 & 0 \\ 0 & 1 \end{pmatrix} > 0.$$

The corresponding barrier function is:

$$\phi(x) = -\log(5 - x) - \log(1 + x).$$

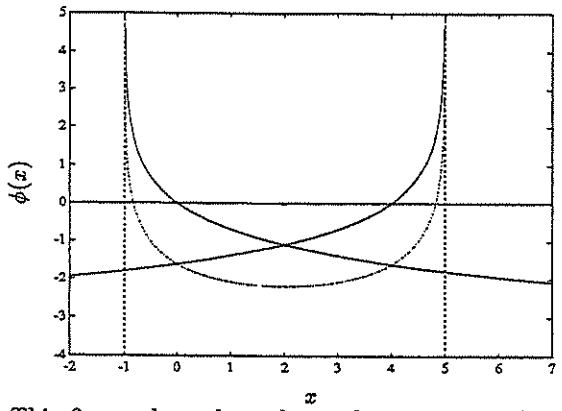

Figure 5.1: This figure shows how the analytic center is found for two one-dimensional LMIs: $5 - x > 0$ and $1 + x > 0$. The full lines are the barrier functions of the individual constraints. The dash-dotted line is the barrier function of the combination of the two constraints. The analytic center is indicated with a star. The analytic center is defined as the x that minimizes the barrier function. $x = 2$ is obviously the analytic center.

The barrier function for each of the two constraints separately and for the two constraints combined is shown in figure 5.1. From the figure it is clear that the value of x that minimizes the barrier is $x = 2$. This is the analytic center for these two (easy) constraints.

Using this definition of analytic center, it also depends on the non-active constraints. This is illustrated in figure 5.2. A third LMI $6 - x > 0$ is added to the two constraints. This constraint will never be active: x has to be less than 5 due to the first constraint. Nevertheless, introducing this constraints pushes the analytic center away from the added constraint. The new analytic center is $x = 1.1475$.

5.4.4 Nesterov and Nemirovsky's Newton Algorithm

To find the analytic center a Newton algorithm is used:

$$x_{k+1} = x_k - \alpha_k H(x_k)^{-1} g(x_k),$$

where α_k is the damping factor of the kth iteration.

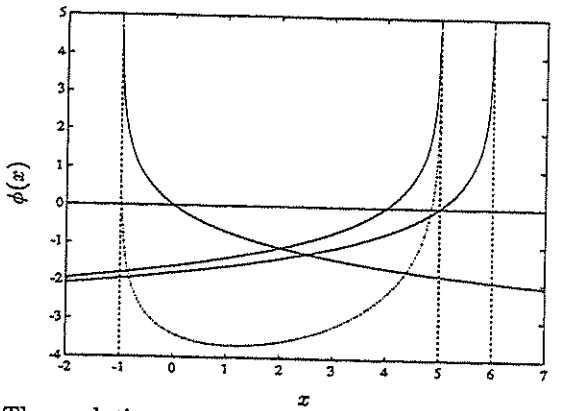

Figure 5.2: The analytic center is dependent on all the constraints, even the non-active ones. This is illustrated in this figure. A constraint $6 - x > 0$ is added. The analytic center, indicated by the star, is pushed away from the additional constraint.

In [13] it is shown that the undamped Newton step is the solution of a least squares problem:

$$\begin{aligned} -H(x)^{-1}g(x) &= \underset{x \in \mathbb{R}^m}{\operatorname{argmin}} \left\| F(x)^{-1/2} F(x - v) F(x)^{-1/2} \right\|_F \\ &= \underset{x \in \mathbb{R}^m}{\operatorname{argmin}} \left\| I - \sum_{i=1}^{m} v_i F(x)^{-1/2} F_i F(x)^{-1/2} \right\|_F . \end{aligned} \quad (5.24)$$

Nesterov and Nemirovsky derived a damping factor that ensures feasibility of x_{k+1} if x_k is feasible. ([13],[80]). The damping factor depends on the *Newton decrement* $\delta(x)$ of $\phi(x)$. The Newton decrement is defined as

$$\delta(x) \triangleq \|H(x)^{-1/2} g(x)\|.$$

If $\delta(x_k)$ is known the Nesterov-Nemirovsky damping factor is:

$$\begin{cases} \alpha_k = 1 & \text{if } \delta(x_k) \leq .25, \\ \alpha_k = \frac{1}{1+\delta(x_k)} & \text{if } \delta(x_k) > .25. \end{cases}$$

It is easily proved using the inner ellipsoid approximation ([13]), that this damping factor assures feasibility of x_{k+1} if x_k is feasible. Moreover, if

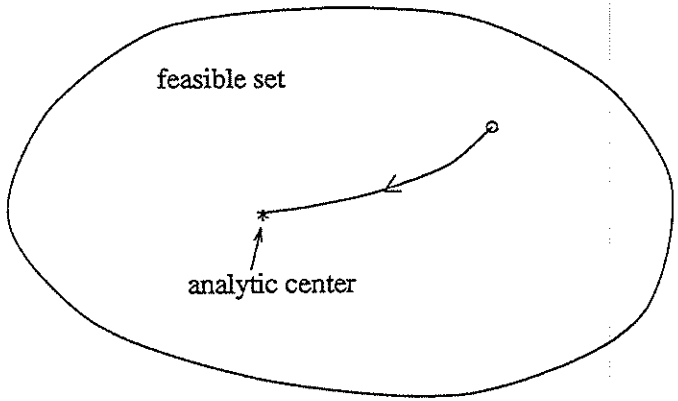

Figure 5.3: From each point in the feasible set, Nesterov and Nemirovsky's Newton algorithm follows a path to the analytic center.

$\delta(x_k) < .25$, the algorithm converges quadratically towards the analytic center, when undamped Newton steps are taken.

$\delta(x_k)$ can easily be computed when the solution v of (5.24) is known:

$$\delta(x_k) = \left\| \sum_{i=1}^{m} v_i F(x)^{-1/2} F_i F(x)^{-1/2} \right\|_F .$$

The algorithm stops when $\delta(x)$ becomes small.

Instead of using the Nesterov-Nemirovsky damping factor, it is also possible to do a line search. The line search can be done with very little extra effort compared to the number of computations to solve the least squares problem. The number of iterations, however, is usually much lower using the line search.

From each point in the feasible set, a path is followed to the analytic center. This is shown in figure 5.3.

5.5 Inversion of the Analytic Centering

Consider again the minimum rank problem we want to solve:

$$\min_{x \in \mathbb{R}^m} \text{Rank } F(x) \qquad \text{subject to} \begin{cases} F(x) \geq 0 \\ C(x) \geq 0. \end{cases} \tag{5.25}$$

where $F(x)$ and $C(x)$ are symmetric affine matrix functions:

$$\begin{aligned} F(x) &= F_0 + x_1 F_1 + x_2 F_2 + \ldots + x_m F_m, \\ C(x) &= C_0 + x_1 C_1 + x_2 C_2 + \ldots + x_m C_m, \end{aligned}$$

with $F_i = F_i^t \in \mathbb{R}^{n_f \times n_f}$ and $C_i = C_i^t \in \mathbb{R}^{n_c \times n_c}$, $i = 0 \ldots m$. The feasible sets are denoted by:

$$\mathcal{X}_f = \{x \in \mathbb{R}^m \mid F(x) \geq 0\}, \quad \mathcal{X}_c = \{x \in \mathbb{R}^m \mid C(x) \geq 0\}.$$

The inverted centering method is based on the following: The vectors x for which $F(x)$ is rank deficient are located on the boundary of the set $\mathcal{X}_f$. This is where the objective function $\log\det F(x)^{-1}$ becomes infinity. From each point on the boundary, there is a path to the analytic center which is followed by the Newton algorithm. Furthermore, assume $F(x)$ has $n_f - 1$ eigenvalues 1 and one small eigenvalue $\epsilon > 0$, then $\log\det F(x) = -\log\epsilon$. If there are $n_f - 2$ eigenvalues equal to 1 and two small eigenvalues ϵ_1 and ϵ_2 then is $-\log\det F(x) = -\log\epsilon_1 - \log\epsilon_2$ which is larger. Thus the higher the value of the barrier the lower the rank of $F(x)$. The intuitive idea is to solve minimum rank problems by finding the maximum of the barrier function, by tracing back the steepest path from the analytic center to the boundary. This is shown in figure 5.4. This is, however, not a convex problem. We could denote our objective as

$$\max_x \; -\log\det F(x) \qquad \text{subject to } F(x) \geq 0.$$

5.5.1 Without Constraints $C(x) \geq 0$

We describe first how the algorithm works when there are no constraints $C(x) > 0$. The algorithm starts at a point in the neighbourhood of the analytic center of the constraint $F(x) > 0$. To find the updating direction the Newton step is computed as in (5.24). However, the opposite direction is taken. We want to move away from the center towards the boundary.

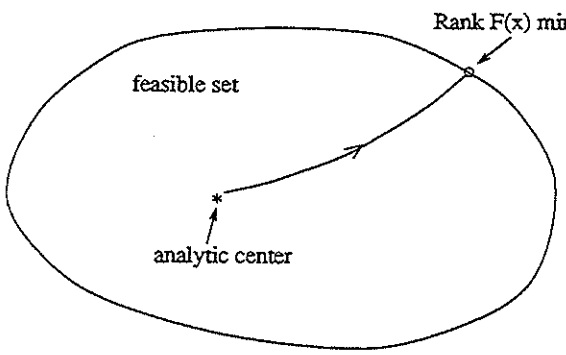

Figure 5.4: The intuitive idea for the inverted analytic centering method is to trace back the steepest path from the analytic center to the 'highest' point on the boundary.

To ensure feasibility of the step the Nesterov-Nemirovsky damping factor is used:

$$\alpha = \frac{1}{1+\delta(x)},$$

where $\delta(x)$ is the Newton decrement.

$\delta(x)$ has another nice property when x approaches the boundary of $F(x)$. When $\delta(x)^2$ is rounded towards the nearest integer, it indicates the number of decreasing eigenvalues. This is shown in section 5.6.2. These are the eigenvalues that tend to zero. Thus $\delta(x)^2$ indicates the resulting corank of $F(x)$. Experimental results show that $\delta(x)^2$ quickly converges to a constant value. Based on $\delta(x)^2$ the following stopping criterion is used. The eigenvalues are assumed to be zero if they are smaller than a given tolerance, e.g. 10^{-8}. Suppose that the nearest integer to $\delta(x)^2$ is k. In each step the eigenvalues of $F(x)$ are sorted from small to large. If the kth smallest eigenvalue is smaller than the tolerance, then the algorithm stops. The resulting rank of $F(x)$ is $n_f - k$.

Until now only the rank minimization of $F(x)$ is described, without taking into account the constraints $C(x)$. To ensure that the algorithm is started at a feasible point, the analytic center of the constraints $F(x) \geq 0$ and $C(x) \geq 0$ is computed first. If the constraints are not taken into account,

they will be violated in most cases. How the constraints can be taken into account is explained in the following subsections.

5.5.2 All the Constraints are Taken Into Account

The constraints can be added using barrier functions. Here we maximize a function, so the barrier function should be $-\infty$ at the boundaries of $\mathcal{X}_c$. Therefore the following function was proposed:

$$\psi(x) = -\log\det F(x) + \log\det C(x).$$

The gradients with respect to x of $-\log\det F(x)$ and $-\log\det C(x)$ will be called $g_f(x)$ and $g_c(x)$, respectively. The Hessians will be called $H_f(x)$ and $H_c(x)$. The gradient of the $\psi(x)$ is $g(x) = g_f(x) - g_c(x)$. The Hessian of $\psi(x)$ is $H(x) = H_f(x) - H_c(x)$. The Newton direction is thus:

$$v(x) = -H(x)^{-1}g(x).$$

The Newton direction of this function is not easily calculated via a least squares problem. As $F(x)$ becomes singular the gradient $g_f(x)$ and the Hessian $H_f(x)$ grow enormously. The numerical calculation of $H_f(x)^{-1}g_f(x)$ will become dubious. Therefore we adapted the least squares problem to include the constraints. However, in that case we do not obtain the real Newton direction any more.

First, we recall how the Newton direction can be calculated via a least squares problem. Suppose we want to find the analytic center of the constraints $F(x) \geq 0$ and $C(x) \geq 0$. The Newton direction towards the analytic center of

$$-\log\det F(x) - \log\det C(x)$$

can be solved as

$$-H^{-1}g = \underset{v}{\operatorname{argmin}} \left\| \begin{pmatrix} I_f & 0 \\ 0 & I_c \end{pmatrix} - \sum_i v_i \begin{pmatrix} Z_F & 0 \\ 0 & Z_C \end{pmatrix} \begin{pmatrix} F_i & 0 \\ 0 & C_i \end{pmatrix} \begin{pmatrix} Z_F & 0 \\ 0 & Z_C \end{pmatrix} \right\|_F^2$$

where $Z_F = F(x)^{-1/2}$ and $Z_C = C(x)^{-1/2}$.
To find a reduced order solution $F(x)$ subject to some constraints $C(x) \geq 0$, this was modified to

$$\underset{v}{\operatorname{argmin}} \left\| \begin{pmatrix} I_f & 0 \\ 0 & I_c \end{pmatrix} - \sum_i v_i \begin{pmatrix} Z_F & 0 \\ 0 & Z_C \end{pmatrix} \begin{pmatrix} F_i & 0 \\ 0 & -C_i \end{pmatrix} \begin{pmatrix} Z_F & 0 \\ 0 & Z_C \end{pmatrix} \right\|_F^2.$$

The solution is

$$v = -(H_f(x) + H_c(x))^{-1}(g_f(x) - g_c(x)).$$

However, this is not the Newton direction of $-\log\det F(x) + \log\det C(x)$. Nevertheless, it is easy to scale this direction such that the updated x is again in the inner ellipsoid, now based on the constraints $F(x) \geq 0$ *and* $C(x) \geq 0$. The new x satisfies the constraints.

The scaling of the v is again $\frac{1}{1+\delta(x)}$ where $\delta(x)$ is now defined as

$$\delta(x)^2 = \left\| \sum_i v_i \begin{pmatrix} Z_F & 0 \\ 0 & Z_C \end{pmatrix} \begin{pmatrix} F_i & 0 \\ 0 & -C_i \end{pmatrix} \begin{pmatrix} Z_F & 0 \\ 0 & Z_C \end{pmatrix} \right\|_F^2.$$

Near the boundary, $\delta(x)^2$ also indicates the number of decreasing eigenvalues. However, a better measure for the number of eigenvalues of $F(x)$ that converge towards zero, is given by

$$\delta_f(x)^2 = \left\| \sum_i v_i Z_F F_i Z_F \right\|_F^2.$$

$v(x)$ is in both cases the optimal solution of the least squares problem.

When this algorithm is used, a reduced rank solution is found. However, the rank does not decrease very much. Numerical experiments showed that in most examples the lowest possible rank is not attained. The influence of the constraints on the result is quite strong. This is a disadvantage. Therefore, other methods with less influence of the constraints are studied.

A second disadvantage is that while some eigenvalues tend to zero, others can diverge.

5.5.3 The Constraints Are Taken Into Account if Needed

A straightforward method, although not very efficient from the computational point of view, is to add the constraint in the calculation of v only if needed. First, we calculate v without constraints. Then, for each constraint individually, it is checked if the new x satisfies it. If all the constraints are satisfied, x is updated with that v: $x_{k+1} = x_k + v$. Of course the stepsize is scaled, as mentioned above. If some constraints are violated, a new v is computed only taking into account those constraints. The algorithm of the previous section is used. Again all the constraints are tested if they are satisfied. If not, the ones that are now violated are added to the ones

that had been violated previously, and a new v is computed. This process is repeated until all the constraints are satisfied. It can easily be checked that this process will stop. In the worst case all the constraints are included. The resulting update of x, will satisfy the constraints.

The advantage is that only the necessary constraints influence the updating. It is thus less likely to encounter diverging eigenvalues.

The main disadvantage is of course the increase in computations. All the constraints are checked separately, and sometimes v has to be computed several times, before x is updated.

5.5.4 Reduction of the Influence of the Constraints

As mentioned in the previous sections, the constraints have a large influence on the path followed by the algorithm. However, they have to be included in some way to obtain feasible results. In the previous section, the influence of the bounds was already reduced by only taking them into account when they are needed. To reduce the influence even further, a parameter r is introduced. This parameter r weights the influence of the constraints in the least squares problem:

$$v(x) = \underset{v}{\operatorname{argmin}} \left\| \begin{pmatrix} I_f & 0 \\ 0 & I_c \end{pmatrix} - \sum_i v_i \begin{pmatrix} Z_F & 0 \\ 0 & Z_C \end{pmatrix} \begin{pmatrix} F_i & 0 \\ 0 & -rC_i \end{pmatrix} \begin{pmatrix} Z_F & 0 \\ 0 & Z_C \end{pmatrix} \right\|_F^2.$$

The resulting v determines the updating direction. The step size is $\frac{1}{1+\delta(x)}$, where $\delta(x)$ is given by

$$\delta(x)^2 = \left\| \sum_i v_i \begin{pmatrix} Z_F & 0 \\ 0 & Z_C \end{pmatrix} \begin{pmatrix} F_i & 0 \\ 0 & -rC_i \end{pmatrix} \begin{pmatrix} Z_F & 0 \\ 0 & Z_C \end{pmatrix} \right\|_F^2.$$

The number of eigenvalues of $F(x)$ tending to zero is given by

$$\delta_f(x)^2 = \left\| \sum_i v_i Z_F F_i Z_F \right\|_F^2.$$

Some examples give a lower rank when r is reduced. However, reducing r cannot be done without some extra checks during the loop. The updated x sometimes continues to violate the original constraints, even when the constraints are taken into account to find v. If this is the case, r has to be increased and a new v has to be computed. This results in a slower computation.

5.6 The Potential Reduction Method

In this section we motivate the use of a potential reduction method to solve minimum rank problems involving LMIs. The potential reduction method was originally developed to solve convex problems. Therefore, we will start by describing briefly how these problems are solved. Afterwards we show how it can be generalized to solve minimum rank problems. In the second subsection the implementation is discussed. In the third subsection some properties are proved.

5.6.1 Description of the Algorithm

The potential reduction method is used to solve the following problems:

$$\min_{x\in\mathbb{R}^m} c^t x \qquad \text{subject to } C(x)\geq 0, \tag{5.26}$$

where $C(x)$ is a symmetric affine matrix function: $C(x)=C_0+x_1C_1+\ldots+x_mC_m$ with $C_i=C_i^t\in\mathbb{R}^{n_c\times n_c}$. c is a vector in $\mathbb{R}^m$. Call $\mathcal{X}$ the set of feasible points x:

$$\mathcal{X}=\{x\in\mathbb{R}^m \mid C(x)\geq 0\}.$$

A barrier function is constructed from the LMI $C(x)\geq 0$:

$$\phi(x)=\begin{cases}\log\det C(x)^{-1} & x\in\mathcal{X}\\ \infty & x\notin\mathcal{X}.\end{cases}$$

With this definition of a barrier function, an objective function is constructed to solve (5.26):

$$\varphi(x)=\begin{cases}q\log\left(c^tx-l\right)+\phi(x) & x\in\mathcal{X}, c^tx>l\\ \infty & x\notin\mathcal{X}\\ -\infty & x\in\mathcal{X} \text{ and } c^tx\leq l.\end{cases}$$

The first term is a concave term that tends to $-\infty$ as c^tx decreases towards l. The second term is a normal barrier function that tends to ∞ as x approaches the boundary of the feasible set $\mathcal{X}$. To solve the optimization problem, $\varphi(x)$ is minimized with l sufficiently low. When the minimum is reached, l is increased and $\varphi(x)$ is minimized again. This is repeated until c^tx converges.

To minimize $\varphi(x)$ the Newton method of Nesterov and Nemirovsky for convex optimization could be used ([80]). As there is a concave term in the potential function, the Nesterov-Nemirovsky theory can not be applied immediately. However when the concave term is linearized, their theory can be used. The factor q that has been introduced is also important. It has to be larger than n_c to ensure that the sublevel sets are bounded.

This procedure can also be used to solve a so called phase I problem. A phase I problem tries to find a feasible point for $C(x)>0$. To start with a positive definite LMI a term is added to $C(x)$ multiplied with a parameter t:

$$C_t(x,t)=C(x)+(I-C(x_0))t,$$

where x_0 is any given initial vector. In this case $C_t(x_0,1)>0$ holds and can serve as an initial point for the optimization procedure. Then the following potential function is minimized:

$$\varphi(x,t)=q\log t-\log\det C_t(x,t). \tag{5.27}$$

When a solution x_{opt} is found with $t=0$ this implies $C(x_{opt})>0$, a feasible point has been found. A feasible solution only exists when $\varphi(x,t)$ becomes $-\infty$.

Reconsider now the minimum rank problem we want to solve:

$$\min_{x\in\mathbb{R}^m} \text{Rank } F(x), \qquad \text{subject to } \begin{cases}F(x)\geq 0\\ C(x)\geq 0,\end{cases} \tag{5.28}$$

where $F(x)$ and $C(x)$ are symmetric affine matrix functions:

$$F(x)=F_0+x_1F_1+x_2F_2+\ldots+x_mF_m,$$

$$C(x)=C_0+x_1C_1+x_2C_2+\ldots+x_mC_m,$$

with $F_i=F_i^t\in\mathbb{R}^{n_f\times n_f}$ and $C_i=C_i^t\in\mathbb{R}^{n_c\times n_c}$. The feasible sets are denoted by:

$$\mathcal{X}_f=\{x\in\mathbb{R}^m \mid F(x)\geq 0\}, \quad \mathcal{X}_c=\{x\in\mathbb{R}^m \mid C(x)\geq 0\}.$$

Both sets are convex.

The reduced rank matrices $F(x)$ are located on the boundary of the set $\mathcal{X}_f$, and in the set $\mathcal{X}_c$. The desired solutions have determinant zero: $\det F(x)=0$. Therefore we propose to construct the following objective function:

$$\varphi(x)=q\log\det F(x)-\log\det\begin{pmatrix}C(x) & 0\\ 0 & F(x)\end{pmatrix}. \tag{5.29}$$

The first term is a concave term that becomes $-\infty$ when $F(x)$ becomes singular. The second term is again a barrier function that ensures that x remains inside the feasible sets $\mathcal{X}_c$ and $\mathcal{X}_f$. It might look strange that $F(x)$ is also included in the convex term. This does not matter if q is high enough. (5.29) is equivalent with

$$\varphi(x) = (q-1)\log\det F(x) - \log\det C(x).$$

The implementation is easier when $F(x)$ is also in the convex term.

Reduced rank solutions $F(x)$ are obtained by minimizing $\varphi(x)$. When $\varphi(x) = -\infty$ a singular matrix $F(x)$ is reached. In fact (5.29) is just a generalization of a phase I optimization using a potential reduction method. Does there exist a x such that $F(x)$ is rank deficient and $C(x) > 0$? However, the objective function $\varphi(x)$ can have several local minima, while the potential function used for convex optimization has only one minimum. The existence of multiple minima is of course a serious disadvantage. Still in most cases a reduced rank solution is found.

To minimize $\varphi(x)$ the Newton method of Nesterov and Nemirovsky is used ([13],[80],[97]). Due to the concave term their theory cannot be applied immediately. The concave term is linearized first in each step. The linearized function satisfies the conditions of the Nesterov-Nemirovsky theory. Using this theory the next step is computed. As the first term is concave, $\varphi(x)$ will be lower than the linearized function. The concave term is again linearized in the new point x and the next step is computed. This is repeated until x converges. The Newton direction is easily computed solving a least squares problem. The damping factor of the Nesterov-Nemirovsky theory ensures feasibility of the different steps ([13],[80]), if the initial point is feasible. We suggest to start from the analytic center x^* of the constraints $C(x) > 0$ and $F(x) > 0$. The algorithm starts inside the feasible set and moves to the boundary where $F(x)$ is singular. More details of the implementation are given in the next section.

5.6.2 Implementation

In this section we describe in more detail how the objective function $\varphi(x)$ can be minimized using Nesterov and Nemirovsky's Newton algorithm [80]. Consider the algorithm:

$$x_{k+1} = x_k - \alpha_k H(x_k)^{-1} g(x_k), \tag{5.30}$$

where $g(x_k)$ is the gradient and $H(x_k)$ is the Hessian of $\varphi(x)$. α_k is the damping factor of the kth iteration. As already mentioned, the concave term has to be linearized first to apply the Nesterov-Nemirovsky theory. The Newton direction of the linearized function is computed via a least squares problem. The damping factor is determined by the Nesterov-Nemirovsky theory. It is also shown what stopping criteria can be used.

Linearization of the Concave Term

The objective function that has to be minimized is

$$\varphi(x) = q\log\det F(x) - \log\det\begin{pmatrix} C(x) & 0 \\ 0 & F(x) \end{pmatrix}.$$

Call

$$C_e(x) = \begin{pmatrix} C(x) & 0 \\ 0 & F(x) \end{pmatrix}.$$

As $\varphi(x)$ is not convex the Nesterov-Nemirovsky theory cannot be applied immediately. The concave term has to be linearized first in each step. Let $\psi(x)$ denote $\varphi(x)$ linearized in x_k:

$$\psi(x) = qg_F^t x - \log\det\begin{pmatrix} C(x) & 0 \\ 0 & F(x) \end{pmatrix} + c,$$

where g_F represents the gradient of $\log\det F(x)$ in x_k:

$$g_F = \begin{pmatrix} g_1 \\ g_2 \\ \vdots \\ g_m \end{pmatrix},$$

with

$$g_i = \text{trace } F(x_k)^{-1} F_i,$$

and c is a constant: $c = q(\log\det F(x_k) - g_F^t x_k)$.

As the first term of $\varphi(x)$ is concave, $\varphi(x) \leq \psi(x)$. The equality only holds when $x = x_k$. Thus when the linearized function is minimized, the corresponding value of $\varphi(x)$ will be lower. $\varphi(x)$ is linearized in each point of the iteration.

The Newton Direction

To compute the Newton direction, a symmetric matrix D has to be found such that ([15],[97]):

$$\text{trace } DC_e(x) = g_P^t x + c. \tag{5.31}$$

It is straightforward to show that (5.31) holds up to a constant with

$$D = \begin{pmatrix} 0 & 0 \\ 0 & F(x_k)^{-1} \end{pmatrix}. \tag{5.32}$$

The constant term does not matter for the computation of the optimization direction.
When D is known, it is shown in [80] and [97] how to construct a least squares problem to compute the Newton direction:

$$-H^{-1}g = \underset{v \in \mathbb{R}^m}{\text{argmin}} \left\| I - qZ^tDZ - \sum_{i=1}^{m} v_i Z^{-1} C_{e_i} Z^{-t} \right\|_F, \tag{5.33}$$

where $C_e(x_k) = ZZ^t$. Z is also a block diagonal matrix:

$$Z = \begin{pmatrix} Z_c & 0 \\ 0 & Z_f \end{pmatrix},$$

with $C(x_k) = Z_c Z_c^t$ and $F(x_k) = Z_f Z_f^t$. It is straightforward to show that (5.33) is equivalent to:

$$-H^{-1}g = \underset{v \in \mathbb{R}^m}{\text{argmin}} \left\| I_c - \sum_{i=1}^{m} v_i Z_c^{-1} C_i Z_c^{-t} \right\|_F^2 + \left\| I_f(1-q) - \sum_{i=1}^{m} v_i Z_f^{-1} F_i Z_f^{-t} \right\|_F^2. \tag{5.34}$$

$F(x)^{-1}$ does not need to be computed explicitly to construct (5.34). The factors Z_c and Z_f can be determined such that Z_c^{-1} and Z_f^{-1} are easily constructed.

The Damping Factor

To ensure that x_{k+1} is still inside the feasible set the Nesterov-Nemirovsky damping factor is taken. It is based on the so-called Newton decrement $\delta(x)$ ([13], [80]), which is defined as:

$$\delta(x) = \|H(x)^{-1/2} g(x)\|.$$

With this measure the following damping factor ensures that x_{k+1} is feasible:

$$\begin{cases} \alpha = \frac{1}{1+\delta(x)} & \text{if } \delta(x) > .25, \\ \alpha = 1 & \text{if } \delta(x) \leq .25. \end{cases}$$

With v the solution of (5.34), $\delta(x)$ is easily computed as ([13], [15]):

$$\begin{aligned} \delta(x) &= \left\| \sum_{i=1}^{m} v_i Z^{-1} C_{e_i} Z^{-t} \right\|_F \\ &= \left(\left\| \sum_{i=1}^{m} v_i Z_c^{-1} C_i Z_c^{-t} \right\|_F^2 + \left\| \sum_{i=1}^{m} v_i Z_f^{-1} F_i Z_f^{-t} \right\|_F^2 \right)^{\frac{1}{2}}. \end{aligned}$$

Determination of The Corank of $F(x)$

In this section it is shown how the corank of the resulting $F(x)$ can be determined during the optimization process. This means that the number of decreasing eigenvalues of $F(x)$ can be estimated near the boundary of $\mathcal{X}_f$. The following notation will be used:

$$\begin{aligned} F &= F_0 + \textstyle\sum_{i=1}^m x_{k_i} F_i, & C &= C_0 + \textstyle\sum_{i=1}^m x_{k_i} C_i, \\ V_f &= \textstyle\sum_{i=1}^m v_i F_i, & V_c &= \textstyle\sum_{i=1}^m v_i C_i. \end{aligned}$$

The Newton direction is computed via a least squares problem:

$$-H^{-1}g = \underset{v}{\text{argmin}} \left\| I + C^{-1}V_c \right\|_F^2 + \left\| (1-q)I + F^{-1}V_f \right\|_F^2.$$

Near the boundary of $\mathcal{X}_f$ the term in F will dominate. Thus v minimizes

$$\|(1-q)I + F^{-1}V_f\|_F^2. \tag{5.35}$$

This is equivalent to

$$\sum_{i=1}^{n_f} \left(1 - q + \lambda_i(F^{-1}V_f)\right)^2.$$

Near the boundary of $\mathcal{X}_f$, v is determined such that as much eigenvalues of $F^{-1}V_f$ as possible become $q-1$, the other λ_i will remain approximately 0. This corresponds to maximizing the corank of $I(1-q) + F^{-1}V_f$. An

example is shown in Appendix 1 of this chapter. The resulting minimal value for (5.35) is

$$(1-q)^2(n_f - c_r), \tag{5.36}$$

where c_r is the corank of $I(1-q)+F^{-1}V_f$ and thus of $F+V_f\frac{1}{1-q}$. As V_f minimizes (5.35), the following holds

$$\begin{aligned} \|(1-q)I+F^{-1}V_f\|_F^2 &= n_f(1-q)^2 - \|F^{-1}V_f\|_F^2 \\ &= (1-q)^2\left(n_f - \left(\frac{\|F^{-1}V_f\|_F}{q-1}\right)^2\right). \end{aligned} \tag{5.37}$$

Comparing (5.36) and (5.37) yields

$$c_r \simeq \left(\frac{\|F^{-1}V_f\|_F}{q-1}\right)^2 = \left(\frac{\|\sum_{i=1}^m v_i Z_F^{-1}F_i Z_F^{-t}\|_F}{q-1}\right)^2.$$

Near the boundary, v is computed such that the rank of $F(x)$ is reduced in the direction of v. As shown, the rank of $F(x+\frac{v}{1-q})$ is $n_f - c_r$.

The derivation corresponds to experimental results that will be presented in section 5.10. When this number is rounded towards the nearest integer, it indicates the number of decreasing eigenvalues of $F(x)$. In fact most of the time this number is close to an integer. Except when a new eigenvalue starts decreasing or if an eigenvalue stops decreasing, it takes intermediate values going from one integer to another.

Stopping Criteria

An important aspect of the routines are stopping criteria. Here we have to keep in mind that two situations can occur. Either x gets close to the boundary of $\mathcal{X}_F$ and thus some of the eigenvalues of $F(x)$ will become very small, or the algorithms stops when a finite local minimum is found. This implies that no reduced rank $F(x)$ has been found. The latter case is easily detected. It is well known in that $\delta(x)$ becomes small when a minimum is reached. Once a $\delta(x)$ is smaller than .25 the algorithm will converge quadratically towards the optimum.

To detect a point near the boundary the following procedure is used. The eigenvalues of $F(x)$ are considered to be 0 if they are smaller than a given tolerance. In the previous section it is shown that a good estimate of

the number of eigenvalues that tend to zero is given by

$$\delta_F(x_k)^2 = \left(\frac{\|\sum_{i=1}^m v_i Z_F^{-1}F_i Z_F^{-t}\|_F}{q-1}\right)^2$$

with v the solution of (5.34). The stopping criterion can then be formulated as: Sort the eigenvalues from small to large and check if the eigenvalue indicated by $\delta_F(x)^2$ is smaller than the tolerance. If so, stop, else continue. The resulting rank of $F(x_k)$ is $n_f - \lceil\delta_F(x_k)^2\rfloor$, where $\lceil y\rfloor$ is the integer closest to y. E.g. if $\lceil\delta_F(x)^2\rfloor = 4$, check if the 4th smallest eigenvalue is smaller than the tolerance. If it is, stop. The solution $F(x)$ has a rank $n_f - 4$.

5.6.3 Some Properties

In this section a lower bound for q is derived and the linear convergence of the eigenvalues of $F(x)$ is proved.

A Lower Bound for q

A good choice of q is important. q has to be large enough to emphasize the minimization of $F(x)$. However, when q is too large it might create spurious local minima. No good heuristic rule to chose q has been found yet. In this section a lower bound for q is derived. In section 5.7 we illustrate the influence of q with some examples.

When a line search is done, we want to find a minimum for a finite value and not a minimum at ∞. If h is the line search parameter, we want that the objective function becomes ∞ if $h \to \infty$. This yields a lower bound for q.

Suppose a given direction v is found, then the line search is used to find the h that minimizes the objective function:

$$\operatorname*{argmin}_h \; q\log\det(F+hV_f) - \log\det\begin{pmatrix} C+hV_c & 0 \\ 0 & F+hV_f \end{pmatrix}, \tag{5.38}$$

where

$$\begin{aligned} F &= F_0 + \textstyle\sum_{i=1}^m x_i F_i, & C &= C_0 + \textstyle\sum_{i=1}^m x_i C_i, \\ V_f &= \textstyle\sum_{i=1}^m v_i F_i, & V_c &= \textstyle\sum_{i=1}^m v_i C_i. \end{aligned}$$

(5.38) is equivalent with

$$\begin{aligned} &= \operatorname*{argmin}_h \ (q-1)\log\det(F+hV_f) - \log\det(C+hV_c) \\ &= \operatorname*{argmin}_h \ (q-1)\log\det(I+hF^{-1/2}\,V_f\,F^{-1/2}) \\ &\qquad - \log\det(I+hC^{-1/2}\,V_c\,C^{-1/2}) + c. \end{aligned}$$

The constant c term does not play any role in the optimization of h. So, it is dropped.

$$= \operatorname*{argmin}_h \ (q-1)\log\prod_{i=1}^{n_f}(1+h\lambda_i(P_F)) - \log\prod_{j=1}^{n_c}(1-h\lambda_j(P_c))$$

where

$$P_F = \sum_{i=1}^{m} v_i F^{-1/2} F_i F^{-1/2}, \qquad P_C = \sum_{j=1}^{m} v_j C^{-1/2} C_j C^{-1/2}.$$

$$= \operatorname*{argmin}_h \ (q-1)\sum_{i=1}^{n_f}\log(1+h\lambda_i(P_F)) - \sum_{j=1}^{n_c}\log(1+h\lambda_j(P_C)).$$

Taking the exponential of this function does not change the location of the extrema:

$$= \operatorname*{argmin}_h \ \frac{\prod_{i=1}^{n_f}(1+h\lambda_i(P_F))^{q-1}}{\prod_{j=1}^{n_c}(1+h\lambda_j(P_C))}.$$

We are only interested in a line search in the Newton direction, thus for positive h. When $h \to \infty$ this function has to go to ∞ to ensure a finite optimal h. Because $(1+h\lambda_i(P_F))$ and $(1+h\lambda_i(P_C))$ have to remain positive, h can only tend to ∞ if all the eigenvalues $\lambda_i(P_F)$ and $\lambda_i(P_C)$ are positive. As $h \to \infty$ the ones can be neglected:

$$\begin{aligned} \operatorname*{argmin}_h \ \frac{\prod_{i=1}^{n_f}(h\lambda_i(P_F))^{q-1}}{\prod_{j=1}^{n_c}(h\lambda_j(P_C))} &= \operatorname*{argmin}_h \ \frac{h^{(q-1)n_f}}{h^{n_c}}\frac{\prod_{i=1}^{n_f}\lambda_i(P_F)^{q-1}}{\prod_{j=1}^{n_c}\lambda_j(P_C)} \\ &= \operatorname*{argmin}_h \ h^{(q-1)n_f-n_c}\frac{\prod_{i=1}^{n_f}\lambda_i(P_F)^{q-1}}{\prod_{j=1}^{n_c}\lambda_j(P_C)}. \end{aligned}$$

The function will tend to ∞ as $h \to \infty$ if the following condition holds:

$$(q-1)n_f - n_c > 0,$$

or

$$q > 1 + \frac{n_c}{n_f}. \tag{5.39}$$

The lower bound on q ensures a finite line search. All the points will end in a local minimum. However, this local minimum can be a finite local minimum where $F(x)$ does not drop rank. These local minima can occur as q increases. This is illustrated with examples in section 5.8.3.

The Eigenvalues Decrease Linearly

In this section it is shown that the eigenvalues of $F(x)$ decrease almost linearly on a logarithmic scale, when the damping factor is $\frac{1}{1+\delta(x)}$ and $\delta(x)$ is constant. The following equality holds:

$$\log\det(F+\alpha V) = \log\det F + \log\det(I+\alpha F^{-1}V), \tag{5.40}$$

where

$$F = F_0 + \sum_{i=1}^{m} x_i F_i, \qquad V = \sum_{i=1}^{m} v_i F_i.$$

α denotes the damping factor. (5.40) is equivalent with

$$\sum_{i=1}^{n_f}\log\lambda_i^{k+1} = \sum_{i=1}^{n_f}\log\lambda_i^{k} + \sum_{i=1}^{n_f}\log\left(1+\alpha\lambda_i(F^{-1}V)\right), \tag{5.41}$$

where

$$\lambda_i^k = \lambda_i(F), \qquad \lambda_i^{k+1} = \lambda_i(F+\alpha V).$$

Near the boundary, V is such that $\|I(1-q)+F^{-1}V\|_F^2$ is minimized. This is equivalent with

$$\min_v \sum(1-q+\lambda_i(F^{-1}V))^2.$$

The minimum is reached by taking as many eigenvalues as possible equal to $q-1$. The others will be almost 0. This corresponds to maximizing the corank of $I(1-q)+F^{-1}V$. c_r denotes the corank of F. Using this fact and

substituting the damping factor $\alpha = \frac{1}{1+\delta(x)}$, (5.41) becomes:

$$\begin{aligned}\sum_{i=1}^{n_f} \log \lambda_i^{k+1} &= \log \sum_{i=1}^{n_f} \lambda_i^k + \sum_{i=1}^{c_r} \log\left(1 + \frac{q-1}{1+\delta(x)}\right) \\ &= \sum_{i=1}^{n_f} \log \lambda_i^k + \sum_{i=1}^{c_r} \log \frac{\delta(x)+q}{1+\delta(x)}.\end{aligned}$$

This can be rewritten as:

$$\sum_{i=1}^{c_r} \log \lambda_i^{k+1} + \sum_{i=c_r+1}^{n_f} \log \lambda_i^{k+1} = \sum_{i=1}^{c_r} \log \frac{\delta(x)+q}{1+\delta(x)} \lambda_i^k + \sum_{i=c_r+1}^{n_f} \log \lambda_i^k.$$

This implies that c_r eigenvalues will decrease almost linearly on a logarithmic scale, when a path gets in the neighborhood of the boundary of $\mathcal{X}_f$. How to determine c_r is shown in a previous paragraph.

5.7 A Comparison of the Two Methods

In this section the two methods are compared. As the reduced rank solutions are located at the boundary of the set $\mathcal{X}_f$, both methods move from inside the feasible set to the boundary. The objective functions are similar:

inversion of analytic centering:	$\max_x \ [-\log\det F(x) + \log\det C(x)]$
potential reduction:	$\min_x \ [q\log\det F(x) - \log\det C(x)]$

A factor q is introduced for the potential reduction method, that weights the term in $F(x)$. The main difference however is the computation of the optimization direction.

In the inverted analytic centering method the following least squares problem is solved to find the optimization direction:

$$\underset{v}{\text{argmin}} \left\| \begin{pmatrix} I_f & 0 \\ 0 & I_c \end{pmatrix} - \sum_{i=1}^{m} v_i \begin{pmatrix} Z_f^{-1} & 0 \\ 0 & Z_c^{-1} \end{pmatrix} \begin{pmatrix} F_i & 0 \\ 0 & -rC_i \end{pmatrix} \begin{pmatrix} Z_f^{-t} & 0 \\ 0 & Z_c^{-t} \end{pmatrix} \right\|_F.$$

For the potential reduction method, the least squares problem that has to be solved is

$$\underset{v}{\text{argmin}} \left\| \begin{pmatrix} I_f(1-q) & 0 \\ 0 & I_c \end{pmatrix} - \sum_{i=1}^{m} v_i \begin{pmatrix} Z_f^{-1} & 0 \\ 0 & Z_c^{-1} \end{pmatrix} \begin{pmatrix} F_i & 0 \\ 0 & C_i \end{pmatrix} \begin{pmatrix} Z_f^{-t} & 0 \\ 0 & Z_c^{-t} \end{pmatrix} \right\|_F.$$

The computation of the optimization direction of the inverted analytic centering method resembles the centering method. The main difference is a minus sign before the C block. Further an extra scalar r is also introduced to weight the importance the different blocks. If r is small the influence of the C block is reduced. The computed direction is then:

$$v = -(H_f + r^2 H_c)^{-1}(g_f - r g_c),$$

where g_f and g_c are the gradients of $-\log\det F(x)$ and $-\log\det C(x)$, and H_f and H_c the Hessians. This is however not a Newton direction, while the computed direction for the potential reduction method is the Newton direction of the linearized objective function.

The direction of the inverted centering method will tend more towards the center of $F(x)$ when r is small, thus the update will tend more towards the boundary of $F(x)$. However, due to the lower weighting of the Hessian of $C(x)$ you are not assured that the next x will be in $\mathcal{X}_c$. However, the r has to be reduced in order to weight more the search for a minimum rank solution. This is an advantage of the potential reduction method. The q parameter emphasizes the search for a minimum rank solution ensuring the feasibility of $C(x)$.

Due to the parameter q, the potential method function converges much faster than the inverted analytic centering method. The updating direction, which is the real Newton direction of the linearized potential function is directed more towards the minimum rank solutions. However taking q high also has it disadvantages. The first term of the potential reduction method is concave. Taking q too high can introduce additional local minima.

To reduce the influence of the constraints $C(x)$, without taking r to low, the following procedure was used: The constraints are not added to compute a new updating direction. It is checked if the new x satisfies all the constraints. If so, continue with a new iteration. If one or more constraints are violated, compute a new step with the violated constraints added in the least squares problem. Check again if all the constraints are satisfied. If this is not the case, add the violated constraints and compute a new v. Continue until a feasible new point is found. Finally all the constraints can be used to find a new point. This is a long and time consuming procedure. All the constraints have to be checked at each iterations. If at least one of them is violated, a new least squares problem has to be solved. This might happen several times in one iteration. The potential function reduction method includes all the constraints at each step. In each iteration only one least squares problem is solved. As the feasibility of the step is guaranteed, the constraints

do not have to be checked. Furthermore, the potential method requires less iterations than the inverted centering method in most cases. This makes the procedure even faster: It needs less iterations and the iterations are faster.

The lack of putting weight on $F(x)$ and the conditional use of the blocks $C(x)$ made it hard to solve some reduced rank problems using the inverted centering method: Due to the conditional addition of the constraints, the inverted centering method can get stuck in a loop. This can be understood as follows: A step can be taken without taking the constraints into account. To compute the next step the constraints have to be taken into account again, as they would be violated otherwise. However, due to the constraints that are taken into account, the point is pushed away in the neighborhood of the first point. Again a step can be taken without introducing the constraints. This will be in the direction of the first step, ... So the steps go back and forth without convergence. The potential reduction method does not suffer from this problem. The constraints are always taken into account.

5.8 Convergence properties

5.8.1 Optimization paths

To obtain a better insight in how the algorithms work, plots of the optimization paths of simple problems are shown in this section. The examples have only two unknowns to allow an easy graphical representation. The paths of the potential reduction method as well as the inverted potential method are also compared. All the routines used to generate the plots, have a similar structure. First the analytic center of the LMIs $F(x) > 0$ and $C(x) > 0$ is computed. Then the optimization paths are computed from 40 points in the neighborhood of this analytic center. The paths are shown until convergence at the boundary or in a local minimum. The boundaries of $\mathcal{X}_f$ are represented in full lines, the boundaries of $\mathcal{X}_c$ as dashed lines. The computed analytic center is indicated with a star. In this section we always use for the potential reduction method $q = 2(n_f + n_c)$. For the inverted analytic centering method, we use $r = 1$.

Without Constraints $C(x)$

In this section some optimization paths are shown when no constraints $C(x)$ are present. Only the rank of $F(x)$ has to be minimized. Consider first an example where the feasible set is a polytope. The feasible set $\mathcal{X}_f$ consists of

all points (x_1, x_2) satisfying:

$$\begin{cases} 2x_1 & -5x_2 & +33 & \geq & 0, \\ -2x_1 & -x_2 & +21 & \geq & 0, \\ -4x_1 & +3x_2 & +17 & \geq & 0, \\ x_1 & +3x_2 & -8 & \geq & 0, \\ 5x_1 & +x_2 & -12 & \geq & 0. \end{cases}$$

The corresponding $F(x)$ is

$$F(x) = \text{diag}\begin{pmatrix} 33 \\ 21 \\ 17 \\ -8 \\ -12 \end{pmatrix} + \text{diag}\begin{pmatrix} 2 \\ -2 \\ -4 \\ 1 \\ 5 \end{pmatrix} x_1 + \text{diag}\begin{pmatrix} -5 \\ -1 \\ 3 \\ 3 \\ 1 \end{pmatrix} x_2.$$

The boundaries of $F(x) \geq 0$ are the straight lines shown in figure 5.5. The paths followed by the potential reduction method to minimize the rank of $F(x)$, are also shown in figure 5.5. The paths start around the analytic center $(4.36, 5.44)$. All the paths end in one of the corners of the polytope. The resulting rank of $F(x)$ is thus always 3. A contour plot is also shown. Within the feasible set the potential function is rather flat. Near the boundary the slopes are steep. q is 10 in this case.

To compare this with the inverted centering procedure, consider figure 5.6. The followed paths are very similar. However, it can also be observed that the potential reduction method takes larger steps and thus it will be faster.

In the previous example there are five points the give a rank 3 solution. In one of the points extra constraints will be added such that the rank drops more in that corner. The following LMIs are added to $F(x)$:

$$\begin{cases} x_1 & +x_2 & -4 & \geq & 0, \\ 4x_1 & +2x_2 & -12 & \geq & 0, \\ 2x_1 & +4x_2 & -12 & \geq & 0. \end{cases}$$

$F(x)$ is now an 8×8 matrix. The result is shown in figure 5.7. Unfortunately, not all the paths tend to the corner $(2, 2)$. Some still tend to the other corners where the rank of $F(x)$ drops only 2 instead of 5. There is even one line going directly from the analytic center to the middle of a line of the boundary, resulting in a solution which is only one lower than the nominal rank of $F(x)$.

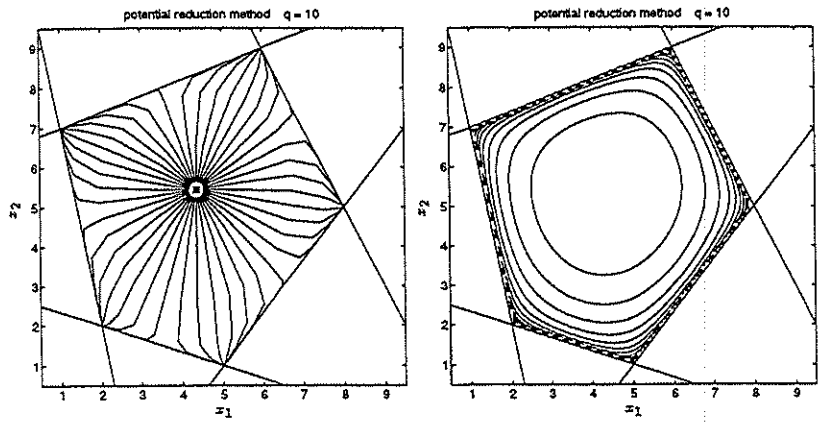

Figure 5.5: The left plot shows the paths followed by the potential reduction method to find reduced rank points. The endpoints are all in the cornerpoints of the polytopes. This corresponds to rank 3 solution for $F(x)$. The contour lines of the objective function for the potential reduction method are shown in the right plot.

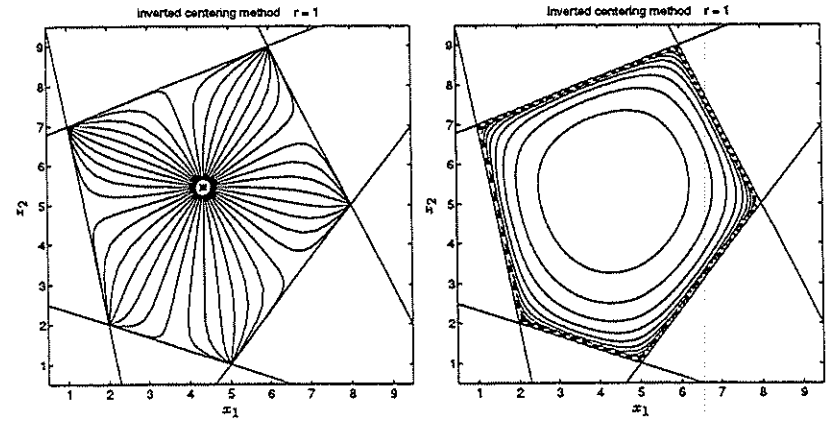

Figure 5.6: The paths followed by the inverted centering method on the left. The paths are similar to those used by the potential reduction method. The paths are smoother than the ones of the potential reduction method, due to the smaller stepsize of the inverted centering method. The right plot shows the contour lines of the objective function.

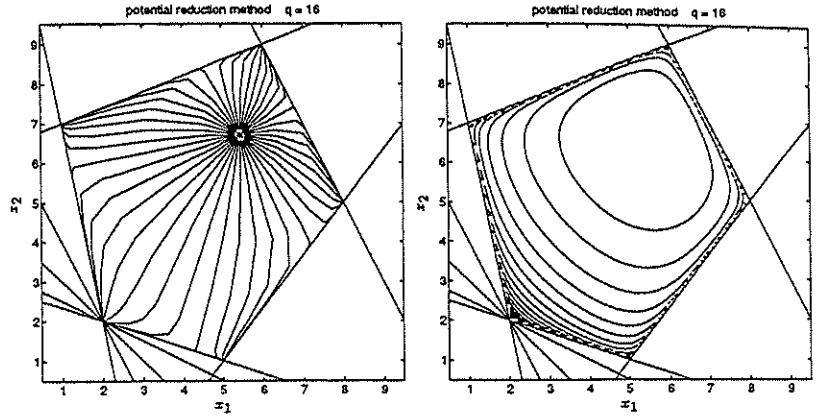

Figure 5.7: The paths followed by the potential reduction method for an example where one of the corners of the polytope has a much lower rank than the other corners. Unfortunately many paths will tend to the other corners. However, it is clear that there are more points from which the paths will tend towards the corner with the lowest rank. The right plot shows the contour lines of the objective function.

This corresponds to experiments with the inverted centering method. The 'lobe' of paths tending towards the lowest has however enlarged compared to the case where all the points are equal. The contour plot of the objective function is also shown in figure 5.7.

In the previous plots only linear bounds are used. Then most paths tend towards the intersections of the boundaries. At these points the rank of $F(x)$ is reduced most. In most cases the feasible set will not be a polytope (with linear boundaries). Most boundaries will have some curvature. This is studied next. Consider the following example:

$$\begin{cases} \begin{pmatrix} 9-x_1 & 3 \\ 3 & 9-x_2 \end{pmatrix} \geq 0, \\ x_1 - 1 \geq 0, \\ x_2 - 1 \geq 0. \end{cases} \tag{5.42}$$

The analytic center of the feasible set is $(4.08, 4.08)$. The resulting paths are shown in figure 5.8. In this case not all the paths tend to the corners. Many paths end on the curved boundary, where the rank of $F(x)$ drops only by

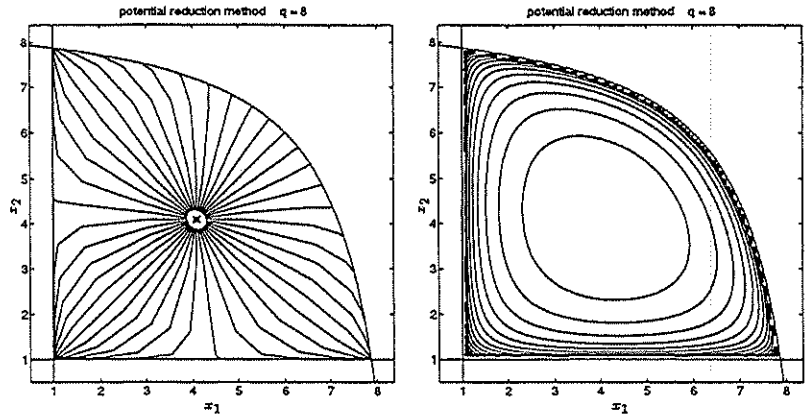

Figure 5.8: The paths of the potential reduction method in the case of curved boundaries. Not all the paths tend to the intersections of the boundaries any more. Many of them stop on the curved boundary where the rank only drops 1. The right plot is the contour plot of the objective function.

1 instead of by 2 in the corners of the boundary. The boundary is reached faster than in the case of the inverted centering method.

With Constraints $C(x)$.

In this section, the paths are studied when extra constraints $C(x)$ are present. Consider first an example with only one extra (linear) constraint. Take $F(x)$ as in (5.42). The extra constraint is:

$$C(x) = -x_1 + x_2 + 5 > 0.$$

The initial starting point is the analytic center of the constraints $F(x) > 0$ and $C(x) > 0$ combined. For this example the analytic center is: $(3.29, 4.95)$. The resulting paths are shown in figure 5.9. By computing the analytic center using $F(x)$ and $C(x)$ the initial point moves into one of the lobes of the unconstrained rank minimization of $F(x)$. All the paths go towards reduced rank solutions. In this case they all move to the same corner. This is similar to the inverted analytic centering method. The contour plot of the potential function is also shown in figure 5.9.

Consider also the case that the paths start at the analytic center of $F(x)$. The paths are shown in figure 5.10. In this case not all the paths tend towards

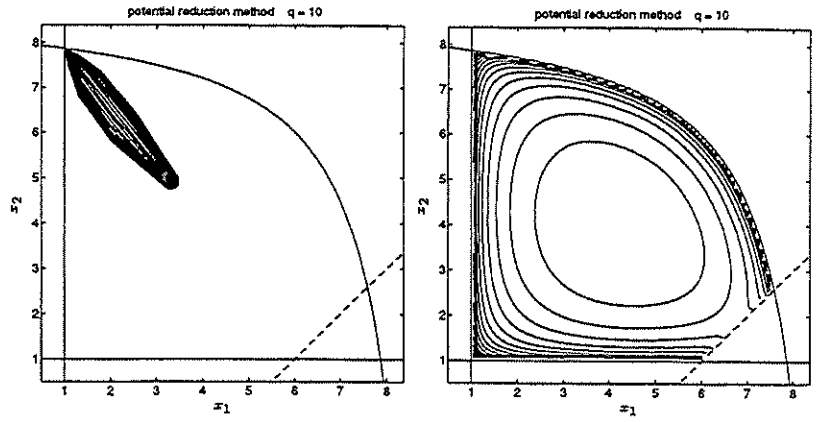

Figure 5.9: The paths followed by the potential reduction method. The paths start at points around the analytic center of $F(x) > 0$ *and* $C(x) > 0$. The analytic center is moved away from the extra constraint, compared to the unconstrained problem. All the paths end on rank reduced points. The contour lines are shown in the right plot. The value of the objective function is high near the repelling constraint.

the same corner. The paths start more or less as in the unconstrained case. The paths tending towards the repelling constraint, are turned smoothly away from the boundary. The same problem is also solved using the inverted analytic centering method. As long as the constraint is not violated, the unconstrained problem is solved. Only when the constraints are violated they are taken into account in computing the next step. This results in a rather zigzagging path around the constraint, shown in figure 5.10. The paths are less smooth in the neighbourhood of the boundary of $\mathcal{X}_c$. The smoothness of the paths is an advantage of the potential reduction method. The path of the inverted analytic centering method is not smooth as the constraints are only taken into account when they are violated. Remark that it is much more likely to find reduced rank solutions in the neighborhood of the boundary $\mathcal{X}_c$ than when the potential reduction method is used.

The previous example had only one extra constraint. How does the algorithm perform when more constraints are present? In the next example the constraints $C(x)$ are chosen such that only a small part of the boundary of $\mathcal{X}_f$ is feasible with respect to $C(x) > 0$. Take $F(x)$ as in (5.42) and $C(x)$

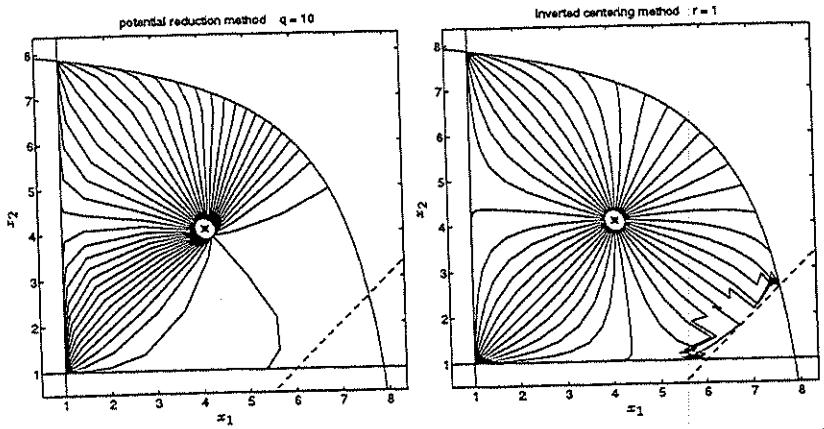

Figure 5.10: On the left the paths followed by the potential reduction method. On the right the paths followed the inverted centering method. The paths start at points around the analytic center of $F(x)$ (not of $C(x)$). Again all the paths start in all the directions. In the case of the potential reduction method, the paths in the direction of the repelling constraints are nicely bowed away from the constraint. In the inverted centering method the paths are equal to the unconstrained problem unless the extra constraint $C(x)$ is violated. The paths are not so smooth around the boundary of $\mathcal{X}_c$ compared to the potential reduction method.

consists of the following LMIs:

$$\begin{cases} -x_1 - x_2 + 10 > 0, \\ x_1 - 2 > 0, \\ x_2 - 2 > 0. \end{cases}$$

The paths are shown in figure 5.11. The paths starts around the analytic center of $F(x)$. Many paths go towards a reduced rank point ($F(x)$ is of lower rank). However, some paths get into a center without a rank reduction of $F(x)$. The algorithm detects easily that a center is reached by checking $\delta(x)$. It is also clear that the paths are nicely repelled by the constraints $C(x)$. Compare these paths with the paths of the inverted analytic centering method in figure 5.11. These paths are not as smooth. Sometimes the algorithm gets stuck in a local minimum. As $\delta(x)$ is not checked this is only found due to the fact that the maximum number of iterations is exceeded. As can be observed, the inverted centering method has some trouble when a local finite minimum is encountered. Because no good stopping criterion exists in this case and due to the conditional adding of constraints, the algorithm keeps jumping around. This is a disadvantage of the inverted analytic centering method.

It is a disappointing fact that the function can have local minima. These are local minima where the objective function does not become $-\infty$. These local minima can appear when a concave and a convex function are added. As the algorithm that is used is basically a Newton algorithm, it will get stuck in these local minima. This is illustrated with a one dimensional example. Consider the following LMIs $F(x)$ and $C(x)$:

$$F(x) = \begin{pmatrix} x-1 & 0 \\ 0 & 7-x \end{pmatrix} > 0,$$

$$C(x) = \begin{pmatrix} x-2 & 0 \\ 0 & 8-x \end{pmatrix} > 0.$$

The objective function is shown in figure 5.12. The full line is the concave function $q \log\det F(x)$. The bounds of $F(x) \geq 0$ are indicated with dash-dot lines. The boundaries of $C(x)$ are indicated with dotted lines. The objective function

$$q \log\det F(x) - \log\det \begin{pmatrix} C(x) & 0 \\ 0 & F(x) \end{pmatrix}$$

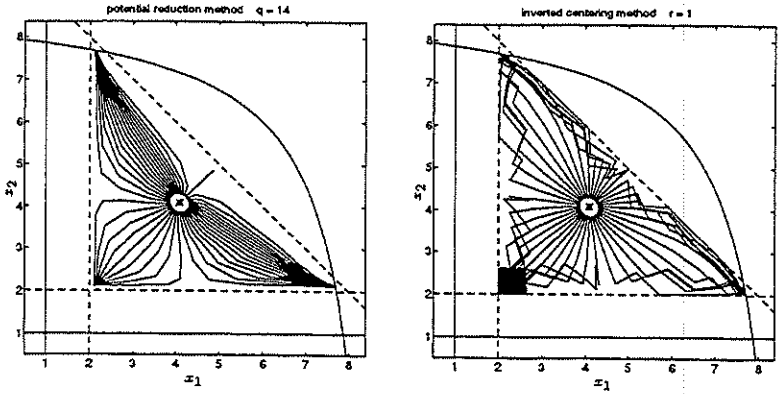

Figure 5.11: The left figure represents the paths followed by the potential reduction method for an example with many constraints. Not all of the paths end into a point of reduced rank. There are local minima of the objective function that do not correspond to reduced rank solutions. The right plot shows the paths followed by the inverted centering method. The paths are not as smooth as those of the potential reduction method.

is represented by a dashed line ($q = 8$). The function has a local minimum near 2 where $F(x)$ is not rank deficient. If the initial x is chosen too far left, the optimization will get stuck into the local minimum.

5.8.2 The Influence of r

In this section the influence of the parameter r in the method based on the inversion of the analytic center method, is studied. Consider the last two dimensional example. The paths followed by the algorithm with $r = .5$ and $r = .125$ are shown in figure 5.13. Compare this also with figure 5.11 where $r = 1$ for the inverted centering method. The curves are much smoother as r decreases.

Another example can be found in [24]. The following problem has to be solved:

$$\min_{R,S} \text{Rank} \begin{pmatrix} R & I \\ I & S \end{pmatrix} \geq 0,$$

$$AR + RA^t < \gamma BB^t, \quad A^tS + SA < \gamma C^tC.$$

This problem has to be solved to find a low order stabilizing controller. A, B

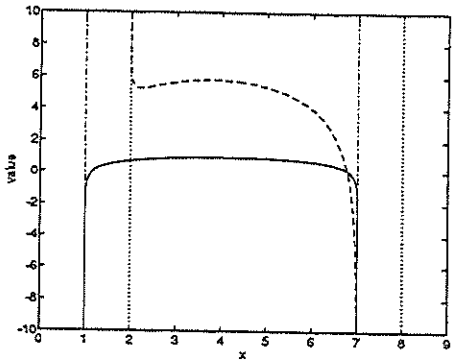

Figure 5.12: The potential reduction function for a one dimensional function. The full line is the concave part of the function. The dash-dotted line is the boundary of $F(x) \geq 0$. The dotted lines are the boundary of $C(x) > 0$. The dashed lines represent the potential function. Due to the summation of a concave and a convex function, the potential function can have local minima that are not rank reduced points of $F(x)$.

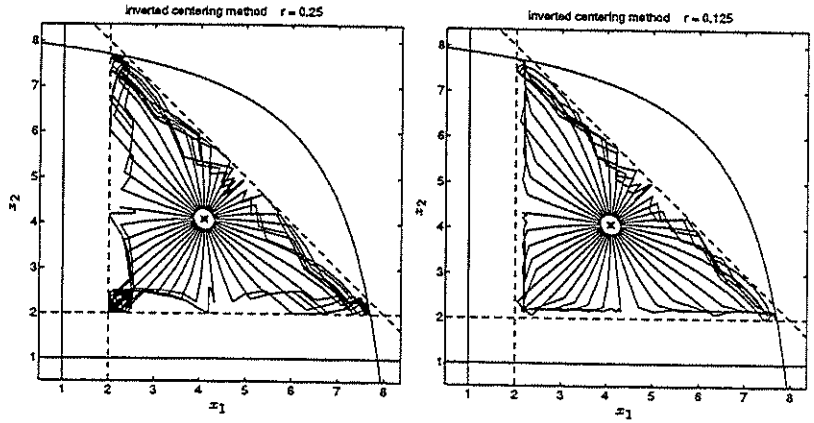

Figure 5.13: The paths followed by the inverted centering method for an example with few feasible rank reduced solutions $F(x)$. The left plot shows the inverted centering method with $r = 0.25$. The right plot is the same problem with $r = 0.125$. The curves are much smoother as r decreases.

and C are the state space matrices of the plant. The lower the rank of

$$\begin{pmatrix} R & I \\ I & S \end{pmatrix}, \tag{5.43}$$

the lower the order of the controller. The resulting rank depends not only on γ but also on the r used in the inverted centering algorithm. The example in [24] is an unstable $4th$ order system ($A \in \mathbb{R}^{4\times4}$). The resulting rank of 5.43 as a function of γ and r is given in the next table:

	2^3	2^4	2^5	2^6	2^7	2^8	2^9	2^{10}	2^{11}	2^{12}	γ
1	6	6	6	5	5	5	5	5	5	5	
.5	5	5	5	5	5	5	5	5	5	5	
.25	5	5	5	5	5	5	5	4	4	4	
.125	5	5	5	5	4	4	4	4	4	4	
.0625	5	5	5	5	4	4	4	4	4	4	
r											

In this case the rank can be reduced by increasing γ and decreasing r. However, this is not always the case. More examples are shown in [24].

5.8.3 The Influence of q

In this section the influence of the parameter q in the potential reduction method is studied. Consider first the one-dimensional example of the previous section. Instead of taking $q = 2(n_f + n_c) = 8$ as previously, the value of the potential function with $q = 3$ is shown in figure 5.14 (dashed line). In this case there is no spurious local minimum any ¡more. Starting form any feasible point, the optimal $x = 7$ will be found.

Changing the value of q also changes the paths in other examples. E.g. the example with the curved boundary and the many additional constraints. In figure 5.15 the paths are shown for $q = 4$. Less paths get stuck in a local minimum. q can take other values than integer ones. The paths for $q = 3.5$ are also shown in figure 5.15. Still not all the paths tend to a rank reduced solution. When the symmetry is broken, this problem also disappears. E.g. when the constraint

$$10 - x_1 - x_2 > 0,$$

is transformed into

$$10 - x_1 - 0.95x_2 > 0.$$

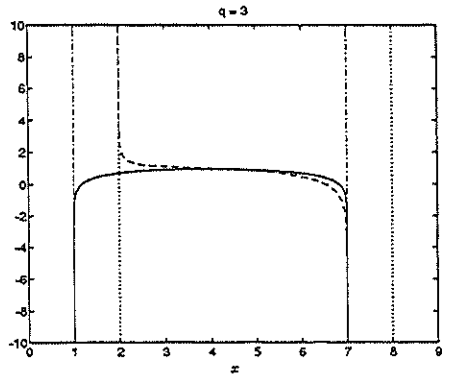

Figure 5.14: The potential reduction function for a one dimensional function. The full line is the concave part of the function. The dash-dotted line is the boundary of $F(x) \geq 0$. The dotted lines are the boundary of $C(x) > 0$. The dashed lines represent the potential function. Different values of q can introduce spurious local minima or let them disappear.

The resulting paths are shown in figure 5.16. Taking q too small does not work either. $q = 2$ for the modified problem is shown in figure 5.16. All the paths that start in the neighborhood of the analytic center, end in a local minimum instead of at the boundary of $F(x)$, although q is larger than the proposed lower bound $1 + \frac{n_c}{n_f}$, as $n_c = 3$ and $n_f = 4$. A better lower bound is needed.

Until now, bounds on q were looked for via linearization. In this case other methods will be needed.

5.9 Other Minimum Rank Problems

In this section we describe some other problems that can be cast as minimum rank LMI problems. The first two examples are also controller design problems. The third one is an identification problem.

5.9.1 Reduced Order Output Feedback Design

A first example of an output feedback control problem that can be formulated as a minimum rank problem is described. It is the design of a low order

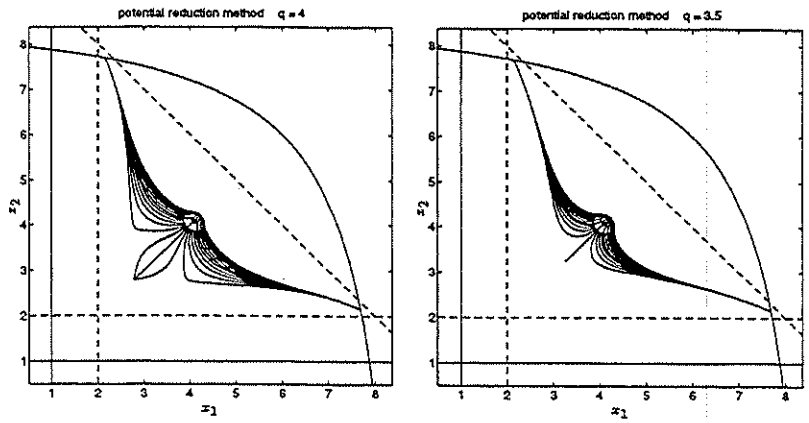

Figure 5.15: Changing q has a serious influence. The left figure shows the curved boundary example with $q = 4$. Less paths get stuck into the spurious local minimum. The local minimum is less deep. q can also be a real number. The right figure shows the curved boundary example with $q = 3.5$. Only two paths get stuck into a local optimum. The optimum is a saddle point. The paths can get stuck in it because the problem is symmetric.

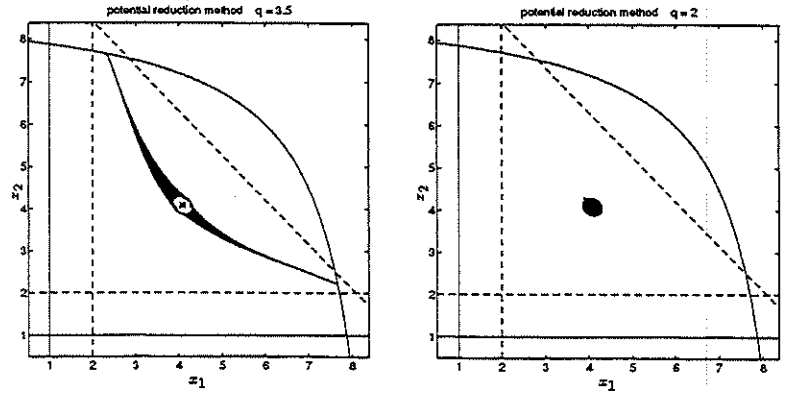

Figure 5.16: In the left plot it is shown that when the symmetry of the problem is broken, the saddle points can disappear. The right plot shows an example where q has been chosen too low. When q is chosen too low, the paths can all run into a center. q has to be chosen large enough to put enough weight on the rank minimization of $F(x)$.

linear dynamic controller that quadratically stabilizes a norm-bound linear differential inclusion (NLDI) ([14]). Quadratic stability implies that there exists a quadratic Lyapunov function $V(x) = x^t P x$, that proves the stability of the plant, where P is a positive definite matrix of appropriate size. The derivation follows arguments of [14] and [47]. Only the result will be stated.

Consider the following state space realization of a NLDI:

$$\begin{cases} \dot{x} &= Ax + B_u u + B_p p \\ y &= C_y x + D_{yu} u + D_{yp} p \\ q &= C_q x + D_{qu} u + D_{qp} p, \end{cases} \tag{5.44}$$

$$p = \Delta(t) q, \qquad \|\Delta(t)\| \leq 1,$$

where $\Delta(t)$ is a time varying uncertainty with norm lower than 1 at each time instant. $\|.\|$ denotes the induced 2-norm for matrices. Without loss of generality D_{yu} is assumed to be 0. When a controller is computed with a zero D_{yu}, the obtained controller can always be adapted to take into account the non-zero D_{yu} ([56]).

Using arguments of [14] and [47] the following theorem is easily derived.

Theorem 14 *A controller of order n_c that quadratically stabilizes the NLDI (5.44) exists if a $P, Q \in \mathbb{R}^{n \times n}$ and $\sigma \in \mathbb{R}$ can be found such that $P = P^t > 0$, $Q = Q^t > 0$ and $\sigma > 0$ which satisfy the following inequalities:*

$$\begin{pmatrix} P & I \\ I & Q \end{pmatrix} \geq 0, \tag{5.45}$$

$$\begin{pmatrix} QA^t + AQ + B_p B_p^t & QC_q^t + B_p D_{qp}^t \\ C_q Q + D_{qp} B_p^t & -I + D_{qp} D_{qp}^t \end{pmatrix} < \sigma \begin{pmatrix} B_u \\ D_{qu} \end{pmatrix} \begin{pmatrix} B_u^t & D_{qu}^t \end{pmatrix}, \tag{5.46}$$

$$\begin{pmatrix} A^t P + PA + C_q^t C_q & PB_p + C_q^t D_{qp} \\ B_p^t P + D_{qp}^t C_q & -I + D_{qp}^t D_{qp} \end{pmatrix} < \sigma \begin{pmatrix} C_y^t \\ D_{yp}^t \end{pmatrix} \begin{pmatrix} C_y & D_{yp} \end{pmatrix}, \tag{5.47}$$

and

$$Rank \begin{pmatrix} P & I \\ I & Q \end{pmatrix} \leq n + n_c.$$

□

σ can be removed from equations (5.46) and (5.47) by multiplying (5.46) from the left and the right with the null space of $\begin{pmatrix} B_u^t & D_{qu}^t \end{pmatrix}$ and (5.47) with the null space of $\begin{pmatrix} C_y & D_{yp} \end{pmatrix}$ ([14]).

The order of the controller that can be designed is determined by the rank of (5.45). To design a controller of lowest possible order the rank of (5.45) has to be reduced as much as possible. This nicely fits in the general framework of the minimum rank problems.

The formulas can also be used to design a reduced order stabilizing controller for a linear time invariant system. The equations represent a linear time-invariant system if $B_p = 0$, $D_{yp} = 0$, $C_q = 0$, $D_{qu} = 0$ and $D_{qp} = 0$. The formulas are necessary and sufficient for linear time invariant systems.

5.9.2 Reduced Order H_2 Control

In this section we show how a reduced order H_2 controller for a linear time invariant system can be designed. First we briefly recapitulate the computation of the H_2 norm of linear time invariant systems.

The H_2 norm of a stable linear time invariant plant $G(s)$ with state space realization:

$$\begin{cases} \dot{x} &= Ax &+Bw \\ z &= Cx &+Dw, \end{cases}$$

is

$$\|G(s)\|_2^2 = \int_0^\infty \text{trace}\,(G(j\omega)^* G(j\omega))\,d\omega.$$

The feedthrough term D has to be 0 to obtain a finite H_2 norm. It is well known that the H_2 norm can be computed as:

$$\|G(s)\|_2^2 = \text{trace}\,(B^t P B),$$

where P is the solution of

$$PA + A^t P + C^t C = 0.$$

This is also equal to

$$\|G(s)\|_2^2 = \min_P \text{trace}\,(B^t P B),$$

for Ps satisfying

$$PA + A^t P + C^t C < 0.$$

The derivation of the formulas for the design of a reduced order H_2 controller, is based on [14] and [47]. Consider the following state space realization of the plant:

$$\begin{cases} \dot{x} &= Ax &+B_w w &+B_u u \\ z &= C_z x &+D_{zw} w &+D_{zu} u \\ y &= C_y x &+D_{yw} w &+D_{yu} u, \end{cases} \tag{5.48}$$

where $A \in \mathbb{R}^{n\times n}$, $B_w \in \mathbb{R}^{n\times n_w}$, $B_u \in \mathbb{R}^{n\times n_u}$, $C_z \in \mathbb{R}^{n_z\times n}$, $C_y \in \mathbb{R}^{n_y\times n}$, $D_{zw} \in \mathbb{R}^{n_z\times n_w}$, $D_{zu} \in \mathbb{R}^{n_z\times n_u}$, $D_{yw} \in \mathbb{R}^{n_y\times n_w}$, $D_{yu} \in \mathbb{R}^{n_y\times n_u}$. The problem is to minimize the H_2 norm of the closed loop transfer function from z to w:

$$\min_C \|T_{zw}\|_2.$$

The state space realization of the controller C is denoted by:

$$\begin{cases} \dot{x}_c &= A_c x_c + B_c y \\ u &= C_c x_c + D_c y, \end{cases} \tag{5.49}$$

with $A_c \in \mathbb{R}^{n_c\times n_c}$, $B_c \in \mathbb{R}^{n_c\times n_y}$, $C_c \in \mathbb{R}^{n_u\times n_c}$ and $D_c \in \mathbb{R}^{n_u\times n_y}$.

The following assumptions are made:

1. $D_{zw} = 0$.
2. $D_{yw} = 0$.
3. $D_{yu} = 0$.

The first and the second assumption are necessary to ensure a finite H_2 norm of the transfer function from w to z. To obtain a finite H_2 norm the feedthrough term has to be 0. The third assumption can easily be removed. Once a controller is computed a non-zero D_{yu} can always be taken into account afterwards.

The following can easily be proved:

Theorem 15 *A controller of order n_c that makes the H_2 norm of the closed loop of the plant (5.48) and the controller (5.49) less than α exists if a*

$P, Q \in \mathbb{R}^{n\times n}$ and $\sigma \in \mathbb{R}$ can be found such that $P = P^t > 0$, $Q = Q^t > 0$ and $\sigma > 0$ which satisfy the following inequalities:

$$trace\,(B_w^t P B_w) < \alpha^2, \tag{5.50}$$

$$\begin{pmatrix} P & I \\ I & Q \end{pmatrix} \geq 0, \tag{5.51}$$

$$\begin{pmatrix} A^tP + PA & C_z^t \\ C_z & -I \end{pmatrix} < \sigma \begin{pmatrix} C_y^t \\ 0 \end{pmatrix} \begin{pmatrix} C_y & 0 \end{pmatrix}, \tag{5.52}$$

$$\begin{pmatrix} QA^t + AQ & QC_z^t \\ C_zQ & -I \end{pmatrix} < \sigma \begin{pmatrix} B_u \\ D_{zu} \end{pmatrix} \begin{pmatrix} B_u^t & D_{zu}^t \end{pmatrix}, \tag{5.53}$$

and

$$Rank \begin{pmatrix} P & I \\ I & Q \end{pmatrix} \leq n + n_c.$$

Proof:
The closed loop of the generalized plant (5.48) and the controller (5.49) is

$$\begin{cases} \dot{\tilde{x}} &= (\tilde{A} + \tilde{B}_u K \tilde{C}_y)\tilde{x} \quad + \tilde{B}_w w \\ z &= (\tilde{C}_z + \tilde{D}_{zu} K \tilde{C}_y)\tilde{x}, \end{cases}$$

where

$$\tilde{x} = \begin{pmatrix} x \\ x_c \end{pmatrix}, \quad K = \begin{pmatrix} A_c & B_c \\ C_c & D_c \end{pmatrix},$$

$$\tilde{A} = \begin{pmatrix} A & 0 \\ 0 & 0 \end{pmatrix}, \quad \tilde{B}_w = \begin{pmatrix} B_w \\ 0 \end{pmatrix}, \quad \tilde{B}_u = \begin{pmatrix} 0 & B_u \\ I & 0 \end{pmatrix},$$

$$\tilde{C}_z = \begin{pmatrix} C_z & 0 \end{pmatrix}, \quad \tilde{D}_{zw} = D_{zw}, \quad \tilde{D}_{zu} = \begin{pmatrix} 0 & D_{zu} \end{pmatrix},$$

$$\tilde{C}_y = \begin{pmatrix} 0 & I \\ C_y & 0 \end{pmatrix}.$$

To minimize $\|T_{zw}\|_2$, a $\tilde{P} = \tilde{P}^t \in \mathbb{R}^{(n+n_c)\times(n+n_c)}$ has to exist such that:

$$\min_{K,\tilde{P}} \text{trace} \left(\tilde{B}_w^t \tilde{P} \tilde{B}_w\right),$$

where K and $\tilde{P}$ have to satisfy

$$(\tilde{A} + \tilde{B}_u K \tilde{C}_y)^t \tilde{P} + \tilde{P}(\tilde{A} + \tilde{B}_u K \tilde{C}_y) + (\tilde{C}_z + \tilde{D}_{zu} K \tilde{C}_y)^t (\tilde{C}_z + \tilde{D}_{zu} K \tilde{C}_y) < 0.$$

This is equivalent with

$$\begin{pmatrix} \tilde{A}^t\tilde{P} + \tilde{P}\tilde{A} + \tilde{C}_y^t K^t \tilde{B}_u^t \tilde{P} + \tilde{P}\tilde{B}_u K \tilde{C}_y & \tilde{C}_z^t + \tilde{C}_y^t K^t \tilde{D}_{zu}^t \\ \tilde{C}_z + \tilde{D}_{zu} K \tilde{C}_y & -I \end{pmatrix} < 0. \tag{5.54}$$

To obtain LMIs, K can be eliminated from the inequalities (5.54) using the elimination procedure described in [14] and [47]. There exists a K that satisfies (5.54), if and only if there exist a $\tilde{P} > 0$, $\tilde{Q} > 0$ and a scalar $\tilde{\sigma} > 0$ such that

$$\begin{pmatrix} \tilde{A}^t\tilde{P} + \tilde{P}\tilde{A} & \tilde{C}_{z_1}^t \\ \tilde{C}_{z_1} & -I \end{pmatrix} < \tilde{\sigma} \begin{pmatrix} \tilde{C}_y^t \\ 0 \end{pmatrix} \begin{pmatrix} \tilde{C}_y & 0 \end{pmatrix}, \tag{5.55}$$

$$\begin{pmatrix} \tilde{Q}\tilde{A}^t + \tilde{A}\tilde{Q} & \tilde{Q}\tilde{C}_{z_1}^t \\ \tilde{C}_{z_1}\tilde{Q} & -I \end{pmatrix} < \tilde{\sigma} \begin{pmatrix} \tilde{B}_u \\ \tilde{D}_{z_1 u} \end{pmatrix} \begin{pmatrix} \tilde{B}_u^t & \tilde{D}_{z_1 u}^t \end{pmatrix}, \tag{5.56}$$

where $\tilde{Q} = \tilde{P}^{-1}$. The H_2 norm $\|T_{zw}\|_2$ is lower than α if there exists a $\tilde{P}$ such that the previous inequalities are satisfied and trace $(\tilde{B}_w^t \tilde{P} \tilde{B}_w) < \alpha^2$. These inequalities are no LMIs yet, due to the equality constraint on $\tilde{P} = \tilde{Q}^{-1}$. However, the following theorem of [47] can be used. Let P and Q denote the upper left $n \times n$ blocks of $\tilde{P}$ and $\tilde{Q} \in \mathbb{R}^{(n+n_c)\times(n+n_c)}$, respectively. Then, $\tilde{P} = \tilde{Q}^{-1}$ if

$$\begin{pmatrix} P & I \\ I & Q \end{pmatrix} \geq 0, \qquad \text{Rank} \begin{pmatrix} P & I \\ I & Q \end{pmatrix} \leq n + n_c.$$

This also holds the other way around. If a P and Q exist that satisfy the inequalities, then they are the upper left corners of positive definite matrices $\tilde{P}$ and $\tilde{Q} \in \mathbb{R}^{(n+n_c)\times(n+n_c)}$, such that $\tilde{P} = \tilde{Q}^{-1}$.

From, this it is easily proved that a reduced order H_2 controller exists if a P, Q and σ exist that satisfy the following constraints:

$$\text{trace}\,(\tilde{B}_{w_1}^t \tilde{P} \tilde{B}_{w_1}) = \text{trace}\,(B_{w_1}^t P B_{w_1}) < \alpha^2,$$

$$\begin{pmatrix} P & I \\ I & Q \end{pmatrix} \geq 0, \tag{5.57}$$

$$\begin{pmatrix} A^tP+PA & C_{z_1}^t \\ C_{z_1} & -I \end{pmatrix} < \sigma \begin{pmatrix} C_y^t \\ 0 \end{pmatrix} \begin{pmatrix} C_y & 0 \end{pmatrix}, \tag{5.58}$$

$$\begin{pmatrix} QA^t+AQ & QC_{z_1}^t \\ C_{z_1}Q & -I \end{pmatrix} < \sigma \begin{pmatrix} B_u \\ D_{z_1u} \end{pmatrix} \begin{pmatrix} B_u^t & D_{z_1u}^t \end{pmatrix}. \tag{5.59}$$

We still have to prove that if there exist solutions Q, P and σ satisfying (5.57) to (5.59), there exist a $\tilde{Q}$, $\tilde{P}$ and $\tilde{\sigma} \geq \sigma > 0$ such that the inequalities (5.55) and (5.56) are satisfied. Suppose Q and σ are such that (5.59) is satisfied. $\tilde{Q}$ can be partitioned as

$$\tilde{Q} = \begin{pmatrix} Q & Q_{12} \\ Q_{12}^t & Q_{22} \end{pmatrix}.$$

The inequality (5.56) can then be written as

$$\begin{pmatrix} QA^t+AQ & AQ_{12} & QC_{z_1}^t \\ Q_{12}^tA^t & 0 & Q_{12}^tC_{z_1}^t \\ C_{z_1}Q & C_{z_1}Q_{12} & -I \end{pmatrix} < \tilde{\sigma} \begin{pmatrix} B_uB_u^t & 0 & 0 \\ 0 & I & 0 \\ 0 & 0 & D_{z_1u}D_{z_1u}^t \end{pmatrix}.$$

This is equivalent with

$$\begin{pmatrix} QA^t+AQ & QC_z^t \\ C_zQ & -I \end{pmatrix} - \tilde{\sigma} \begin{pmatrix} B_uB_u^t & 0 \\ 0 & D_{zu}D_{zu}^t \end{pmatrix} + \frac{1}{\tilde{\sigma}} \begin{pmatrix} AQ_{12} \\ C_zQ_{12} \end{pmatrix} \begin{pmatrix} Q_{12}^tA^t & Q_{12}^tC_z^t \end{pmatrix} < 0.$$

From this expression it is obvious that if $\tilde{\sigma}$ is large enough, (5.56) will be satisfied if (5.59) is satisfied.

If a solution is found, $\tilde{P}$ can be constructed and substituted into (5.54). Then a K can be constructed that satisfies these constraints. This completes the proof. □

As shown previously, σ can be removed from the inequalities (5.59) and (5.58).

5.9.3 The Frisch Scheme

The Frisch scheme deals with the problem of identifying linear relations between measured data. Suppose n variables are measured over m time instants. The measurements are aggregated in an $m \times n$ real matrix M. It is

assumed that the number of measurements exceeds the number of variables: $m > n$ so that the matrix M has more rows than columns. This assumption of overdetermination is of course necessary since otherwise the problem would be trivial. An existing linear relation will reveal itself via an n-vector x that belongs to the kernel of the matrix M:

$$Mx = 0.$$

The number of linear independent relations between the variables equals the *corank*. The corank of M is defined as $n - \text{rank}(M)$.
Typically, however, measurements are noisy so that no linear relations between the data exist. A fundamental assumption on the noise is that it is additive and uncorrelated. The measured matrix M can be written as:

$$M = \hat{M} + N,$$

where $\hat{M}$ denotes the noisefree data and N the noise variables. The noise on the different channels is assumed to be uncorrelated, hence:

$$N^tN = \text{ diagonal},$$

and kernel$(N) = 0$. No linear relations between the noise and the exact data exist either:

$$\hat{M}^tN = N^t\hat{M} = 0.$$

The measured, exact and noise Gramians are denoted as:

$$A = M^tM, \quad \hat{A} = \hat{M}^t\hat{M}, \quad D = N^tN.$$

The Frisch scheme can now be formulated as follows:
Given a positive definite matrix A, find a diagonal, positive definite matrix D so that:

1. $\hat{A} = A - D$ is positive semi definite.
2. The corank of $\hat{A}$ is maximal.

To find the maximum number of linear relations, the corank has to be maximized. Generically the rank of $\hat{A}$, cannot be reduced arbitrarily. There exist a generic lower bound, which is called the Wilson-Lederman bound, see e.g. [28] and references therein. The rank of $\hat{A}$ can be reduced under this bound only in special cases.

It is, of course, obvious that the Frisch scheme can be reformulated as minimum rank problem involving linear matrix inequalities:

$$\min_D \text{ Rank } A - D$$

$$\text{subject to } \begin{cases} A - D \geq 0 \\ D > 0, \end{cases}$$

where D is a diagonal matrix.

5.10 Numerical Results

5.10.1 Reduced Order H_∞ Design

In this section a low order H_∞ controller is designed based on the formulas of section 5.2. A 5th order plant was constructed that satisfies the assumptions. The state space representation is:

$$\left(\begin{array}{c|c:c} A & B_1 & B_2 \\ \hline C_1 & 0 & D_{12} \\ \hdashline C_2 & D_{21} & 0 \end{array}\right) =$$

$$\left(\begin{array}{ccccc|ccc:cc} -0.3979 & 1.272 & -1.39 & -0.7975 & -0.2683 & 1.939 & 0 & 0 & 1.339 & 0.421 \\ 0.8643 & -0.03534 & 0.2293 & -0.9367 & -1.082 & -0.8958 & 0 & 0 & 1.222 & -0.4334 \\ -0.1776 & -1.501 & 0.2712 & -0.002433 & 2.014 & -0.3042 & 0 & 0 & -1.596 & 0.7063 \\ 1.874 & 0.3654 & -0.3664 & 0.3961 & 1.944 & 0.5553 & 0 & 0 & -1.068 & 0.2279 \\ 0.1724 & -0.1987 & 1.377 & -0.5087 & -1.522 & -0.3242 & 0 & 0 & -0.7599 & -1.017 \\ \hline 0.1399 & -0.7481 & -0.629 & 1.395 & -1.648 & 0 & 0 & 0 & 0 & 0 \\ 0 & 0 & 0 & 0 & 0 & 0 & 0 & 0 & 1 & 0 \\ 0 & 0 & 0 & 0 & 0 & 0 & 0 & 0 & 0 & 1 \\ \hdashline -2.015 & -1.555 & 0.2449 & -0.5702 & 1.209 & 0 & 1 & 0 & 0 & 0 \\ 0.4917 & -0.1406 & -0.2675 & -0.1873 & -0.6389 & 0 & 0 & 1 & 0 & 0 \end{array}\right).$$

This system is unstable. From standard H_∞ techniques, it is easily derived that the lowest possible H_∞ norm is 3.094.

Suppose we want to design a controller such that the H_∞ norm of the controller is lower than 4.641 ($\gamma = 4.641$). This is 50% higher than the lower bound. The eigenvalues of the matrix

$$F_1 = \begin{pmatrix} R & \gamma^{-1} I \\ \gamma^{-1} I & S \end{pmatrix}$$

as a function of the number of iterations is shown in figure 5.17. The potential reduction method is used with $q = 22$ and the inverted centering

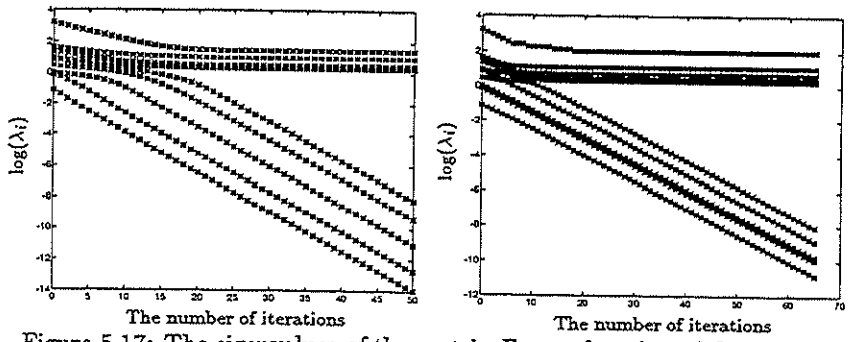

Figure 5.17: The eigenvalues of the matrix F_1 as a function of the number of iterations. The left plot shows the eigenvalues when the potential reduction method is used with $q = 22$. The right plot shows the result of the inverted centering method ($\tau = 1$). In both cases five eigenvalues decrease below the threshold 10^{-8}. Thus the order of the controller will be 5 lower than the order of the plant. This corresponds, in this case, to a 0th order controller, a static controller.

method with $\tau = 1$. The potential reduction method decreases much faster than the inverted centering method. The potential reduction method reduces the minimal rank in 50 iterations while the inverted centering method needs 65 iterations. In both cases, five eigenvalues decrease below the tolerance 10^{-8}. The order of the controller is five lower than the order of the plant. This corresponds to a $0th$ order controller: a static output feedback gain K, $u = Ky$. The static gain of obtained with the potential reduction method is

$$K = \begin{pmatrix} 1.205 & -0.9937 \\ -0.5005 & -0.003085 \end{pmatrix},$$

and the K obtained with the inverted centering method is:

$$K = \begin{pmatrix} 1.252 & -0.8265 \\ -0.5781 & 0.3938 \end{pmatrix}.$$

For this example a static output feedback gain is found that stabilizes the system and reduces the H_∞ norm below $\gamma = 4.641$.

As an illustration low order controllers are computed for different values of the bound γ. This is shown in figure 5.18. The low order H_∞ controller was computed for several values of γ: $\gamma = 3.1, 3.3, \ldots, 4.7$. The controllers

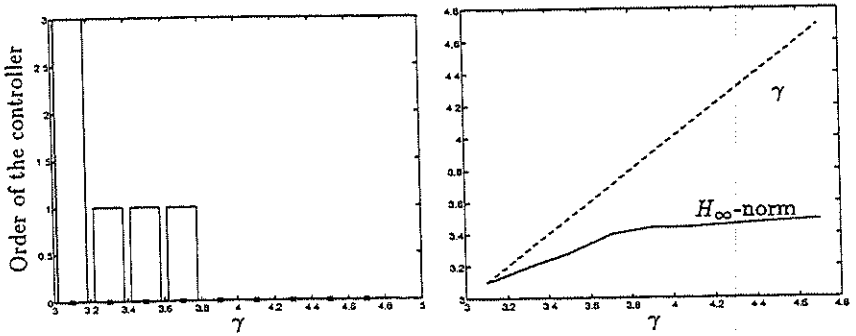

Figure 5.18: The left plot shows the order of the controller for different values of γ. The stars indicate the values of γ for which a low order H_∞ suboptimal controller is computed. A $0th$ order controller is a static output feedback. Apparently, the higher the value of γ, the lower the necessary order of the controller is. The right plot shows the H_∞ norm with a reduced order controller as a function of γ. The full line is the H_∞ norm of the closed loop. The dashed line is γ. The H_∞ remains nicely under γ.

are computed with the potential reduction method because it is much faster than the inverted centering method. It can be seen that the order of the controller increases as γ approaches the optimal (lowest) γ. When γ is large enough a static output feedback is sufficient to obtain the desired γ. As a check, the H_∞ norm of the the closed loop with the obtained controllers is also shown in figure 5.18. The H_∞ norm of the closed loop is always lower than the desired γ.

5.10.2 The Design of a Controller for a NLDI

In this section reduced order controllers are designed for a pendulum with a varying length, shown in figure 5.19. This system can be described as a NLDI:

$$\begin{pmatrix} \dot{\theta}_1 \\ \dot{\theta}_2 \end{pmatrix} = \begin{pmatrix} 0 & 1 \\ -\frac{g}{l_0} & 0 \end{pmatrix}\begin{pmatrix} \theta_1 \\ \theta_2 \end{pmatrix} + \begin{pmatrix} 0 \\ \frac{1}{ml_0} \end{pmatrix} w + \begin{pmatrix} 0 \\ \frac{1}{ml_0} \end{pmatrix} u + \begin{pmatrix} 0 \\ \delta l \end{pmatrix} p$$

$$z = \begin{pmatrix} 1 & 0 \end{pmatrix}\begin{pmatrix} \theta_1 \\ \theta_2 \end{pmatrix}$$

$$y = \begin{pmatrix} 1 & 0 \end{pmatrix}\begin{pmatrix} \theta_1 \\ \theta_2 \end{pmatrix}$$

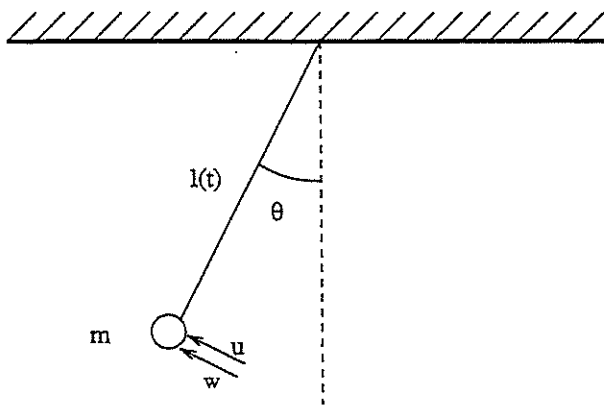

Figure 5.19: The pendulum with varying length setup.

$$q = \begin{pmatrix} \frac{g}{l_0^2} & 0 \end{pmatrix}\begin{pmatrix} \theta_1 \\ \theta_2 \end{pmatrix} - \frac{1}{ml_0^2}w - \frac{1}{ml_0^2}u$$
$$p = \Delta(t)q$$

with $\|\Delta(t)\| < 1$, where $\Delta(t)$ is an unknown bounded time varying uncertainty. l_0 is the nominal length. δl is the maximal deviation from this nominal length. θ_1 is the angle of the pendulum. θ_2 is the angular velocity. m is the mass of the load.

A disturbing input w is assumed, parallel to the control input u. The controlled output is the angle θ. The following values are used:

$$\begin{array}{lcll} l_0 & = & 1 & (m) \\ \delta l & = & .1 & (m) \\ m & = & .5 & (kg) \\ g & = & 9.81 & (m/s^2) \end{array} \tag{5.60}$$

This system is not quadratically stable. To design a stabilizing controller a feasible solution has to be found for

$$F_2 = \begin{pmatrix} P & I \\ I & Q \end{pmatrix} \geq 0,$$

(5.46) and (5.47) in a first step. This is a so called phase I problem (see e.g. [97]).

Once a feasible point is found, the rank of F_2 can be minimized to find a reduced order controller using the potential reduction method. The lower the resulting rank of F_2, the lower the order of the corresponding controller will be.

To compute the controller, the state space matrices of the controller are put into one matrix:

$$K = \begin{pmatrix} A_c & B_c \\ C_c & D_c \end{pmatrix}.$$

The state space matrices of the original plant are embedded into a larger system as shown in [14] and [47]. The state space matrices of the larger system will be denoted with tildes ($\tilde{}$). The size of the matrix K depends on the number of control inputs n_u, the number of measured outputs n_y and the order of the controller n_c, as determined by the rank minimization procedure. The controller matrices can be computed solving a regular convex optimization problem. From the theory it follows that a feasible solution K has to exist. A K has to be found that satisfies:

$$\begin{pmatrix} \tilde{A}^t\tilde{P} + \tilde{P}\tilde{A} & \tilde{P}\tilde{B}_p & \tilde{C}_q^t \\ \tilde{B}_p^t\tilde{P} & -I & \tilde{D}_{qp}^t \\ \tilde{C}_q & \tilde{D}_{qp} & -I \end{pmatrix} + \begin{pmatrix} \tilde{P}\tilde{B}_u \\ 0 \\ \tilde{D}_{qu} \end{pmatrix} K \begin{pmatrix} \tilde{C}_y & \tilde{D}_{yp} & 0 \end{pmatrix} + \begin{pmatrix} \tilde{C}_y^t \\ \tilde{D}_{yp}^t \\ 0 \end{pmatrix} K^t \begin{pmatrix} \tilde{B}_u^t\tilde{P} & 0 & \tilde{D}_{qu}^t \end{pmatrix} < 0,$$

where I is a unit matrix of appropriate dimensions. $\tilde{P}$ is a symmetric $(n + n_c) \times (n + n_c)$ matrix that can be computed from P and Q. In fact a matrix $\tilde{P}$ and a matrix $\tilde{Q}$ have to be found that are positive definite symmetric $(n + n_c) \times (n + n_c)$ matrices such that P and Q are the upper left $n \times n$ subblocks and $\tilde{P} = \tilde{Q}^{-1}$. It is guaranteed that such a $\tilde{P}$ and $\tilde{Q}$ exist as the rank of (5.45) is $n + n_c$ ([47]). Take $\tilde{P}$ and $\tilde{Q}$ e.g.:

$$\tilde{P} = \begin{pmatrix} P & M \\ M^t & -N^\dagger Q M \end{pmatrix}, \quad \tilde{Q} = \begin{pmatrix} Q & N \\ N^t & -M^\dagger P N \end{pmatrix}, \tag{5.61}$$

where $MN^t = I - PQ$ and $M^\dagger$ is the pseudo-inverse of M. This is easily proved.

Probably also closed formulas can be obtained to derive the state space matrices of a controller as e.g. shown in [6] and [52]. However, we prefer

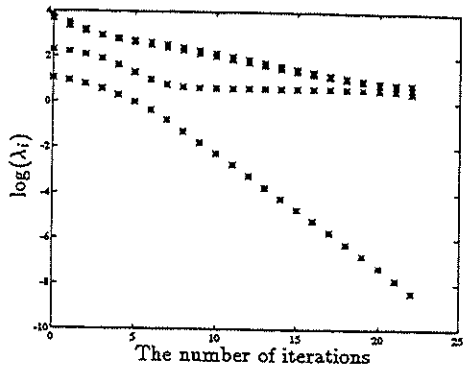

Figure 5.20: The eigenvalues of F_2 as a function of the number of iterations. The order of the controller will be one lower than the order of the plant as one eigenvalue decreases to zero. This implies that the rank of the matrix is only three.

to solve the LMI using convex optimization as it is easier to include other constraints. This is also suggested in [52].

Apply this on the data of the pendulum. First a feasible point has to be found. Once a feasible point is found the rank of (5.45) can be minimized. The evolution of the eigenvalues of (5.45) as a function of the number of iterations is shown in figure 5.20. The rank drops by one. This implies that the order of the controller is one lower than the order of the plant. Thus the system can be stabilized by a first order controller.
The resulting P and Q are:

$$P = \begin{pmatrix} 3.716 & -1.105 \\ -1.105 & 4.947 \end{pmatrix}, \quad Q = \begin{pmatrix} 4.024 & -0.4173 \\ -0.4173 & 0.2786 \end{pmatrix}.$$

Using (5.61) a positive definite $\tilde{P}$ and $\tilde{Q}$ can easily be constructed:

$$\tilde{P} = \begin{pmatrix} 3.716 & -1.105 & -3.640 \\ -1.105 & 4.947 & 1.644 \\ -3.640 & 1.644 & 3.871 \end{pmatrix},$$

$$\tilde{Q} = \begin{pmatrix} 4.024 & -0.4173 & 3.961 \\ -0.4173 & 0.2786 & -0.5107 \\ 3.961 & -0.5107 & 4.199 \end{pmatrix}.$$

The matrices $\tilde{P}$ and $\tilde{Q}$ are each other's inverses.
With $\tilde{P}$ a suitable first order controller K can be computed:

$$\left(\begin{array}{c|c} A_c & B_c \\ \hline C_c & D_c \end{array}\right) = \left(\begin{array}{c|c} -1.517 & 1.408 \\ \hline 0.8592 & 4.039 \end{array}\right).$$

This controller quadratically stabilizes the NLDI, a suitable Lyapunov function is given by $\tilde{P}$. The poles of the nominal closed loop system are stable:

$$-0.69156 \pm 1.0334i, \quad -0.13395.$$

The L_2 gain of the closed loop plant with this stabilizing controller is 14.81. We want to design a controller such that the closed loop L_2 gain is smaller, e.g. a L_2 gain less than 1. In a first stage a λ and μ have to be found such that the rank of

$$F_3 = \left(\begin{array}{cc} \lambda & 1 \\ 1 & \mu \end{array}\right) \geq 0$$

is 1, subject to (5.7), (5.8) and (5.9). The evolution of the eigenvalues of F_3 is shown in figure 5.21. One eigenvalue goes to 0. Thus a solution $\lambda = \mu^{-1}$ exists, such that the other inequalities are satisfied:

$$\lambda = 4.1404e-03, \qquad \mu = 2.4152e+02.$$

When λ and μ are fixed, the order of the controller can also be reduced by minimizing the rank of

$$F_4 = \left(\begin{array}{cc} P & I \\ I & Q \end{array}\right) \geq 0$$

subject to (5.8) and (5.9). When P, Q and the rank of F_4 are known, the order of the controller and the corresponding matrix $\tilde{P}$ can be found.

Finally the controller is designed, solving a convex feasibility problem for a feasible K. If solutions λ, μ, P and Q are found we know from the theory that a solution K has to exist. Usually a whole set of reduced order controllers exists that satisfy the constraints. Extra conditions can also be taken into account.

With λ and μ fixed, the rank of F_4 can be reduced subject to (5.8) and (5.9). The evolution of the eigenvalues of F_4 is shown in figure 5.22. The final rank of F_4 is 3, implying a first order controller. The state space realization of the controller is

$$\left(\begin{array}{c|c} A_c & B_c \\ \hline C_c & D_c \end{array}\right) = \left(\begin{array}{c|c} -5.302 & 35.35 \\ \hline 3.456 & -31.66 \end{array}\right).$$

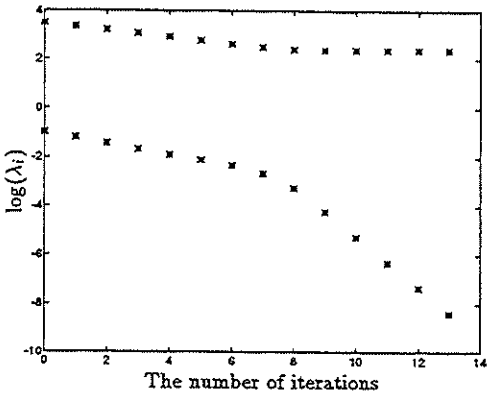

Figure 5.21: The example of the pendulum with varying length. The eigenvalues of F_3 as a function of the number of iterations. One of the eigenvalues goes to zero. This implies that a solution $\lambda = \mu^{-1}$ exists.

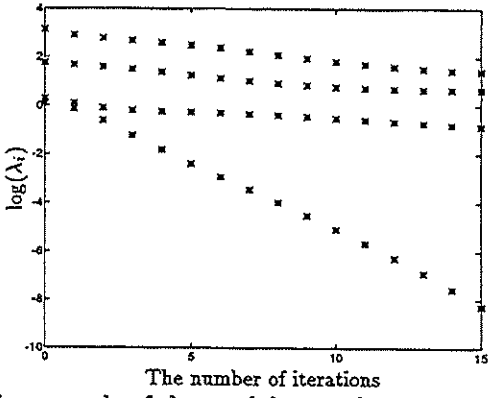

Figure 5.22: The example of the pendulum with varying length. The eigenvalues of F_4 as a function of the number of iterations. One eigenvalue decreases to zero. This implies that the rank of the matrix is only three. The order of the controller will be one lower than the order of the plant.

The actual L_2-gain is 0.1296, which is much lower than the given bound. It is thus possible to reduce the H_∞ norm even lower.

5.10.3 Reduced Order H_2 Design

Consider the following random 5th order plant with state space model:

$$\left(\begin{array}{c|c|c} A & B_w & B_u \\ \hline C_z & D_{zw} & D_{zu} \\ \hline C_z & D_{zw} & D_{zu} \end{array}\right)$$

$$= \left(\begin{array}{ccccc|cc|c} 1.389 & -0.7673 & 1.874 & 0.3654 & -0.3664 & 0.3961 & 1.944 & 0.5553 \\ 1.364 & 0.3644 & 0.1724 & -0.1987 & 1.377 & -0.5087 & -1.522 & -0.3242 \\ 0.6582 & -0.3979 & 1.272 & -1.39 & -0.7975 & -0.2683 & 1.939 & 1.339 \\ 0.4913 & 0.8643 & -0.03534 & 0.2293 & -0.9367 & -1.082 & -0.8958 & 1.222 \\ 0.8007 & -0.1776 & -1.501 & 0.2712 & -0.002433 & 2.014 & -0.3042 & -1.596 \\ \hline -1.068 & -0.7599 & 0.421 & -0.4334 & 0.7063 & 0 & 0 & -0.1406 \\ 0.2279 & 0.1399 & -0.629 & -1.648 & 0.4917 & 0 & 0 & 0.2449 \\ \hline -1.017 & -0.7481 & 1.395 & -2.015 & -1.555 & 0 & 0 & -0.2675 \end{array}\right).$$

This plant is unstable. It has two disturbance inputs and one controlled output. The controller acts on one input and takes its measurements from two outputs. The matrices D_{zw} and D_{yw} are zero, satisfying the constraints for reduced order H_2 design.

From a convex optimization problem we know that the lowest attainable H_2 norm is 9.169. The goal is to obtain a reduced order controller such that the closed loop H_2 norm is only 2% worse than the optimal one. Therefore take $\alpha = 1.02 \times 9.169 = 9.353$.

First a feasible point has to be found that satisfies the constraints (5.50) to (5.52). Once a suitable initial point is found the order of the controller can be reduced by minimizing the rank of

$$F_5 = \begin{pmatrix} P & I \\ I & Q \end{pmatrix} \geq 0,$$

subject to (5.50), (5.52) and (5.53). The eigenvalues of F_5 in different iterations are shown in figure 5.23. Two eigenvalues go to zero. The order of the controller is thus two lower than the order of the plant: a $3th$ order controller. From the resulting P and Q, $\tilde{P}$ can be constructed:

$$\tilde{P} = \begin{pmatrix} P & M \\ M^t & -N^\dagger Q M \end{pmatrix}.$$

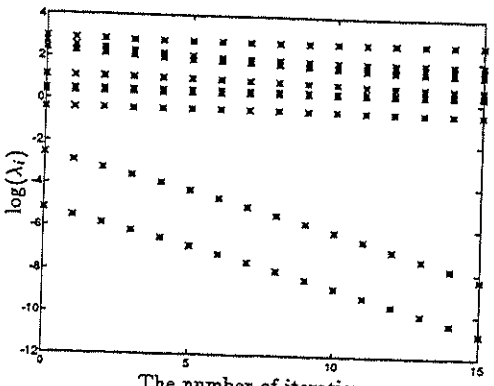

Figure 5.23: The eigenvalues of F_5 as a function of the number of iterations. Two eigenvalues decrease to 0. The order of the controller will be two lower than the order of the plant. A 3rd order controller satisfies the constraints.

To compute the state space matrices of the reduced order controller, $\tilde{P}$ is substituted in (5.54) and a convex feasibility problem is solved. A controller the satisfies the constraints is:

$$K = \left(\begin{array}{c|c} A_c & B_c \\ \hline C_c & D_c \end{array}\right) = \left(\begin{array}{ccc|cc} 29.63 & 3.242 & -0.1267 & -4.855 & -3.903 \\ 33.91 & 3.593 & -0.0476 & -4.987 & -4.339 \\ 30.96 & 4.742 & -0.7086 & -4.894 & -4.358 \\ \hline -90.6 & -9.462 & -0.3881 & 14.7 & 11.37 \end{array}\right).$$

The resulting closed loop is stable. The poles are:

$$\begin{array}{ll} -3.6756e+00 & \pm 5.9879e+00i, \\ -5.8290e-01 & \pm 2.2715e+00i, \\ -1.0505e+00 & \pm 3.7202e-01i, \\ -2.0274e-02, & -9.3683e-01. \end{array}$$

The H_2 norm of the closed loop with the reduced order controller is 9.307. This is, of course, higher than the optimal H_2 norm, but is lower than the bound α.

5.10.4 The Frisch Scheme

In this section some numerical examples are shown for the Frisch scheme. First 2×2 examples are solved, to illustrate some facts graphically.

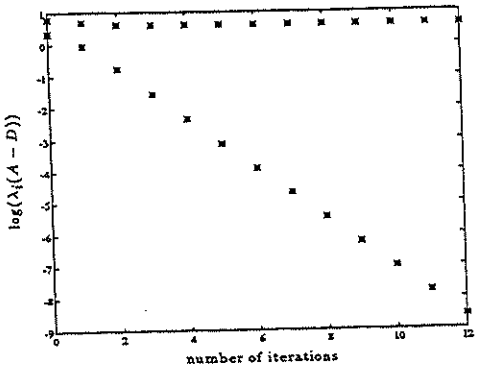

Figure 5.24: The logarithm of the eigenvalues of $A - D$ for a simple 2×2 example as a function of the number of iterations. One eigenvalue decreases to 0. The resulting rank of $A - D$ is thus 1. Note how the eigenvalue reduces linearly on this logarithmic plot.

Consider the following example:

$$A = \begin{pmatrix} 8 & 2 \\ 2 & 7 \end{pmatrix}.$$

The lowest possible rank for $A - D$ is 1. The rank minimization algorithm starts at the analytic center of $A - D > 0$ and $D > 0$. The evolution of the eigenvalues is shown in figure 5.24. If D is represented by:

$$D = \begin{pmatrix} x & 0 \\ 0 & y \end{pmatrix}.$$

The steps of the algorithm can be represented in an xy-plane. This is shown in figure 5.25. Also the boundaries of the feasible region are plotted. The boundary of the feasible region consists of the axes $x = 0$ and $y = 0$. The curved line represents the boundary where $\det(A - D) = 0$. All the points on that boundary represent matrices of rank 1. The algorithm starts in the analytic center of the feasible region: $(3.49, 3.06)$. In a few steps the algorithm moves to a singular point on the boundary: $(5.86, 5.13)$.

In figure 5.25 also the paths followed by the optimization algorithm are shown starting from 40 points around the analytic center. All the paths tend to the boundary of the feasible region where the rank of $A - D$ equals 1.

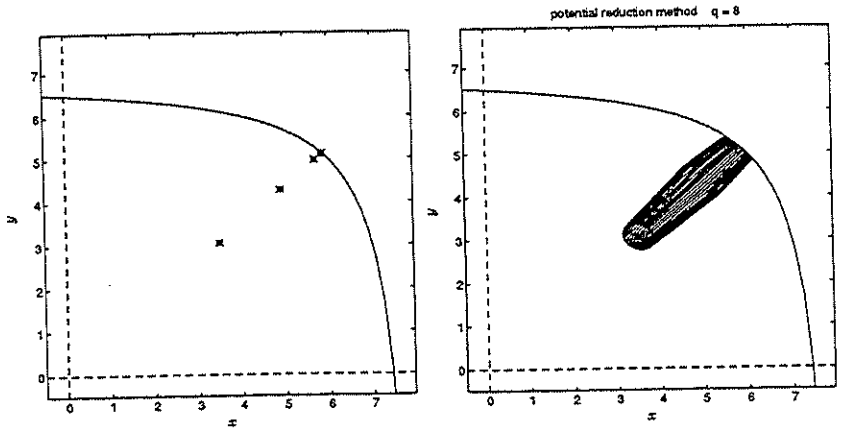

Figure 5.25: The figure on the left shows the steps taken by the algorithm starting from the analytic center of the feasible region. The curved line is the boundary where $A - D$ is rank deficient. The algorithm quickly moves from the analytic center of the feasible region towards the boundary. The right figure shows the paths followed starting from 40 points around the analytic center. All the paths move to the boundary where the rank of $A - D$ equals 1.

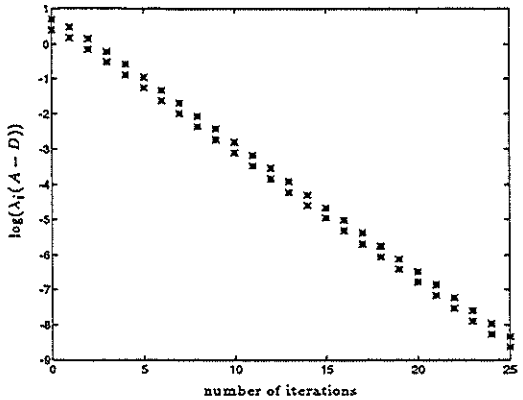

Figure 5.26: The logarithm of the eigenvalues for a special 2×2 example as a function of the number of iterations. Two eigenvalues decrease to 0. The resulting rank of $A - D$ is thus 0. Remark how the eigenvalues reduce linearly on this logarithmic plot.

In the previous example, all the rank deficient matrices had rank 1. Consider the following 2×2 matrices where the minimal possible rank is 0:

$$A = \begin{pmatrix} 10 & 0 \\ 0 & 5 \end{pmatrix}.$$

Again the algorithm is started from the analytic center of the feasible region. In this case two eigenvalues tend to 0. The different steps converge to the intersection of the two boundaries $x = 10$ and $y = 5$ where the rank of $A - D$ is 0. This is shown in figures 5.26 and 5.27.

In figure 5.27 also the paths followed by the optimization algorithm are shown starting from 40 points around the analytic center of the feasible region. All the paths tend to the corner point of the boundary of the feasible region where the rank of $A - D$ equals 0.

The method is not restricted to small examples. Consider the following 10×10 example:

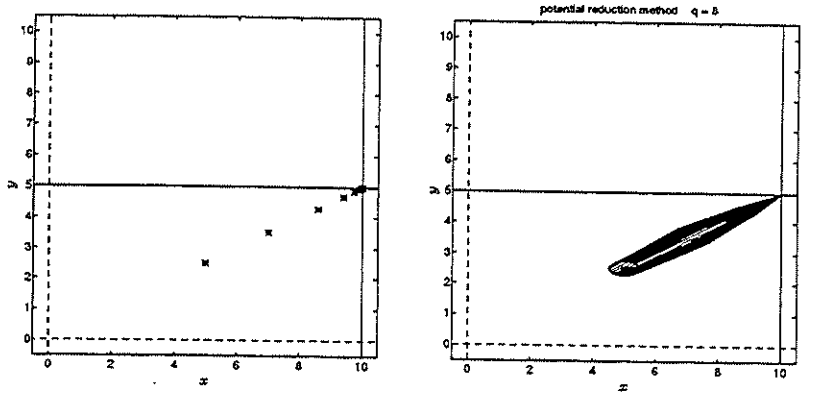

Figure 5.27: The left figure shows the steps taken by the algorithm starting from the analytic center of $A - D > 0$ and $D > 0$. The point with the lowest rank of $A - D$ is $(10, 5)$. The algorithm moves quickly towards that point. The right figure shows the paths followed by the optimization algorithm starting from 40 points around the analytic center. All the paths move to the corner point of the boundary where the rank of $A - D$ is 0.

$$A = \begin{pmatrix}
3.67 & 1.78 & -1.68 & 1.30 & -1.64 & 2.47 & 0.25 & 4.01 & 2.13 & -0.35 \\
1.78 & 1.57 & -0.22 & -0.02 & -0.80 & 0.91 & -0.18 & 1.47 & 0.74 & 0.93 \\
-1.68 & -0.22 & 2.82 & -1.43 & 0.71 & -0.71 & -0.47 & -2.13 & -1.87 & 2.32 \\
1.30 & -0.02 & -1.43 & 1.95 & -0.66 & 1.27 & 0.45 & 2.15 & 1.25 & -1.48 \\
-1.64 & -0.80 & 0.71 & -0.66 & 1.76 & -1.42 & -0.14 & -2.07 & -0.94 & 0.04 \\
2.47 & 0.91 & -0.71 & 1.27 & -1.42 & 3.65 & 0.35 & 3.92 & 1.11 & 0.44 \\
0.25 & -0.18 & -0.47 & 0.45 & -0.14 & 0.35 & 0.70 & 0.55 & 0.35 & -0.61 \\
4.01 & 1.47 & -2.13 & 2.15 & -2.07 & 3.92 & 0.59 & 6.45 & 2.49 & -0.78 \\
2.13 & 0.74 & -1.87 & 1.25 & -0.94 & 1.11 & 0.35 & 2.49 & 1.88 & -1.56 \\
-0.35 & 0.93 & 2.32 & -1.48 & 0.04 & 0.44 & -0.61 & -0.78 & -1.56 & 3.58
\end{pmatrix}.$$

This matrix is a positive definite matrix of full rank. The matrix is constructed such that the minimal rank for the Frisch scheme is known. A is constructed as $A = BB^t + D_1$, with $B \in \mathbb{R}^{10 \times 3}$, a random matrix. D_1 is a diagonal matrix with strictly positive elements. The minimal obtainable rank of $A - D$ is thus 3. The eigenvalues as a function of the iterations are shown in figure 5.28. Seven eigenvalues decrease. The rank of the resulting matrix is thus 3. The optimal D is exactly D_1. Note that this is not a *typical* order 10 example, since the Wilson-Lederman bound for $n = 10$ equals 6.

As a last example the evolution of the eigenvalues for a random 7×7 matrix A are shown in figure 5.29:

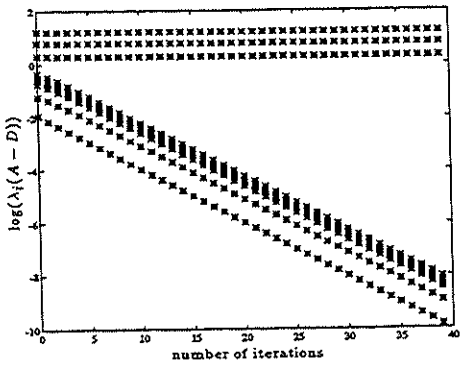

Figure 5.28: The logarithm of the eigenvalues of $A - D$ for an artificially constructed 10×10 example as a function of the number of iterations. Seven eigenvalues decrease to 0. The resulting rank of $A - D$ is thus 3.

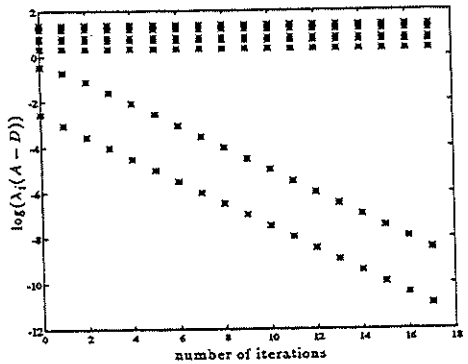

Figure 5.29: The logarithm of the eigenvalues of $A - D$ for a random 7×7 example as a function of the number of iterations. Two eigenvalues decrease to 0. The resulting rank of $A - D$ is thus 5.

$$A = \begin{pmatrix} 6.157 & -5.434 & 4.433 & -0.4415 & -1.17 & 1.227 & -3.578 \\ -5.434 & 13.45 & -4.839 & 1.944 & 4.976 & -1.737 & 2.56 \\ 4.433 & -4.839 & 9.128 & -5.036 & -2.579 & -2.126 & 0.9752 \\ -0.4415 & 1.944 & -5.036 & 6.401 & 3.822 & 4.124 & -0.6081 \\ -1.17 & 4.976 & -2.579 & 3.822 & 6.669 & 3.881 & 0.2779 \\ 1.227 & -1.737 & -2.126 & 4.124 & 3.881 & 7.352 & -1.911 \\ -3.578 & 2.56 & 0.9752 & -0.6081 & 0.2779 & -1.911 & 6.122 \end{pmatrix}$$

Two eigenvalues decrease. The resulting rank of $A - D$ is 5. This is higher than the Wilson-Lederman bound, which is 4 for a 7×7 matrix. This is correct as the Wilson-Lederman bound is only a generic *lower* bound. The resulting elements of D are:

$$D = \text{diag} \begin{pmatrix} 0.008258 & 2.475 & 0.0109 & 0.01552 & 0.2606 & 0.8981 & 0.01883 \end{pmatrix}.$$

5.10.5 The Ventilator Setup

As a last example an H_2 and an H_∞ controller are designed for the ventilator. The controllers obtained with classical techniques are shown in the introduction. These controllers are usually of high order. We will try to design low order controllers without losing too much of the closed loop performance. To design low order controllers, the potential reduction method is used.

Consider first the H_∞ controller. The lowest possible H_∞ norm is 159.66. We will try to design a low order controller such that the H_∞ norm is less than 2% higher: $\gamma = 162.9$. The eigenvalues of the matrix

$$F_6 = \begin{pmatrix} R & \gamma^{-1} I \\ \gamma^{-1} I & S \end{pmatrix}$$

as a function of the number of iterations is shown in figure 5.30. Only one eigenvalue decreases to 0. This implies that with the obtained P and Q matrices, the order of the controller is only one lower than the order of the plant. The obtained controller is a fourth order controller:

$$\left(\begin{array}{c|c} A_c & B_c \\ \hline C_c & D_c \end{array}\right) = \left(\begin{array}{cccc|c} 154.7 & -1.307 & 2.568 & -2.005 & 1554 \\ 3.015e+04 & -254.9 & 500.1 & -389.2 & 3.025e+05 \\ -1.555e+04 & 131.5 & -258 & 200.8 & -1.561e+05 \\ -1.731e+04 & 146.3 & -287.1 & 223 & -1.737e+05 \\ \hline 104.1 & -0.8793 & 1.728 & -1.347 & 1045 \end{array}\right).$$

The H_∞ norm of the closed loop with this controller is 160.5. In this case, the order of the resulting low order controller is not lower than the order of

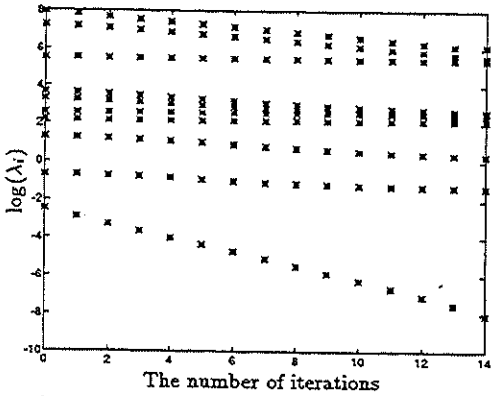

Figure 5.30: The eigenvalues of F_6 as a function of the number of iterations to design a low order H_∞ controller for the ventilator setup. One eigenvalue decrease to 0. The order of the controller will be one lower than the order of the plant. A $4th$ order controller satisfies the constraints.

the optimal H_∞. However, it is one lower than the order of the corresponding suboptimal H_∞ controller computed with the standard techniques.

To compute a reduced order H_2 controller, the plant has to be modified slightly. The disturbance input of the measurement is removed. This makes it hard to compare the results with the results of [33]. The lowest possible H_2 norm of the closed loop is 0.8681. We want to design a controller such that the H_2 norm is less than $\alpha = 0.9549$. The formulas of a preceeding section are used. The eigenvalues of

$$F_7 = \begin{pmatrix} P & I \\ I & Q \end{pmatrix}$$

are shown in figure 5.31. Again only one eigenvalue decreases to 0. The corresponding order of the controller is 4. A feasible fourth order controller is:

$$\left(\begin{array}{c|c} A_c & B_c \\ \hline C_c & D_c \end{array}\right) = \left(\begin{array}{cccc|c} -181.9 & -0.986 & 0.1955 & 32.31 & 1.335e+05 \\ -305.1 & -1.805 & 0.225 & 38.05 & 2.241e+05 \\ 176.1 & 0.9825 & -0.1785 & -21.96 & -1.294e+05 \\ 518.6 & 2.81 & -0.5599 & -92.19 & -3.808e+05 \\ \hline -186 & -1.055 & 0.1654 & 23.13 & 1.366e+05 \end{array}\right).$$

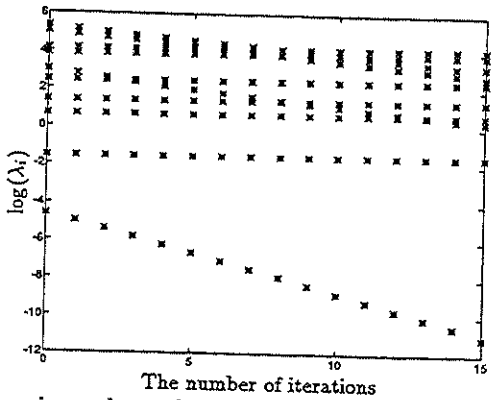

Figure 5.31: The eigenvalues of F_7 as a function of the number of iterations in the design of a low order H_2 controller for the ventilator setup. One eigenvalue decreases to 0. The order of the controller will be one lower than the order of the plant. A $4th$ order controller satisfies the constraints.

The H_2 norm of the closed loop with this controller is 0.9516. The order of this controller is one less than the order of the optimal H_2 controller.

Instead of the potential reduction method, the inverted analytic centering method has also been used with $r = 1$ and $r = 0.125$. However, no controllers of lower order have been obtained using the inverted analytic centering method.

5.11 Conclusions and Remarks

In this section algorithms are proposed to solve minimum rank problems involving linear matrix inequalities. These problems arise in different fields in control and identification. Several examples are given: such as the design of reduced order H_∞ controllers, the design of controllers for norm bounded linear differential inclusions. In this chapter, we also showed how the Frisch scheme and the design of a low order H_2 controller for LTI systems, can be cast in this framework. Many more examples exist where these problems arise: such as the design of gain scheduled controllers, and controllers that bound the reachable sets ([14]).

Two algorithms are proposed. The first one is based on the inversion of the analytic centering method for convex optimization. The second is

an extension of the potential reduction method also for convex optimization over a set of linear matrix inequalities. In both cases a trajectory is followed from inside the feasible set to the boundary which consists of the reduced rank solutions. The minimum rank problems are not convex. This is a serious disadvantage. When a reduced rank solution is found, it is never sure that it is the minimal feasible rank. However, in most cases reduced rank solutions are obtained.

For both algorithms it is shown how they can be implemented. The updating direction can be computed via a least squares problem. The feasibility of the step can be ensured. The number of decreasing eigenvalues can be estimated. Based on that estimate a stopping criterion is suggested. It is also shown that the eigenvalues decrease almost linearly on a logarithmic scale. For the potential reduction method a lower bound on q is derived. It is shown that the potential reduction method is better than the inverted centering method. It is faster and the path are smoother. It is also possible to define better stopping criteria.

In Chapter 3 we also looked at a problem where reduced rank solutions of an affine matrix function have to be found. However, the problem differs from the problems studied in this chapter. The solution in Chapter 3 does not need to be symmetric positive semi definite. A rank reduced solution can be found for any square matrix. However in Chapter 3 the rank drops only by 1. While in this chapter we look for a minimum rank solution. The rank can drop by more than 1. Furthermore there are no extra constraints that have to be satisfied in the problem of Chapter 3.

Appendix 1: An Example of the Least Squares Solution near the Boundary

In this appendix we illustrate the conjecture in section 5.2.2 that to minimize $\|(1-q)I + F^{-1}V_f\|_F^2$, V_f is determined such that as much eigenvalues of $F^{-1}V_f$ as possible become $q-1$. This step will also try to maximize the corank of $F(x)$.
Consider the following simple problem:

$$\begin{cases} 2-x-y & > & 0 \\ x & > & 0 \\ y & > & 0. \end{cases}$$

Find a point of minimal rank such that

$$\min \text{Rank} \begin{pmatrix} 2-x-y & & \\ & x & \\ & & y \end{pmatrix} \geq 0.$$

Suppose we start in the feasible point $x_0 = (.1, 1.8)$. The nearest point of rank 1 is $(0,2)$. For q we take $q = 2$.

$$F(x_0) = \begin{pmatrix} .1 & & \\ & .1 & \\ & & 1.8 \end{pmatrix}$$

$$F(x_0)^{-1}V = \begin{pmatrix} 10 & & \\ & 10 & \\ & & .55 \end{pmatrix} \left[v_1 \begin{pmatrix} -1 & & \\ & 1 & \\ & & 0 \end{pmatrix} + v_2 \begin{pmatrix} -1 & & \\ & 0 & \\ & & 1 \end{pmatrix} \right].$$

The following least squares problem has to be solved:

$$\min_{v_1, v_2} (-1 + 10v_1 + 10v_2)^2 + (-1 - 10v_1)^2 + (-1 - 0.55v_2)^2$$

$$\begin{aligned} \frac{\partial \mathcal{L}}{\partial x} &: 10(-1 + 10v_1 + 10v_2) - 10(-1 - 10v_1) = 0 \\ \frac{\partial \mathcal{L}}{\partial y} &: 10(-1 + 10v_1 + 10v_2) - 0,55(-1 - 0.55) = 0 \end{aligned}$$

or

$$\begin{cases} 200v_1 + 100v_2 &= 0 \\ 100v_1 + 100.25v_2 &= 9.45. \end{cases}$$

The solution is $v_1 \simeq -0.1$ and $v_2 \simeq 0.2$. This step would take us exactly to the point of minimal rank.
We also claimed that as the corank is 2 in that point, there will be two eigenvalues of $F^{-1}V$ that will be approximately $1-q$, and one that is approximately 0:

$$\begin{aligned} \lambda_1 &= -10v_1 - 10v_2 \simeq -1 \\ \lambda_2 &= 10v_1 \simeq -1 \\ \lambda_3 &= 0.55v_2 \simeq 0.1. \end{aligned}$$

The observation seems to hold well in this case.

Chapter 6

Conclusions

In this thesis we present algorithms to analyze and design robust controllers. In the first part some topics in system analysis are discussed. It is shown how directional aspects of two transfer matrices relative to one another, can be studied. An algorithm is described to compute the 2-parameter margin. The second part deals with controller design. It is shown how a mixed H_2/H_∞ controller can be designed by separating the H_2 and the H_∞ part. Finally we presented algorithms to solve minimum rank problems involving linear matrix inequalities. This problem occurs in the design of reduced order controllers.

In Chapter 2 directional aspects of two transfer matrices relative to one another are studied. It is shown that the quotient singular value decomposition (QSVD) is the appropriate tool. The extremal directions are given by it. It is also shown how to represent directional aspect of transfer matrices graphically. It is well-known how this can be done for one transfer matrix in the output space. We show how the directional aspects of one transfer matrix can be represented in the input space and how to represent relative directional aspects of two transfer matrices.
In the case of two transfer matrices two situations can occur:

1. The two transfer matrices have the same input and different outputs.
2. The two transfer matrices have separate inputs and their outputs are added.

In the first case the relative output energies are studied, given a certain input direction. In the second case the proportion of the input energies is studied

for signals that generate the same output direction. So, it can be determined what transfer matrix has the largest influence on the output.

To quantify the relative directional aspects two new norms are defined: the QH_2 norm and the QH_∞ norm. It are extensions of the classical H_2 norm and H_∞ norm. It is shown how they can be computed. The formulas for the QH_2 norms are derived. A level set algorithm to compute the QH_∞ norm is also developed.

It is shown how these norms can be used to study signal-to-noise ratios at different frequencies. In this thesis we only use them for analysis. However, based on the defined norms, a controller could also designed that minimizes the norms. In this way controllers could be designed that minimize signal-to-noise ratios, if necessary by introducing appropriate directional weighting functions.

The QSVD is only one generalization of the singular value decomposition to two matrices. It is well-known that there exist infinitely many generalizations. Norms between transfer matrices could also be based on these other generalizations. However, we do not know how to interprete these norms.

In Chapter 3 systems with real parameters are studied. The entries of the state space matrices are assumed to be polynomially or rationally dependent on the parameters. In [44], [45] and [46], the q-parameter stability margin and the q-parameter performance margin are defined. The q-parameter stability margin is the largest q-norm of the parameter vector for which stability of the system is ensured. The q-parameter performance margin is the largest q-norm of the parameter vector for which a given H_2-performance is ensured. In [46] a quadratic convergent algorithm is presented to find the 2-parameter margins. However, the number of parameters is restricted to two. In Chapter 3 it is shown how the 2-parameter margins can be computed, when there are more than two parameters. An algorithm that was developed to solve structured total least squares problems ([35]), can be used.

In [44] and [46], it is shown how the parameter stability margins and the parameter performance margins can be reformulated as determinantal problems. The parameter margin is the smallest norm of the parameter vector for which the determinant becomes zero. The computation of the 2-parameter margins is similar to problems in structured total least squares. In [35] it is shown how they can be transformed into a so-called non-linear singular value problem. Algorithms based on the inverse power method are suggested to solve this problem. The advantage of this algorithms is that the number of parameters is not restricted to two. However, convergence to the global minimum is not guaranteed. The convergence properties of the algorithm should still be studied more carefully.

In Chapter 4 the general mixed H_2/H_∞ control design problem is studied. We propose to design a controller considering the H_∞ constraint and the H_2 optimization separately. It is well-known that there exists a whole set of controllers that solve the H_∞ problem ([56]). This set can be parameterized using a controller generator and a stable, H_∞ norm bounded parameter. The idea is to compute the controller generator and attach it to the original plant. Then we look in the set of admissible controllers to find the controller that optimizes the H_2 norm. This is an optimization over the stable, H_∞ norm bound parameter. Unfortunately, no analytic solution has been found for this problem. The optimum has to be computed numerically. Necessary conditions for the solution are given.

For further research we suggest to look for sufficient conditions for the problem and for a better numerical optimization method.

In Chapter 5 algorithms are suggested for solving minimum rank problems involving linear matrix inequalities. The rank of a LMI $F(x) \geq 0$ has to be minimized subject to another LMI $C(x) \geq 0$. These problems arise in the design of reduced order controllers. It is shown that the minimum rank problems are NP-hard. Two heuristic algorithms are suggested to solve these problems. In many practical cases reduced rank solutions are obtained. However, we do not claim that the minimal rank is always found. Although the minimum rank problem is not convex, the algorithms are based on concepts of convex optimization involving linear matrix inequalities.

The first method is based on an inversion of the analytic centering method. Start at the analytic center and trace back the steepest path to the boundary of the feasible set. The boundary consists of the rank reduced solutions. It is also shown how the constraints can be included in the optimization. The search direction can be computed by solving a least squares problem. Feasibility of the step is ensured by an appropriate damping factor. The second method is an extension of the potential reduction method for convex optimization. It is shown how the objective function can be linearized such that the theory of Nesterov and Nemirovsky can be applied. As for the inverted centering method, the search direction can be computed solving a least squares problem. The feasibility of the step is ensured by an appropriate damping factor. The corank of the resulting solution can be estimated. Based on the corank a stopping criterion is suggested. A lower

bound for the parameter q in the potential reduction method is derived. Finally it is shown that the eigenvalues of $F(x)$ decrease almost linearly to zero.

Minimum rank problems do not appear only in control design problems. The Frisch scheme can also be cast as a minimum rank problem. We think that H_∞ identification via Nevanlinna-Pick interpolation can also be formulated as a minimum rank problem. This still has to be looked at more carefully. Probably many more problems in other domains than control and identification, can be cast as minimum rank problems.

Bibliography

[1] B.D.O. Anderson and Y. Liu, "Controller reduction: concepts and approaches," *IEEE Trans. Autom. Contr.*, **Vol. 34**, pp. 802-812, 1989.

[2] G.J. Balas, J.C. Doyle, K. Glover, A. Packard and R. Smith, *μ-Analysis and Synthesis Toolbox*, The MathWorks, South-Natick, MA, 1991.

[3] B.R. Barmish, P.P. Khargonekhar, Z.C. Shi and R. Tempo, "Robustness margin need not be a continuous function of the problem data," *Systems & Control Letters*, **Vol. 15**, pp. 91-98, 1990.

[4] J.R. Bar-on and E.A. Jonckheere, "Gain margins for multivariable control systems," *Proc. CDC*, Honolulu, Hawaii, pp. 340-346, 1990.

[5] C. Barratt and S. Boyd, "Example of exact trade-offs in linear controller design," *IEEE Control Systems Magazine*, pp. 46-52, 1989.

[6] G. Becker, A. Packard, D. Philbrick and G. Balas, "Control of parametrically-dependent linear systems: A single quadratic Lyapunov approach", *Proc. ACC93*, San Francisco, pp. 2795-2799, June 1993.

[7] D.S. Bernstein, "Robust static and dynamic output-feedback stabilization: deterministic and stochastic perspectives," *IEEE Trans. Autom. Contr.*, **Vol. 32**, pp. 1076-1084, 1987.

[8] D.S. Bernstein and W.M. Haddad, " The optimal projection equations with Petersen-Hollot bounds: robust stability and performance via fixed-order dynamic compensation for systems with structured real-valued parameter uncertainty," *IEEE Trans. Autom. Contr.*, **Vol. 33**, pp. 578-582, 1988.

[9] D.S. Berstein and W.M. Haddad, "LQG control with an H_∞ performance bound: A Riccati equation approach," *IEEE Trans. Autom. Contr.*, **Vol. 34**, pp. 293-305, 1989.

[10] S. Boyd, V. Balakrishnan, C.H. Barratt, N.M. Kraishi, X. Li, D.G. Meyer and S.A. Norman, "A new CAD method and associated architectures for linear controllers," *IEEE Trans. Autom. Contr.*, **Vol. 33**, pp. 268-283, 1988.

[11] S. Boyd and V. Balakrishnan, "A regularity result for the singular values of a transfer matrix and a quadratically convergent algorithm for computing its L_∞-norm", *System & Control Letters*, **Vol. 15**, pp. 1-7, 1990.

[12] S. Boyd and S. Barratt, *Linear Control Design: Limits of Performance*, Prentice-Hall, Englewood Cliffs, 1991.

[13] S. Boyd and L. El Ghaoui, "Method of centers for minimizing generalized eigenvalues," *Linear Algebra and Applications*, **Vol. 188-189**, pp. 63-113, 1993.

[14] S. Boyd, L. El Ghaoui, E. Feron and V. Balakrishnan, *Linear Matrix Inequalities in Systems and Control Theory*, Stanford University, June 1993 draft.

[15] S. Boyd and L. Vandenberghe, "Notes on Interior-Point Methods for Positive-Definite Programming," Lecture Notes, Tutorial Workshop on Convex Optimization Techniques in Robust Control, CDC 1993, San Antonio.

[16] R.D. Braatz, P.M. Young, J.C. Doyle and M. Morari, "Computational complexity of μ calculation," *Proc. ACC93*, San Francisco, pp. 1682-1683, 1993.

[17] F.M. Callier and C.A. Desoer, *Multivariable Feedback Systems*, Springer-Verlag, New York, 1982.

[18] J. Chen, C.N. Nett and M.K.H. Fan, "Worst-case system identification in H_∞: Validation of apriori information, essentially optimal algorithms and error bounds," *Proc. ACC92*, Chicago, IL, pp. 251-257, 1992.

[19] Y. Cheng and B. De Moor, "A Multidimensional Realization Algorithm for Parametric Uncertainty Modeling and Multiparameter Margin Problems," ESAT-SISTA report 92-50, Dept. Elec. Eng. K.U.Leuven, Belgium, 1993. Accepted for publication in International Journal of Control.

[20] J. David and B. De Moor, "The quotient SVD and directional aspects of two transfer matrices", *Proc. CompEuro92*, The Hague, pp. 316-321, 1992.

[21] J. David, B. De Moor and J. Vandewalle, "The quotient SVD and H_∞ norms," *Proc. ACC92*, Chicago, pp. 2215-2216, June 1992.

[22] J. David and B. De Moor, "H_2 controller design with an H_∞ bounded controller," *Proc. ACC93*, San Francisco, pp. 248-249, June 1993.

[23] J. David and B. De Moor, "On the calculation of the Euclidean parameter margin," *Proc. ECC93*, Groningen, pp. 380-384, June 1993.

[24] J. David and B. De Moor, "On solving minimum rank problems," ESAT-SISTA report 93-6, Dept. Elec. Eng., K.U.Leuven, 1993.

[25] J. David and B. De Moor, "The opposite of analytic centering for solving minimum rank problems in control and identification," *Proc. 32nd CDC*, San Antonio, Texas, pp. 2901-2902, 1993.

[26] J. David and B. De Moor, "Computing solutions of the Frisch scheme using a potential reduction method," ESAT-SISTA report 1993-54I, Dept. Elec. Eng., K.U.Leuven, 1993. Accepted for IFAC SYSID'94, Copenhagen.

[27] J. David and B. De Moor, "Designing reduced order output feedback controllers using a potential reduction method," ESAT-SISTA report 1993-55I, Dept. Elec. Eng., K.U.Leuven, 1993. Accepted for 1994ACC, Baltimore.

[28] B. De Moor, *Mathematical concepts and techniques for modelling of static and dynamic systems*, Ph.D. thesis, Dept. Elec. Eng., K.U.Leuven, 1988.

[29] B. De Moor, J. Staar and J. Vandewalle, "Oriented energy and oriented signal-to-signal ratio concepts in the analysis of vector sequences and time series," *SVD AND SIGNAL PROCESSING: Algorithms, Applications and Architectures*, E.F. Deprettere (Editor), Elsevier Science Publishers B.V. (North Holland), pp. 209-232, 1988.

[30] B. De Moor and G. Golub, "Generalized singular value decompositions: a proposal for a standardized nomenclature," ESAT-SISTA Re-

port 1989-10, Dept. Elec. Eng., Katholieke Universiteit Leuven, Belgium, 1989. (Also Numerical Analysis Project Manuscript NA-89-04, Department of Computer Science, Stanford University.)

[31] B. De Moor and S. Boyd, "Analytic properties of singular values and vectors," ESAT-SISTA Report 1989-28, Dept. Elec. Eng., Katholieke Universiteit Leuven, Belgium, 1989.

[32] B. De Moor, and H. Zha, "A tree of generalizations of the ordinary singular value decomposition," *Linear Algebra and Applications*, special issue on Canonical Forms of Matrices, **147**, 469-500, 1991.

[33] B. De Moor, J. David, J. Vandewalle, M. De Moor and D. Berckmans, "Trade-offs in linear control system design: A practical example," *Optimal Control Applications & Methods*, **Vol. 13**, pp. 121-144, 1992.

[34] B. De Moor and J. David, "Total linear least squares and the algebraic Riccati equation," *System & Control Letters*, **Vol. 18**, 5, pp. 329-337, 1992.

[35] B. De Moor, "Structured total least squares and L_2 approximation problems", Special Issue of *Linear Algebra and its Applications* on Numerical Linear Algebra in Systems & Control (eds: Van Dooren, Ammar, Nichols, Mehrmann), **Vol. 188-189**, pp. 163-207, 1993.

[36] J.C. Doyle, "Guaranteed margins for LQG regulators," *IEEE Trans. Autom. Contr.*, **Vol. 23**, pp. 756-757, 1978.

[37] J.C. Doyle and G. Stein, "Multivariable feedback design: Concepts for a classical/modern synthesis," *IEEE Trans. Autom. Contr.*, **Vol. 26**, pp. 4-16, 1981.

[38] J.C. Doyle, "Analysis of feedback systems with structured uncertainties," *IEE Proceedings*, Part D, **Vol. 129**, pp. 242-250, 1982.

[39] J. Doyle, *Advances in Multivariable Control,* Lecture Notes at ONR/Honeywell Workshop. Minneapolis, MN, Oct. 8-10, 1984.

[40] J.C. Doyle, K. Glover, P.P. Khargonekar and B.A. Francis, "State-space solutions to standard H_2 and H_∞ control problems,", *IEEE Trans. Autom. Contr.*, **Vol. 34**, pp. 831-847, 1989.

[41] J.C. Doyle, K. Zhou, and B. Bodenheimer, "Optimal control with mixed H_2 and H^∞ performance objectives," *Proc. ACC89*, Pittsburgh, PA, pp. 2065-2070, 1989.

[42] J. Doyle, A. Packard and K. Zhou, "Review of LFTs, LMIs and μ", *Proc. CDC91*, Brighton, England, pp. 1227-1232, 1991.

[43] J.C. Doyle, B.A. Francis and A.R. Tannenbaum, *Feedback Control Theory*, MacMillan Publishing Company, New York, 1992.

[44] L. El Ghaoui, *Robustness of Linear Systems to Parameter Variations*, Ph.D. thesis, Stanford University, 1990.

[45] L. El Ghaoui, "A measure of parametric robustness in H_2 performance", *Proc.* 1st *ECC*, Grenoble, France, pp. 2278-2282, 1991.

[46] L. El Ghaoui, "Fast computation of the largest stability radius for a two-parameter linear system", *IEEE Trans. Autom. Contr.*, **Vol. 37**, pp. 1033-1037, 1992.

[47] L. El Ghaoui and P. Gahinet, "Rank minimization under LMI constraints: A framework for output feedback problems", *Proc. ECC93*, Groningen, The Netherlands, pp. 1176-1179, 1993.

[48] L. El Ghaoui, personal communication, 1993.

[49] B.A. Francis, *A course in H_∞ control theory,* (Lecture Notes in Control and Information Sciences, Vol. 88), Springer-Verlag, New York, 1987.

[50] J.S. Freudenberg, "Analysis and design for ill-conditioned plants. Part 1. Lower bounds on the structured singular value", *Int. J. Control*, **Vol. 49**, pp. 851-871, 1989.

[51] P. Gahinet, "A convex parameterization of H_∞ suboptimal controllers," Proc. 31th CDC, Tucson, Arizona, pp. 937-942, 1992.

[52] P. Gahinet and P. Apkarian, "State-space H_∞ control: A complete solution via convex Riccati inequalities", submitted to Special Issue on H_∞ Control of *Int. Jour. of Robust, Nonlinear Control*, 1992.

[53] M.R. Garey and D.S. Johnson, *Computers and Intractability. A Guide to the Theory of NP-Completeness*, W.H. Freeman and Company, San Francisco, 1979.

[54] T.T. Georgiou and M.C. Smith, "Optimal robustness in the gap metric," *IEEE Trans. Autom. Contr.*, **Vol. 35**, pp. 673-686, 1990.

[55] K. Glover, "All optimal Hankel-norm approximations of linear multivariable systems and their L_∞-error bounds," *Int. J. Control*, **Vol. 39**, pp. 1115-1193, 1984.

[56] K. Glover and J. Doyle, "State-space formulae for all stabilizing controllers that satisfy an H_∞ bound and relations to risk sensitivity", *Systems & Control Letters*, **Vol. 11**, pp. 167-172, 1988.

[57] K. Glover, D. Limebeer, J. Doyle, E. Kasenally and M. Safanov, "A characterization of all solution to the H_∞ four block problem," *SIAM J. Control Optim.*, **Vol. 29**, pp. 283-324, 1991.

[58] G.H. Golub and C.F. Van Loan, *Matrix Computations* (2nd ed.), Johns Hopkins Univ. Press., 1989.

[59] G. Gu and P.P. Khargonekar, "A Class of Algorithms for Identification in H_∞," *Automatica*, **Vol. 28**, pp. 299-312, 1992.

[60] S. Hara, T. Sugie and R. Kondo, "H_∞ control problem with $j\omega$-axis zeros," *Automatica*, **Vol. 28**, pp. 55-70, 1992.

[61] C.V. Hollott and A.V. Bartlett, "Some discrete-time counterparts to Kharitonov's stability criterion for uncertain systems," *IEEE Trans. Autom. Contr.*, **Vol. 31**, pp. 355-356, 1986.

[62] C.V. Hollott, *Extreme Point Results in Robust Control Legacy of Kharitonov's Theorem*, Lecture Notes at the $11th$ Benelux Meeting on Systems and Control, Veldhoven, The Netherlands, March 1992.

[63] H.X. Hu and N.K. Loh, "Robust optimal parametric LQ control with a guaranteed cost bound and applications," *Int. J. Control*, **Vol. 50**, pp. 2489-2502, 1989.

[64] D.C. Hyland and D.S. Berstein, "The optimal projection equations for fixed-order dynamic compensation," *IEEE Trans. Autom. Contr.*, **Vol. 29**, pp. 1034-1037, 1984.

[65] E.A. Jonckheere and L.M. Silverman, "A new set of invariants for linear systems - Applications to reduced order compensator design," *IEEE Trans. Autom. contr.*, **Vol. 28**, pp. 953-964, 1983.

[66] E.I. Jury, *Inners and Stability of Dynamic Systems*, John-Wiley & Sons, Inc., New York, 1974.

[67] R.E. Kalman, "System identification from noisy data", *Proc. Int. Symp. on Dynamical Systems* (Gainesville, Florida, 1981) edited by A. Bednarek, Academic Press, 1982.

[68] P.P. Khargonekar and M.A. Rotea, "Mixed H_2/H_∞ control: A convex optimization approach," *IEEE Trans. Autom. Contr.*, **Vol. 36**, pp. 824-837, 1991.

[69] V.L. Kharitonov, "Asymptotic stability of an equilibrium position of a family of systems of linear differential equations", *Differential Equations*, **Vol. 14**, pp. 1483-1485, 1979.

[70] L. Lee and A.L. Tits, "On continuity/discontinuity in robustness indicators," *Proc. CDC91*, Brighton, England, pp. 547-548, 1991.

[71] D.J.N. Limebeer, B.D.O. Anderson, P.P. Khargonekar and M. Green, "A game theoretic approach to H^∞ control for time-varying systems," *SIAM J. Control and Optimization*, **Vol. 30**, pp. 262-283, 1992.

[72] J.L. Lin, I. Postlethwaithe and D. Gu, "$\mu-K$ iteration: a new algorithm for μ-synthesis," report 91-14, dept. eng., University of Leicester, 1991.

[73] L. Ljung, *System Identification: Theory for the User*, Prentice Hall, Englewood Cliffs, N.J., 1987.

[74] J.M. Maciejowski, *Multivariable Feedback Design*, Addison Wesley, 1989.

[75] D.G. MacMartin, R.S. Hall and D. Mustafa, "On a cost functional for H_2/H_∞ minimization," *Proc. 29th Conference on Decision and Control*, Hawaii, pp. 1010-1012, 1990.

[76] P.M. Makula and H.T. Toivonen, "Computational methods for parametric LQ problems," *IEEE Trans. Autom. Contr.*, **Vol. 32**, pp. 658-671, 1987.

[77] D.C. McFarlane and K. Glover, *Robust Controller Design Using Normalized Coprime Factor Plant Descriptions*, Lecture Notes in Control and Information Sciences, 138, M. Thomas and A. Wyner (Eds.), Springer-Verlag, Berlin, 1989.

[78] B.C. Moore, "Principal component analysis in linear systems: controllability, observability and model reduction," *IEEE Trans. Autom. Contr.*, **Vol. 26**, pp. 17-32, 1981.

[79] D. Mustafa, *Minimum Entropy H_∞ Control*, PhD Thesis, University of Cambridge, 1989.

[80] Y. Nesterov and A. Nemirovsky, *Interior point polynomial methods in convex programming: Theory and applications*, SIAM, 1993.

[81] K. Ogata, *Discrete time control systems*, Prentice-Hall, 1987.

[82] A. Packard, K. Zhou, P. Pandey and G. Becker, "A collection of robust control problems leading to LMIs," *Proc. CDC*, Brighton, England, pp. 1245-1250, 1991.

[83] C.C. Paige and M.A. Saunders, "Towards a generalized singular value decomposition," *SIAM J. Numer. Anal.*, **Vol. 18**, pp. 398-405, 1981.

[84] J. Partington, "Robust identification and interpolation in H_∞," *Int. J. Contr.*, **Vol. 54**, pp. 1281-1290, 1991.

[85] I.R. Petersen, "A stabilizing algorithm for a class of uncertain linear systems," *Systems & Control Letters*, **Vol. 8**, pp. 351-357, 1987.

[86] D.B. Ridgely, L. Valavani, M. Dahleh and G. Stein, "Solution to the general mixed H_2/H_∞ control problem - Necessary conditions for optimality," *Proc. ACC92*, Chicago, IL, pp. 1348-1352, 1992.

[87] M.A. Rotea and P.P. Khargonekar, "H^2-optimal control with an H^∞-constraint: The state Feedback case," *Automatica*, **Vol. 27**, pp. 307-316, 1991.

[88] M.G. Safanov and Peng-Hin Lee, "A multiplier method for computing real multivariable stability margins," *Proc. 1993 IFAC World Congress*, Sydney, Australia, pp. 275-278, 1993.

[89] T. Söderström, P. Stoica, *System Identification*, Prentice-Hall International Series in Systems and Control Engineering, M.J. Grimble (Ed.), Prentice-Hall, New-York, 1989.

[90] J. Staar, *Concepts for reliable modeling of linear systems with application to on-line identification of multivariable state space descriptions*, Ph.D. thesis, Dept. Elec. Eng., K.U.Leuven, Belgium, 1982.

[91] M. Steinbuch and O. Bosgra, "Necessary conditions for static and fixed order dynamic mixed H_2/H_∞ optimal control," *Selected Topics in Identification, Modelling and Control*, Delft University Press, **Vol. 2**, 1990.

[92] M. Steinbuch and O. Bosgra, "Robust performance in H_2/H_∞ optimal control," *Proc. CDC91*, Brighton, England, pp. 549-550, 1991.

[93] A.A. Stoorvogel, "The robust H_2 control problem: a worst case design," *Proc. CDC91*, Brighton, England, pp. 194-199, 1991.

[94] A.A. Stoorvogel, *The H_∞ Control Problem*, Prentice-Hall International Series in Systems and Control Engineering, M.J. Grimble (Ed.), Prentice-Hall, New-York, 1992.

[95] G. Tadmor, "H^∞ in the time domain: The standard four block problem," *Math. Control Syst. Signal Processing*, **Vol. 3**, pp. 301-324, 1990.

[96] A. Tesi and A. Vicino, "Robust stability of state-space models with structured uncertainties," *IEEE Trans. Autom. Contr.*, **Vol. 35**, pp. 191-195, 1990.

[97] L. Vandenberghe and S. Boyd, "Primal-dual potential reduction method for problems involving matrix inequalities", to appear *Mathematical Programming Series B*, 1993.

[98] C.F. Van Loan, "Generalizing the singular value decomposition", *SIAM J. Numer. Anal.*, **Vol. 13**, pp. 76-83, 1976.

[99] P. Van Overschee and B. De Moor, "N4SID: Subspace algorithms for the identification of combined deterministic-stochastic systems," *Automatica*, Special issue on statistical signal processing and control, **Vol. 30**, pp. 75-93, 1994.

[100] M. Vidyasagar, *Control System Synthesis: A Factorization approach*, The MIT Press, Cambridge, MA, 1985.

[101] J.C. Willems, "Least-squares stationary optimal control and the algebraic Riccati equation," *IEEE Trans. Autom. Contr.*, **Vol. 16**, pp. 621-634, 1971.

[102] H.-H. Yeh, S.S. Banda, B.-C. Chang, "Necessary and sufficient conditions for mixed H_2 and H_∞ optimal control," *IEEE Trans. Autom. Contr.*, **Vol. 37**, pp. 355-358, 1992.

[103] G. Zames, "Feedback and optimal sensitivity: model reference transformations, multiplicative seminorms and approximate inverses," *IEEE Trans. Autom. Contr.*, **Vol. 26**, pp. 301-320, 1982.